TU WIEN **bl.**

Doctoral Thesis

ON THE INFLUENCE OF DESIGN CHANGES ON BUCKLING AND POSTBUCKLING OF ELASTIC STRUCTURES

submitted in satisfaction of the requirements for the degree of
Doctor of Technical Sciences in Civil Engineering
of Vienna University of Technology, Department of Civil Engineering

Dissertation

ZUM EINFLUSS VON ENTWURFSÄNDERUNGEN AUF DAS BEULEN UND NACHBEULEN ELASTISCHER STRUKTUREN

ausgeführt zum Zwecke der Erlangung des akademischen Grades eines
Doktors der technischen Wissenschaften
eingereicht an der Technischen Universität Wien, Fakultät für Bauingenieurwesen

von
Xin JIA, M. Eng.
Matrikelnummer 0626084
Institut für Mechanik der Werkstoffe und Strukturen,
Technische Universität Wien,
Karlsplatz 13/202, 1040 Wien, Österreich

Gutachter: Em. O. Univ. Prof. Dipl. -Ing. Dr.techn. Dr.h.c.mult. Herbert A. MANG, Ph.D.
Institut für Mechanik der Werkstoffe und Strukturen,
Technische Universität Wien,
Karlsplatz 13/202, 1040 Wien, Österreich

Gutachter: Univ. Prof. Dipl. -Ing. Dr.techn. Josef FINK
Institut für Tragkonstruktionen-Stahlbau,
Technische Universität Wien,
Karlsplatz 13/212, 1040 Wien, Österreich

Wien, im Dezember 2010 _____

Acknowledgments

Abstract

In structural stability, apart from determination of the buckling load, the postbuckling behavior maybe of interest. The reason for this is that the behavior of the real, i.e. of an imperfect structure depends on the postbuckling behavior of the corresponding perfect structure.

The aim of this work is to study the influence of design changes on buckling and on the postbuckling behavior of elastic structures. Of special interest in this context is the conversion of imperfection-sensitive structures into imperfection-insensitive ones in the course of sensitivity analysis based on modifying the original design. Such a conversion will only be useful if the improvement of the postbuckling behavior does not entail a decrease in the buckling load. By choosing proper design parameters such as the stiffness of additional structural members, the geometric form of the structure, etc., the aforementioned conversion is frequently feasible.

The present dissertation consists of seven published papers. Symmetric bifurcation, zero-stiffness postbuckling, and conversion of imperfection-sensitive structures into imperfection-insensitive ones were chosen as the main topics of this work.

Many structures exhibit symmetric bifurcation which, however, is not required for the conversion of an imperfection-sensitive structure into an imperfection-insensitive one. A less restrictive necessary condition for imperfection insensitivity of structures is presented in this work.

As a special case of postbuckling behavior, zero-stiffness postbuckling may occur in the course of sensitivity analysis of the initial postbuckling behavior. Unfortunately, Koiter's initial postbuckling analysis, representing a computational tool that permits classification of structures as either imperfection sensitive or insensitive, is not sufficient for the diagnosis of zero-stiffness postbuckling. It is shown that bifurcation buckling from a membrane stress state is a necessary condition for this special mode of postbuckling behavior. An example with two degrees of freedom was chosen to demonstrate that for imperfections of first kind, characterized by preservation of bifurcation buckling as the mode of loss of stability, zero-stiffness postbuckling represents a genuine transition from imperfection sensitivity to imperfection insensitivity. For imperfections of second kind, however, resulting in snap-through as the mode of loss of stability, the structure is already imperfection insensitive. Furthermore, by investigating the potential energy, it was shown that the zero-stiffness postbuckling path is stable.

To be of use for engineering practice, conversion from imperfection-sensitive structures into imperfection-insensitive ones must be feasible for real-life structures. An arch bridge was designed to demonstrate the practical feasibility of such a conversion. In its original design, the bridge is without hangers connecting the two arches with the deck. Loss of stability occurs by symmetric bifurcation of the deck, characterized by an antisymmetric buckling mode. The original structure is imperfection sensitive. The arch bridge becomes imperfection insensitive by adding sufficiently stiff hangers which overcompensate the decrease in the load carried by the deck in the postbuckling regime.

Kurzfassung

Abgesehen von der Ermittlung der Beullast kann bei Stabilitätsuntersuchungen auch das Nachbeulverhalten von Interesse sein. Der Grund dafür besteht darin, dass das Verhalten der tatsächlichen, also einer imperfekten Struktur vom Nachbeulverhalten der entsprechenden perfekten Struktur abhängt.

Ziel der vorliegenden Arbeit ist das Studium des Einflusses von Änderungen des ursprünglichen Entwurfs auf das Beulen sowie das Nachbeulverhalten elastischer Strukturen. Von besonderem Interesse ist dabei die Umwandlung imperfektionssensitiver in imperfektionsinsensitive Strukturen im Verlauf von Sensitivitätsanalysen auf der Grundlage von Modifikationen des ursprünglichen Entwurfs. Eine derartige Umwandlung ist allerdings nur dann technisch sinnvoll, wenn die Verbesserung des Nachbeulverhaltens keine Abnahme der Beullast nach sich zieht. Durch Wahl geeigneter Entwurfsparameter, wie der Steifigkeit zusätzlicher Tragglieder, der geometrischen Form der Struktur usw., lässt sich die zuvor erwähnte Umwandlung in vielen Fällen bewerkstelligen.

Die vorliegende Dissertation besteht aus sieben veröffentlichten Aufsätzen. Symmetrische Verzweigung, sogenanntes „zero-stiffness Nachbeulverhalten" und die Umwandlung imperfektionssensitiver in imperfektionsinsensitive Strukturen sind die Hauptthemen dieser Dissertation.

Bei vielen Strukturen erfolgt der Stabilitätsverlust in Form von symmetrischer Verzweigung. Bei dieser Form von Stabilitätsverlust handelt es sich aber um keine notwendige Voraussetzung für die zuvor erwähnte Umwandlung. In der vorliegenden Dissertation wird eine weniger restriktive notwendige Bedingung für imperfektionsinsensitive Strukturen beschrieben.

Als spezielle Form von Nachbeulverhalten kann „zero-stiffness postbuckling" im Verlauf einer Sensitivitätsanalyse des initialen Nachbeulverhaltens auftreten. Leider reicht Koiters initiale Nachbeulanalyse – ein Rechenverfahren, das die Klassifizierung von Strukturen als imperfektionssensitiv bzw. -insensitiv erlaubt – zur Diagnose von „zero-stiffness postbuckling" nicht aus. Es wird gezeigt, dass Verzweigungsbeulen von einem Membranspannungszustand eine notwendige Bedingung für diese spezielle Form des Nachbeulverhaltens darstellt. Ein Beispiel mit zwei Freiheitsgraden dient zum Nachweis, dass im Falle von Imperfektionen erster Art, gekennzeichnet durch Beibehaltung von Verzweigungsbeulen als Form des Stabilitätsverlusts, im Zuge der Sensitivitätsanalyse bei Vorliegen von „zero-stiffness postbuckling" ein echter Übergang von Imperfektionssensitivität zu Imperfektionsinsensitivität stattfindet. Im Falle von Imperfektionen zweiter Art hingegen, die zu Durchschlagen als Form des Stabilitätsverlusts der Struktur führen, ist die Struktur bei Vorliegen von „zero-stiffness postbuckling" bereits imperfektionsinsensitiv. Dementsprechend hat eine Untersuchung der mit dem Nachbeulpfad verbundenen potentiellen Energie ergeben, dass dieser Pfad bei „zero-stiffness postbuckling" stabil ist.

Der Nutzen der Umwandlung von imperfektionssensitiven in imperfektionsinsensitive Strukturen für die Ingenieurpraxis hängt von der Realisierbarkeit einer solchen Transformation für reale Strukturen – im Gegensatz zu akademischen Beispielen – ab. Wie anhand der Sensitivitätsanalyse des Nachbeulverhaltens einer Bogenbrücke gezeigt wird, ist diese Realisierbarkeit gegeben. Der ursprüngliche Entwurf der Brücke enthält noch keine Hängestangen, welche die beiden Bögen mit der Fahrbahnkonstruktion verbinden. Der Stabilitätsverlust erfolgt durch symmetrische Verzweigung, gekennzeichnet durch eine antimetrische Beulform der Fahrbahnkonstruktion. Die ursprüngliche Struktur ist imperfektionssensitiv. Durch Anbringung hinreichend dehnsteifer Hängestangen, die die Abnahme der von der ausbeulenden Fahrbahnkonstruktion aufgenommenen Belastung überkompensieren, wird die Struktur imperfektionsinsensitiv.

Table of Contents

Chapter III

Conditions for Symmetric, Antisymmetric, and Zero-Stiffness Bifurcation
in View of Imperfection Sensitivity and Insensitivity   45

Chapter IV

Hilltop Buckling as the Alpha and Omega in Sensitivity Analysis
of the Initial Postbuckling Behavior of Elastic Structures   68

Chapter V

Three Pending Questions in Structural Stability   89

Chapter VI

Imperfection Sensitivity or Insensitivity of Zero-stiffness Postbuckling ... that is the Question   109

Chapter VII

Necessary and Sufficient Conditions for Zero-Stiffness Postbuckling   115

Chapter VIII

Conversion of Imperfection-sensitive Elastic Structures into Imperfection-insensitive Ones
by Adding Tensile Members 119

Chapter I

Summary
of the Contents of Papers Representing the Dissertation

1. Introduction

1.1. State of the art

In 1757, Leonhard Euler derived a formula for the critical load of a long, slender, ideal column subjected to an axial vertical load [1]. This may be regarded as the starting point of the analysis of structural stability. Two centuries later, the stability of structures had been studied already by numerous scientific scholars e.g. [6, 8, 9]. Buckling analysis has been extended from buckling of Euler columns to lateral buckling of beams, e.g. [2], buckling of plates e.g. [4], and of shells e.g. [7], plastic buckling e.g. [10], dynamic buckling e.g. [12], etc. With the availability of the Finite Element Method (FEM) [5, 16], buckling analysis of real-life structures became feasible. Because of the difficulty of deriving equilibrium equations for the postbuckling path, postbuckling analysis was not feasible until Koiter's pioneering work on initial postbuckling analysis [6] was translated into the English language. Koiter utilized asymptotic series expansions to represent the secondary path at the bifurcation point. His approach was integrated in the FEM e.g. by Reitinger [15].

From an engineering viewpoint, optimization of the buckling behavior of structures is an important topic. In early research on this topic, efforts were focused on optimization of the buckling load e.g. [8]. In addition to the buckling load, frequently the postbuckling behavior of structures is of interest. The reason for this interest is the influence of imperfections on the postbuckling behavior of ideal, i.e. perfect structures. Work on optimization of the postbuckling behavior was done e.g. by Budiansky [9], Mróz *et al.* [13, 18], and Bochenek *et al.* [19, 20].

The focus of the work of the Stability Group at the Institute for Mechanics of Materials and Structures of Vienna University of Technology is on computational sensitivity analysis of the initial postbuckling behavior of elastic structures. The present research activities of this group were preceded by work of Helnwein [17] who proposed the so-called consistently linearized eigenproblem for the purpose of estimating the stability limit. Information extracted from the solution of this problem was utilized by [21, 33] in the frame of Koiter's asymptotic series expansions. Depending on the stress state in the prebuckling regime, the following distinction between two classes was made: (1) buckling from a general stress state; and (2) buckling from a membrane stress state. This classification plays a great role in sensitivity analysis of bifurcation buckling of elastic structures.

The main purpose of sensitivity analysis of the postbuckling behavior of elastic structures is to investigate the feasibility of converting imperfection-sensitive structures into imperfection-insensitive ones through minor changes of the original design. At first sight, it might appear that such a conversion is restricted to symmetric bifurcation. However, Steinboeck *et al* [23] have shown that symmetric bifurcation is not necessary for transition from imperfection sensitivity to insensitivity. Steinboeck *et. al.* [25] have also shown that linear prebuckling paths and linear stability problems are not mutually conditional.

In the course of sensitivity analysis of the initial postbuckling behavior of structures, hilltop buckling and zero-stiffness postbuckling may occur. Definitions of these two special cases and examples can be found in [26] and [25]. Later on, Höfinger [27] presented a mathematical proof that hilltop buckling is necessarily imperfection-sensitive. Jia [28] showed that zero-stiffness postbuckling is imperfection insensitive. Mang [29, 30] derived a necessary and sufficient condition for zero-stiffness postbuckling.

Academic examples with remarkable postbuckling paths were reported in [22, 23, 24, 25]. An arch bridge was designed and analyzed by Jia [31]. This analysis illustrates the feasibility of converting imperfection-sensitive structures other than academic examples into imperfection-insensitive structures.

1.2. List of publications representing this dissertation

This dissertation consists of seven scientific papers. The following list contains references to these works.

> 1. Andreas Steinböck, **Xin Jia**, Gerhard Höfinger, Helmut Rubin, Herbert A. Mang:
> "Remarkable Postbuckling Paths Analyzed by Means of the Consistently Linearized Eigenproblem"
> International Journal for Numerical Methods in Engineering, 76, 156-182, 2008.
>
> 2. Andreas Steinböck, **Xin Jia**, Gerhard Höfinger, Herbert A. Mang:
> "Conditions for Symmetric, Antisymmetric, and Zero-Stiffness Bifurcation in View of Imperfection Sensitivity and Insensitivity"
> Computer Methods in Applied Mechanics and Engineering, 197(45-48), 3623-3636, 2008.
>
> 3. Herbert A.Mang, **Xin Jia,** Gerhard Höfinger:
> "Hilltop Buckling as the Alpha and Omega in Sensitivity Analysis of the Initial Postbuckling Behavior of Elastic Structures"
> Journal of Civil Engineering and Management, 15(1), 35-46, 2009.
>
> 4. Andreas Steinböck, Gerhard Hoefinger, **Xin Jia**, Herbert A. Mang:
> "Three Pending Questions in Structural Stability"
> Journal of the International Association for Shell and Spatial Structures, 50(1), 51-64, 2009.
>
> 5. **Xin Jia**, Gerhard Höfinger, Herbert A.Mang:
> "Imperfection Sensitivity or Insensitivity of Zero-stiffness Postbuckling ... that is the Question"
> In Computational Structural Engineering: Proceedings of the International Symposium on Computational Structural Engineering, Springer, Shanghai, China, 103-110, 2009.
>
> 6. **Xin Jia**, Gerhard Höfinger, Herbert A. Mang:
> "Necessary and Sufficient Conditions for Zero-Stiffness Postbuckling"
> To appear in PAMM - Proceedings in Applied Mathematics and Mechanics, 2010.

7. **Xin Jia**, Herbert A. Mang:
"Conversion of Imperfection-sensitive Elastic Structures into Imperfection-insensitive Ones by Adding Tensile Members"
In Proceedings of the International Association for Shell and Spatial Structures (IASS) Symposium 2010, Spatial Structures – Permanent and Temporary, November 8-12, 2010, Shanghai, China; accepted also for publication in the Journal of IASS.

These papers and several other ones not included in the above list were written during the period of the doctoral studies of Xin Jia (April 2006 – December 2010). His contributions to all of these works were significant and dominant where he is the lead author. The topics of symmetric bifurcation, zero-stiffness postbuckling, and the conversion of an imperfection-sensitive arch bridge into an imperfection-insensitive one were chosen as the main topics of this dissertation.

1.3.   Scope of work

The summary of publications representing this dissertation is organized as follows: Section 2 is devoted to the theoretical basis including formulation of the equilibrium conditions in the framework of the FEM, Koiter's initial postbuckling analysis, the condition for imperfection insensitivity and the so-called consistently linearized eigenproblem. The question whether transition from imperfection sensitivity to insensitivity of elastic structures requires symmetric bifurcation is discussed in Section 3. At first, symmetric bifurcation with respect to (*w.r.t.*) the parameter η for the secondary path is defined. Then, the condition for symmetric bifurcation is formulated. By comparing this condition with the one for imperfection insensitivity, the above question is answered. An example with 2 degrees of freedom (*d.o.f.*) is chosen for verification of the theoretical considerations. In Section 4, the special case of zero-stiffness postbuckling is investigated. With the help of the imperfection parameter ε, it is shown that the zero-stiffness postbuckling path is imperfection insensitive. Furthermore, the potential energy surface of an example with 2 *d.o.f.* is plotted to show that the zero-stiffness postbuckling path is stable. Section 5 contains the design of an arch bridge and its analysis for loss of stability and for its postbuckling behavior. By adding sufficiently stiff hangers connecting the two arches with the deck, the structure is converted from imperfection sensitivity to imperfection insensitivity. In Section 6, concluding remarks are made. *Corrigenda* of errors in published papers are summarized in Section 7.

This work is restricted to static, conservative systems with N *d.o.f.*, conforming to the FEM. Loss of stability at multiple bifurcation points is not taken into account.

2.   Theoretical basis

For a static, conservative system with N *d.o.f.*, the equilibrium conditions can be expressed as

$$\mathbf{G}(\mathbf{u}, \lambda) := \mathbf{F}^I(\mathbf{u}) - \lambda \overline{\mathbf{P}} = \mathbf{0} \tag{1}$$

where $\mathbf{u}$ is the displacement vector, λ is a dimensionless scalar scaling a constant reference load $\overline{\mathbf{P}}$, and $\mathbf{F}^I$ stands for the vector of internal forces. Eq. (1) defines equilibrium paths of the system. If two

equilibrium paths intersect, the system is said to bifurcate at the point of intersection. A bifurcation point is denoted as $(\mathbf{u}_S, \lambda_S)$, see e.g. point S in Fig. 1. The equilibrium path which contains the undeformed state is called primary or (up to the stability limit) prebuckling path $(\tilde{\mathbf{u}}(\lambda), \lambda)$. Other equilibrium paths that contain the stability limit are referred to as secondary or postbuckling paths.

The differential form of Eq. (1), representing the basis of incremental-iterative analysis for the solution of mechanical problems, is obtained as [25]

$$\mathbf{K}_T \cdot d\mathbf{u} - d\lambda \overline{\mathbf{P}} = \mathbf{0} \tag{2}$$

with $\mathbf{K}_T = \partial \mathbf{G}(\mathbf{u})/\partial \mathbf{u}$ standing for the tangent stiffness matrix. For the primary path, (2) can be written as

$$\tilde{\mathbf{K}}_T \cdot d\tilde{\mathbf{u}} = d\lambda \overline{\mathbf{P}} \tag{3}$$

with $\tilde{\mathbf{K}}_T := \mathbf{K}_T\left(\tilde{\mathbf{u}}(\lambda)\right)$. If $d\lambda = 0$, resulting in

$$\tilde{\mathbf{K}}_T \cdot d\tilde{\mathbf{u}} = \mathbf{0}, \tag{4}$$

and the nullity of $\tilde{\mathbf{K}}_T$ is one, *snap-through buckling* occurs. The snap-through point, represents a local maximum on the primary path.

At the bifurcation point, $\tilde{\mathbf{K}}_T$ becomes singular. The zero eigenvector $\mathbf{v}_1$ is defined as

$$\tilde{\mathbf{K}}_T \cdot \mathbf{v}_1 = \mathbf{0}. \tag{5}$$

At S,

$$\mathbf{v}_1^T \cdot \mathbf{P} = 0 \ \wedge \ \tilde{\mathbf{K}}_T \cdot d\tilde{\mathbf{u}} \neq \mathbf{0}. \tag{6}$$

Premultiplying Eq.(3) by $\mathbf{v}_1^T$ yields

$$\mathbf{v}_1^T \cdot \tilde{\mathbf{K}}_T \cdot d\tilde{\mathbf{u}} = d\lambda\left(\mathbf{v}_1^T \cdot \overline{\mathbf{P}}\right). \tag{7}$$

If $d\lambda = 0 \ \wedge \ \mathbf{v}_1^T \cdot \mathbf{P} = 0$, the bifurcation point S coincides with the snap-through point, indicating the special case of *hilltop buckling*. For this case, the nullity of $\tilde{\mathbf{K}}_T$ is two.

Koiter utilized $\mathbf{v}(\eta)$ and $\lambda(\eta)$ (see Fig. 1) to describe the secondary path. $\mathbf{v}(\eta)$ represents the offset of the displacement of a point on the secondary path, defined by the path parameter η, from the point on the primary path with the same load level. $\mathbf{v}(\eta)$ and $\lambda(\eta)$ are expanded at the bifurcation point S into asymptotic series. For sensitivity analysis, characterized by a variation of the original design of the structure with the help of the design parameter κ, the dependence of the coefficients $\lambda_1, \lambda_2, \dots$ and of the vectors $\mathbf{v}_1, \mathbf{v}_2, \dots$ on κ must be considered:

$$\Delta\lambda(\kappa, \eta) = \lambda_1(\kappa)\eta + \lambda_2(\kappa)\eta^2 + \lambda_3(\kappa)\eta^3 + \lambda_4(\kappa)\eta^4 + \dots. \tag{8}$$

$$\mathbf{v}(\kappa,\eta) = \mathbf{v}_1(\kappa)\eta + \mathbf{v}_2(\kappa)\eta^2 + \mathbf{v}_3(\kappa)\eta^3 + \mathbf{v}_4(\kappa)\eta^4 + ... \tag{9}$$
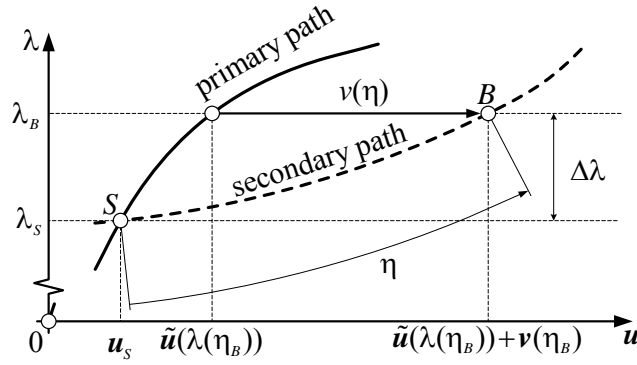
Fig. 1: Nonlinear primary path and secondary path for a specific value of the design parameter κ [23]

With

$$\mathbf{u}(\eta) = \tilde{\mathbf{u}}(\lambda(\eta)) + \mathbf{v}(\eta), \tag{10}$$

specialization of (1) for the secondary path reads as

$$\mathbf{G}(\eta) := \mathbf{G}\big(\tilde{\mathbf{u}}(\lambda(\eta)) + \mathbf{v}(\eta), \lambda(\eta)\big) = \mathbf{0}. \tag{11}$$

Inserting the series expansions (8) and (9) into (11), yields

$$\mathbf{G}(\eta) = \mathbf{G}_{0S} + \mathbf{G}_{1S}\eta + \mathbf{G}_{2S}\eta^2 + \mathbf{G}_{3S}\eta^3 + O(\eta^4) = \mathbf{0} \tag{12}$$

where $\mathbf{G}_{nS} = \mathbf{G}_{,\eta^n}\big|_{\eta=\eta_S=0} / n! \; \forall n \in \mathbb{N}$. Satisfaction of (12) for an arbitrary value of η requires

$$\mathbf{G}_{nS} = \mathbf{0} \tag{13}$$

which allows successive computation of the unknown pairs $(\lambda_1, \mathbf{v}_1), (\lambda_2, \mathbf{v}_2), ...$

A necessary and sufficient condition for imperfection insensitivity is

$$\lambda_m > 0 \tag{14}$$

where λ_m is the first non-vanishing term in (8) and m is an even number [23].

Originally, the so-called consistently linearized eigenproblem was used to estimate the stability limit *ab initio*, i.e. without an incremental analysis [17]. The importance of this eigenproblem rests with its role in the derivation of a mathematical condition for bifurcation buckling from a membrane stress state in [33]. The mathematical formulation of this eigenproblem for the first eigenpair $\big(\lambda_1^*(\lambda) - \lambda, \mathbf{v}_1^*(\lambda)\big)$ is

$$\Big[\tilde{\mathbf{K}}_T + (\lambda^* - \lambda_1)\tilde{\mathbf{K}}_{T,\lambda}\Big] \cdot \mathbf{v}_1^* = \mathbf{0} \tag{15}$$

where $\tilde{\mathbf{K}}_{T,\lambda}$ is the first derivative of $\tilde{\mathbf{K}}_T$ *w.r.t.* λ. At the stability limit,

$$\lambda_1^* = \lambda, \quad \mathbf{v}_1^* = \mathbf{v}_1, \quad \tilde{\mathbf{K}}_T \cdot \mathbf{v}_1 = \mathbf{0}, \tag{16}$$

with (16.3) representing the condition for loss of stability of equilibrium of the primary path.

3.   Is symmetric bifurcation necessary for imperfection insensitivity?

Symmetric bifurcation represents a qualitative property of a structure that simplifies postbuckling analysis. Frequently, symmetric bifurcation is considered as a necessary condition for imperfection insensitivity of the initial postbuckling behavior of elastic structures. In [25] it is shown that this is not the case.

The potential energy function V plays a pivotal role in determining the load-displacement behavior of a structure. With the help of V, symmetric bifurcation can be defined as

$$V(\mathbf{u},\lambda) = V(\mathbf{T}(\mathbf{u}),\lambda) \tag{17}$$

where $\mathbf{T}:\mathbb{R}^N \to \mathbb{R}^N$ is an element of a symmetry group.

If

$$\mathbf{T} := \begin{bmatrix} 1 & & & \\ & \ddots & \mathbf{0} & \\ & \mathbf{0} & 1 & \\ & & & -1 \end{bmatrix} = \left[T_{ij}\right] = \left[\delta_{ij}\left(1 - 2\delta_{ij}\right)\right], \tag{18}$$

and

$$\mathbf{T}(\mathbf{u}) = \left[\delta_{ij}\left(1 - 2\delta_{ij}\right)\right]_{i=1..N,\,j=1..N} \cdot \mathbf{u}, \tag{19}$$

the symmetric structure of $\tilde{\mathbf{K}}_{T,\lambda^n}$ with $n \in \mathbb{N}$ can be used to demonstrate that symmetry is characterized by

$$\begin{aligned} &\mathbf{v}_1 = \left[0,...,0,p\right]^T, p \in \mathbb{R}\setminus\{0\}, \\ &\mathbf{v}_1 \cdot \mathbf{v}_i = 0 \ \forall \ i > 1, \\ &\mathbf{v}_i = \mathbf{0} \ \forall \ i \in \{3,5,7,...\}. \end{aligned} \tag{20}$$

Necessary and sufficient conditions for the symmetry of the secondary path *w.r.t.* η are then obtained as

$$\lambda(\eta) = \lambda(-\eta) \ \wedge \ \mathbf{v}(\eta) = \mathbf{T}(\mathbf{v}(-\eta)) \ \wedge \ \tilde{\mathbf{u}}(\lambda) = \mathbf{T}(\tilde{\mathbf{u}}(\lambda)). \tag{21}$$

Substituting (20.1) into (8) yields

$$\lambda_{2i-1} = 0 \ \forall \ i \in \mathbb{N}. \tag{22}$$

Since symmetric bifurcation is merely a matter of choice of the coordinates, only symmetry with respect to a scalar variable η is addressed herein.

Comparing the condition for symmetric bifurcation according to (22) with the condition for imperfection insensitivity according to (14), it is evident that imperfection insensitivity does not require symmetric bifurcation. This is shown for the 2 *d.o.f.* example in Fig. 2. A detailed analysis of this problem is contained in [23]. The meaning of the design parameter κ follows from Fig. 2. The

structure is imperfection sensitive for $\kappa \in [0, 0.0454)$ and imperfection insensitive for $\kappa \geq 0.0454$. For $\kappa = 0.0454$,

$$\lambda_1 = 0, \ \lambda_2 = 0, \ \lambda_3 = 0, \ \lambda_4 = 9.79 \times 10^{-3}, \lambda_5 = -9.27 \times 10^{-3},$$
$$\mathbf{v}_1 = [0,1]^T, \ \mathbf{v}_2 = [0.048,0]^T, \ \mathbf{v}_3 = [0,0]^T, \ \mathbf{v}_4 = [-0.011,0]^T, \ \mathbf{v}_5 = [0,0]^T.$$

Although, the structure is imperfection insensitive for $\kappa = 0.0454$, the postbuckling path is *not* symmetric with regard to η.
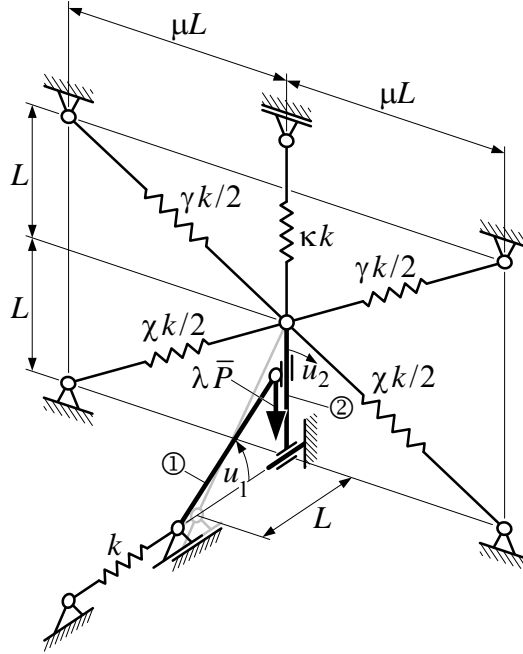
Fig. 2: System with an unsymmetric secondary path [23]

4. Is zero-stiffness postbuckling imperfection insensitive?

Zero-stiffness postbuckling is characterized by a secondary load-displacement path along which the load remains constant. Hence, for zero-stiffness postbuckling,

$$\lambda_i = 0 \ \ \forall \ i \in \mathbb{N}. \tag{23}$$

In sensitivity analysis of the initial postbuckling path, zero-stiffness is viewed as a borderline case between imperfection sensitivity and insensitivity. However, it is not clear whether zero-stiffness postbuckling is imperfection sensitive or insensitive. In order to clarify this issue, imperfections were introduced to perfect structures which experience zero-stiffness postbuckling in the course of sensitivity analysis of the initial postbuckling behavior, and a new definition of imperfection insensitivity was given.

For perfect systems undergoing bifurcation buckling, imperfections are classified in two categories depending on whether or not the imperfect system has a bifurcation point. With the help of the potential energy function referring to the imperfect structure, $V^* = V^*(\mathbf{u}, \lambda, \varepsilon)$, where $\varepsilon \in \mathbb{R}$ denotes the imperfection parameter and * marks variables or functions referring to the imperfect structure, the imperfection vector is defined as

$$\mathbf{E}\left(\lambda,\varepsilon\right) := V^*_{,\mathbf{u}\varepsilon}\Big|_{\mathbf{u}=\tilde{\mathbf{u}}} = \frac{\partial^2 V^*}{\partial\mathbf{u}\partial\varepsilon}\left(\mathbf{u}=\tilde{\mathbf{u}}\right). \tag{24}$$

The following classification of imperfections is given in [28]:

$\mathbf{E}^T\cdot\mathbf{v}_1 = 0 \;\forall\; \lambda\in\mathbb{R},\; \varepsilon_I\in\mathbb{R}/\{0\}$ for imperfections of the first kind for which the imperfection parameter is denoted as ε_I; $\tag{25}$

$\mathbf{E}^T\cdot\mathbf{v}_1 \neq 0 \;\forall\; \lambda\in\mathbb{R},\; \varepsilon_{II}\in\mathbb{R}/\{0\}$ for imperfections of the second kind for which the imperfection parameter is denoted as ε_{II}. $\tag{26}$

For the definition of imperfection insensitivity in case of imperfections of the first kind, it is sufficient to consider $\varepsilon_I\in[-\varsigma,\varsigma]$ where ς is an arbitrary, small positive value. If all imperfect structures in this interval are still stable at the bifurcation point S^*, then the initial postbuckling path of the corresponding perfect structure is imperfection insensitive *w.r.t.* ε_I. Actually, ε_I is equivalent to the design parameter for sensitivity analysis. For each value of ε_I, it can be found out by checking (14) whether the structure is imperfection sensitive or insensitive.

For the definition of imperfection insensitivity in case of imperfections of the second kind, it is sufficient to consider $\varepsilon_{II}\in[-\varsigma,\varsigma]\setminus\{0\}$. If no imperfect structure in this interval has a load-displacement path with a snap-through point $\left(\mathbf{u}_{D*},\lambda_{D*}\right)$ with $\lambda_{D*} < \lambda_S$, then the initial postbuckling path of the corresponding perfect structure is imperfection insensitive *w.r.t.* ε_{II}.

A structure with 2 *d.o.f.* (see Fig. 3) was studied in [28], considering four different imperfections. The results (see Fig. 4) from this analysis show that zero-stiffness postbuckling is a case of a real transition from imperfection sensitivity to imperfection insensitivity for imperfections of the first kind and that it is imperfection insensitive for imperfections of the second kind.
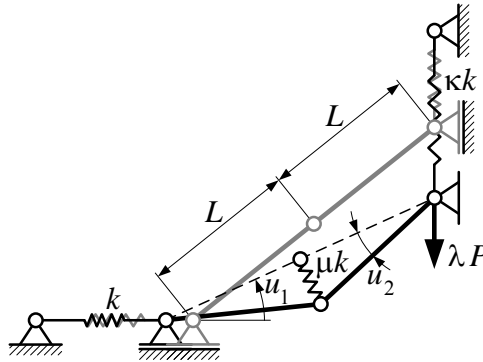
Fig. 3: A two-bar system [28]
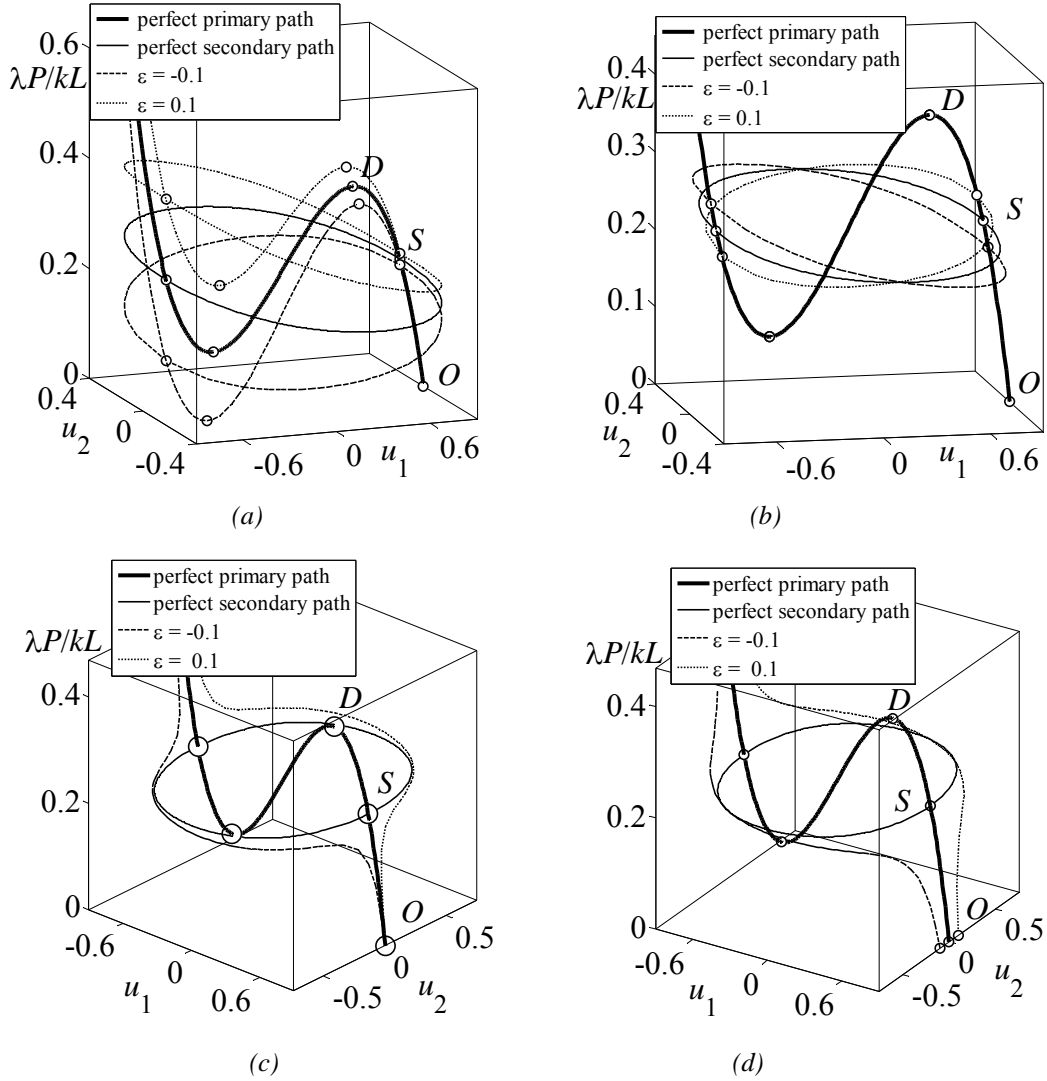
Fig. 4: Equilibrium paths of perfect and imperfect structures (a) imperfection of stiffness of top spring; (b) imperfection of stiffness of lateral spring; (c) shift of load; (d) change of initial angle between two rods [28]

Moreover, Fig. 5 shows the intersection of the potential energy function $V(\mathbf{u}, \lambda)$ for the present example with the hyper-plane $\lambda = \lambda_s$, denoted as $V'(u_1(\eta), u_2(\eta))$. The closed, plane, horizontal curve $\gamma(\eta)$ on V' represents the potential energy along the zero-stiffness postbuckling path. Hence, the potential energy along such a path is constant. At each point on $\gamma(\eta)$, $\delta^2 V \geq 0$, indicating stable equilibrium. The local maximum of the surface V', denoted as C, corresponding to a deformation state of the two bars being horizontal and in line, is characterized by unstable equilibrium, i.e. $\delta^2 V < 0$.
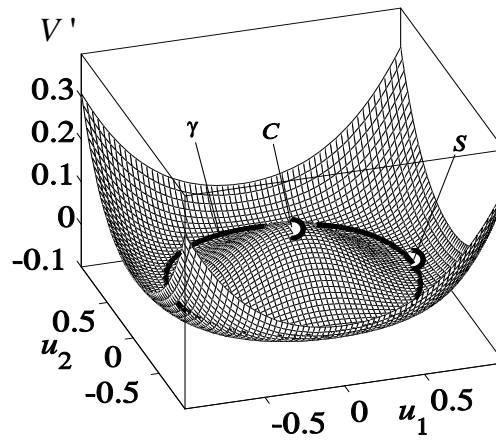
Fig. 5: Surface $V'(u_1, u_2)$ containing the plane horizontal curve $\gamma(\eta) = V'(u_1(\eta), u_2(\eta)) = V(u_1(\eta), u_2(\eta), \lambda_S)$, related to zero-stiffness postbuckling [28]

5. Conversion of an imperfection-sensitive arch bridge into an imperfection-insensitive one by adding tensile members

If a vertical spring of sufficient stiffness is attached to the top of a *von Mises* truss (see Fig. 6), the structure becomes imperfection insensitive. To utilize the positive influence of a tensile member on the postbuckling behavior, an arch bridge, shown in Fig. 7, was designed and analyzed.
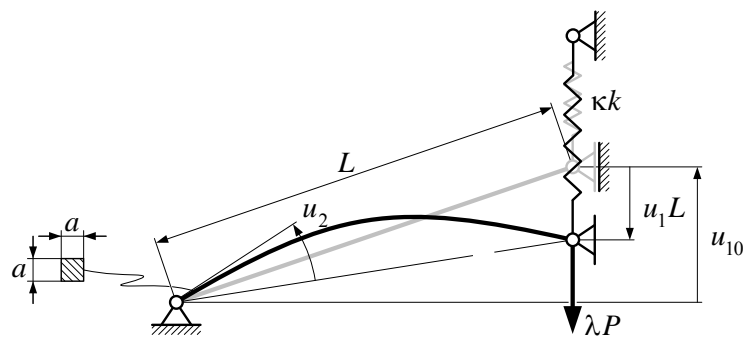
Fig. 6: Left half of a von Mises truss with a vertical elastic spring attached to the load point [24]
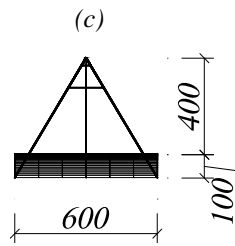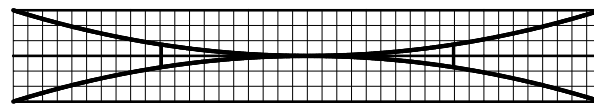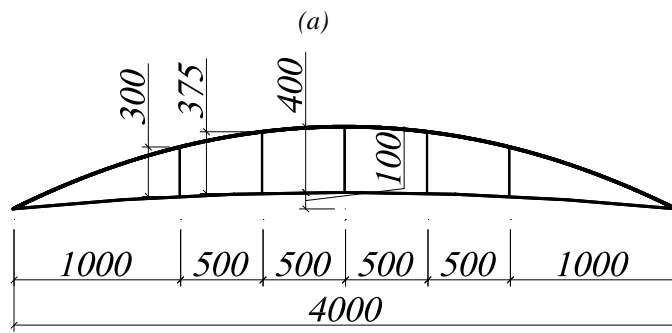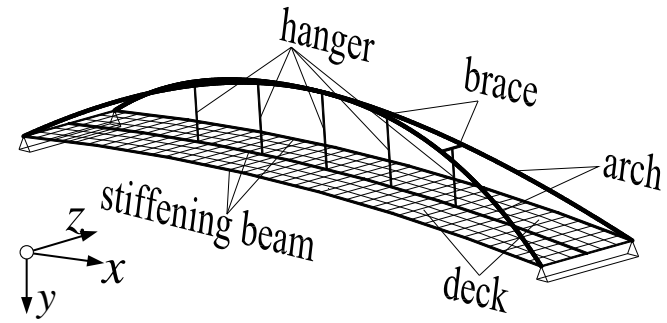
Fig. 7: (a) Arch bridge, (b) view from the side; (c) floor plan, (d) front view; unit
of numerical data: cm unit of dimensions: cm [31]
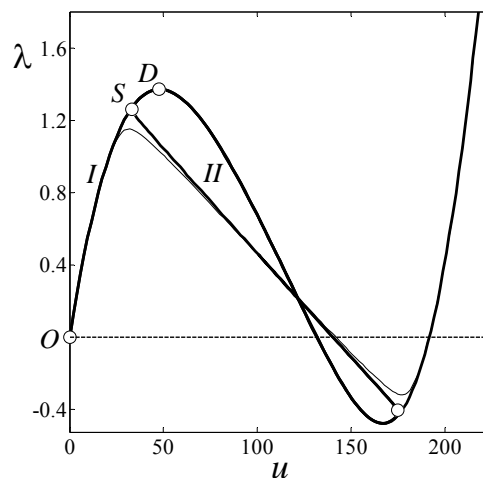
(a)
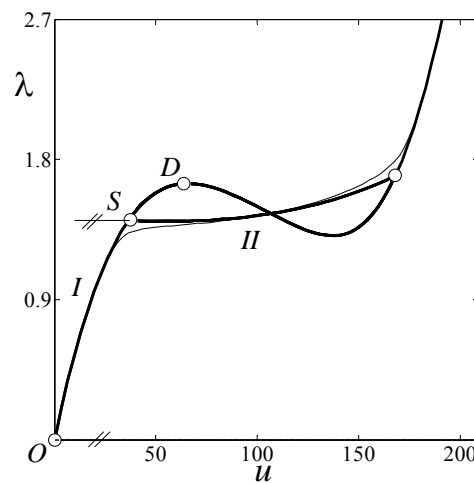
(b)
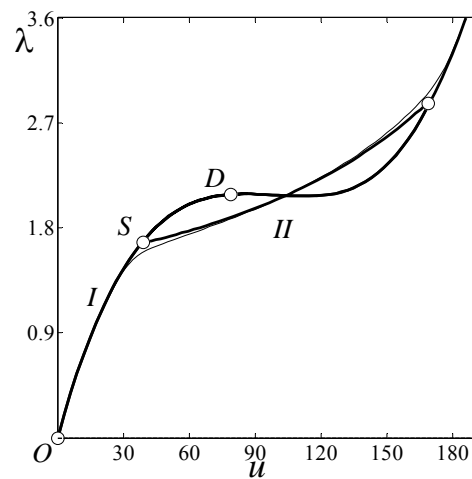
(c)

Fig. 8: Load-displacement paths of the midpoint of the deck of an arch bridge for three different values of the stiffness of the hangers; (a) $\kappa = 0$ *, (c)* $\kappa = 0.6182$, *(d)* $\kappa = 0.8000$ *(* κ *is related to the diameter of the cross section of the hangers) [31]*

Fig. 8 shows selected results from sensitivity analysis of the prebuckling and the postbuckling behavior of the arch bridge where λ denotes the load parameter by which the uniformly distributed reference load of the deck is multiplied and u stands for the vertical displacement of the midpoint of the deck of the bridge. The thick lines represent the primary and secondary paths of the perfect structures, and the thin lines refer to the load-displacement paths of imperfect structures. The imperfections were chosen as perturbations of the geometric shapes of the perfect structures, affine to the respective eigenvector $\mathbf{v}_1$. As follows from Fig. 8, the slope of the projection of the secondary path onto the u-λ plane at the bifurcation point S changes from negative to positive, indicating that the postbuckling behavior of the structure can be significantly improved by adding sufficiently stiff hangers which overcompensate the decrease in the load carried by the deck in the postbuckling regime. At the same time, also the buckling load is increased.

6. Concluding remarks and recommendations for future work

Imperfection-insensitive structures can carry loads that are larger than the stability limit of the respective perfect structures. Hence, investigating the possibility of a conversion of originally imperfection-sensitive structures into imperfection-insensitive ones can be useful. To make sense, such a conversion should result in an improvement of the postbuckling path without decrease of the buckling load. By choosing proper design parameters such as the stiffness of additional tensile members, the rise of the structure, the reduction of non-axial deformations by means of a change of the original form of the structures etc., the mentioned conversion can be achieved.

In this work, Koiter's initial postbuckling analysis was used as a tool for investigating the initial postbuckling behavior. The consistently linearized eigenproblem was utilized within Koiter's approach that represents the theoretical basis for sensitivity analysis.

It was shown that symmetric bifurcation, characterized by $\lambda_{2i-1} = 0, i \in \mathbb{N}$, is not necessary for conversion of imperfection-sensitive structures into imperfection-insensitive ones. What is necessary for such a conversion, however, is $\lambda_1 = 0 \ \forall \ \kappa$.

In the course of sensitivity analysis of the initial postbuckling path, zero-stiffness postbuckling may occur in bifurcation buckling analysis. For this special case, all load coefficients in (8) vanish. Hence, the condition for imperfection insensitivity, as given by (14), is not applicable. By investigating a 2 *d.o.f.* structure for four types of imperfections, zero-stiffness postbuckling was shown to represent a genuine transition from imperfection sensitivity to imperfection insensitivity for imperfections of the first kind, but to be imperfection insensitive for imperfections of the second kind. Furthermore, by investigating the potential energy, it was shown that the zero-stiffness postbuckling path is stable (see Fig. 5).

An arch bridge was designed and analyzed to illustrate the practical applicability of converting imperfection-sensitive structures into imperfection-insensitive ones. The design results in symmetric

bifurcation of the deck, with an antisymmetric buckling mode. The original design is characterized by imperfection sensitivity of the bridge. The structure becomes imperfection insensitive by adding sufficiently stiff hangers which overcompensate the decrease in the load carried by the deck in the postbuckling regime.

Further work should focus on investigating the reason for a structure being either imperfection sensitive or imperfection insensitive. On the basis of this dissertation, the degree of tensile stiffness of a structure has a significant influence on its postbuckling behavior. Obviously, such a qualitative statement needs further quantitative corroboration.

7. Corrigenda

Error 1:

In [26], Eq. (84) is incorrect. It is based on the erroneous assumption of

$$\lambda_2\left(\overline{\kappa}\right) = a_1\left(\overline{\kappa}\right) = a_1^*\left(\overline{\kappa}\right) = 0 \tag{27}$$

which was insinuated by numerical work pursued by Schranz and reported in [22]. The mentioned error also appeared in [29, 30].

Error 2:

In [26], Fig. 4(a) and Fig. 5(a) are incorrect, because $\lambda_2 = 0$ does not occur for the same value of the design parameter as $a_1 = 0$.

Error 3:

In [30], Eq. (8) is incorrect. In [31], the curvature of the secondary path at the bifurcation in Fig. 7(c) is positive, indicating that $\lambda_4\big|_{\lambda_2=0} > 0$.

Error 4:

Eq. (4) in [29] and Eq. 3 in [30] are incorrect. The two eqations were based on the wrong assumption of "restricted asymmetry". The example in Section 4.5 of [25] shows that $\lambda_2\left(\overline{\kappa}\right) = 0$ but $\lambda_3\left(\overline{\kappa}\right) \neq 0$.

8. References

[1] Euler L. *De motu vibratorio tympanorum*. Novi Commentari Acad, Petropolit, 10, 243-260, 1766.

[2] Flint A.R. *The influence of restraints on the stability of beams*. The Structural Engineer, London, U.K., 29(9), 235-246, 1951.

[3] Timoshenko, S. P., and Gere, J. M. *Theory of elastic stability*, 2 ed. McGraw-Hill, 1961.

[4] Wittrick W.H., Ellen C.H. *Buckling of tapered rectangular plates in compression*. The Aeronautical Quarterly. 13(4), 308–326, 1962.

[5] Zienkiewicz O.C., Cheung Y.K. *The Finite element method in structural and continuum mechanics*. McGraw-Hill, New York, 1967.

[6] Koiter W.T. *On the stability of elastic equilibrium.* (translation of 'over de stabiliteit van het elastisch evenwicht', (1945)). Technical report, Polytechnic Institute Delft, H.J. Paris Publisher Amsterdam, NASA TT F-10, 833, 1967.

[7] Arbocz J. and Babcock C. D. *The effect of general imperfections on the buckling of cylindrical shells.* ASME Journal of Applied Mechanics, 36:28 – 38, 1969.

[8] Thompson J.M.T., Lewis G.M. O*n the optimum design of thin-walled compression members.* Journal of the Mechanics and Physics of Solids, 20(2), 1010-109, 1972.

[9] Budiansky B. *Theory of buckling and postbuckling behavior of elastic structures.* In Chia-Shun Yih, (Editor), Advances in Applied Mechanics, Elsevier, 14, 1-65, 1974.

[10] Tvergaard V. Buckling of eccentrically stiffened elastic-plastic panels on two simple supports or multi-supported. International Journal of Solids Structures, 11, 647-663, 1975.

[11] Brush D.O., Almroth B.O. *Buckling of bars, plates and shells.* McGraw-Hill, 1975.

[12] Lindberg HE, Florence AL. Dy*namic pulse buckling-theory and experiment.* Martinus Nijhoff Publishers, 1987.

[13] Mróz Z., Haftka R.T. *Design sensitivity analysis of non-linear structures in regular and critical states.* International Journal of Solids and Structures, 31(15), 2071-2098, 1994.

[14] Godoy L.A. *Sensitivity of post-critical states to changes in design parameters.* International Journal of Solids and Structures, 33(15), 2177-2192, 1996.

[15] Reitinger R. *Stabilität und Optimierung imperfektionsempfindlicher Tragwerke.* PHD thesis, Universität Stuttgart, 1994.

[16] Bathe K.J. F*inite element procedures.* Prentice Hall, Upper Saddle River, New Jersey 07458, 1996.

[17] Helnwein P. *Zur initialen Abschätzbarkeit von Stabilitätsgrenzen auf nichtlinearen Last-Verschiebungspfaden elastischer Strukturen mittels der Methode der Finiten Element*e [in German; *On ab initio assessability of stability limits on nonlinear load-displacement paths of elastic structures by means of the finite element method*]. PHD thesis, Vienna University of Technology, 1997.

[18] Mróz Z., Piekarski J. *Sensitivity analysis and optimal design of non-linear structures.* International Journal of Numerical Methods in Engineering, 42, 1231-1262, 1998.

[19] Bochenek B., Krużelecki J. *A new concept of optimization for postbuckling behavior.* Engineering Optimization, 33(4), 503-522, 2001.

[20] Bochenek B. *Problem of structural optimization for post-buckling behavior.* Structural and Multidisciplinary Optimization, 25, 423-425, 2003.

[21] Mang H.A., Schranz C. Mackenzie-Helnwein P. C*onversion from imperfection-sensitive into imperfection-insensitive elastic structures I, theory.* Computer Methods in Applied Mechanics and Engineering, 195(13-16), 1422-1457, 2006**.**

[22] Schranz. C., Krenn B. Mang H.A. *Conversion from imperfection-sensitive into imperfection-insensitive elastic structures II, numerical investigation.* Computer Methods in Applied Mechanics and Engineering, 195(13-16), 1458-1479, 2006.

[23] Steinboeck A., Jia X., Hoefinger G., Mang H. A. *Conditions for symmetric, antisymmetric, and zero-stiffness bifurcation in view of imperfection sensitivity and insensitivity.* Computer Methods in Applied Mechanics and Engineering, 197(45-48), 3623-3636, 2008.

[24] Steinboeck A., Jia X., Hoefinger G., Rubin H., Mang H. A. *Remarkable postbuckling paths analyzed by means of the consistently linearized eigenproblem.* International Journal for Numerical Methods in Engineering, 76,156-182, 2008.

[25] Steinboeck A., Hoefinger G., Jia X., Mang H. A. *Three pending questions in structural stability.* Journal of the International Association for Shell and Spatial Structures, 50(1), 51-64, 2009.

[26] Mang H. A., Jia X., Hoefinger G. *Hilltop buckling as the Alpha and Omega in sensitivity analysis of the initial postbuckling behavior of elastic structures*. Journal of Civil Engineering and Management, International Research and Achievements. Vilnius: Technika, 15(1), 35-46, 2009.

[27] Höfinger G., Jia X., Mang H.A. *Is hilltop buckling imperfection sensitive or insensitive?* PAMM-Proceedings in Applied Mathematics and Mechanics, 9, 249–250, 2009.

[28] Jia X., Höfinger G., Mang H. A. *Imperfection sensitivity or insensitivity of zero-stiffness postbuckling ... that is the Question*. In Computational Structural Engineering: Proceedings of the International Symposium on Computational Structural Engineering, Shanghai, China, Springer, p.103-110, 2009.

[29] Mang H.A., Höfinger G., Jia X. *On the predictability of zero-stiffness postbuckling*. ZAMM-Zeitschrift für Angewandte Mathematik und Mechanik, 90(10-11); 837-846, 2010.

[30] Jia X., Höfinger G., Mang H. A. *Necessary and sufficient conditions for zero-stiffness postbuckling*. To appear in PAMM-Proceedings in Applied Mathematics and Mechanics, 2010.

[31] Jia X., Mang H.A. *Conversion of imperfection-sensitive elastic structures into imperfection-insensitive ones by adding tensile members*. In Proceedings of the International Association for Shell and Spatial Structures (IASS) Symposium 2010, Spatial Structures – Permanent and Temporary, November 8-12, 2010, Shanghai, China, accepted for publication in Journal of IASS.

[32] Mang H.A., Hoefinger G., Jia X. *Sensitivity analysis of the postbuckling behavior of elastic structures.* Computational Technology Reviews, 2, 1-22, 2010.

[33] Mang H.A., Hoefinger G. *Bifurcation buckling from a membrane stress state.* Submitted for publication, 2010.

Chapter II

Remarkable Postbuckling Paths Analyzed by Means of the Consistently Linearized Eigenproblem

Andreas Steinboeck [1], Xin Jia [1], Gerhard Hoefinger [1], Helmut Rubin [2], and Herbert A. Mang [1]

[1] *Institute for Mechanics of Materials and Structures, Vienna University of Technology, Karlsplatz 13/202, 1040 Vienna, Austria*
[2] *Institute for Structural Statics, Vienna University of Technology, Karlsplatz 13/211, 1040 Vienna, Austria*

Abstract

In addition to determination of load levels at critical points of stability problems, frequently the postbuckling behavior is of interest. For nonlinear problems, the so-called consistently linearized eigenvalue problem is a suitable tangent linearization method, which facilitates determination of stability limits. The solution process of the eigenproblem is significantly simplified by appropriate coordinate transformations. Within this process, characteristic shapes of eigenvalue curves allow identification of bifurcation buckling modes, snap-through modes, and hilltop buckling modes. Mathematical properties of the eigenvalue curves are addressed and conclusions regarding the shape of postbuckling paths are drawn. Considerations also touch upon the conversion from imperfection sensitivity into insensitivity. The theoretical findings are corroborated by examples dealing with a von Mises truss and a similar discrete system, showing a remarkable postbuckling behavior such as a zero-stiffness equilibrium path. For both systems, the same approach of stiffness increase allows conversion from imperfection sensitivity into insensitivity.

Keywords

bifurcation, consistently linearized eigenproblem, hilltop buckling, imperfection insensitivity, snap-through, *von Mises* truss.

1. Introduction

1.1. Motivation

Major tasks in the analysis of static, nonlinear stability problems are: (i) determination of the stability limit and (ii) assessment of the postbuckling behavior. A common method of determining stability limits in the context of the Finite Element Method (FEM) is to search along the nonlinear prebuckling path for points at which the tangent stiffness matrix $\mathbf{K}_T$ becomes singular. To this end, Gallagher and Yang [1] developed a secant linearization technique representing an extension of conventional linear stability analysis. Brendel [2] gave an overview of incremental secant methods and suggested a new approach which was applied to nonlinear structures by Brendel *et al.* [3].

For finite dimensional systems, Helnwein [4] introduced the so-called *consistently linearized eigenproblem* which associates the tracing of a nonlinear prebuckling path with an *accompanying eigenvalue problem*. In a series of studies ([4-6]]), this approach was used to estimate stability limits *ab initio*, i.e., without an incremental analysis. Mang *et al.* [7] extended the considerations to the postbuckling regime insofar as they investigated the possibility of converting an *imperfection-sensitive* into an *imperfection-insensitive* system by means of minor structural modifications, which is the second aforementioned task.

Originally, Koiter [8] proposed a mathematical scheme to analyze postbuckling paths in the vicinity of the bifurcation point representing the stability limit. In Koiter's approach, asymptotic series expansions play a pivotal role. Hence, the considerations focus on *initial* postbuckling behavior. Mang *et al.* [7] integrated Koiter's scheme and Helnwein's consistently linearized eigenproblem for the purpose of specifying diagnostics for the conversion from imperfection sensitivity into insensitivity. Several algorithms have been developed for *optimizing* the postbuckling behavior, e.g. [9-12]. However, it seems that there is still a lack of knowledge of *designing a structure for imperfection insensitivity* right from the outset.

1.2. Scope of this work

An objective of this work is to identify characteristic properties of eigenvalue curves which occur in the process of solving the consistently linearized eigenproblem. These properties may be beneficial for engineers intending to convert designs of imperfection-sensitive structures into imperfection-insensitive ones. For this purpose, theoretical considerations about characteristic shapes of eigenvalue curves will be carried out in Section 2, followed by a discussion of remarkable load-displacement paths and corresponding eigenvalue curves in Section 3, as may appear in simple static systems. An intuitive method of conversion from imperfection sensitivity into insensitivity [7] will be delineated and its effectiveness will be demonstrated. Section 3 will be concluded by an example showing how a system with infinitely many degrees of freedom can be approximated by a two-degrees-of-freedom model. Justification for using the approximation in practical analyses will be given by comparison of

the approximate and the exact solution. The simplified model allows an analysis of the structure by means of the consistently linearized eigenproblem.

In this work, static, conservative systems with N degrees of freedom will be considered. Restriction to finite values of N is no limitation insofar as this approach conforms to the FEM. Only perfect structures subjected to dead load will be investigated. The assumed material behavior is either linear elastic or rigid. The considerations include bifurcation from *nonlinear* prebuckling paths. In addition, *snap-through* and the special case of *hilltop buckling* [13] will be considered as possible modes of loss of stability.

1.3. Equilibrium conditions

$V(\mathbf{u}, \lambda): \mathbb{R}^N \times \mathbb{R} \rightarrow \mathbb{R}$ is the expression of the potential energy of a conservative system with N degrees of freedom. $\mathbf{u} \in \mathbb{R}^N$ is the vector of displacement coordinates and $\lambda \in \mathbb{R}$ is a load multiplier, which scales a constant reference load vector $\mathbf{P} \in \mathbb{R}^N$. Introduction of the so-called out-of-balance force

$$\mathbf{G} := V_{,\mathbf{u}} = \mathbf{F}^{\mathrm{I}}(\mathbf{u}) - \lambda \mathbf{P}, \tag{1}$$

allows to formulate the equilibrium conditions as $\mathbf{G} = \mathbf{0}$. The differential of this expression,

$$\mathbf{K}_T \cdot d\mathbf{u} - d\lambda \mathbf{P} = \mathbf{0}, \tag{2}$$

with the tangent-stiffness matrix

$$\mathbf{K}_T := V_{,\mathbf{uu}}(\mathbf{u}, \lambda), \tag{3}$$

permits the solution of nonlinear problems by the FEM.

1.4. Consistently linearized eigenproblem

In the context of the solution of such problems by the FEM, *Helnwein* [4] defined the consistently linearized eigenproblem as

$$\left(\tilde{\mathbf{K}}_T + (\lambda^* - \lambda) \tilde{\mathbf{K}}_{T,\lambda} \right) \cdot \mathbf{v}^* = \mathbf{0}. \tag{4}$$

Because of its well-natured mathematical behavior, it has proved valuable in computing points of the load displacement path where the tangent-stiffness matrix $\mathbf{K}_T$ experiences a rank deficiency. An upper tilde denotes quantities that are evaluated along the primary equilibrium path. In (4), $(\lambda^* - \lambda) \in \mathbb{R}$ is the eigenvalue corresponding to the eigenvector $\mathbf{v}^* \in \mathbb{R}^N$. λ^* and $\mathbf{v}^*$ are functions of λ. The eigenproblem (4) is a set of implicit equations defining N curves in the λ^*-λ-space. Hence, it has got N solutions $(\lambda_j^*, \mathbf{v}_j^*)$ $j \in \{1, 2, \ldots, N\}$, referred to as *eigenpairs*. The eigenvalue curves $\lambda_j^*(\lambda)$ allow identification of characteristic properties of the postbuckling behavior. $[\bullet]_{,\lambda}$ denotes the special rule of differentiation along the primary path, as defined by [7]. To distinguish it from the partial derivative, the latter will be written as $[\bullet]_{;\lambda}$.

Moreover, the equation

$$\lambda^* - \lambda = 0 \tag{5}$$

defines a straight line in this space. At points where both, (4) and (5) are satisfied, i.e., at points of intersection of two curves defined by (4) and (5), $\tilde{\mathbf{K}}_T$ is singular. The stability limit C is the first value

of λ where this happens when λ is either increased or decreased starting from $\lambda = 0$. Quantities evaluated at C are labeled by a subscript $_C$. Hence, the load level at the bifurcation point C is λ_C. Without loss of generality, only positive values of λ will be considered in the following, since the sign of $\mathbf{P}$ in (1) can be defined at will. Although snap-through points are not excluded from this analysis, it is generally assumed that the relevant mode of loss of stability is bifurcation buckling. A new vector $\mathbf{v}_1 \in \mathbb{R}^N$ defined by the equation

$$\tilde{\mathbf{K}}_{TC} \cdot \mathbf{v}_1 = \mathbf{0} \tag{6}$$

is introduced, i.e., $\mathbf{v}_1$ is a zero-eigenvector of $\tilde{\mathbf{K}}_{TC}$ and it describes the initial buckling shape. As suggested by Mang *et al.* [7], indices of the N eigenpairs $(\lambda_j^*, \mathbf{v}_j^*)$ are chosen such that $\mathbf{v}_{1C}^* = \mathbf{v}_1$. Therefore, $\lambda_{1C}^* = \lambda_C$. Because of this definition, $\lambda = \lambda_1^*$ is the bifurcation point.

2. Theory

2.1. Derivatives of the eigenvalue curve

The first and second derivative of (4) with respect to λ follow as:

$$\left(\lambda_{,\lambda}^* \tilde{\mathbf{K}}_{T,\lambda} + (\lambda^* - \lambda) \tilde{\mathbf{K}}_{T,\lambda\lambda} \right) \cdot \mathbf{v}^* + \left(\tilde{\mathbf{K}}_T + (\lambda^* - \lambda) \tilde{\mathbf{K}}_{T,\lambda} \right) \cdot \mathbf{v}_{,\lambda}^* = \mathbf{0}, \tag{7}$$

$$\left(\lambda_{,\lambda\lambda}^* \tilde{\mathbf{K}}_{T,\lambda} + (2\lambda_{,\lambda}^* - 1) \tilde{\mathbf{K}}_{T,\lambda\lambda} + (\lambda^* - \lambda) \tilde{\mathbf{K}}_{T,\lambda\lambda\lambda} \right) \cdot \mathbf{v}^*$$
$$+ 2 \left(\lambda_{,\lambda}^* \tilde{\mathbf{K}}_{T,\lambda} + (\lambda^* - \lambda) \tilde{\mathbf{K}}_{T,\lambda\lambda} \right) \cdot \mathbf{v}_{,\lambda}^* \tag{8}$$
$$+ \left(\tilde{\mathbf{K}}_T + (\lambda^* - \lambda) \tilde{\mathbf{K}}_{T,\lambda} \right) \cdot \mathbf{v}_{,\lambda\lambda}^* = \mathbf{0},$$

Premultiplying (7) by $\mathbf{v}^{*\mathrm{T}}$, taking $\tilde{\mathbf{K}}_T = \tilde{\mathbf{K}}_T^\mathrm{T}$ into account, and substitution of (4) yields

$$\mathbf{v}^{*\mathrm{T}} \cdot \left(\lambda_{,\lambda}^* \tilde{\mathbf{K}}_{T,\lambda} + (\lambda^* - \lambda) \tilde{\mathbf{K}}_{T,\lambda\lambda} \right) \cdot \mathbf{v}^* = \mathbf{0} \tag{9}$$

and, consequently,

$$\lambda_{,\lambda}^* = -(\lambda^* - \lambda) \frac{\mathbf{v}^{*\mathrm{T}} \cdot \tilde{\mathbf{K}}_{T,\lambda\lambda} \cdot \mathbf{v}^*}{\mathbf{v}^{*\mathrm{T}} \cdot \tilde{\mathbf{K}}_{T,\lambda} \cdot \mathbf{v}^*}. \tag{10}$$

Treating (8) in the same way gives

$$\lambda_{,\lambda\lambda}^* = -\mathbf{v}^{*\mathrm{T}} \cdot \frac{\left((2\lambda_{,\lambda}^* - 1) \tilde{\mathbf{K}}_{T,\lambda\lambda} + (\lambda^* - \lambda) \tilde{\mathbf{K}}_{T,\lambda\lambda\lambda} \right) \cdot \mathbf{v}^* + 2 \left(\lambda_{,\lambda}^* \tilde{\mathbf{K}}_{T,\lambda} + (\lambda^* - \lambda) \tilde{\mathbf{K}}_{T,\lambda\lambda} \right) \cdot \mathbf{v}_{,\lambda}^*}{\mathbf{v}^{*\mathrm{T}} \cdot \tilde{\mathbf{K}}_{T,\lambda} \cdot \mathbf{v}^*}. \tag{11}$$

2.2. Points of the eigenvalue curve with zero slope

Because of (10), the vanishing of $\lambda_{1,\lambda}^*$ requires

$$\underbrace{\left(\lambda_1^* - \lambda = 0 \quad \wedge \quad \left| \frac{\mathbf{v}_1^{*\mathrm{T}} \cdot \tilde{\mathbf{K}}_{T,\lambda\lambda} \cdot \mathbf{v}_1^*}{\mathbf{v}_1^{*\mathrm{T}} \cdot \tilde{\mathbf{K}}_{T,\lambda} \cdot \mathbf{v}_1^*} \right| < \infty \right)}_{\text{trivial case}}$$

$$\vee \tag{12}$$

$$\underbrace{\left(\mathbf{v}_1^{*\mathrm{T}} \cdot \tilde{\mathbf{K}}_{T,\lambda\lambda} \cdot \mathbf{v}_1^* = 0 \quad \wedge \quad \left| \frac{\lambda_1^* - \lambda}{\mathbf{v}_1^{*\mathrm{T}} \cdot \tilde{\mathbf{K}}_{T,\lambda} \cdot \mathbf{v}_1^*} \right| < \infty \right)}_{\text{nontrivial case}}.$$

In the nontrivial case, (11) degenerates to

$$\lambda_{1,\lambda\lambda}^*\Big|_{\lambda_{1,\lambda}^*=0} = -(\lambda_1^* - \lambda)\frac{\mathbf{v}_1^{*\mathrm{T}} \cdot \tilde{\mathbf{K}}_{T,\lambda\lambda} \cdot \mathbf{v}_1^* + 2\mathbf{v}_1^{*\mathrm{T}} \cdot \tilde{\mathbf{K}}_{T,\lambda} \cdot \mathbf{v}_{1,\lambda}^*}{\mathbf{v}_1^{*\mathrm{T}} \cdot \tilde{\mathbf{K}}_{T,\lambda} \cdot \mathbf{v}_1^*}. \tag{13}$$

Examples of horizontal tangents of eigenvalue curves will be given in Section 3 (cf. Figs. 2 and 6). The trivial case of (12) indicates loss of stability, since $\tilde{\mathbf{K}}_T$ becomes singular. This case always coincides with a horizontal tangent ($\lambda_{1,\lambda}^* = 0$), unless the second part of the trivial case of condition (12) is not satisfied.

2.3.   Derivation of the eigenvector $\mathbf{v}_1^*$

It follows from (4) that

$$\mathbf{v}_j^{*\mathrm{T}} \cdot \tilde{\mathbf{K}}_T \cdot \mathbf{v}_1^* = 0, \quad \mathbf{v}_j^{*\mathrm{T}} \cdot \tilde{\mathbf{K}}_{T,\lambda} \cdot \mathbf{v}_1^* = 0 \quad \forall j \in \{2,3,\dots,N\}. \tag{14}$$

Since the eigenvectors $\mathbf{v}_i^*$ $i \in \{1,2,\dots,N\}$ are a basis of $\mathbb{R}^N$, $\mathbf{v}_{1,\lambda}^*$ can be written as

$$\mathbf{v}_{1,\lambda}^* = \sum_{i=1}^N c_{1i}\,\mathbf{v}_i^*. \tag{15}$$

Inserting (15) into (7), premultiplying the obtained expression by $\mathbf{v}_j^{*\mathrm{T}}$, making use of (14) and substituting

$$\mathbf{v}_j^{*\mathrm{T}} \cdot \left(\tilde{\mathbf{K}}_T + (\lambda_j^* - \lambda)\tilde{\mathbf{K}}_{T,\lambda}\right) \cdot \mathbf{v}_j^* = \mathbf{0} \tag{16}$$

yields

$$c_{1j} = -\frac{\lambda_1^* - \lambda}{\lambda_1^* - \lambda_j^*}\frac{\mathbf{v}_j^{*\mathrm{T}} \cdot \tilde{\mathbf{K}}_{T,\lambda\lambda} \cdot \mathbf{v}_1^*}{\mathbf{v}_j^{*\mathrm{T}} \cdot \tilde{\mathbf{K}}_{T,\lambda} \cdot \mathbf{v}_j^*} \quad \forall j \in \{2,3,\dots,N\}. \tag{17}$$

c_{11} cannot be determined by applying this scheme. At first sight, c_{11} may take arbitrary values, which would also follow from the definition (4). However, the normalization condition

$$\left|\mathbf{v}_1^{*\mathrm{T}} \cdot \tilde{\mathbf{K}}_{T,\lambda} \cdot \mathbf{v}_1^*\right| = 1 \tag{18}$$

is used in order to define the length of $\mathbf{v}_1^*$ and, consequently, the value of c_{11}. Thus, $\mathbf{v}_1^{*\mathrm{T}} \cdot \tilde{\mathbf{K}}_{T,\lambda} \cdot \mathbf{v}_1^*$ is piecewise continuous and piecewise continuously differentiable. Excluding points where $\mathbf{v}_1^{*\mathrm{T}} \cdot \tilde{\mathbf{K}}_{T,\lambda} \cdot \mathbf{v}_1^*$ changes its sign, the derivation of (18) with respect to λ gives

$$2\mathbf{v}_1^{*\mathrm{T}} \cdot \tilde{\mathbf{K}}_{T,\lambda} \cdot \mathbf{v}_{1,\lambda}^* + \mathbf{v}_1^{*\mathrm{T}} \cdot \tilde{\mathbf{K}}_{T,\lambda\lambda} \cdot \mathbf{v}_1^* = 0. \tag{19}$$

Substitution of (15) into (19) and consideration of (10) and (14) yields

$$c_{11} = -\frac{1}{2}\frac{\mathbf{v}_1^{*\mathrm{T}} \cdot \tilde{\mathbf{K}}_{T,\lambda\lambda} \cdot \mathbf{v}_1^*}{\mathbf{v}_1^{*\mathrm{T}} \cdot \tilde{\mathbf{K}}_{T,\lambda} \cdot \mathbf{v}_1^*} = \frac{\lambda_{1,\lambda}^*}{2(\lambda_1^* - \lambda)}. \tag{20}$$

As expected, this expression becomes infinite at the excluded points.

In case of linear prebuckling behavior, $\tilde{\mathbf{K}}_{T,\lambda}$ is constant and $\tilde{\mathbf{K}}_{T,\lambda\lambda} = \mathbf{0}$. Consequently, (4) yields a constant solution $\lambda^*(\lambda)$ and $c_{1i} = 0 \ \forall i \in \{1,2,\dots,N\}$. This is the rationale for sometimes referring to c_{11} as *nonlinearity coefficient*. However, $c_{11} = 0$ is only a necessary condition for linear prebuckling behavior [7].

2.4. Structure of the tangent stiffness matrix

It is assumed that $\mathbf{K}_T^{FE}$ is the tangent stiffness matrix defined for an arbitrary coordinate system with

displacement coordinates $\mathbf{q}$. For instance, $\mathbf{K}_T^{FE}$ may be thought of as the tangent stiffness matrix

generated by the finite element method. Since $\mathbf{K}_T^{FE}$ is symmetric, it is always possible to diagonalize it

through transformation of coordinates. New displacement coordinates $\mathbf{u}$ are introduced such that

$$d\mathbf{q} := \mathbf{T} \cdot d\mathbf{u}, \tag{21}$$

where $\mathbf{T} : \mathbb{R}^N \to \mathbb{R}^N$ is generally a variable linear mapping, sometimes denoted as *Jacobian matrix*.

Hence,

$$\frac{\partial}{\partial \mathbf{u}} = \frac{\partial}{\partial \mathbf{q}} \cdot \mathbf{T}. \tag{22}$$

The columns of

$$\mathbf{T} := \begin{bmatrix} \mathbf{t}_1 & \mathbf{t}_2 & \cdots & \mathbf{t}_N \end{bmatrix} \tag{23}$$

can be defined by the eigenproblem

$$\mathbf{K}_T^{FE} \cdot \mathbf{t}_i = \mathbf{t}_i \tau_i \quad \forall\, i \in \{1, 2, \dots, N\}. \tag{24}$$

The eigenvectors $\mathbf{t}_i$ are orthogonal with respect to each other, since $\mathbf{K}_T^{FE} = \mathbf{K}_T^{FE\mathrm{T}}$. In addition, it is

stipulated that they are normalized to unit length, i.e.,

$$\mathbf{t}_i \cdot \mathbf{t}_j := \begin{cases} 1 & i = j \\ 0 & i \neq j \end{cases}. \tag{25}$$

Left-hand multiplication of

$$\mathbf{K}_T^{FE} \cdot \mathbf{T} = \mathbf{T} \cdot \mathrm{diag}\{\tau_1, \tau_2, \dots, \tau_N\} \tag{26}$$

by $\mathbf{T}^{\mathrm{T}}$ and consideration of $\mathbf{T}^{\mathrm{T}} \cdot \mathbf{T} = \mathbf{I}$ as well as of (3) and (22) yields the diagonal matrix

$$\mathrm{diag}\{\tau_1, \tau_2, \dots, \tau_N\} = \mathbf{T}^{\mathrm{T}} \cdot \mathbf{K}_T^{FE} \cdot \mathbf{T} = \mathbf{T}^{\mathrm{T}} \cdot \frac{\partial^2 V}{\partial \mathbf{q}^{\mathrm{T}} \partial \mathbf{q}} \cdot \mathbf{T} = \frac{\partial^2 V}{\partial \mathbf{u}^{\mathrm{T}} \partial \mathbf{u}} = \mathbf{K}_T. \tag{27}$$

Hence, without loss of generality, it can be assumed that the tangent stiffness matrix and also its

derivatives with respect to λ evaluated along the primary path have the following structure

$$\tilde{\mathbf{K}}_{T,\lambda^n} = \left[V_{,u_i u_j, \lambda^n}(\tilde{\mathbf{u}}, \tilde{\lambda}) \right] = \begin{bmatrix} & & & \vdots & 0 \\ & \tilde{\mathbf{K}}_{T,\lambda^n}^{\text{upper left}} & & \vdots & \vdots \\ & & & \vdots & 0 \\ \hline 0 & \cdots & 0 & \vdots & V_{,u_N u_N, \lambda^n} \end{bmatrix}, \tag{28}$$

where the buckling coordinate is u_N. By permutation of coordinates it is always possible to ensure that

$V_{,u_N u_N}$ is the first vanishing eigenvalue of $\tilde{\mathbf{K}}_T$ as λ is increased. The upper-left submatrix may be

diagonal.

It is emphasized that solving (24) and computing (27) can be numerically cumbersome if the number

of degrees of freedom is large. However, in this Subsection it was shown that, in principle, it is always

possible to obtain a diagonal structure of $\tilde{\mathbf{K}}_{T,\lambda^n}$. As will be seen in the following Subsections, this

diagonal structure facilitates many theoretical considerations.

2.5. Orthogonality of eigenvectors with respect to $\tilde{\mathbf{K}}_{T,\lambda^n}$

Orthogonality of the eigenvectors $\mathbf{v}_1^*$ and $\mathbf{v}_j^*$ ($j \in \{2,3,\ldots,N\}$) with respect to $\tilde{\mathbf{K}}_{T,\lambda^n}$ leads to simplifications of the analysis of eigenvalue curves. In particular, it facilitates the computation of higher derivatives of λ^* with respect to λ. It will be shown in this Subsection that, if the assumptions stipulated in the previous Subsection hold and the suggested coordinate transformations are applied, orthogonality is a consequence of (28).

Specialization of the lower right component of $\tilde{\mathbf{K}}_{T,\lambda^n}$ from (28) for $n=0$ and the stability limit C yields

$$V_{,u_N u_N C} = 0, \tag{29}$$

which reflects the vanishing of an eigenvalue of $\tilde{\mathbf{K}}_T$ at C.

$$\mathbf{v}_1^* = \begin{bmatrix} 0 & \cdots & 0 & p \end{bmatrix}^T \quad p \in \mathbb{R} \quad \wedge \quad \lambda_1^* = \lambda - \frac{V_{,u_N u_N}}{V_{,u_N u_N,\lambda}} \tag{30}$$

is a solution of the consistently linearized eigenproblem (4) specialized by means of (28). At C, $\mathbf{v}_{1C}^* = \mathbf{v}_1$ and $\lambda_{1C}^* = \lambda = \lambda_C$ hold. Because of (14) and the specialization of (28) for $n=0$ or $n=1$,

$$\mathbf{v}_j^* = \begin{bmatrix} v_{j1}^* & v_{j2}^* & \cdots & v_{jN-1}^* & 0 \end{bmatrix}^T \qquad \forall\, j \in \{2,3,\ldots,N\}. \tag{31}$$

Consequently,

$$\mathbf{v}_j^{*T} \cdot \tilde{\mathbf{K}}_{T,\lambda^n} \cdot \mathbf{v}_1^* = 0 \qquad \forall\,(j,n) \in \{2,3,\ldots,N\} \times \mathbb{N}. \tag{32}$$

The implications of this remarkable orthogonality will be analyzed in the following Subsections.

2.6. Derivatives of the eigenvalue curve

Specialization of (10) for the first eigenpair reads as

$$\lambda_{1,\lambda}^* = -(\lambda_1^* - \lambda) \frac{\mathbf{v}_1^{*T} \cdot \tilde{\mathbf{K}}_{T,\lambda\lambda} \cdot \mathbf{v}_1^*}{\mathbf{v}_1^{*T} \cdot \tilde{\mathbf{K}}_{T,\lambda} \cdot \mathbf{v}_1^*}. \tag{33}$$

For the first derivative of the eigenvector $\mathbf{v}_{1,\lambda}^*$, it follows from (32), that $c_{1j} = 0 \;\forall\, j \in \{2,3,\ldots,N\}$ and

$$\mathbf{v}_{1,\lambda}^* = c_{11} \mathbf{v}_1^* = \frac{\lambda_{1,\lambda}^*}{2(\lambda_1^* - \lambda)} \mathbf{v}_1^*, \tag{34}$$

where (17) and (20) were used. That is, the direction of $\mathbf{v}_1^*$ is constant. Substitution of (34) into the specialization of (11) for the first eigenpair and consideration of (33) results in

$$\lambda_{1,\lambda\lambda}^* = \frac{\lambda_{1,\lambda}^* (2\lambda_{1,\lambda}^* - 1)}{(\lambda_1^* - \lambda)} - (\lambda_1^* - \lambda) \frac{\mathbf{v}_1^{*T} \cdot \tilde{\mathbf{K}}_{T,\lambda\lambda\lambda} \cdot \mathbf{v}_1^*}{\mathbf{v}_1^{*T} \cdot \tilde{\mathbf{K}}_{T,\lambda} \cdot \mathbf{v}_1^*}. \tag{35}$$

Derivation of (34) with respect to λ yields

$$\mathbf{v}_{1,\lambda\lambda}^* = \frac{1}{2(\lambda_1^* - \lambda)} \left(\lambda_{1,\lambda\lambda}^* - \frac{\lambda_{1,\lambda}^* (\lambda_{1,\lambda}^* - 2)}{2(\lambda_1^* - \lambda)} \right) \mathbf{v}_1^*. \tag{36}$$

Generally, after further derivations

$$\mathbf{v}_{1,\lambda^n}^* \propto \mathbf{v}_1^* \quad \forall\, n \in \mathbb{N}. \tag{37}$$

In order to analyze characteristic properties of the eigenvalue curve, (35) is specialized for points which have a nontrivial horizontal tangent, i.e., $\lambda_{1,\lambda}^* = 0$ and $\lambda_1^* \neq \lambda$. In this case

$$\lambda_{1,\lambda\lambda}^* \Big|_{\lambda_{1,\lambda}^* = 0} = -(\lambda_1^* - \lambda) \frac{\mathbf{v}_1^{*T} \cdot \tilde{\mathbf{K}}_{T,\lambda\lambda} \cdot \mathbf{v}_1^*}{\mathbf{v}_1^{*T} \cdot \tilde{\mathbf{K}}_{T,\lambda} \cdot \mathbf{v}_1^*}. \tag{38}$$

2.7. The limit case $\lambda \to \lambda_1^*$ for bifurcation points

At bifurcation points, the fraction in (33) will generally remain finite. It becomes infinite, however, at snap-through points and, in particular, for the special case of hilltop buckling [13], where a bifurcation point coincides with a snap-through point. A discussion of snap-through phenomena and hilltop buckling is postponed to Subsection 2.8. Hence, at C,

$$\lim_{\lambda \to \lambda_1^*} \lambda_{1,\lambda}^* = 0 \tag{39}$$

holds. Assuming that

$$\left| \frac{\mathbf{v}_{1C}^{*T} \cdot \tilde{\mathbf{K}}_{T,\lambda\lambda C} \cdot \mathbf{v}_{1C}^*}{\mathbf{v}_{1C}^{*T} \cdot \tilde{\mathbf{K}}_{T,\lambda C} \cdot \mathbf{v}_{1C}^*} \right| < \infty, \tag{40}$$

insertion of (33) into (35) and computation of the limit yields

$$\lim_{\lambda \to \lambda_1^*} \lambda_{1,\lambda\lambda}^* = \frac{\mathbf{v}_{1C}^{*T} \cdot \tilde{\mathbf{K}}_{T,\lambda C} \cdot \mathbf{v}_{1C}^*}{\mathbf{v}_{1C}^{*T} \cdot \tilde{\mathbf{K}}_{T,\lambda C} \cdot \mathbf{v}_{1C}^*} = -2c_{11C}. \tag{41}$$

However, the situation is different if a point with a horizontal tangent ($\lambda_{1,\lambda}^* = 0$) approaches the stability limit $\lambda = \lambda_1^*$. In this case,

$$\lim_{\lambda \to \lambda_1^*} \left(\lambda_{1,\lambda\lambda}^* \Big|_{\lambda_{1,\lambda}^* = 0} \right) = 0 \tag{42}$$

follows from (38), provided that (40) is satisfied. (42) requires that the point with the horizontal tangent ($\lambda_{1,\lambda}^* = 0$) "moves" in the λ-λ_1^*- space. This is tied to parameter changes of the structure.

2.8. The limit case $\lambda \to \lambda_1^*$ for snap-through points

In the following, snap-through instability will be indentified from the $\lambda_j^*(\lambda)$ curves. For this purpose, the first and the second derivative of these curves at the snap-through point D will be computed. However, compared to Subsection 2.7, a different approach is required.

The considerations are applicable to any eigenpair $(\lambda_j^*, \mathbf{v}_j^*)$ $j \in \{1, 2, \ldots, N\}$. At D, the equilibrium path has a local extremum in terms of the load multiplier λ, i.e., $d\lambda = 0$. Hence, derivatives $d/d\lambda$ will generally produce infinite or indeterminate results, and λ is not a good choice for parameterizing the equilibrium path in the vicinity of D. To circumvent this problem, the new path parameter $\xi \in \mathbb{R}$ is introduced, which by definition vanishes at D. It follows that, if D is a local maximum,

$$\lambda_{,\xi D} = 0, \quad \lambda_{,\xi\xi D} < 0. \tag{43}$$

The derivative of $\tilde{\mathbf{K}}_T$ with respect to λ can be rewritten as

$$\tilde{\mathbf{K}}_{T,\lambda} = \frac{\tilde{\mathbf{K}}_{T,\xi}}{\lambda_{,\xi}}. \tag{44}$$

Substitution of (44) into the specialization of (4) for the j-th eigenpair and left-hand multiplication by $\lambda_{,\xi}\, \mathbf{v}_j^{*\mathrm{T}}$ yields the scalar equation

$$\mathbf{v}_j^{*\mathrm{T}} \cdot \left(\lambda_{,\xi}\, \tilde{\mathbf{K}}_T + (\lambda_j^* - \lambda)\, \tilde{\mathbf{K}}_{T,\xi} \right) \cdot \mathbf{v}_j^* = 0. \tag{45}$$

Insertion of the series expansions

$$\lambda_j^* - \lambda = \lambda_{j,\xi D}^*\, \xi + (\lambda_{j,\xi\xi D}^* - \lambda_{,\xi\xi D})\xi^2/2 + \mathcal{O}(\xi^3),$$
$$\mathbf{v}_j^* = \mathbf{v}_{jD}^* + \mathbf{v}_{j,\xi D}^*\, \xi + \mathbf{v}_{j,\xi\xi D}^*\, \xi^2/2 + \mathcal{O}(\xi^3),$$
$$\tilde{\mathbf{K}}_T = \tilde{\mathbf{K}}_{TD} + \tilde{\mathbf{K}}_{T,\xi D}\, \xi + \tilde{\mathbf{K}}_{T,\xi\xi D}\, \xi^2/2 + \mathcal{O}(\xi^3), \tag{46}$$
$$\tilde{\mathbf{K}}_{T,\xi} = \tilde{\mathbf{K}}_{T,\xi D} + \tilde{\mathbf{K}}_{T,\xi\xi D}\, \xi + \tilde{\mathbf{K}}_{T,\xi\xi\xi D}\, \xi^2/2 + \mathcal{O}(\xi^3)$$

into (45) and consideration of coefficients up to order ξ^2 yields

$$\lambda_{,\xi}\, \mathbf{v}_{jD}^{*\mathrm{T}} \cdot \tilde{\mathbf{K}}_{TD} \cdot \mathbf{v}_{jD}^* + \left(2\,\lambda_{,\xi}\, \mathbf{v}_{j,\xi D}^{*\mathrm{T}} \cdot \tilde{\mathbf{K}}_{TD} \cdot \mathbf{v}_{jD}^* + (\lambda_{,\xi} + \lambda_{j,\xi D}^*)\, \mathbf{v}_{jD}^{*\mathrm{T}} \cdot \tilde{\mathbf{K}}_{T,\xi D} \cdot \mathbf{v}_{jD}^* \right)\xi$$
$$+ \left(\lambda_{,\xi}\, \mathbf{v}_{j,\xi\xi D}^{*\mathrm{T}} \cdot \tilde{\mathbf{K}}_{TD} \cdot \mathbf{v}_{jD}^* + \lambda_{,\xi}\, \mathbf{v}_{j,\xi D}^{*\mathrm{T}} \cdot \tilde{\mathbf{K}}_{TD} \cdot \mathbf{v}_{j,\xi D}^* + 2(\lambda_{,\xi} + \lambda_{j,\xi D}^*)\, \mathbf{v}_{j,\xi D}^{*\mathrm{T}} \cdot \tilde{\mathbf{K}}_{T,\xi D} \cdot \mathbf{v}_{jD}^* \right.$$
$$\left. + (\lambda_{j,\xi\xi D}^* - \lambda_{,\xi\xi D})/2\, \mathbf{v}_{jD}^{*\mathrm{T}} \cdot \tilde{\mathbf{K}}_{T,\xi D} \cdot \mathbf{v}_{jD}^* + (\lambda_{,\xi}/2 + \lambda_{j,\xi D}^*)\, \mathbf{v}_{jD}^{*\mathrm{T}} \cdot \tilde{\mathbf{K}}_{T,\xi\xi D} \cdot \mathbf{v}_{jD}^* \right)\xi^2 + \mathcal{O}(\xi^3) = 0. \tag{47}$$

It follows from (43) that $\lambda_{,\xi} = \mathcal{O}(\xi)$. On the premise that $\xi \ll 1$, terms in (47) up to order ξ can be reshaped as

$$\frac{\lambda_{j,\xi D}^*}{\lambda_{,\xi}} = -\xi^{-1}\, \frac{\mathbf{v}_{jD}^{*\mathrm{T}} \cdot \tilde{\mathbf{K}}_{TD} \cdot \mathbf{v}_{jD}^*}{\mathbf{v}_{jD}^{*\mathrm{T}} \cdot \tilde{\mathbf{K}}_{T,\xi D} \cdot \mathbf{v}_{jD}^*} - 1 - 2\, \frac{\mathbf{v}_{j,\xi D}^{*\mathrm{T}} \cdot \tilde{\mathbf{K}}_{TD} \cdot \mathbf{v}_{jD}^*}{\mathbf{v}_{jD}^{*\mathrm{T}} \cdot \tilde{\mathbf{K}}_{T,\xi D} \cdot \mathbf{v}_{jD}^*} + \mathcal{O}(\xi). \tag{48}$$

The limit of (48) for $\xi \to 0$, i.e., $\lambda_{j,\xi D}^* / \lambda_{\xi D}$ is the desired first derivative $\lambda_{j,\lambda D}^*$. At first, (48) is specialized for the case of a snap-through mode $\mathbf{v}_{jD}^*$, which means that $\tilde{\mathbf{K}}_{TD} \cdot \mathbf{v}_{jD}^* = \mathbf{0}$. Then, computation of the limit $\xi \to 0$ of (48) results in

$$\lambda_{j,\lambda D}^* = -1. \tag{49}$$

As a second possibility, (48) is specialized for the case that $\mathbf{v}_{jD}^*$ does not represent the snap-through mode. If hilltop buckling [13] is excluded, $\tilde{\mathbf{K}}_{TD} \cdot \mathbf{v}_{jD}^* \neq \mathbf{0}$ and hence,

$$\lambda_{j,\lambda D}^* = \pm\infty. \tag{50}$$

The sign depends on the sign of ξ as the limit $\xi \to 0$ is calculated, but has no practical relevance.

For determination of $\lambda_{j,\lambda\lambda D}^*$, $\lambda_{j,\lambda\lambda}^*$ is written in terms of the path parameter ξ

$$\lambda_{j,\lambda\lambda}^* = \left(\frac{\lambda_{j,\xi}^*}{\lambda_{,\xi}} \right)_{,\lambda} = \frac{1}{\lambda_{,\xi}} \left(\frac{\lambda_{j,\xi\xi}^*}{\lambda_{,\xi}} - \frac{\lambda_{j,\xi}^*}{\lambda_{,\xi}} \frac{\lambda_{,\xi\xi}}{\lambda_{,\xi}} \right). \tag{51}$$

Insertion of the Taylor series expansions

$$\lambda_{j,\xi}^* = \lambda_{j,\xi D}^* + \lambda_{j,\xi\xi D}^*\, \xi + \mathcal{O}(\xi^2), \qquad \lambda_{j,\xi\xi}^* = \lambda_{j,\xi\xi D}^* + \lambda_{j,\xi\xi\xi D}^*\, \xi + \mathcal{O}(\xi^2) \tag{52}$$

and truncation after the constant term gives

$$\lambda_{j,\lambda\lambda}^* = \frac{1}{\lambda_{,\xi}} \left(\frac{\lambda_{j,\xi\xi D}^*}{\lambda_{,\xi}} - \frac{\lambda_{j,\xi D}^*}{\lambda_{,\xi}} \frac{\lambda_{,\xi\xi}}{\lambda_{,\xi}} \right) + \mathcal{O}(\xi). \tag{53}$$

(47) is reshaped to get

$$\frac{\lambda^*_{j,\xi\xi D}}{\lambda_{,\xi}} =$$

$$-\frac{2}{\mathbf{v}^{*T}_{jD} \cdot \tilde{\mathbf{K}}_{T,\xi D} \cdot \mathbf{v}^*_{jD}} \Big(\mathbf{v}^{*T}_{jD} \cdot \tilde{\mathbf{K}}_{TD} \cdot \mathbf{v}^*_{jD} \, \xi^{-2}$$

$$+ \Big(2\,\mathbf{v}^{*T}_{j,\xi D} \cdot \tilde{\mathbf{K}}_{TD} \cdot \mathbf{v}^*_{jD} + (1 + \lambda^*_{j,\xi D} / \lambda_{,\xi}) \, \mathbf{v}^{*T}_{jD} \cdot \tilde{\mathbf{K}}_{T,\xi D} \cdot \mathbf{v}^*_{jD} \Big) \xi^{-1} \qquad (54)$$

$$+ \Big(\mathbf{v}^{*T}_{j,\xi D} \cdot \tilde{\mathbf{K}}_{TD} \cdot \mathbf{v}^*_{j,\xi D} + \mathbf{v}^{*T}_{j,\xi\xi D} \cdot \tilde{\mathbf{K}}_{TD} \cdot \mathbf{v}^*_{jD} + 2(1 + \lambda^*_{j,\xi D} / \lambda_{,\xi}) \, \mathbf{v}^{*T}_{j,\xi D} \cdot \tilde{\mathbf{K}}_{T,\xi D} \cdot \mathbf{v}^*_{jD}$$

$$+ (1/2 + \lambda^*_{j,\xi D} / \lambda_{,\xi}) \, \mathbf{v}^{*T}_{jD} \cdot \tilde{\mathbf{K}}_{T,\xi\xi D} \cdot \mathbf{v}^*_{jD} \Big) \xi^0 \Big) + \frac{\lambda_{,\xi\xi D}}{\lambda_{,\xi}} \xi^0 + \mathcal{O}(\xi).$$

Finally, insertion of (48) and (54) into (53) and truncation after terms of order ξ^{-1} yield

$$\lambda^*_{j,\lambda\lambda} = \frac{1}{\lambda_{,\xi}} \Bigg(-\frac{2}{\mathbf{v}^{*T}_{jD} \cdot \tilde{\mathbf{K}}_{T,\xi D} \cdot \mathbf{v}^*_{jD}} \Big(\mathbf{v}^{*T}_{jD} \cdot \tilde{\mathbf{K}}_{TD} \cdot \mathbf{v}^*_{jD} \, \xi^{-2}$$

$$+ \Big(2\,\mathbf{v}^{*T}_{j,\xi D} \cdot \tilde{\mathbf{K}}_{TD} \cdot \mathbf{v}^*_{jD} + (1 + \lambda^*_{j,\xi D} / \lambda_{,\xi}) \, \mathbf{v}^{*T}_{jD} \cdot \tilde{\mathbf{K}}_{T,\xi D} \cdot \mathbf{v}^*_{jD} \Big) \xi^{-1} \Big) \qquad (55)$$

$$+ \frac{\mathbf{v}^{*T}_{jD} \cdot \tilde{\mathbf{K}}_{TD} \cdot \mathbf{v}^*_{jD}}{\mathbf{v}^{*T}_{jD} \cdot \tilde{\mathbf{K}}_{T,\xi D} \cdot \mathbf{v}^*_{jD}} \frac{\lambda_{,\xi\xi}}{\lambda_{,\xi}} \xi^{-1} + \mathcal{O}(\xi^0) \Bigg).$$

Hence,

$$\lambda^*_{j,\lambda\lambda D} = \pm\infty \quad \forall j \in \{1, 2, \ldots, N\}, \qquad (56)$$

irrespectively of the value of $\tilde{\mathbf{K}}_{TD} \cdot \mathbf{v}^*_{jD}$. The sign of $\lambda^*_{j,\lambda\lambda D}$ depends on the sign of $\lambda_{,\xi}$ as the limit $\xi \to 0$ is computed, but has no practical relevance.

For the special case of hilltop buckling [13],

$$\lambda^*_{j,\lambda D} = -1, \quad \lambda^*_{j,\lambda\lambda D} = \pm\infty, \qquad (57)$$

hold for both, the buckling mode and the snap-through mode, since $C = D$ and $\tilde{\mathbf{K}}_{TC} \cdot \mathbf{v}^*_{jC} = \tilde{\mathbf{K}}_{TD} \cdot \mathbf{v}^*_{jD} = \mathbf{0}$. For $j = 1$, $\mathbf{v}^*_{jC} = \mathbf{v}^*_{jD} = \mathbf{0}$ holds as a consequence of (18) and (44).

2.9.   The limit case $\lambda_1 \to \lambda^*_1$ for saddle points

In analogy to the previous Subsection, a path parameter $\xi \in \mathbb{R}$ is introduced, which vanishes by definition at the saddle point D. It follows that

$$\lambda_{,\xi D} = 0, \quad \lambda_{,\xi\xi D} = 0, \quad \lambda_{,\xi\xi\xi D} \neq 0. \qquad (58)$$

Without loss of generality, it is assumed that $\xi = u_j$ $(j \neq 1)$ is the only coordinate which changes its value at D. This deflection mode will be referred to as *saddle mode*. The assumed situation can be established by the coordinate transformation introduced in Subsection 2.4; throughout this Subsection, it is assumed that $\tilde{\mathbf{K}}_T$ has a diagonal structure. Thus, $\mathbf{u}_{,\xi}$ is the j-th unit vector and

$$\mathbf{u}_{,\xi\xi} = \mathbf{0}. \qquad (59)$$

Dividing (2) by $d\xi$, specializing the result for D, and insertion of (58) yields

$$\tilde{\mathbf{K}}_{TD} \cdot \mathbf{u}_{,\xi D} = \mathbf{0}. \qquad (60)$$

Hence, $\tilde{\mathbf{K}}_{TD}$ is singular and following from the specialization of (4) for D

$$p\,\mathbf{v}^*_{jD} = \mathbf{u}_{,\xi D}, \quad p \in \mathbb{R} \backslash \{0\}, \qquad (61)$$

where $\mathbf{v}_{jD}^*$ describes the saddle mode. Division of (2) by $d\xi$ derivation of the result with respect to ξ, insertion of (59), specialization for D, and insertion of (58) yields

$$\tilde{\mathbf{K}}_{T,\xi D} \cdot \mathbf{u}_{,\xi D} = \mathbf{0}. \tag{62}$$

Insertion of (61) results in

$$\tilde{\mathbf{K}}_{T,\xi D} \cdot \mathbf{v}_{jD}^* = \mathbf{0}. \tag{63}$$

It is emphasized that (63) is based on $\lambda_{,\xi\xi D} = 0$, i.e., it generally does not hold for snap-through points.

Since $\tilde{\mathbf{K}}_T$ is a diagonal matrix, the relation

$$\mathbf{v}_{j,\xi^n}^* \propto \mathbf{v}_j^* \quad \forall n \in \mathbb{N} \tag{64}$$

can be deduced in analogy to (37) referring to the first eigenvector $\mathbf{v}_1^*$. Insertion of $\tilde{\mathbf{K}}_{TD} \cdot \mathbf{v}_{jD}^* = \mathbf{0}$, (63), and the specialization of (64) for D into (47) and solving the result for $\lambda_{j,\xi D}^*/\lambda_{,\xi}$ yields

$$\frac{\lambda_{j,\xi D}^*}{\lambda_{,\xi}} = -\frac{1}{2} + \mathcal{O}(\xi). \tag{65}$$

Finally, computation of the limit $\xi \to 0$ of (65) gives

$$\lambda_{j,\lambda D}^* = \frac{\lambda_{j,\xi D}^*}{\lambda_{,\xi D}} = -\frac{1}{2}. \tag{66}$$

Similar to the deduction of (55) and (56), it can be shown that in this case

$$|\lambda_{j,\lambda\lambda D}^*| < \infty. \tag{67}$$

Hence, $\lambda_j^*(\lambda)$, corresponding to the saddle mode, is a smooth curve. However, for the remaining eigenvalues $\lambda_i^*(\lambda)$ $(i \neq j)$, (50) and (56) still hold, implying that their tangent is vertical.

2.10. Disintegration of (7) and (8)

Because of (4) and (34), the specialization of (7) for the first eigenpair disintegrates into

$$\left(\lambda_{1,\lambda}^* \tilde{\mathbf{K}}_{T,\lambda} + (\lambda_1^* - \lambda)\tilde{\mathbf{K}}_{T,\lambda\lambda}\right) \cdot \mathbf{v}_1^* = \mathbf{0}, \qquad \left(\tilde{\mathbf{K}}_T + (\lambda_1^* - \lambda)\tilde{\mathbf{K}}_{T,\lambda}\right) \cdot c_{11}\,\mathbf{v}_1^* = \mathbf{0}. \tag{68}$$

It follows from (68) that

$$\lambda_{1,\lambda}^* = 0 \quad \wedge \quad \lambda_1^* - \lambda \neq 0 \quad \Rightarrow \quad \tilde{\mathbf{K}}_{T,\lambda\lambda} \cdot \mathbf{v}_1^* = \mathbf{0}, \tag{69}$$

which describes the nontrivial case of (12). Substitution of (37) into the specialization of (8) for the first eigenpair and consideration of (4) and (68) show that (8) disintegrates into

$$\left(\lambda_{1,\lambda\lambda}^* \tilde{\mathbf{K}}_{T,\lambda} + (2\lambda_{1,\lambda}^* - 1)\tilde{\mathbf{K}}_{T,\lambda\lambda} + (\lambda_1^* - \lambda)\tilde{\mathbf{K}}_{T,\lambda\lambda\lambda}\right) \cdot \mathbf{v}_1^* = \mathbf{0}, \qquad \left(\lambda_{1,\lambda}^* \tilde{\mathbf{K}}_{T,\lambda} + (\lambda_1^* - \lambda)\tilde{\mathbf{K}}_{T,\lambda\lambda}\right) \cdot c_{11}\,\mathbf{v}_1^* = \mathbf{0},$$
$$\left(\tilde{\mathbf{K}}_T + (\lambda_1^* - \lambda)\tilde{\mathbf{K}}_{T,\lambda}\right) \cdot p\,\mathbf{v}_1^* = \mathbf{0} \quad p \in \mathbb{R}. \tag{70}$$

Proceeding in this manner, it can be shown that higher derivatives of the eigenproblem (4) also disintegrate as a consequence of (37). It is possible to compute derivatives λ_{1,λ^n}^* from these equations. E.g., (68) and (70) give (33) and (35), respectively.

It is once more emphasized that the Subsections 2.5 through 2.7 as well as 2.10 essentially use the structure of $\tilde{\mathbf{K}}_{T,\lambda^n}$ given in (28). In Subsection 2.9, it is even assumed that $\tilde{\mathbf{K}}_{T,\lambda^n}$ is diagonal. These

are no limitations, since the postulated structure of $\tilde{\mathbf{K}}_{T,\lambda^n}$ can be established by means of a coordinate transformation.

2.11. Imperfection sensitivity versus imperfection insensitivity

A system is imperfection sensitive if it is not guaranteed that the ultimate load of the imperfect system exceeds the theoretical limit load λ_C of the perfect system. In order to analyze this for a specific structure by means of the FEM, it has proved useful to expand the load multiplier $\lambda(\eta)$ into an asymptotic series with respect to $\eta \in \mathbb{R}$. η is a scalar which parameterizes the postbuckling path, and by definition $\eta_C = 0$. Hence,

$$\lambda(\eta) = \lambda_C + \lambda_1 \eta + \lambda_2 \eta^2 + \lambda_3 \eta^3 + \mathcal{O}(\eta^4). \tag{71}$$

The coefficients $\lambda_i \in \mathbb{R}$ can be computed from FEM results (cf. [4, 5, 7, 14]]). Sometimes, the buckling coordinate is chosen as the path parameter η. With the help of

$$m_{\min} := \min\{m \mid m \in \mathbb{N}\backslash\{0\} \wedge \lambda_m \neq 0\}, \tag{72}$$

a necessary and sufficient condition for imperfection insensitivity [14], in a mathematical sense, is obtained as

$$m_{\min} \text{ is even } \wedge \ \lambda_{m_{\min}} > 0. \tag{73}$$

If this condition is not satisfied, the system is imperfection sensitive.

2.12. Discussion of theoretical results

At first, the following considerations focus on the point $(\lambda_C, \lambda_1^*(\lambda_C))$ at which the curve $\lambda_1^*(\lambda)$ intersects the straight line $\lambda_j^* = \lambda$ for the first time, i.e., for the smallest value of λ. (39) or in case of hilltop buckling (57) reveal that $\lambda_{1,\lambda C}^* < 1$. Therefore, since C is the first point of intersection of $\lambda_1^*(\lambda)$ and λ and since only positive values of λ are considered,

$$\lambda_1^*(\lambda) - \lambda > 0 \quad \forall \lambda < \lambda_C. \tag{74}$$

For $\lambda < \lambda_C$, stability requires that $\tilde{\mathbf{K}}_T$ is positive definite. Consequently, this applies also to the scalar $V_{,u_N u_N}$, which vanishes at C. Generally, as λ exceeds λ_C, $V_{,u_N u_N} < 0$, at least in the vicinity of the stability limit. The existence of such points requires $C \neq D$, i.e., hilltop buckling is excluded. Therefore,

$$V_{,u_N u_N,\lambda}(\lambda) < 0 \qquad \forall \lambda \in (\lambda_C - a, \lambda_C + a), \tag{75}$$

where $(\lambda_C - a, \lambda_C + a)$ is a sufficiently small domain including the stability limit. (75) implies that in the considered domain $\tilde{\mathbf{K}}_{T,\lambda}$ is not positive semidefinite. Moreover, (75) implies

$$\mathbf{v}_1^{*\mathrm{T}} \cdot \tilde{\mathbf{K}}_{T,\lambda} \cdot \mathbf{v}_1^* < 0 \qquad \forall \lambda \in (\lambda_C - a, \lambda_C + a). \tag{76}$$

Using this result, it follows from (33) that the sign of the slope of the eigenvalue curve $\lambda_{1,\lambda}^*$ is essentially determined by the sign of $V_{,u_N u_N,\lambda\lambda}$. A physical interpretation of the foregoing can be given based on the fact that $V_{,u_N u_N}$ represents the tangential stiffness of the structure with respect to the

buckling displacement u_N. As described by (75), this stiffness reduces as the load multiplier λ is increased. The rate at which $V_{,u_N u_N}$ decreases may change, which is quantified by $V_{,u_N u_N,\lambda\lambda}$. Assuming $V_{,u_N u_N,\lambda\lambda C} \neq 0$, $\lambda^*_{1,\lambda}$ changes its sign at C (cf. (33)).

In case of a point with a nontrivial horizontal tangent ($\lambda^*_{1,\lambda} = 0 \wedge \lambda^*_1 \neq \lambda$), $\lambda^*_{1,\lambda\lambda}$ is defined by (38). In essence, its sign is determined by the sign of $V_{,u_N u_N,\lambda\lambda\lambda}$, which does not allow a straightforward physical interpretation. However, (42) indicates that $\lambda^*_{1,\lambda\lambda}$ changes its sign as the considered point characterized by a horizontal tangent passes the stability limit.

For snap-through points D, it was shown in Subsection 2.8, that the slope of the eigenvalue curve λ^*_j belonging to the snap-through mode $\mathbf{v}^*_j$ is -1, i.e., that it has a finite value. However, the curvature is infinite, and consequently, D is a cusp of the $\lambda^*_j(\lambda)$ curve. Hence,

$$\lambda^*_j(\lambda) - \lambda \geq 0 \tag{77}$$

with the equality sign holding at the cusp D. If, on the other hand, $\mathbf{v}^*_j$ is neither a snap-through mode nor a hilltop buckling mode, $\lambda^*_j(\lambda)$ has a vertical tangent at D. Since both, the first and the second derivative are infinite in this case, the curvature may be finite or infinite. It follows from (20) that in this case

$$c_{11D} = \pm\infty, \tag{78}$$

which is just another indicator for snap-through points. In case of hilltop buckling, (77) also holds for λ^*_1, which corresponds to the bifurcation mode. Insertion of (57) and (77) into (20) results in

$$c_{11C} = -\infty. \tag{79}$$

In Subsection 2.9 it was shown that, if the load-displacement path contains a saddle point D, $\lambda^*_{j,\lambda D} = -1/2$ and $|\lambda^*_{j,\lambda\lambda D}| < \infty$ hold for the associated eigenvalue curve. Eigenvalue curves not corresponding to the saddle mode have a vertical tangent at D.

Examples given in the following Section will corroborate these theoretical findings. The examples refer to symmetric bifurcation behavior [14], i.e., the sign of the buckling coordinate is not relevant.

3. Structures with remarkable postbuckling paths

3.1. Two-bar system

A planar, static, conservative system with two degrees of freedom, as shown in Fig. 1, is considered. Both rigid bars, ① and ② have the same length L and in the non-buckled state they are in-line. The bars are linked at one end and supported by turning-and-sliding joints at their other ends. A horizontal linear elastic spring of stiffness k and a vertical linear elastic spring of stiffness κk are attached to turning-and-sliding joints.
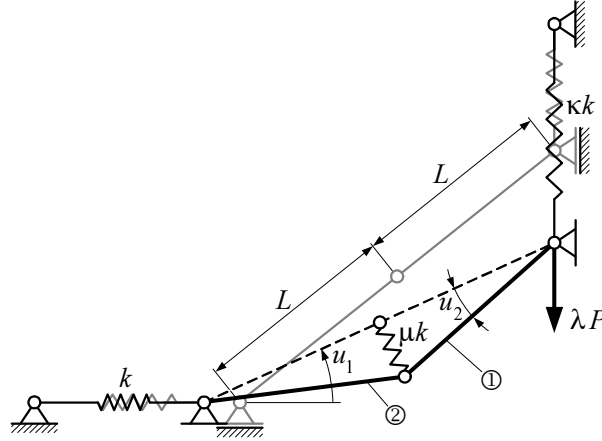
Fig. 1: Two-bar system

A spring of stiffness μk "pulls" the two bars back into their in-line position. The system is loaded by a vertical load λP at the vertical turning-and-sliding joint. The two displacement coordinates are the angles u_1 and u_2, summarized in the vector $\mathbf{u} = [u_1, u_2]^{\text{T}}$. In order to write the out-of-balance force $\mathbf{G}$ in the structure defined in (1), other coordinates would need to be chosen. In fact, the angle u_1 would need to be replaced by the vertical position of the upper turning-and-sliding joint. This would only require a simple coordinate transformation. For convenience, however, the angle u_1 was chosen as a coordinate. The unloaded position, delineated in gray, is defined by $\mathbf{u} = [u_{10}, 0]^{\text{T}}$. This system was originally suggested by Schranz *et al.* [15]. The potential energy expression follows as

$$V(\mathbf{u}, \lambda) = 2\kappa k L^2 \left(\sin(u_{10}) - \sin(u_1)\cos(u_2)\right)^2 + \frac{\mu k}{2} L^2 \sin^2(u_2) + 2 k L^2 \left(\cos(u_{10}) - \cos(u_1)\cos(u_2)\right)^2$$
$$- \lambda P 2 L \left(\sin(u_{10}) - \sin(u_1)\cos(u_2)\right).$$

(80)

The equilibrium equations $V_{,u_1} = 0$ and $V_{,u_2} = 0$ are satisfied for the primary path

$$u_2 = 0,$$
$$\lambda = \frac{2 L k}{P} \left((1 - \kappa)\sin(u_1) - \cos(u_{10})\tan(u_1) + \kappa \sin(u_{10})\right),$$

(81)

and for the secondary path

$$u_2 = \pm \arccos\left(\frac{4}{4 - \mu} \frac{\cos(u_{10})}{\cos(u_1)}\right),$$
$$\lambda = \frac{2 L k}{P} \left(\frac{\mu - 4\kappa}{4 - \mu}\cos(u_{10})\tan(u_1) + \kappa \sin(u_{10})\right).$$

(82)

Since a perfect system is assumed, the sign of u_2 is indeterminate, i.e., it is not known into which direction the two bars will buckle. The tangent-stiffness matrix follows as

$$\tilde{\mathbf{K}}_T = 4 k L^2 \operatorname{diag}\left\{\kappa\left(1 + \sin(u_{10})\sin(u_1) - 2\sin^2(u_1)\right) + 1 + \cos(u_{10})\cos(u_1) - 2\cos^2(u_1) - \lambda \frac{P}{2 k L}\sin(u_1);\right.$$
$$\left. \kappa\left(\sin(u_{10})\sin(u_1) - \sin^2(u_1)\right) + \cos(u_{10})\cos(u_1) - \cos^2(u_1) - \lambda \frac{P}{2 k L}\sin(u_1)\right\}.$$

(83)

Its derivative with respect to λ can be computed by

$$\tilde{\mathbf{K}}_{T,\lambda} = V_{,\mathbf{uuu}} \cdot \tilde{\mathbf{u}}_{,\lambda} + V_{,\mathbf{uu};\lambda}, \tag{84}$$

where $\tilde{\mathbf{u}}_{,\lambda}$ is the derivative of the displacement vector along the primary path, which can be determined from the linear equation

$$\tilde{\mathbf{G}}_{,\lambda} = \tilde{\mathbf{K}}_T \cdot \tilde{\mathbf{u}}_{,\lambda} + \tilde{\mathbf{G}}_{;\lambda} = \mathbf{0}. \tag{85}$$

The expression of $\tilde{\mathbf{K}}_{T,\lambda}$ looks similar to (83). For the sake of conciseness, it has been omitted. Hence, all terms necessary for solving the eigenproblem (4) have been deduced.

$u_{10} \in (-\pi/2, \pi/2)$, $\mu \in \mathbb{R}^+$ and $\kappa \in \mathbb{R}^+$ are parameters that can be varied in order to achieve qualitative changes of the system. However, in this work, only κ was modified. The remaining two parameters were taken as $\mu = 3/5$ and $u_{10} = 0.67026$, in which case hilltop buckling occurs for $\kappa = 0$. The load-displacement path for hilltop buckling and its projection onto the plane $u_2 = 0$ are shown in Fig. 2(a) and (b), respectively. S labels the unloaded state. As the load is increased, the state will move up along the primary path until $C = D$ is reached. In case of a load-controlled system, snap-through will occur. However, a displacement-controlled system would bifurcate and the state would traverse one branch of the secondary path. The corresponding eigenvalue curve is given in Fig. 2(c). As expected from the theoretical result (57), both curves have a cusp at $C = D$, where the slope of their common tangent is -1.

If $\eta = u_2$, the relevant coefficients of the series expansion (71) generally follow as

$$\lambda_1 = 0, \qquad \lambda_2 = \frac{kL}{P} \frac{(\kappa - \mu/4)}{\sqrt{1 - \frac{\cos^2(u_{10})}{(1 - \mu/4)^2}}}, \qquad \lambda_3 = 0, \qquad \lambda_4 = -\frac{\lambda_2}{12} \frac{1 - 4\frac{\cos^2(u_{10})}{(1 - \mu/4)^2}}{1 - \frac{\cos^2(u_{10})}{(1 - \mu/4)^2}}. \tag{86}$$

Thus, $\lambda_4 \propto \lambda_2$. For $\kappa = 0$, this system is imperfection sensitive ($\lambda_2 < 0$), and λ_C exceeds the ultimate load of any imperfect system. Increasing the parameter κ, i.e., the stiffness of the vertical spring, improves the postbuckling behavior insofar as λ_2 increases monotonically. The system is imperfection insensitive for $\kappa > \mu/4$. Load-displacement paths and eigenvalue curves for the transition case $\kappa = \mu/4$ are shown in Figs. 2(d) and (e), respectively. Remarkably, $\lambda = \lambda_C$ holds along the whole postbuckling path, i.e., the motion occurs with zero-stiffness. From an engineering viewpoint, this is not better than snap-through behavior, because under load control the system will undergo a discontinuous displacement associated with high accelerations. Fig. 2(e) confirms (39) and (50) for the eigenvalue λ_1^* (thick line) corresponding to the bifurcation mode, as well as (49) and (56) for the eigenvalue λ_2^* (thin line) corresponding to the snap-through mode. It is noted that cases where $u_{1C} < u_{1D}$ are possible, if u_{10} would be reduced. However, this is not elaborated here, since it is only relevant for displacement-controlled systems.

As κ is further increased, the critical displacement u_{1D} at the onset of snap-through approaches 0. Eventually, at $\kappa = 1 - \cos(u_{10})$, the two turning points meet at $\mathbf{u} = \mathbf{0}$, where the primary path exhibits a

saddle point D. This situation is shown in Fig. 2(f). Its theoretical background was discussed in Subsection 2.9. Fig. 2(g) verifies that $\lambda_{2,\lambda D}^{*} = -1/2$ and that the curvature of λ_{2}^{*} at D is finite. Hence, the eigenvalue curve does not show a cusp.

For $\kappa > 1 - \cos(u_{10})$, the only possible mode of loss of stability is bifurcation. The system remains imperfection insensitive. If

$$\kappa = 1 + \frac{1 - \mu/4}{2\frac{\cos^2(u_{10})}{(1 - \mu/4)^2} - 3} = 0.364, \tag{87}$$

λ_{1}^{*} has a saddle point at C, as demonstrated by Fig. 2(i) (thick line). λ_{2}^{*} (thin line) does not intersect the line $\lambda^{*} = \lambda$, which reflects the fact that snap-through cannot occur.

Generally, as κ is increased, the projection of the secondary path approaches the primary path, as may be concluded from a comparison of the Figs. 2(d), (f), and (h). Equating λ from (81) and λ from (82) yields that for $\kappa = 1$, the difference between the primary path and the projection of the secondary path vanishes, whereas the displacement u_2 is nonzero. In fact λ depends only on u_1 but not on the buckling coordinate u_2. This special case is shown in Fig. 2(j). The corresponding eigenvalue curve is plotted in Fig. 2(k). The second eigenvalue curve is outside the plotting frame; it does not intersect the straight line $\lambda^{*} = \lambda$.

If $\kappa > 1$ and $u_1 > 0$, the projection of the secondary path exceeds the primary path in terms of λ. That is, the secondary path carries higher loads than the primary path. It is unclear, whether this effect is of practical use, since the large deflection u_2 may be unacceptable.

In Subsection 2.12, it was concluded that $c_{11C} = -\infty$ for hilltop buckling. This is verified by Fig. 3, where c_{11C} approaches a vertical asymptote at $\lambda_2 = -0.387$ and $\lambda_4 = -0.516$, for $\kappa \to 0$. Apart from the three special cases $\kappa = \mu/4$, $\kappa = 1 - \cos(u_{10})$ and $\kappa = 1$, which were already discussed, two more noteworthy points are highlighted in Fig. 3, i.e., $\kappa = 0.346$ and $\kappa = 0.692$. The latter marks the maximum of c_{11C}, which splits c_{11C} into two monotonically decreasing sections. For $\kappa \to +\infty$, the curve asymptotically approaches 0. However, it is emphasized that this is a rather unrealistic case, since the vertical spring would become rigid and the buckling load λ_C infinitely large. As expected from (41), c_{11C} also vanishes for $\kappa = 0.346$, where the curve λ_1^{*} has a saddle point at C (cf. Fig. 2(i)). This example verified the theoretical conclusions of Section 2, especially those concerning the shape of the eigenvalue curves. Their characteristic properties, like intersections with the straight line $\lambda^{*} = \lambda$, cusps, tangents having a specific slope $(0, -1/2, -1, \pm\infty)$, etc., facilitate the analysis of instability phenomena. Moreover, this example proved the existence of remarkable postbuckling paths, such as the zero-stiffness case or the equivalence of a primary path and the projection of a secondary path.
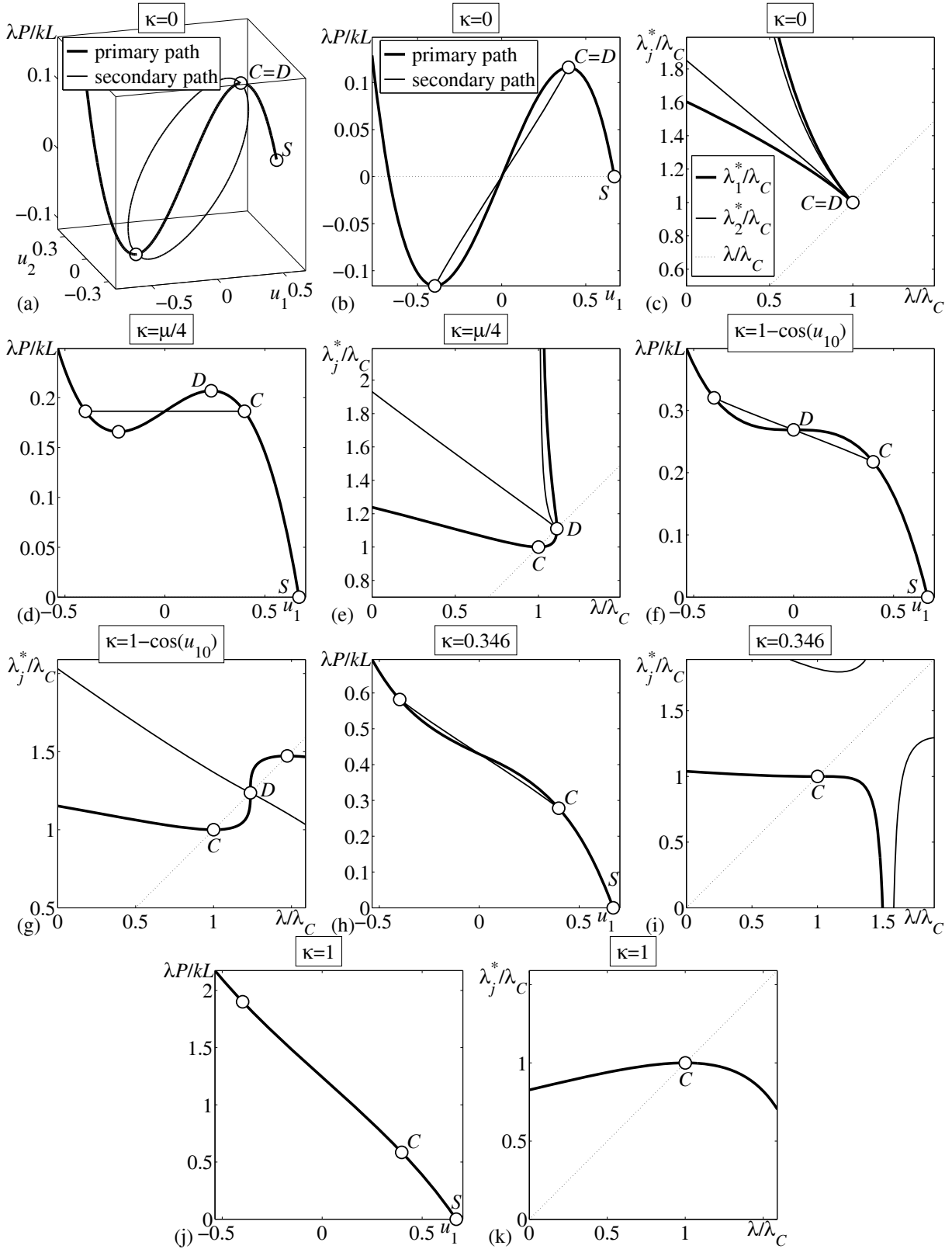
Fig. 2: Load-displacement paths and eigenvalue curves for various values of κ, (a) load displacement path, (b), (d), (f), (h), and (j) projections of load-displacement paths onto the plane $u_2 = 0$, (c), (e), (g), (i), and k) eigenvalue curves (normalized with respect to λ_C, equal scaling on both axes)
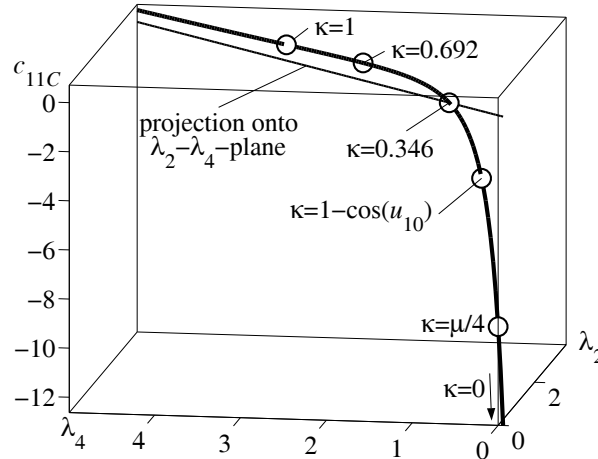
Fig.3: λ_2-λ_4-c_{11C} *curve*

3.2. *Von Mises* **truss**

Fig. 4 shows the geometry of a *von Mises* truss supported by a vertical spring κk, with $k=10^7$ N/m. In fact, only one half of the truss is considered herein. $\kappa \in \mathbb{R}^+$ is a scaling parameter that is varied in order to control the behavior of the planar system. $s \in [0, L=1\text{m}]$ shall be a Lagrangian coordinate of the principal beam, which is straight in the unloaded configuration as shown in gray color. The homogeneous beam has a squared cross section (side length $a=0.2\text{m}$) and the elastic modulus of its material is $E=2.1\cdot10^{11}$ N/m^2. The position of a vertical turning-and-sliding joint is defined by $u_1 L$. The load λP, with $P=10^7$ N, is applied to this joint. The beam and the spring are unstrained if the beam is straight and $u_1 = u_{10} = 0.30901$. Using these parameters, hilltop buckling occurs for $\kappa=0$.

The angle between the tangent to the beam and the line connecting its end points is denoted as $\varphi(s) \in [-u_2, u_2]$, where $\varphi(0) = -\varphi(L) = u_2$. $w(s)$ measures the lateral deflection of the beam with respect to the line connecting its end points. The Euler-Bernoulli hypothesis is the basis of the kinematic relations of the beam. Generally, the system has infinitely many degrees of freedom. Both, the bending and the stretching energy of the beam are taken into account.
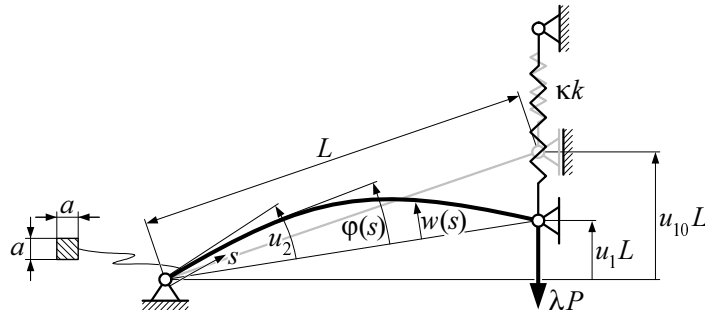
Fig. 4: Von Mises truss

Two solution strategies are pursued: (i) exact nonlinear theory and (ii) approximation of the deformed shape as a sine-curve. In the latter case, it is stipulated that $\mathbf{u} = [u_1, u_2]^\text{T}$ suffices to define the configuration of the system, i.e., the model is reduced to a two-degrees-of-freedom scheme.

For the exact solution (i), the equilibrium equation reads as

$$EI\frac{d^2\varphi}{ds^2} + \frac{\sqrt{1-u_{10}^2+u_1^2}}{u_1}\left(\lambda P - \kappa k L(u_{10}-u_1)\right)\sin(\varphi) = 0 \tag{88}$$

with the boundary conditions

$$\varphi(0) = -\varphi(L) = u_2, \qquad \frac{d\varphi(0)}{ds} = \frac{d\varphi(L)}{ds} = 0. \tag{89}$$

In (88), I denotes the areal moment of inertia. With the help of

$$\frac{d\varphi}{ds} = \sqrt{2\left(\cos(\varphi)-\cos(u_2)\right)\frac{\sqrt{1-u_{10}^2+u_1^2}}{u_1 EI}\left(\lambda P - \kappa k L(u_{10}-u_1)\right)}, \tag{90}$$

which satisfies (88), and the complete elliptic integrals [16]

$$\bar{K}(m) := \int_0^{\pi/2} \frac{dt}{\sqrt{1-m\sin(t)^2}}, \qquad \bar{E}(m) := \int_0^{\pi/2} \sqrt{1-m\sin(t)^2}\, dt \tag{91}$$

of first and second kind, respectively, the length reduction caused by bending can be computed as

$$\Delta L_B = 2L\left(1 - \frac{\bar{E}\left(\sin(u_2/2)^2\right)}{\bar{K}\left(\sin(u_2/2)^2\right)}\right). \tag{92}$$

Neglecting the curvature of the beam, the change of its length caused by stretching reads as

$$\Delta L_N = -\frac{1}{EA}\frac{\sqrt{1-u_{10}^2+u_1^2}}{u_1}\left(\lambda P - \kappa k L(u_{10}-u_1)\right), \tag{93}$$

where $A = a^2$ is the cross-sectional area. The geometric relation

$$\Delta L_B - \Delta L_N = L\left(1 - \sqrt{1-u_{10}^2+u_1^2}\right) \tag{94}$$

complements the set of equations required to obtain the exact solution. The primary path follows with $\varphi = 0$ and $\Delta L_B = 0$ from (93) and (94) as

$$\lambda = \frac{\kappa k L}{P}(u_{10}-u_1) + \frac{u_1 EA}{P}\left(\frac{1}{\sqrt{1-u_{10}^2+u_1^2}}-1\right). \tag{95}$$

(88) through (94) yield the solution for the secondary path

$$u_1 = \pm\sqrt{u_{10}^2 - 1 + \left(2\frac{\bar{E}\left(\sin(u_2/2)^2\right)}{\bar{K}\left(\sin(u_2/2)^2\right)} - 1 - \frac{4I}{AL^2}\bar{K}\left(\sin(u_2/2)^2\right)^2\right)^2} \tag{96}$$

$$\lambda = \frac{4EI}{L^2 P}\bar{K}\left(\sin(u_2/2)^2\right)^2\sqrt{1 + \frac{u_{10}^2 - 1}{\left(2\frac{\bar{E}\left(\sin(u_2/2)^2\right)}{\bar{K}\left(\sin(u_2/2)^2\right)} - 1 - \frac{4I}{AL^2}\bar{K}\left(\sin(u_2/2)^2\right)^2\right)^2}} \tag{97}$$

in terms of the angle u_2. It is possible to develop (97) into a series expansion with respect to u_2. The buckled shape of the beam can be computed as

$$w(\varphi) = \frac{\text{sign}(u_2)\,L}{\bar{K}\left(\sin(u_2/2)^2\right)}\sqrt{\frac{\cos(\varphi)-\cos(u_2)}{2}} \tag{98}$$

$$s(\varphi) = \frac{L}{2} - \frac{L}{\sqrt{2\left(1-\cos(u_2)\right)}\,\bar{K}\left(\sin(u_2/2)^2\right)}\int_0^{\varphi/2}\frac{dt}{\sqrt{1-\frac{2}{1-\cos(u_2)}\sin(t)^2}} \tag{99}$$

with $\varphi \in [-u_2, u_2]$. (99) contains an incomplete elliptic integral of first kind, which can be inverted if Jacobian elliptic functions are employed [16], i.e., computation of $\varphi(s)$ from (99) and insertion into (98) results in $w(s)$.

Quantities of the approximate solution (ii), where the deformed shape of the beam is assumed as

$$w'(s) = \sin(u'_2)\frac{L}{\pi}\sin(\pi s/L), \tag{100}$$

shall be labeled by a quotation mark. Hence, $\varphi'(s)$ and the length reduction caused by bending follow as

$$\varphi'(s) = \arcsin\left(\sin(u'_2)\cos(\pi s/L)\right), \tag{101}$$

$$\Delta L'_B = L - \frac{2L}{\pi}\bar{E}\left(\sin(u'_2)^2\right), \tag{102}$$

respectively. Rewriting (94) for the approximate solution yields

$$\Delta L'_N = \Delta L'_B - L\left(1 - \sqrt{1 - u_{10}^2 + u_1'^2}\right). \tag{103}$$

(101) through (103) allow deduction of the strain energy

$$\frac{EA}{2L}\Delta L_N'^2 = \frac{EAL}{2}\left(\frac{2}{\pi}\bar{E}\left(\sin(u'_2)^2\right) - \sqrt{1 - u_{10}^2 + u_1'^2}\right)^2, \tag{104}$$

$$\frac{EI}{2}\int_0^L\left(\frac{d\varphi'}{ds}\right)^2 ds = \frac{EI\pi^2}{2L}\left(1 - \cos(u'_2)\right) \tag{105}$$

resulting from stretching and bending of the beam, respectively. Summation of the strain energy of the vertical spring κk, the potential of the external load $\lambda'P$, (104), and (105) gives the total potential energy

$$V'(\mathbf{u'}, \lambda') = \frac{\kappa k}{2}L^2(u_{10} - u'_1)^2 - \lambda'PL(u_{10} - u'_1) + \frac{EAL}{2}\left(\frac{2}{\pi}\bar{E}\left(\sin(u'_2)^2\right) - \sqrt{1 - u_{10}^2 + u_1'^2}\right)^2$$
$$+ \frac{EI\pi^2}{2L}\left(1 - \cos(u'_2)\right). \tag{106}$$

The equilibrium equations $V'_{,u'_1} = 0$ and $V'_{,u'_2} = 0$ yield the same primary path as for the exact solution given in (95). The postbuckling solution follows as

$$u'_1 = \pm\sqrt{u_{10}^2 - 1 + \left(\frac{2}{\pi}\bar{E}\left(\sin(u'_2)^2\right) + \frac{EI\pi^3\sin(u'_2)^2}{4EAL^2\cos(u'_2)\left(\bar{E}\left(\sin(u'_2)^2\right) - \bar{K}\left(\sin(u'_2)^2\right)\right)}\right)^2} \tag{107}$$

$$\lambda' = \frac{\kappa k(u_{10} - u'_1)}{P} + \frac{EAu'_1}{P}\left(\frac{2}{\pi}\frac{\bar{E}\left(\sin(u'_2)^2\right)}{\sqrt{1 - u_{10}^2 + u_1'^2}} - 1\right). \tag{108}$$

Insertion of (107) into (108) allows expansion of λ' into a series in terms of u'_2.

The diagonal structure of the tangent stiffness matrix

$$\tilde{\mathbf{K}}'_T = EAL\,\text{diag}\left\{\frac{u_{10}^2 - 1}{\sqrt{\left(1 - u_{10}^2 + u_1'^2\right)^3}} + \frac{\kappa kL}{EA} + 1;\ \frac{1}{2}\left(\sqrt{1 - u_{10}^2 + u_1'^2} - 1\right) + \frac{EI\pi^2}{2EAL^2}\right\} \tag{109}$$

reflects the fact that $u'_2 = 0$ holds along the primary path. With $\tilde{\mathbf{K}}'_T$ from (109) and $\tilde{\mathbf{K}}'_{T,\lambda}$ according to (84), the eigenproblem (4) can be solved.

For the postbuckling analysis, the chosen path parameters are $\eta = u_2$ and $\eta' = u'_2$. A comparison of results for $u_2 = u'_2$ should be carried out with due care, since u_2 and u'_2 do not correspond directly. However, $u_2 = 0$ and $u'_2 = 0$ describe equivalent states of the system. It can be shown that

$$u_{1C} = u'_{1C}, \qquad \lambda_C = \lambda'_C, \qquad \lambda_2 = \lambda'_2, \qquad (110)$$

which is a consequence of the fact that the approximate solution asymptotically approaches the exact solution for $u_2 \to 0$, $u'_2 \to 0$. However, generally λ_4 does not equal λ'_4. It can be shown that $\lambda_2 = \lambda'_2$, λ_4, and λ'_4 depend linearly on κ. Hence, if κ is the only parameter that is varied, there is a linear relationship between $\lambda_2 = \lambda'_2$, λ_4, and λ'_4. The coefficient of κ in the expression of $\lambda_2 = \lambda'_2$ is positive. Consequently, increasing κ will improve the postbuckling behavior.
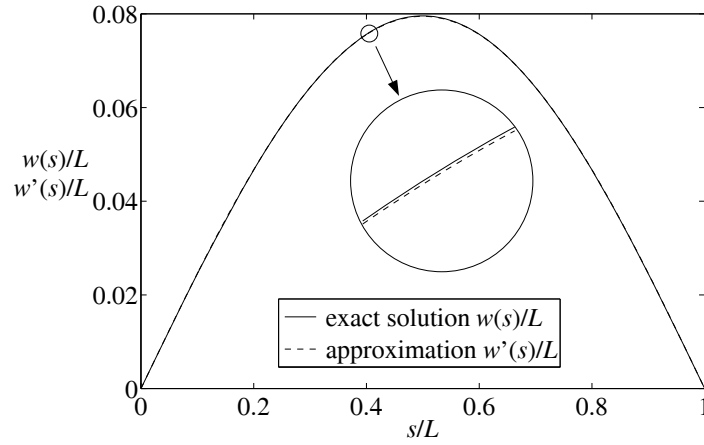
Fig. 5: Bending line of buckled principal beam for $u_1 = u'_1 = 0$

It is emphasized that (96), (97), (107), and (108) give different results for λ and λ' even if $u_1 = u'_1$. For the parameter values chosen in this analysis, their numerical difference did not exceed $\lambda_C / 10^4$. In graphical representations of the results, this difference is hardly visible. Thus, in the following discussion of numerical results, no distinction will be made between exact and approximate results, unless stated otherwise. Another justification for this simplified approach is presented inFig. 5. It shows the bending line of the buckled principal beam for the case $u_1 = u'_1 = 0$, i.e., where both, the lateral deflection $w(s)$ and the compressive normal force of the beam reach a maximum. The differences between the two solutions are small. If the deflections $w(s)$ and $w'(s)$ are compared for several load levels $\lambda = \lambda'$, the maximum error $\|w(s) - w'(s)\|_\infty$ never exceeds $0.13\,\%$ of $|w(L/2)|$.

Load-displacement paths for hilltop buckling ($\kappa = 0$) and their projections onto the plane $u_2 = 0$ are shown in Figs. 6(a) and 6(b), respectively. Again, S labels the unloaded state and $C = D$ the bifurcation point which, at the same time, is a snap-through point. The corresponding eigenvalue curve was computed by means of the potential V' of the approximate solution; it is shown in 6(c). The plot

corroborates (57), since both curves exhibit a cusp and a slope of -1 at $C=D$. For $\kappa=0$, the relevant coefficients of the series expansion (71) follow as

$$\lambda_1 = 0, \qquad \lambda_2 = \lambda'_2 = -38.1, \qquad \lambda_3 = 0, \qquad \lambda_4 = -167.6, \qquad \lambda'_4 = -164.1. \qquad (111)$$

Thus, the system is imperfection sensitive. If κ is increased, the transition from imperfection sensitivity to insensitivity occurs for $\kappa=27.2$, where

$$\lambda_1 = 0, \qquad \lambda_2 = \lambda'_2 = 0, \qquad \lambda_3 = 0, \qquad \lambda_4 = -22.4, \qquad \lambda'_4 = -22.2. \qquad (112)$$

The transition case itself is imperfection sensitive ($\lambda_4 < 0$). Load-displacement paths and eigenvalue curves for this situation are shown in Figs. 6(d) and 6(e). At first sight, the projection of the postbuckling path onto the plane $u_2 = 0$ seems to be a straight line (cf. Figs. 6(b), 6(d), 6(f), and 6(h)) [15]. However, 6(d) contradicts this impression, since the postbuckling path is inclined whereas its tangent at C is horizontal.

In 6(e), the horizontal and vertical tangent of λ_1^{r*} (thick line) at C and D conforms to (39) and (50), respectively. The cusped shape of λ_2^{r*} (thin line) verifies (49) and (56). Figs. 6(c) and (e) are only plotted for positive values of u_1 in order to avoid confusion resulting from additional curves corresponding to the non-relevant bifurcation and snap-through modes in the domain $u_1 < 0$.

As κ is further increased, the two turning points approach the point $\mathbf{u} = \mathbf{0}$, where they merge to a saddle point D on the primary path. That is, turning points and the cusp of the associated eigenvalue curve λ_2^{r*} no longer exist. This special case occurs for the parameter value $\kappa=43.2$. Figs. 6(f) and (g) demonstrate that the situation is similar to the previous example (cf. Figs. 2(f) and (g)). As theoretically addressed in Subsection 2.9, the corresponding eigenvalue curve λ_2^{r*} (thin line) exhibits a finite curvature and a slope of $\lambda_{2,\lambda D}^{*} = -1/2$ at D, whereas λ_1^{*} is characterized by a vertical tangent. Fig. 6(f) shows that the system is imperfection insensitive ($\lambda_2 = 22.5$).

For $\kappa > 43.2$, the primary path is monotonically increasing. The eigenvalue curve λ_1^{*} (thick line) has a positive curvature at C, i.e., $\lambda_{1,\lambda\lambda C}^{r*} > 0$. However, this changes at $\kappa=85.7$, which marks a saddle point of λ_1^{*} at C. Figs. 6(h) and (i) show the relevant graphs for $\kappa=85.7$. As expected, there is no intersection of λ_2^{r*} (thin line) and the line $\lambda_j^{r*} = \lambda'$, reflecting the fact that snap-through is not possible. A situation where the projection of the postbuckling path onto the plane $u_2 = 0$ equals the primary pah, which was observed in the previous example, does not occur for the *von Mises* truss.

Fig.7 shows $\lambda_2 = \lambda'_2$, λ'_4, and c'_{11C} as a function of κ. As expected from (79) and the results (111), c'_{11C} approaches a vertical asymptote at $\lambda_2 = -38.1$ and $\lambda'_4 = -164.1$ for $\kappa \to 0$. In the limit, $c'_{11C} = -\infty$. Apart from the cases $\kappa=27.2$, $\kappa=43.2$, and $\kappa=85.7$ corresponding to $\lambda_2 = 0$, a saddle point D on the primary equilibrium path, and a saddle point of the eigenvalue curve λ_1^{r*} at C, respectively, $\kappa=171.4$ is a point of interest, since it marks the maximum of c'_{11C}. For $\kappa \to +\infty$, c'_{11C}

approaches 0. It is emphasized that the projection of the λ_2-λ'_4-c'_{11C} curve onto the plane $c'_{11C}=0$ is a straight line, which does not contain the point $\lambda_2=\lambda'_4=0$. In fact, this projection is the asymptote of the λ_2-λ'_4-c'_{11C} curve for $\kappa \to +\infty$.
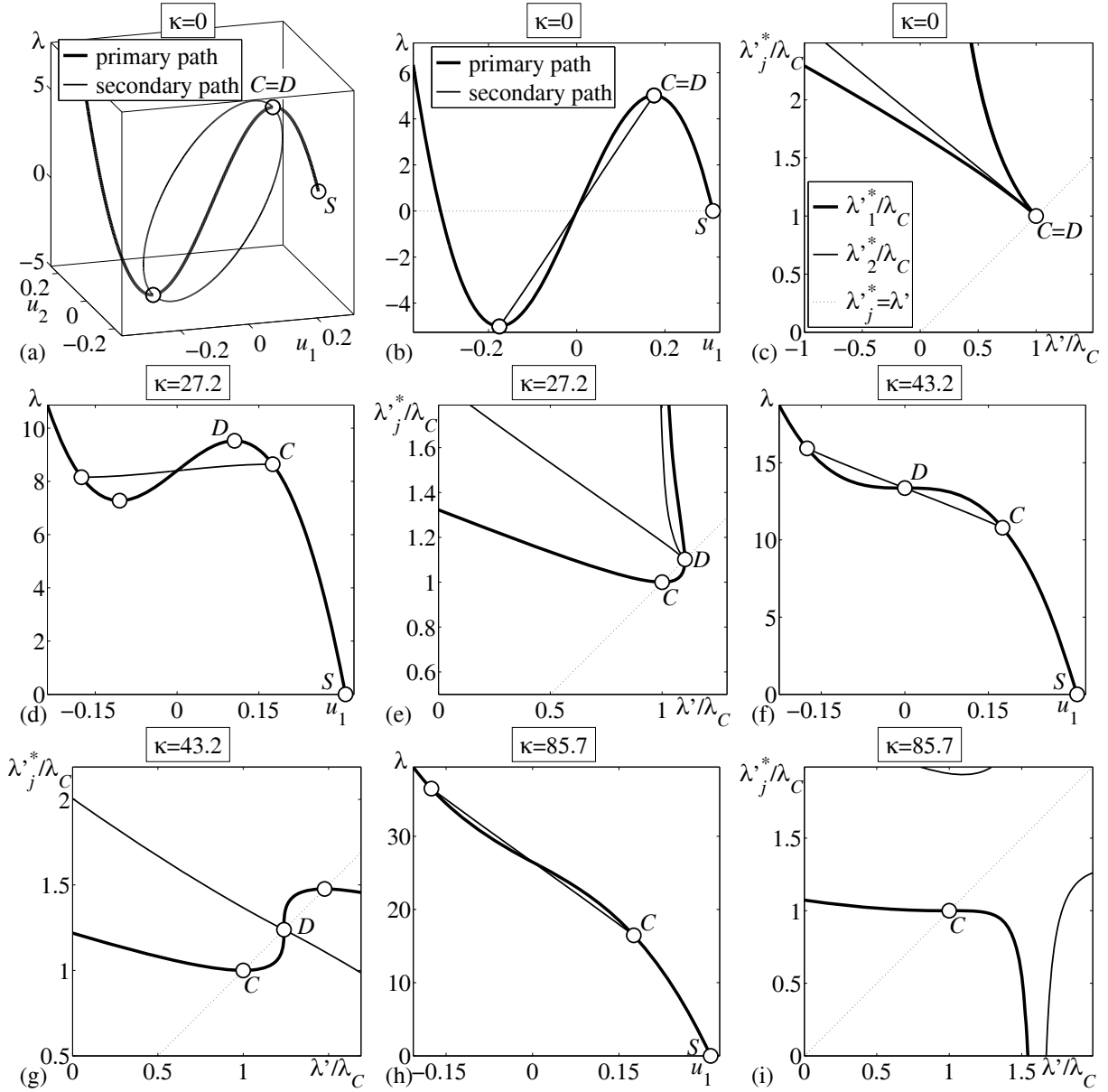
Fig.6 Load-displacement paths and eigenvalue curves for various values of κ, (a) load displacement path, (b), (d), (f), and (h) projections of load-displacement paths onto the plane $u_2=0$, (c), (e), (g), and i) eigenvalue curves (normalized with respect to λ_C, equal scaling on both axes)
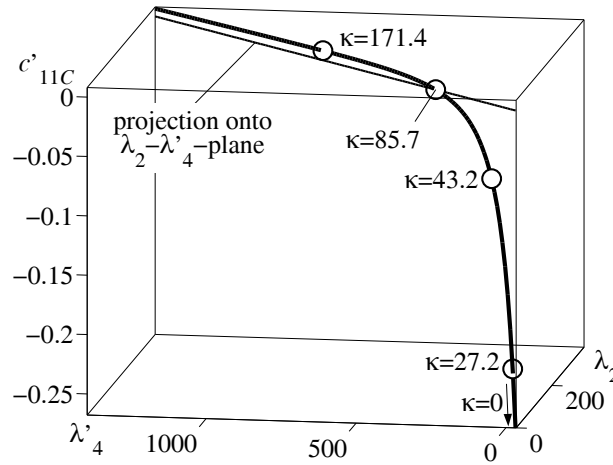
Fig.7: λ_2-λ'_4-c'_{11C} *curve*

This example corroborated some theoretical findings deduced in Section 2. Again, characteristic properties of eigenvalue curves could be identified and thereupon employed for analyzing the behavior of the system. In contrast to the previous example, remarkable types of postbuckling paths such as straight lines or projections of secondary paths which equal primary paths were not observed. This corresponds to the fact that the von Mises truss is a continuous system (infinitely many degrees of freedom), whereas in the previous example a discrete system was addressed.

Moreover, this example demonstrated that for engineering purposes the approximation of the buckled shape of the principal beam by a sine curve is sufficiently accurate. This approximation allows an exact computation of the primary path as well as of the critical load λ_c and of the coefficient λ_2 in the series expansion (71). In fact, these quantities are sufficient for qualifying the system as imperfection sensitive or insensitive. For this example, increasing the stiffness of a vertical supporting spring κk proved successful in converting the system from imperfection sensitivity into insensitivity.

4. Conclusions

The merits and limits of the consistently linearized eigenproblem as a means of computing (i) the stability limit and assessing (ii) the initial postbuckling behavior of a structure were discussed. Characteristic points and qualitative shapes of eigenvalue curves $\lambda_j^*(\lambda)$ were analyzed.

It was shown that after an appropriate coordinate transformation, the direction of the eigenvector $\mathbf{v}_1^*$ is constant whereas its length is still defined by the normalization condition (18). The method of constructing such coordinate transformations was demonstrated in Subsection 2.4. Orthogonalities of eigenvectors with respect to $\tilde{\mathbf{K}}_{T,\lambda^n}$ and a considerably simplified solution process of the consistently linearized eigenproblem are the most significant consequences of the aforementioned coordinate transformation.

For eigenvalue curves corresponding to bifurcation modes, points with a horizontal tangent ($\lambda_{1,\lambda}^{*}=0$) occur at the bifurcation point C. The curvature $\lambda_{1,\lambda\lambda C}^{*}$ at such points is proportional to a nonlinearity coefficient c_{11C}, which may be a helpful parameter for classifying the system behavior (cf. Figs. 3 and 7). Moreover, horizontal tangents may occur at points which do not mark stability limits. Such special cases are coupled to the vanishing of $\tilde{\mathbf{K}}_{T,\lambda\lambda}\cdot\mathbf{v}_{1}^{*}$.

It was shown that snap-through modes entail cusped shapes of eigenvalue curves, where the cusp marks the stability limit D and its tangent is perpendicular to the straight line $\lambda^{*}-\lambda=0$. At snap-through stability limits D, eigenvalue curves corresponding to bifurcation modes have a vertical tangent. However, the situation is different for hilltop buckling ($C=D$), where both, the eigenvalue curve belonging to the bifurcation mode and the one referring to the snap-through mode exhibit a cusp at which their common tangent is perpendicular to the line $\lambda^{*}-\lambda=0$. Another noteworthy case is the occurrence of a saddle point D on the primary path, reflected by an associated eigenvalue curve which is smooth and has a slope of $-1/2$ at D.

In the framework of *Koiter*'s initial postbuckling analysis, a necessary and sufficient condition for imperfection insensitivity was given. The proposed check is based on the computation of a few scalar coefficients λ_{i}. This condition is readily applicable to the FEM.

For two examples, the consequences of modifying a structural parameter κ, which controls the stiffness of a linear elastic spring, were studied. For both cases, it was shown that λ_{2}, which is the coefficient relevant to imperfection sensitivity or insensitivity, depends linearly on κ, which likewise applies to λ_{4}. Therefore, increasing κ improved the system and eventually brought about the desired conversion from imperfection sensitivity into insensitivity. Moreover, for sufficiently large values of κ, snap-through behavior was remedied which entailed the occurrence of a transition case characterized by a saddle point. Both examples show symmetric equilibrium paths.

In the course of varying κ, some remarkable postbuckling paths were observed for the example in Subsection 3.1. Zero-stiffness postbuckling means that λ is constant along the secondary path. Moreover, it proved feasible that λ depends only on u_{1} but not on the buckling coordinate u_{2} in which case the projection of the postbuckling path onto the plane $u_{2}=0$ equals the primary path.

The analysis of the *von Mises* truss in Subsection 3.2 demonstrated the possibility of replacing rigorous solutions by approximations without deteriorating results relevant to qualify a system as imperfection sensitive or insensitive. In fact, results for the primary path, the buckling load λ_{C} and the coefficient λ_{2} are not influenced by the change from rigorous analysis to the simplified model.

Considerations made herein to systems analyzed by the FEM leave scope for future scientific work. Moreover, the meaning of other peculiarities of eigenvalue curves, like singularities, planar points, loops, etc., should be investigated. Such remarkable types of eigenvalue curves have been observed for

more complicated examples ([4, 5, 15]), but their role is yet partially unclear, especially as regards the mode of conversion from imperfection sensitivity into imperfection insensitivity.

Acknowledgements

References

[1] Gallagher R.H., Yang H.T.Y. *Elastic instability predictions four doubly-curved shells*. In Proceedings of the Second Conference on Matrix Methods in Structural Mechanics, Wright-Patterson A. F. Base, Ohio, New Jersey, 711-739, 1968.

[2] Brendel B. *Geometrisch nichtlineare Elastostatik* [in German; *Geometrically nonlinear elastostatics*]. Ph.D. Thesis, Institut für Baustatik der Universität Stuttgart, Deutschland, 1979.

[3] Brendel B., Ramm E., Fischer F.D., Rammerstorfer F.G, *Linear and nonlinear stability analysis of thin cylindrical shells under wind loads*. Journal of Structural Mechanics, 9, 91-113, 1981.

[4] Helnwein P. *Zur initialen Abschätzbarkeit von Stabilitätsgrenzen auf nichtlinearen Last-Verschiebungspfaden elastischer Strukturen mittels der Methode der Finiten Elemente [in German; On ab initio assessability of stability limits on nonlinear load-displacement paths of elastic structures by means of the finite element method]*. Ph.D. Thesis, Technische Universität Wien, Österreichischer Kunst- und Kulturverlag, Wien, 1997.

[5] Helnwein P., Mang H.A. *An asymptotic approach for the evaluation of errors resulting from estimations of stability limits in nonlinear elasticity*. Acta Mechanica, 125, 235-254, 1997.

[6] Mang H.A., Helnwein P. *Second-order a-priori estimates of bifurcation points on geometrically nonlinear prebuckling paths*. In Proceeding of the International Conference of Computational Engineering Science, Hawaii, USA. Springer: Berlin, II, 1511-1516, 1995.

[7] Mang H.A, Schranz C, Mackenzie-Helnwein P. *Conversion from imperfection-sensitive into imperfection-insensitive elastic structures I: Theory*. International Journal of Computer Methods in Applied Mechanics and Engineering, 195, 1422-1457, 2006.

[8] Koiter W. *On the stability of elastic equilibrium*, Translation of '*Over de Stabiliteit van het Elastisch Evenwicht*' (1945). In NASA TT F-10833, Polytechnic Institute Delft, H.J. Paris Publisher: Amsterdam, 1967.

[9] Bochenek B. *Problems of structural optimization for post-buckling behaviour*. Struct. Multidisciplinary Optim., 25, 423-435, 2003.

[10] Godoy L. *Sensitivity of post-critical states to changes in design parameters*. Int. J. Solids Struct., 33, 2177-2192, 1996.

[11] Mróz R, Haftka R. *Design sensitivity analysis of non-linear structures in regular and critical states*. Int. J. Solids Struct., 31, 2071-2098, 1994.

[12] Reitinger R. *Stabilität und Optimierung imperfektionsempfindlicher Tragwerke* [in German; *Stability and optimization of imperfection-sensitive structures*]. Ph.D. Thesis, Universität Stuttgart, Institute of Structural Mechanics, 1994; Bericht Nr. 17.

[13] Fujii F, Noguchi H. *Multiple hill-top branching*. In Proceedings of the 2nd International Conference on Structural Stability and Dynamics, World Scientific, Singapore, 2002.

[14] Steinboeck A, Jia X, Hoefinger G, Mang H.A. *Symmetry and imperfection insensitivity - two independent properties of a structure?* In Proceedings of the 8th HSTAM (Hellenic Society for Theoretical and Applied Mechanics) International Congress on Mechanics, Patras, Greece, 12-14 July, 2007.

[15] Schranz C, Krenn B, Mang H.A. *Conversion from imperfection-sensitive into imperfection-insensitive elastic structures II: Numerical investigation.* International Journal of Computer Methods in Applied Mechanics and Engineering, 195, 1458-1479, 2006.

[16] Abramowitz M, Stegun I.A. *Handbook of Mathematical Functions.* Dover Publications, 1965.

Chapter III

Conditions for
Symmetric, Antisymmetric, and Zero-Stiffness Bifurcation in View of Imperfection Sensitivity and Insensitivity

Andreas Steinboeck[1], Xin Jia[2], Gerhard Hoefinger[2], and Herbert A. Mang[2]

[1]*Automation and Control Institute, Complex Dynamical Systems Group, Vienna University of Technology, Gußhausstraße 27-29/376, 1040 Vienna, Austria*
[2]*Institute for Mechanics of Materials and Structures, Vienna University of Technology, Karlsplatz 13/202, 1040 Vienna, Austria*

Abstract

So far, it is not clear how to design structures such that they are ab initio imperfection insensitive, i.e., without modifications of the original design after the diagnosis of imperfection sensitivity. Symmetry and antisymmetry of bifurcation paths, representing qualitative properties of a structure, not only simplify the postbuckling analysis, but also have an influence on the behavior of real, i.e., imperfect structures. The special case of a zero-stiffness postbuckling path incorporates both, symmetry and antisymmetry. Mathematical definitions of the three categories symmetric, antisymmetric, and zero-stiffness equilibrium paths are given. It is shown that symmetry as well as antisymmetry causes the vanishing of specific coefficients in an asymptotic series expansion, following from Koiter's initial postbuckling analysis. Thereupon, methods of checking for the three categories of bifurcation behavior are discussed. Finally, the three categories are investigated in terms of necessary and/or sufficient conditions for imperfection insensitivity. For instance, a horizontal tangent of the postbuckling path at the bifurcation point is required for imperfection insensitivity. Four examples illustrate non-symmetric, symmetric, and antisymmetric bifurcation as well as zero-stiffness postbuckling behavior. For the first two examples, the approach of increasing the stiffness results in the conversion of the system from imperfection sensitivity into insensitivity. Remarkably, this happens without changing the prebuckling behavior and the buckling load of the structure. The third example demonstrates that imperfection sensitivity is an inevitable implication of antisymmetric bifurcation.

Keywords

antisymmetric bifurcation, imperfection insensitivity, Koiter's postbuckling analysis, symmetric bifurcation, vanishing of coefficients of series expansion, zero-stiffness postbuckling behavior.

1. Introduction

1.1. Motivation

Koiter [6] proposed a mathematical scheme to investigate postbuckling paths in the vicinity of the bifurcation point representing the stability limit. Koiter's calculus proved to be suitable for analyzing static stability problems. However, it appears that there is still a lack of knowledge of designing a structure for imperfection insensitivity *r*ight from the outset.

Several algorithms have been developed for optimizing the postbuckling behavior, e.g. in [1, 9]. Usually, they are of iterative nature, i.e., quantitative parameters defining a structure are modified within algorithmic loops. Apart from the computational cost, the difficulty with these algorithms is that they do not allow deduction of general design rules, since they only work on a case-by-case basis. Similar problems are faced in design sensitivity analyses ([4, 8, 10]), which focus on quantitative properties of the load-displacement behavior of a structure.

The objective of this work is to identify categories of qualitative properties of equilibrium paths and to clarify their influence on the conversion process of imperfection-sensitive into imperfection-insensitive structures. The nature of imperfections is that their shapes and amplitudes are unknown, at least at the design stage of a structure. Therefore, structural analysis is frequently based on models of the ideal system. However, for the fact that an improvement of the ideal system goes hand in hand with an improvement of the real, imperfect system, this is no limitation. In this sense, a first attempt to designing for imperfection insensitivity is made. Eventually, this requires formulation of design rules which either allow designing for imperfection insensitivity *ab initio*, or at least facilitate the conversion from imperfection sensitivity into imperfection insensitivity. In this context, the question of necessary and sufficient conditions for imperfection insensitivity is raised.

Mirror symmetry and antisymmetry of equilibrium paths as well as so-called zero-stiffness postbuckling paths are three prominent categories of bifurcation behavior. Their mathematical definitions will be given in Subsections 3.1, 4.1, and 5.1, respectively, appended by examples. In [12], elastic structures showing zero-stiffness equilibrium paths are presented. There, zero-stiffness behavior is denoted as neutral equilibrium. In [1, 7] it is stated that symmetric bifurcation is a requirement for imperfection insensitivity. However, it will be shown that none of the three categories, in a rigorous mathematical sense, is necessary for the conversion of an imperfection-sensitive into an imperfection-insensitive structure [11]. Symmetric bifurcation is generally better understood and investigated than antisymmetry, mainly because it occurs more frequently in the design of engineering structures.

1.2. Preliminaries

Static, conservative systems with N degrees of freedom will be considered. Restriction to finite values of N does not limit the scope of this work insofar as this restriction conforms to the Finite Element Method (FEM). Only perfect structures subjected to dead loads will be analyzed, and the assumed

material behavior is either rigid or linear elastic. The analysis allows for bifurcation from nonlinear prebuckling paths.

In addition, snap-through will be considered as a mode of loss of stability. Despite the fact that real, imperfect systems practically never exhibit bifurcation behavior but only snap-through or no loss of stability, the main focus of this work is on bifurcation. This approach is justifiable, since conversion of an imperfection-sensitive, ideal, bifurcation system into an imperfection-insensitive system ensures that the associated snap-through buckling path of the corresponding imperfect system is replaced by a monotonically increasing load-displacement path, at least in the vicinity of the theoretical bifurcation point.

For simplicity, *multiple bifurcation* and *hilltop buckling* will be excluded. Moreover, it will be refrained from touching upon *catastrophe theory* ([5, 13]), a commonly employed method in structural stability. Koiter's approach [6] appears to be transferable to the FEM regime more straightforwardly than results from catastrophe theory.

In structural analysis, many systems are known to behave *symmetrically*. Herein, the term symmetric refers to load-displacement paths exhibiting *mirror symmetry*. Similarly, *antisymmetry* means that load displacement paths show antisymmetries. This should not be confused with antisymmetric buckling modes, which may for instance occur in buckling of transversally loaded shallow arches. There, antisymmetry is a geometric property of the buckling shape. Antisymmetric buckling modes usually correspond to symmetric bifurcation (cf. [3, 13]).

It is emphasized that symmetric and antisymmetric bifurcation behavior are not intrinsic properties of a structure, but rather a matter of the choice of coordinates. Identification of a system as symmetric (antisymmetric) requires a statement on the parameter with respect to which symmetry (antisymmetry) is observed. In this work, only symmetry (antisymmetry) with respect to a scalar variable η will be addressed. Obviously, there are systems that are not symmetric (antisymmetric) and that cannot be rendered symmetric (antisymmetric) through diffeomorphic coordinate transformations.

2. Series expansion in the framework of Koiter's initial postbuckling analysis

2.1. Koiter's initial postbuckling analysis

Fig. 1 shows a projection of the load-displacement paths of a system bifurcating at point *C*. The solid line represents a primary path, whereas the dashed line is a secondary path. The latter is parameterized by $\eta \in \mathbb{R}$, defined as zero at *C*. Herein, the subscript $_c$ means evaluation of a quantity at *C*. The reference load $\bar{\mathbf{P}}$ is scaled by a dimensionless load factor λ; $\mathbf{u}$ denotes the vector of generalized displacement coordinates.
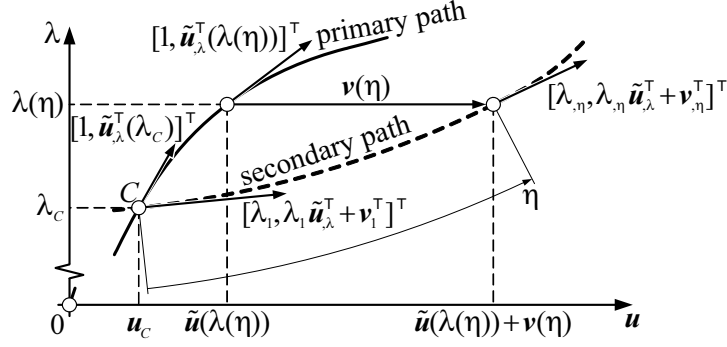
Fig.1: On the series expansion of the secondary path at the bifurcation point C

In [7, 11], Koiter's initial postbuckling analysis [6] was used to expand the out-of-balance force

$$\mathbf{G}(\mathbf{u}, \lambda) := \mathbf{F}^{\mathrm{I}}(\mathbf{u}) - \lambda\, \overline{\mathbf{P}} \in \mathbb{R}^N, \tag{1}$$

where $\mathbf{F}^{\mathrm{I}}(\mathbf{u})$ denotes the internal forces, into an asymptotic series at C. For a static, conservative system, $\mathbf{G}$ can be derived from the potential function V as

$$\mathbf{G} = \frac{\partial V}{\partial \mathbf{u}}. \tag{2}$$

$\mathbf{G}$ vanishes along equilibrium paths in the $\mathbf{u}$-λ-space. $\lambda(\eta)$ is the load parameter at the point of the secondary path defined by η as outlined in Fig. 1. The point on the primary path characterized by the same load is described by the displacement vector $\tilde{\mathbf{u}}(\lambda(\eta))$. Quantities evaluated along the primary path are labeled by an upper tilde. The displacement at the corresponding point of the secondary path can be expressed as $\mathbf{u}(\eta) = \tilde{\mathbf{u}}(\lambda(\eta)) + \mathbf{v}(\eta),$ where $\mathbf{v}$ is the displacement offset which vanishes trivially at C. Hence,

$$\mathbf{G}(\eta) = \mathbf{G}(\tilde{\mathbf{u}}(\lambda(\eta)) + \mathbf{v}(\eta), \lambda(\eta)) = \mathbf{0} \tag{3}$$

must hold along the secondary path. Insertion of the asymptotic series expansions

$$\lambda(\eta) = \lambda_C + \lambda_1\, \eta + \lambda_2\, \eta^2 + \lambda_3\, \eta^3 + \mathcal{O}(\eta^4) \tag{4}$$

$$\mathbf{v}(\eta) = \quad\quad \mathbf{v}_1\, \eta + \mathbf{v}_2\, \eta^2 + \mathbf{v}_3\, \eta^3 + \mathcal{O}(\eta^4) \tag{5}$$

into (3) and expanding the resulting expression into a series in terms of η yields

$$\mathbf{G} = \mathbf{G}_{0C} + \mathbf{G}_{1C}\, \eta + \mathbf{G}_{2C}\, \eta^2 + \mathcal{O}(\eta^3), \tag{6}$$

with

$$\mathbf{G}_{nC} = \frac{\mathbf{G}_{,\eta^n C}}{n!} \quad \forall\, n \in \mathbb{N}. \tag{7}$$

$\mathbb{N}$ denotes the set of natural numbers including zero. Throughout this paper, $(\bullet)_{,\lambda}$ indicates the special rule of differentiation with respect to λ along a direction that is parallel to the primary path [7]. To show its mathematical definition, an arbitrary tensorial quantity $f(\mathbf{u}, \lambda) : \Gamma \to \Lambda$ is introduced. Its argument $(\mathbf{u}, \lambda) \in \Gamma \subset \mathbb{R}^{N+1}$ is a tuple of N generalized displacement coordinates u_i and the load factor λ. Then, $f_{,\lambda}(\mathbf{u}, \lambda) : \Gamma \to \Lambda$ reads as

$$f_{,\lambda}(\mathbf{u}, \lambda) := \frac{\partial \mathbf{f}(\mathbf{u}, \lambda)}{\partial \lambda} + \left. \frac{\partial \mathbf{f}(\mathbf{u} + \alpha\, \tilde{\mathbf{u}}_{,\lambda}(\lambda), \lambda)}{\partial \alpha} \right|_{\alpha=0}, \quad \alpha \in \mathbb{R}. \tag{8}$$

Examples for the coefficients appearing in (6) are

$$\mathbf{G}_{,\eta} = \mathbf{G}_{,\lambda}\,\lambda_{,\eta} + \mathbf{G}_{,\mathbf{u}}\cdot\mathbf{v}_{,\eta},$$

$$\mathbf{G}_{,\eta\eta} = \mathbf{G}_{,\lambda}\,\lambda_{,\eta\eta} + \mathbf{G}_{,\lambda\lambda}\,\lambda_{,\eta}^2 + 2\mathbf{G}_{,\mathbf{u}\lambda}\cdot\mathbf{v}_{,\eta}\,\lambda_{,\eta} + \mathbf{G}_{,\mathbf{uu}}:\mathbf{v}_{,\eta}\otimes\mathbf{v}_{,\eta} + \mathbf{G}_{,\mathbf{u}}\cdot\mathbf{v}_{,\eta\eta} \tag{9}$$

and thus

$$\mathbf{G}_{0C} = \mathbf{0},$$

$$\mathbf{G}_{1C} = \mathbf{G}_{,\mathbf{u}C}\cdot\mathbf{v}_1, \tag{10}$$

$$\mathbf{G}_{2C} = \mathbf{G}_{,\mathbf{u}\lambda C}\cdot\mathbf{v}_1\,\lambda_1 + \frac{1}{2}\mathbf{G}_{,\mathbf{uu}C}:\mathbf{v}_1\otimes\mathbf{v}_1 + \mathbf{G}_{,\mathbf{u}C}\cdot\mathbf{v}_2 ,$$

where the identity

$$\mathbf{G}_{,\lambda^n C} = \mathbf{0} \quad \forall\, n\in\mathbb{N} \tag{11}$$

was used.

Since (3) must hold for any point along the secondary path, i.e., for arbitrary values of η, each coefficient $\mathbf{G}_{nC}$ of the series must vanish. This condition paves the way for successive calculation of the pairs of unknowns $\mathbf{v}_1, \lambda_1, \mathbf{v}_2, \lambda_2$, etc. Premultiplying (6) by $\mathbf{v}_1$ is one of the basic steps of this calculation scheme. The tensor contractions $\mathbf{v}_1\cdot\mathbf{G}_{nC}$ are scalar polynomials in the λ_m ($m\in\{1,2,\ldots,n-1\}$), i.e.,

$$\mathbf{v}_1\cdot\mathbf{G}_{nC} = \sum_{\substack{i_1,\ldots,i_{n-1}\in\mathbb{N} \\ i_1+\ldots+i_{n-1}<n}} A_{n,i_1,\ldots,i_{n-1}}\,\lambda_1^{i_1}\cdots\lambda_{n-1}^{i_{n-1}} = \sum_{i=0}^{n-1} a_{n,i}\,\lambda_1^{i} \qquad \forall\, n\in\mathbb{N}, \quad A_{n,i_1,\ldots,i_{n-1}}\in\mathbb{R}. \tag{12}$$

As indicated by (12), the order $i_1+\ldots+i_{n-1}$ of the monomials $\lambda_1^{i_1}\cdots\lambda_{n-1}^{i_{n-1}}$ is always smaller than n. The coefficients $A_{n,i_1,\ldots,i_{n-1}}$ are constants, i.e., λ_m does not appear in their expressions. $\mathbf{v}_1\cdot\mathbf{G}_{nC}$ may alternatively be interpreted as a polynomial in λ_1, as shown by the rightmost expression of (12). This will be addressed in more detail in the following Sections.

2.2. Coefficients of series expansion

The coefficients $a_{n,i}$ in (12) are themselves polynomials in λ_r ($r\in\mathbb{N}\backslash\{0,1\}$). The lengthy mathematical expressions of the coefficients $A_{n,i_1,\ldots,i_{n-1}}$ and $a_{n,i}$ are listed in Mang *et al.* [7]. For a concise overview, the coefficients $a_{n,i}$ were arranged as a triangular array

$$
\begin{array}{llllll}
\underline{a_{1,0}} & & & & & \\
a_{2,1} & \underline{a_{2,0}} & & & & \\
a_{3,2} & \underline{a_{3,1}} & \underline{a_{3,0}} & & & \\
a_{4,3} & \underline{a_{4,2}} & a_{4,1} & \underline{a_{4,0}} & & \\
\vdots & \ddots & & & \ddots & \\
a_{n,n-1} & \cdots & a_{n,i} & \cdots & & \underline{a_{n,0}} \\
\vdots & & \ddots & & & \ddots \\
\end{array}
\tag{13}
$$

The underlining is only relevant for symmetric bifurcation. Its meaning will become clear later on. The last element in each row of (13) can be written as

$$a_{n,0} = a_n - \lambda_{n-1} \qquad \forall\, n\in\mathbb{N}\backslash\{0,1\}. \tag{14}$$

2.3. Imperfection sensitivity versus imperfection insensitivity

With the help of

$$m_{\min} := \min\{m \mid m \in \mathbb{N}\backslash\{0\}, \lambda_m \neq 0\}, \tag{15}$$

a necessary and sufficient condition for imperfection insensitivity is obtained as

$$m_{\min} \text{ is even } \wedge \; \lambda_{m_{\min}} > 0. \tag{16}$$

If this condition is not satisfied, the system is imperfection sensitive. According to Bochenek [1], symmetric behavior in the *vicinity* of C, characterized by $\lambda_1 = 0$ and satisfaction of $\lambda_{,\eta}(\eta)\,\mathrm{sign}(\eta) \geq 0$ in a local domain around C, is necessary and sufficient for imperfection insensitivity. This is equivalent to (16).

3. Symmetric bifurcation

3.1. Definition

Bifurcation behavior is qualified as *symmetric* with respect to the parameter η if it obeys the definition:

$$\lambda(\eta) = \lambda(-\eta) \quad \wedge \tag{17}$$
$$\mathbf{v}(\eta) = \mathbf{T}(\mathbf{v}(-\eta)) \quad \wedge \tag{18}$$
$$\tilde{\mathbf{u}}(\lambda(\eta)) = \mathbf{T}(\tilde{\mathbf{u}}(\lambda(\eta))), \tag{19}$$

where the linear mapping $\mathbf{T}: \mathbb{R}^N \to \mathbb{R}^N$ is an element of a symmetry group. Insertion of (4) into (17) yields

$$\lambda_1 = \lambda_3 = \lambda_5 = ... = 0. \tag{20}$$

A convenient method of testing if a system satisfies the postulated conditions (17)-(19) will be developed in the following. Only situations where $\mathbf{T}$ is defined by

$$\mathbf{T} := \begin{bmatrix} 1 & & & \\ & \ddots & & \mathbf{0} \\ & & 1 & \\ \mathbf{0} & & & -1 \end{bmatrix} = \begin{bmatrix} T_{ij} \end{bmatrix} = \begin{bmatrix} \delta_{ij}(1 - 2\delta_{iN}) \end{bmatrix} \tag{21}$$

will be considered. This is no restriction, because for symmetric systems it is always possible to find coordinates such that (17)-(19) hold together with the definition (21). As will be demonstrated in the example 6.2, it is possible to construct systems that bifurcate symmetrically simply by supplementing a non-symmetric bifurcation system by its mirror image.

3.2. Vanishing of the coefficients $a_{n,0}$

Eq. (12) represents polynomials in λ_1, which must vanish along any equilibrium path. Therefore, $\lambda_1 = 0$ implies

$$a_{n,0} = 0 \qquad \forall\, n \in \mathbb{N}\backslash\{0\}, \tag{22}$$

i.e., for symmetric bifurcation, the last element of each row of (13) must be zero.

3.3. Potential energy

It is assumed that the continuously differentiable expression of the potential energy $V(\mathbf{u}, \lambda): \Gamma \to \mathbb{R}$ obeys the symmetry condition

$$V(\mathbf{u}, \lambda) = V(\mathbf{T} \cdot \mathbf{u}, \lambda) \quad \forall\, (\mathbf{u}, \lambda) \in \Gamma. \tag{23}$$

It follows from (21) and (23) that an equilibrium path exists which is restricted to the hyperplane $u_N = 0$. Usually, it is referred to as the primary path. This proves (19). Moreover, (1), (2), and (23) prove (17).

3.4. Tensors derived from V

In the mathematical analysis of the postbuckling behavior, tensors are used which are derivations of V with respect to $\mathbf{u}$ and/or λ. The components of these tensors are

$$V_{\underbrace{ij...}_{m\text{ times}},\lambda^n} := \left[\frac{\partial^m V}{\partial u_i \partial u_j ...} \right]_{,\lambda^n} \qquad i, j,... \in \{1,2,...,N\}, \quad n \in \mathbb{N}. \tag{24}$$

$(\bullet)_{,\lambda^n}$ means that the differentiation operation $(\bullet)_{,\lambda}$ defined in (8) is applied n times. Because of (23),

$$\left. V_{\underbrace{ij...}_{m\text{ times}},\lambda^n} \right|_{u_N=0} = 0 \quad \text{if } N \text{ appears in the } m\text{-tuple of indices } (ij...) \text{ an odd number of times.}$$

$$\tag{25}$$

Eq. (25) is essentially based on the fact that the operation $(\bullet)_{,\lambda}$ allows only infinitesimal displacements within the hyperplane $u_N = 0$, i.e., no differentiations with respect to u_N are permitted. For example, the tangent stiffness matrix along the primary path and its derivatives with respect to λ have the structure

$$\tilde{\mathbf{K}}_{T,\lambda^n} = \left[V_{,ij,\lambda^n}(\tilde{\mathbf{u}}, \tilde{\lambda}) \right] = \begin{bmatrix} & & & \vdots & 0 \\ & \tilde{\mathbf{K}}_{T,\lambda^n}^{\text{upper left}} & & \vdots & \vdots \\ & & & \vdots & 0 \\ \hline 0 & \cdots & 0 & \vdots & V_{,NN,\lambda^n} \end{bmatrix}. \tag{26}$$

That is, $\mathbf{G}_{,\mathbf{u}\lambda^n} = \tilde{\mathbf{K}}_{T,\lambda^n}$. Specialization of the lower right component for C and $n = 0$ yields

$$V_{,NN,\lambda^0 C} = 0, \tag{27}$$

which reflects the vanishing of an eigenvalue of $\tilde{\mathbf{K}}_T$ at C. In the following, additional examples of tensors derived from V will be given. The expressions may be deduced from (2)-(12) or can be found in [7].

$$\begin{aligned} \tilde{\mathbf{K}}_{T,\mathbf{u}} &= V_{,\mathbf{uuu}} \\ \tilde{\mathbf{K}}_{T,\lambda} &= V_{,\mathbf{uu},\lambda} = V_{,\mathbf{uuu}} \cdot \tilde{\mathbf{u}}_{,\lambda} \\ \tilde{\mathbf{K}}_{T,\mathbf{u}\lambda} &= V_{,\mathbf{uuu},\lambda} = V_{,\mathbf{uuuu}} \cdot \tilde{\mathbf{u}}_{,\lambda} \\ \tilde{\mathbf{K}}_{T,\lambda\lambda} &= V_{,\mathbf{uu},\lambda^2} = V_{,\mathbf{uuuu}} : \tilde{\mathbf{u}}_{,\lambda} \otimes \tilde{\mathbf{u}}_{,\lambda} + V_{,\mathbf{uuu}} \cdot \tilde{\mathbf{u}}_{,\lambda\lambda} \end{aligned} \tag{28}$$

The vectors $\tilde{\mathbf{u}}_{,\lambda}, \tilde{\mathbf{u}}_{,\lambda\lambda}, \ldots$ are the partial derivatives of the displacements with respect to λ. These vectors are used to realize the operation $(\bullet)_{,\lambda}$ in the computation of the tensors.

3.5. Structure of the vectors $\mathbf{v}_i$

Apart from a scaling parameter, the eigenvector $\mathbf{v}_1$ is defined by the equation

$$\tilde{\mathbf{K}}_{TC} \cdot \mathbf{v}_1 = \mathbf{0}, \tag{29}$$

which, because of (27), always has a non-trivial solution. Hence,

$$\mathbf{v}_1 = \begin{bmatrix} 0 & \cdots & 0 & p \end{bmatrix}^{\mathrm{T}} \qquad p \in \mathbb{R} \backslash \{0\}. \tag{30}$$

Apart from their length, the remaining vectors $\mathbf{v}_i$ $(i \neq 1)$ are uniquely defined in [7] if the *orthogonality condition*

$$\mathbf{v}_1 \cdot \mathbf{v}_i = 0 \qquad \forall i > 1, \tag{31}$$

proposed in [2], is introduced. It follows from (5), (30), and (31) that

$$u_N = v_N(\eta) = p\eta. \tag{32}$$

Because of (21) and (23), V is invariant with respect to sign changes of u_N. However, it is generally not invariant with respect to sign changes of u_i $(i \neq N)$. If V is formulated as a function of η, symmetry requires that $V(\eta) = V(-\eta)$. Therefore, the displacements u_i $(i \neq N)$ must not depend on the sign of η. Together with (23) and (32), this proves $\mathbf{u}(\eta) = \mathbf{T} \cdot \mathbf{u}(-\eta)$, which implies (18). The results of this Subsection can be summarized as follows:

$$\begin{aligned} \mathbf{v}_1 &= \begin{bmatrix} 0 & \cdots & 0 & p \end{bmatrix}^{\mathrm{T}} & p &\in \mathbb{R} \backslash \{0\} \\ \mathbf{v}_1 \cdot \mathbf{v}_i &= \mathbf{0} & \forall i &> 1 \\ \mathbf{v}_i &= \mathbf{0} & \forall i &= \{3, 5, 7, \ldots\}. \end{aligned} \tag{33}$$

3.6. Vanishing of coefficients

According to the definition given in Subsection 2.1, $\mathbf{G}_{nC}$ $(n \in \mathbb{N})$ is a *linear combination* of terms having the structure

$$\mathbf{G}_{,\mathbf{u}^q \lambda^r C} \vdots \ldots \underbrace{\mathbf{v}_a \otimes \mathbf{v}_b \otimes \ldots}_{q \text{ times}} \cdot \underbrace{\lambda_\alpha \lambda_\beta \ldots}_{r \text{ times}} \qquad a, b, \ldots, \alpha, \beta, \ldots \in \mathbb{N} \backslash \{0\}, \quad q, r \in \mathbb{N}. \tag{34}$$

Because of (7) and the fact that η does not explicitly appear in $\mathbf{G}(\tilde{\mathbf{u}}(\lambda) + \mathbf{v}, \lambda)$ but only in (4) and (5),

$$a + b + \ldots + \alpha + \beta + \ldots = n. \tag{35}$$

Because of (11), i.e., $\mathbf{G}_{,\lambda^n C} \lambda_1^n = \mathbf{0}$, G_{nC} is a polynomial in λ_1 of an order smaller than n, as reflected by (12). Generally, the highest power of λ_1 appearing in $\mathbf{G}_{nC}$ is λ_1^{n-1}. Introduction of the abbreviation $\Diamond := \tilde{\mathbf{K}}_{T,\lambda C} : \mathbf{v}_1 \otimes \mathbf{v}_1 \neq 0$ and multiplication of $\mathbf{G}_{nC}$ by $(-\mathbf{v}_1/\Diamond)$ renders the scalar polynomials in λ_1, which make up the respective rows of (13). $a_{n,i}$ $(i<n)$ is the coefficient of λ_1^i. Hence, $a_{n,i}$ is a linear combination of terms of the structure

$$-\frac{1}{\Diamond} V_{,\mathbf{u}^{q+1} \lambda^r C} \vdots \ldots \underbrace{\mathbf{v}_1 \otimes \mathbf{v}_a \otimes \mathbf{v}_b \otimes \ldots}_{q+1 \text{ times}} \cdot \underbrace{\lambda_\alpha \lambda_\beta \ldots}_{r-i \text{ times}} \qquad a, b, \ldots \in \mathbb{N} \backslash \{0\}, \quad \alpha, \beta, \ldots \in \mathbb{N} \backslash \{0,1\}, \quad q, r \in \mathbb{N},$$
$$\tag{36}$$

where (2) was used. The discussion is now restricted to every second column of (13) characterized by an *even* integer value $n-i$. In this case,

$$1 + a + b + \ldots + \alpha + \beta + \ldots = n - i + 1 \tag{37}$$

from (36) is an *odd* integer, e.g.

$$1 + a + b + \ldots + \alpha + \beta + \ldots = \begin{cases} 3 & \text{for } a_{i+2,i} \\ 5 & \text{for } a_{i+4,i} \\ 7 & \text{for } a_{i+6,i} \\ \vdots & \vdots \end{cases}. \tag{38}$$

If $\{a, b, ..., \alpha, \beta, ...\} \cap \{3, 5, 7, ...\} \neq \{\ \}$, (36) vanishes because of (20) and (33). Otherwise, it contains $\mathbf{v}_1$ an odd number of times and vanishes because of (25). Hence, $a_{n,i} = 0$ if $n - i$ is an even integer, i.e., every second column of (13) vanishes for symmetric bifurcation.

The proof given in this Subsection will be illustrated in the following Subsections 3.7 and 3.8, which explicitly contain the expressions appearing in the second and fourth column of (13).

3.7. Vanishing of the coefficients $a_{i+2,i}$

Introducing the function

$$B_2 := -\frac{1}{\Diamond}\left(\tilde{\mathbf{K}}_T : \mathbf{v}_1 \otimes \mathbf{v}_2 + \frac{1}{2}\mathbf{K}_{T,\mathbf{u}} \vdots \mathbf{v}_1 \otimes \mathbf{v}_1 \otimes \mathbf{v}_1 \right), \tag{39}$$

it follows from the definition of the coefficients $a_{i+2,i}$ (cf. [7]) that

$$a_{i+2,i} = \frac{1}{i!}[B_2]_{,\lambda^i C}. \tag{40}$$

Eq. (40) is not restricted to symmetric bifurcation to which (33) applies. (40) conforms to (36) and (38). Hence, any non-zero component of the tensors $\mathbf{v}_1 \otimes \mathbf{v}_2$ and $\mathbf{v}_1 \otimes \mathbf{v}_1 \otimes \mathbf{v}_1$ has an index that contains N once or three times, respectively. Because of (25), all tensor contractions in (40) yield zero. This shows that for symmetric bifurcation the second column of (13) vanishes.

3.8. Vanishing of the coefficients $a_{i+4,i}$

Introducing the function

$$B_4 := -\frac{1}{\Diamond}\left(\lambda_3 \tilde{\mathbf{K}}_{T,\lambda} : \mathbf{v}_1 \otimes \mathbf{v}_1 + \lambda_2 \left(\tilde{\mathbf{K}}_{T,\lambda} : \mathbf{v}_1 \otimes \mathbf{v}_2 + \frac{1}{2}\mathbf{K}_{T,\mathbf{u}\lambda} \vdots \mathbf{v}_1 \otimes \mathbf{v}_1 \otimes \mathbf{v}_1 \right) + \tilde{\mathbf{K}}_T : \mathbf{v}_1 \otimes \mathbf{v}_4 + \mathbf{K}_{T,\mathbf{u}} \vdots \mathbf{v}_1 \otimes \mathbf{v}_1 \otimes \mathbf{v}_3 \right.$$
$$\left. + \frac{1}{2}\mathbf{K}_{T,\mathbf{u}} \vdots \mathbf{v}_1 \otimes \mathbf{v}_2 \otimes \mathbf{v}_2 + \frac{1}{2}\mathbf{K}_{T,\mathbf{uu}} \vdots\vdots \mathbf{v}_1 \otimes \mathbf{v}_1 \otimes \mathbf{v}_1 \otimes \mathbf{v}_2 + \frac{1}{24}\mathbf{K}_{T,\mathbf{uuu}} \vdots\vdots \mathbf{v}_1 \otimes \mathbf{v}_1 \otimes \mathbf{v}_1 \otimes \mathbf{v}_1 \otimes \mathbf{v}_1 \right), \tag{41}$$

it follows from the definition of the coefficients $a_{n+4,n}$ (cf. [7]) that

$$a_{i+4,i} = \frac{1}{i!}[B_4]_{,\lambda^i C}. \tag{42}$$

Eq. (42) is not restricted to symmetric bifurcation to which (20), (25), and (33) apply. (42) conforms to (36) and (38). Hence, $a_{i+4,i} = 0$. This shows that for symmetric bifurcation the fourth column of (13) vanishes.

By giving the full expressions, it was shown that the coefficients $a_{i+2,i}$ and $a_{i+4,i}$ vanish. The same can be done for the columns 6, 8, etc. of (13), although this involves lengthy mathematical expressions.

3.9. Conditions for the symmetry of λ

So far, it was proved that for symmetric bifurcation all underlined terms in (13) vanish. However, this is not sufficient for $\lambda(\eta) = \lambda(-\eta)$ (cf. (17)). Following (14), it is necessary and sufficient for $\lambda(\eta) = \lambda(-\eta)$ that

$$a_{n,0} - a_n = 0 \qquad \forall\, n \in \{2, 4, ...\}. \tag{43}$$

Since $\lambda_1 = 0$ requires (22), (43) disintegrates. Hence,

$$a_{n,0} = a_n = 0 \qquad \forall\, n \in \{2, 4, ...\} \tag{44}$$

is necessary and sufficient for $\lambda(\eta) = \lambda(-\eta)$.

3.10. Sufficient conditions for symmetric bifurcation

The following conditions are sufficient for symmetric bifurcation (see (17)-(19)):

$$
\begin{aligned}
&\exists\, \tilde{\mathbf{u}}(\lambda) : \tilde{u}_N(\lambda) = 0 && \text{(primary path)}\\
&\wedge\, a_{n,0} = a_n = 0 && \forall\, n \in \{2, 4, ...\}\\
&\wedge\, \mathbf{v}_1 = \begin{bmatrix} 0 & \cdots & 0 & p \end{bmatrix}^{\mathrm{T}} && p \in \mathbb{R}\backslash\{0\}\\
&\wedge\, \mathbf{v}_1 \cdot \mathbf{v}_i = 0 && \forall\, i \neq 1\\
&\wedge\, \mathbf{v}_i = \mathbf{0} && \forall\, i = \{3,5,7,...\}.
\end{aligned}
\tag{45}
$$

Testing a bifurcation problem for symmetry by means of (45) is a difficult task, since satisfaction of *infinitely* many conditions needs to be proved. This is a consequence of the asymptotic series expansion of **G**. Starting out from the expression of the potential energy *V*, only the *single* condition (23) would have to be examined.

4. Antisymmetric bifurcation

4.1. Definition

Bifurcation behavior is qualified as *antisymmetric* with respect to the parameter η if it obeys the definition:

$$\lambda(\eta) - \lambda_C = -(\lambda(-\eta) - \lambda_C) \quad \wedge \tag{46}$$

$$\mathbf{v}(\eta) = -\mathbf{v}(-\eta) \quad \wedge \tag{47}$$

$$\tilde{\mathbf{u}}(\lambda(\eta)) = -\tilde{\mathbf{u}}(\lambda(-\eta)). \tag{48}$$

Hence, any equilibrium path in Γ is *centrosymmetrical* with respect to point $(\tilde{\mathbf{u}}(\lambda_C), \lambda_C)$. In some cases, a situation fulfilling (46)-(48) can be achieved by means of diffeomorphic coordinate transformations. This is the rationale for using these conditions in the sequel without loss of generality. (46) may be reduced to $\lambda(\eta) = -\lambda(-\eta)$ by an appropriate shift of the load level zero. Insertion of (4) and (5) into (46) and (47), respectively, yields

$$\lambda_2 = \lambda_4 = \lambda_6 = ... = 0, \tag{49}$$

$$\mathbf{v}_2 = \mathbf{v}_4 = \mathbf{v}_6 = ... = \mathbf{0}. \tag{50}$$

Therefore, according to the definition given in Subsection 2.3, an antisymmetric bifurcation system is always *imperfection sensitive*. A convenient method of testing if a system satisfies the postulated conditions (46)-(48) will be suggested in the following.

4.2. Potential energy

In contrast to Subsection 3.3, the potential energy is now written as $V(\mathbf{u}, \lambda - \lambda_C) : \Gamma \to \mathbb{R}$ with $(\mathbf{u}, \lambda - \lambda_C) \in \Gamma \subset \mathbb{R}^{N+1}$ and split into four parts which depend only on a subset of the coordinates **u**. For this purpose, the projection matrices

$$\mathbf{T}_1 := \frac{1}{2}(\mathbf{I} + \mathbf{T}), \qquad \mathbf{T}_2 := \frac{1}{2}(\mathbf{I} - \mathbf{T}) = \mathbf{I} - \mathbf{T}_1, \tag{51}$$

with **T** from (21), are introduced. The potential function *V* may be written as

$$V(\mathbf{u}, \lambda - \lambda_C) = V_S(\mathbf{T}_1 \cdot \mathbf{u}) + V_A(\mathbf{T}_2 \cdot \mathbf{u}) + (\lambda - \lambda_C)\left(\overline{V}_A(\mathbf{T}_1 \cdot \mathbf{u}) + \overline{V}_S(\mathbf{T}_2 \cdot \mathbf{u})\right) \quad \forall\, (\mathbf{u}, \lambda - \lambda_C) \in \Gamma,$$
$$(52)$$

since λ scales a reference load. The matrices $\mathbf{T}_1$ and $\mathbf{T}_2$ must not be removed from the arguments of (52), because they ensure that V_S and $\overline{V}_A$ do not depend on u_N, whereas V_A and $\overline{V}_S$ depend only on u_N. The split of the potential according to (52) is no restriction, because a coordinate transformation which diagonalizes $\mathbf{K}_T$ can always be found.

Antisymmetric bifurcation requires that V obeys (52) together with

$$V_S(\mathbf{T}_1 \cdot \mathbf{u}) = V_S(-\mathbf{T}_1 \cdot \mathbf{u}) \quad \wedge \quad V_A(\mathbf{T}_2 \cdot \mathbf{u}) = -V_A(-\mathbf{T}_2 \cdot \mathbf{u}) \quad \wedge$$
$$\overline{V}_A(\mathbf{T}_1 \cdot \mathbf{u}) = -\overline{V}_A(-\mathbf{T}_1 \cdot \mathbf{u}) \quad \wedge \quad \overline{V}_S(\mathbf{T}_2 \cdot \mathbf{u}) = \overline{V}_S(-\mathbf{T}_2 \cdot \mathbf{u}) .$$
$$(53)$$

This does not allow the general conclusion that an equilibrium path restricted to the hyperplane $u_N = 0$ exists.

4.3. Structure of the vectors $\mathbf{v}_i$

Apart from a scaling parameter, the eigenvector $\mathbf{v}_1$ is defined by the equation

$$\tilde{\mathbf{K}}_{TC} \cdot \mathbf{v}_1 = \mathbf{0}, \tag{54}$$

just as for symmetric bifurcation. Following from (52), the mixed derivatives $V_{,iN,\lambda^n}$ $(i \neq N)$ vanish. Hence,

$$\mathbf{v}_1 = \begin{bmatrix} 0 & \cdots & 0 & p \end{bmatrix}^{\mathrm{T}} \qquad p \in \mathbb{R}\backslash\{0\}. \tag{55}$$

The orthogonality condition (31) also applies to antisymmetric bifurcation. Therefore (5), (31), and (55) yield

$$u_N = v_N(\eta) = p\,\eta. \tag{56}$$

4.4. Verification

The equilibrium conditions following from (52) are

$$V_{,\mathbf{u}} = \mathbf{T}_1 \cdot \left(V_{S,\mathbf{u}}(\mathbf{T}_1 \cdot \mathbf{u}) + (\lambda - \lambda_C)\overline{V}_{A,\mathbf{u}}(\mathbf{T}_1 \cdot \mathbf{u})\right) + \mathbf{T}_2 \cdot \left(V_{A,\mathbf{u}}(\mathbf{T}_2 \cdot \mathbf{u}) + (\lambda - \lambda_C)\overline{V}_{S,\mathbf{u}}(\mathbf{T}_2 \cdot \mathbf{u})\right) = \mathbf{0},$$
$$(57)$$

which disintegrate into

$$V_{S,\mathbf{u}}(\mathbf{T}_1 \cdot \mathbf{u}) + (\lambda - \lambda_C)\overline{V}_{A,\mathbf{u}}(\mathbf{T}_1 \cdot \mathbf{u}) = \mathbf{0} \quad \wedge \quad V_{A,\mathbf{u}}(\mathbf{T}_2 \cdot \mathbf{u}) + (\lambda - \lambda_C)\overline{V}_{S,\mathbf{u}}(\mathbf{T}_2 \cdot \mathbf{u}) = \mathbf{0}. \tag{58}$$

Partial derivation of (53) with respect to $\mathbf{u}$ yields

$$V_{S,\mathbf{u}}(\mathbf{T}_1 \cdot \mathbf{u}) = -V_{S,\mathbf{u}}(-\mathbf{T}_1 \cdot \mathbf{u}), \quad V_{A,\mathbf{u}}(\mathbf{T}_2 \cdot \mathbf{u}) = V_{A,\mathbf{u}}(-\mathbf{T}_2 \cdot \mathbf{u}),$$
$$\overline{V}_{A,\mathbf{u}}(\mathbf{T}_1 \cdot \mathbf{u}) = \overline{V}_{A,\mathbf{u}}(-\mathbf{T}_1 \cdot \mathbf{u}), \quad \overline{V}_{S,\mathbf{u}}(\mathbf{T}_2 \cdot \mathbf{u}) = -\overline{V}_{S,\mathbf{u}}(-\mathbf{T}_2 \cdot \mathbf{u}) .$$
$$(59)$$

Insertion of (59) into (58) leads to

$$-V_{S,\mathbf{u}}(-\mathbf{T}_1 \cdot \mathbf{u}) + (\lambda - \lambda_C)\overline{V}_{A,\mathbf{u}}(-\mathbf{T}_1 \cdot \mathbf{u}) = \mathbf{0} \quad \wedge \quad V_{A,\mathbf{u}}(-\mathbf{T}_2 \cdot \mathbf{u}) - (\lambda - \lambda_C)\overline{V}_{S,\mathbf{u}}(-\mathbf{T}_2 \cdot \mathbf{u}) = \mathbf{0}.$$
$$(60)$$

Since (58) and (60) are equivalent,

$$V_{,\mathbf{u}}(\mathbf{u}, \lambda - \lambda_C) = \mathbf{0} \quad \Leftrightarrow \quad V_{,\mathbf{u}}(-\mathbf{u}, -(\lambda - \lambda_C)) = \mathbf{0} \quad \forall\, (\mathbf{u}, \lambda - \lambda_C) \in \Gamma. \tag{61}$$

This directly proves (46) and (48). Since the displacements along the secondary path can be written as $\tilde{\mathbf{u}}(\lambda(\eta)) + \mathbf{v}(\eta)$, (61) also verifies (47). It is emphasized that classification of equilibrium paths as *primary* and *secondary* is generally not as clear-cut as for symmetric bifurcation. In fact, the

statements (52)-(61) are equally applicable to any equilibrium path of an antisymmetric bifurcation system.

4.5. Sufficient conditions for antisymmetric bifurcation

The following conditions are sufficient for antisymmetric bifurcation:

$$
\begin{aligned}
&\exists\,\tilde{\mathbf{u}}(\lambda-\lambda_C):\tilde{\mathbf{u}}(\lambda-\lambda_C)=-\tilde{\mathbf{u}}(-(\lambda-\lambda_C))\\
&\qquad\wedge\lambda_i=0\quad\forall\,i\in\{2,4,6,...\}\\
&\wedge\mathbf{v}_1=\begin{bmatrix}0&\cdots&0&p\end{bmatrix}^{\mathrm{T}}\quad p\in\mathbb{R}\backslash\{0\}\\
&\qquad\wedge\mathbf{v}_1\cdot\mathbf{v}_i=0\quad\forall\,i\neq1\\
&\qquad\wedge\mathbf{v}_i=\mathbf{0}\quad\forall\,i=\{2,4,6,...\}.
\end{aligned}\tag{62}
$$

Testing a bifurcation problem for antisymmetry by means of (62) is a difficult task, since *infinitely* many expressions need to be examined. Again, this is a consequence of the asymptotic series expansion of **G**. Starting out from the expression (52), it would only have to be shown that the conditions (53) were satisfied.

The relations between antisymmetric bifurcation and the vanishing of coefficients in the triangular array (13) are not as straightforward as in case of symmetric bifurcation. Since the specific properties of (13) for antisymmetric bifurcation will not be used in the sequel, they are omitted here.

5. Zero-stiffness postbuckling behavior

5.1. Definition

Whereas symmetric and antisymmetric bifurcation behavior are global properties of all equilibrium paths of a system, zero-stiffness bifurcation concerns only the postbuckling path, but does not determine the shape of other equilibrium paths. Therefore, the zero-stiffness case cannot be defined in terms of a potential function *V* which is valid in the whole domain Γ. Zero-stiffness requires that

$$
\lambda(\eta)-\lambda_C=0\tag{63}
$$

holds along the postbuckling path. Hence, it satisfies both, (17) and (46). Considering the third condition (33) for symmetric bifurcation and the condition (50) for antisymmetric bifurcation, it follows that

$$
\mathbf{v}(\eta)=\eta\,\mathbf{v}_1.\tag{64}
$$

In essence, a zero-stiffness postbuckling path may be thought of as being both, a symmetric and an antisymmetric equilibrium path. This is the rationale for the construction of a system with zero-stiffness postbuckling behavior by augmenting an antisymmetric bifurcation system by its mirror image, as will be demonstrated in the example given in Subsection 6.4. Finally, a suitable definition of a zero-stiffness postbuckling path is

$$
\lambda(\eta)-\lambda_C=0\quad\wedge\tag{65}
$$
$$
\mathbf{v}(\eta)=\mathbf{T}(\mathbf{v}(-\eta))=-\mathbf{v}(-\eta).\tag{66}
$$

Without loss of generality, the definition of **T** given in (21) was used here again.

5.2. Sufficient conditions for zero-stiffness postbuckling behavior

The following conditions are sufficient for zero-stiffness postbuckling behavior:

$$\lambda_i = 0 \quad \forall\, i \in \mathbb{N}\backslash\{0\}$$
$$\wedge\, \mathbf{v}_1 = \begin{bmatrix} 0 & \cdots & 0 & p \end{bmatrix}^{\mathrm{T}} \quad p \in \mathbb{R}\backslash\{0\} \tag{67}$$
$$\wedge\, \mathbf{v}_i = \mathbf{0} \quad \forall\, i \in \mathbb{N}\backslash\{0,1\}.$$

With this definition, in principle, *infinitely* many conditions must be checked. General statements about the coefficients of the triangular array (13) are not possible in this case, since the prebuckling behavior and in turn $\mathbf{K}_T$ is not specified.

6. Examples

In this Section, static, finite-degrees-of-freedom systems will be presented, which bifurcate in one of the distinct categories described in the previous Sections. The simplicity of the analyzed low-dimensional structures allows both, drawing focus on corroborating the foregoing theoretical findings and quick repetition of the relatively simple computations.

6.1. Non-symmetric bifurcation

The general case of non-symmetric bifurcation is characterized by postbuckling behavior that does not exhibit specific symmetry properties. Fig. 2(a) shows a system which bifurcates non-symmetrically. Bar ① is mounted on two turning-and-sliding joints. Bar ② can only rotate with respect to a horizontal axis; u_2 defines the angle of rotation. The angle between this axis and bar ① is denoted as u_1. A vertical load $\lambda \bar{P}$ ($\lambda \in \mathbb{R}$) is exerted on the upper turning-and-sliding joint. The system is supported by four linear elastic springs k, γk, κk, and χk ($\gamma, \kappa, \chi \in [0, +\infty)$). Because of mirror symmetry, the factor $\mu \in \mathbb{R}$ can be restricted to non-negative values without loss of generality. The unloaded position, which is delineated in Fig. 2(a) in gray color, is defined as $(u_1, u_2) = (\pi/4, 0)$.
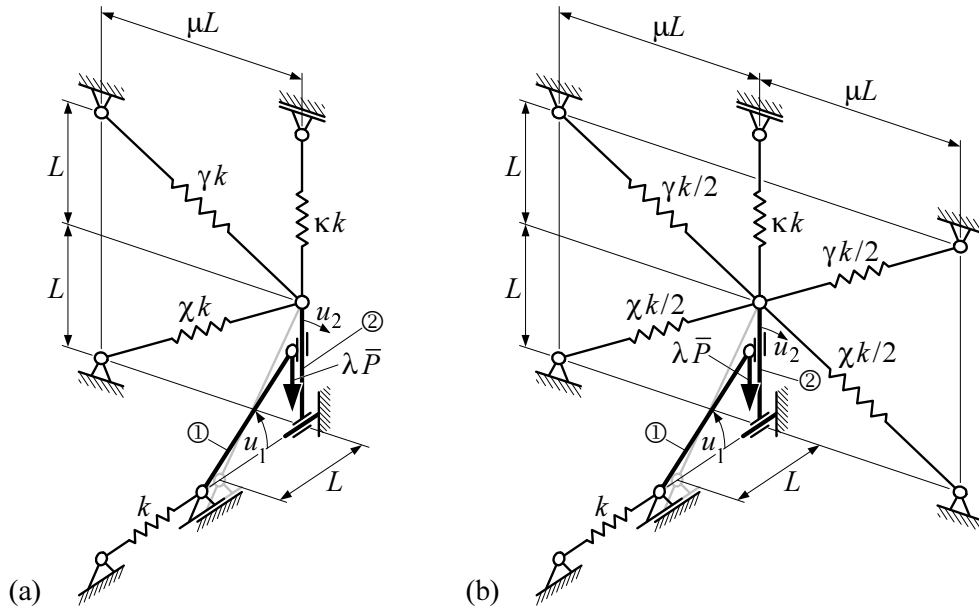

Fig. 2: Static systems with two degrees of freedom, which bifurcate (a) non-symmetrically, (b) symmetrically

The potential energy reads as

$$V(u_1, u_2, \lambda) = U(u_1, u_2) + W(u_1, u_2, \lambda), \tag{68}$$

where

$$U(u_1, u_2) = \frac{1}{2} k L^2 \left(\left(1 - \sqrt{2}\cos(u_1)\right)^2 + \gamma \left(\sqrt{1+\mu^2} - \sqrt{(2-\cos(u_2))^2 + (\mu+\sin(u_2))^2} \right)^2 \right.$$
$$\left. + \kappa \left(1 - \cos(u_2)\right)^2 + \chi \left(\sqrt{1+\mu^2} - \sqrt{\cos(u_2)^2 + (\mu+\sin(u_2))^2} \right)^2 \right) \tag{69}$$

is the strain energy and

$$W(u_1, u_2, \lambda) = -\lambda \bar{P} L \left(1 - \sqrt{2}\sin(u_1)\cos(u_2)\right) \tag{70}$$

is the potential energy of the external load. V is neither symmetric with respect to u_1 nor with respect to u_2. The equilibrium equations are obtained as $V_{,1} = 0$ and $V_{,2} = 0$. The load-displacement relation for the primary path follows as

$$\lambda(u_1) = \frac{kL}{\bar{P}} \left(\sqrt{2}\sin(u_1) - \tan(u_1) \right), \quad u_2 = 0. \tag{71}$$

Analytical solutions for the secondary load-displacement path could not be deduced. Hence, the postbuckling paths were constructed pointwise, using a numerical solver.

Generally, the system does not bifurcate symmetrically. However, a special set of parameters can be found, such that, irrespectively of λ_2, at least $\lambda_1 = \lambda_3 = 0$ holds. This is the case for $\mu = 1.671$ and $\chi/\gamma = 1.717$. The remaining parameter values are chosen as $L = 1$m, $k = 1$N/m, $\chi = 0.05$, and $\bar{P} = 1$N. The structural parameter that is varied for conversion from imperfection sensitivity into imperfection insensitivity is κ, which scales the stiffness of the vertical spring. The system is imperfection sensitive for $\kappa \in [0, 0.0454)$ and imperfection insensitive for $\kappa \geq 0.0454$. For $\kappa = 0.0454$, the components of the triangular array of coefficients (13) are:

$$\begin{matrix} a_{1,0} \\ a_{2,1} & a_{2,0} \\ a_{3,2} & a_{3,1} & a_{3,0} \\ a_{4,3} & a_{4,2} & a_{4,1} & a_{4,0} \\ a_{5,4} & a_{5,3} & a_{5,2} & a_{5,1} & a_{5,0} \end{matrix} = \begin{matrix} 0 \\ -1 & 0 \\ 2.634 & 0 & 0 \\ 14.74 & 0 & p^2/6 & 0 \\ 51.60 & 0 & -0.5392\,p^2 & 0 & 0. \end{matrix} \tag{72}$$

Moreover,

$$\lambda_1 = 0, \qquad \lambda_2 = 0, \qquad \lambda_3 = 0, \quad \lambda_4 = 9.79 \cdot 10^{-3} p^4, \quad \lambda_5 = -9.27 \cdot 10^{-3} p^5,$$
$$\mathbf{v}_1 = \begin{pmatrix} 0 \\ p \end{pmatrix}, \quad \mathbf{v}_2 = \begin{pmatrix} 0.048\,p^2 \\ 0 \end{pmatrix}, \quad \mathbf{v}_3 = \mathbf{0}, \quad \mathbf{v}_4 = \begin{pmatrix} -0.011\,p^4 \\ 0 \end{pmatrix}, \quad \mathbf{v}_5 = \mathbf{0}. \tag{73}$$

Fig.3: Coefficients of asymptotic series expansion of λ for varying κ

It is emphasized that $\lambda_1, \lambda_3, \mathbf{v}_3$, and $\mathbf{v}_5$ as well as the second and the fourth column of (72) only vanish because of the special choice of μ, χ, and γ. Fig. 3 shows λ_2 and λ_4 for $p=1$ and varying κ. It can be shown that the dependence of λ_2 and λ_4 on κ is linear and quadratic, respectively.

According to (71), the shape of the primary path depends only on the initial rise of bar ①, which is 1 in this case. In particular, (71) is independent of γ, κ, μ, and χ. Hence, these parameters only control the postbuckling behavior. Along the primary path, $\tilde{\mathbf{K}}_T$ does not depend on κ. Therefore, also the bifurcation points are independent of κ. $\tilde{\mathbf{K}}_T$ is a diagonal matrix, reflecting that $u_2 = 0$ along the primary path. The non-symmetric equilibrium paths for specific values of κ are shown in Fig. 4. A second bifurcation point C_1 and a snap-through point D are located on an unstable section of the primary path.
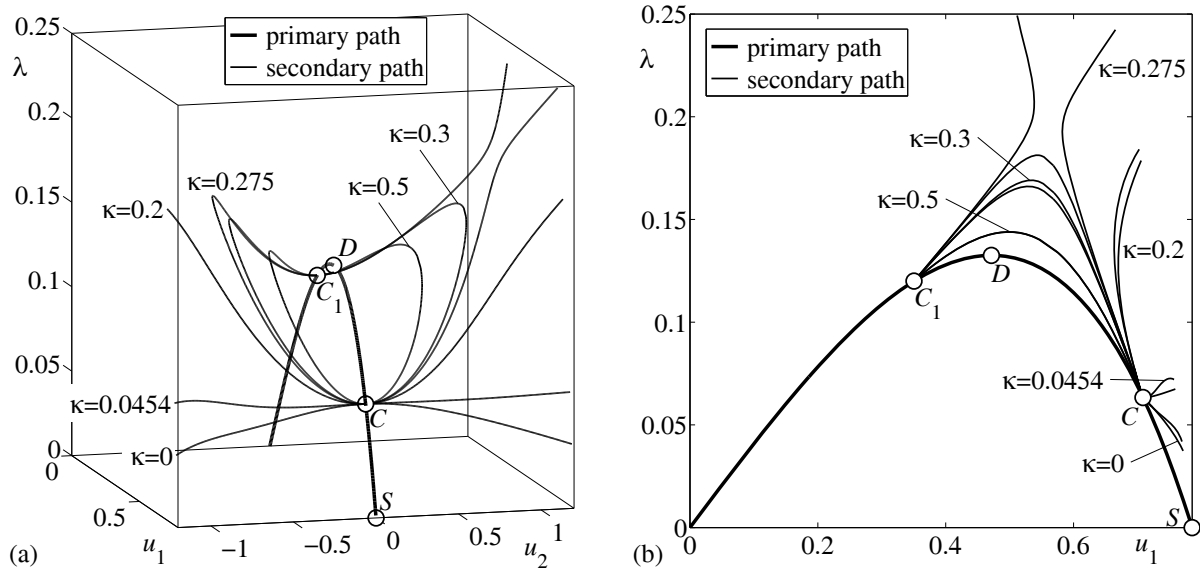
Fig.4: (a) Load-displacement paths of the system shown in Fig. 2(a), (b) projection onto the plane $u_2 = 0$

For sufficiently large values of κ, the limit load of the secondary path exceeds the limit load at the snap-through point D of the primary path. Any *increase* of γ, μ, or χ will increase the buckling load λ_C. Hence, an increase of these parameters such that the system does not bifurcate anymore would *reduce* its ultimate load. Moreover, it can be shown that the maximum value of the ultimate load is obtained for $\kappa = 0.2668$. Therefore, an increase of κ beyond this value is counterproductive, because the ultimate load drops.

This example shows that non-symmetric bifurcation does *not* hamper the conversion from imperfection sensitivity into imperfection insensitivity, as long as $\lambda_1 = 0$ can be realized. In this example, both, $\lambda_1 = 0$ and $\lambda_3 = 0$ were achieved simultaneously. Together with $\lambda_4 > 0$, this is the reason that the transition case $\lambda_2 = 0$ is also imperfection insensitive. $\lambda_1 = 0$ was obtained through variation of parameters. However, there are also cases where enforcing $\lambda_1 = 0$ involves structural

modifications of the original design, which may be undesirable or not feasible from an engineering perspective.

6.2. Symmetric bifurcation

Many simple bifurcation systems behave symmetric without any special design measures. However, any non-symmetric bifurcation system can be rendered symmetric if it is supplemented by its mirror image. This simple principle was applied to the system given in Fig. 2(a), which yields the system shown in Fig. 2(b). It is very similar to the original system, however, it bifurcates symmetrically. In order to keep the buckling load λ_C at the same level, the stiffness of the duplicated springs was halved. The strain energy reads as

$$U(u_1,u_2) = \frac{1}{4}kL^2\left(2\left(1-\sqrt{2}\cos(u_1)\right)^2 + \gamma\left(\sqrt{1+\mu^2} - \sqrt{(2-\cos(u_2))^2 + (\mu+\sin(u_2))^2}\right)^2\right.$$
$$+ \gamma\left(\sqrt{1+\mu^2} - \sqrt{(2-\cos(u_2))^2 + (\mu-\sin(u_2))^2}\right)^2 + \kappa\left(1-\cos(u_2)\right)^2$$
$$\left. + \chi\left(\sqrt{1+\mu^2} - \sqrt{\cos(u_2)^2 + (\mu+\sin(u_2))^2}\right)^2 + \chi\left(\sqrt{1+\mu^2} - \sqrt{\cos(u_2)^2 + (\mu-\sin(u_2))^2}\right)^2\right).$$
$$(74)$$

It is not surprising that (74) is the symmetric part $\left(U(u_1,u_2) + U(u_1,-u_2)\right)/2$ of (69). The potential function of the vertical load $\lambda\bar{P}$ and the solutions for the primary path are the same as in the previous example, given in (70) and (71), respectively. Again, the postbuckling load-displacement paths were constructed using a numerical solver.

Compared to the previous example, the parameter values were not modified. Hence, the buckling load λ_C is the same. Again, κ is used as the parameter for conversion from imperfection sensitivity into imperfection insensitivity. This conversion is achieved for $\kappa = 0.0454$. The system is imperfection sensitive for $\kappa \in [0, 0.0454)$, and imperfection insensitive for $\kappa \geq 0.0454$. For the transition case, the components of (13) are:

$$
\begin{array}{cccccc}
\underline{a_{1,0}} & & & & & 0 \\
a_{2,1} & \underline{a_{2,0}} & & & & -1 \quad 0 \\
a_{3,2} & \underline{a_{3,1}} & \underline{a_{3,0}} & & = & 2.634 \quad 0 \quad\quad 0 \\
a_{4,3} & \underline{a_{4,2}} & \underline{a_{4,1}} & \underline{a_{4,0}} & & 14.74 \quad 0 \quad\quad p^2/6 \quad\quad 0 \\
a_{5,4} & a_{5,3} & a_{5,2} & a_{5,1} & a_{5,0} & 51.60 \quad 0 \quad -0.5392\,p^2 \quad 0 \quad 0.
\end{array}
\qquad (75)
$$

Moreover,

$$\lambda_1 = 0, \qquad \lambda_2 = 0, \qquad \lambda_3 = 0, \quad \lambda_4 = 9.79\cdot10^{-3}\,p^4, \quad \lambda_5 = 0$$
$$\mathbf{v}_1 = \begin{pmatrix} 0 \\ p \end{pmatrix} \quad \mathbf{v}_2 = \begin{pmatrix} 0.048\,p^2 \\ 0 \end{pmatrix}, \quad \mathbf{v}_3 = \mathbf{0}, \quad \mathbf{v}_4 = \begin{pmatrix} -0.011\,p^4 \\ 0 \end{pmatrix}, \quad \mathbf{v}_5 = \mathbf{0}. \qquad (76)$$
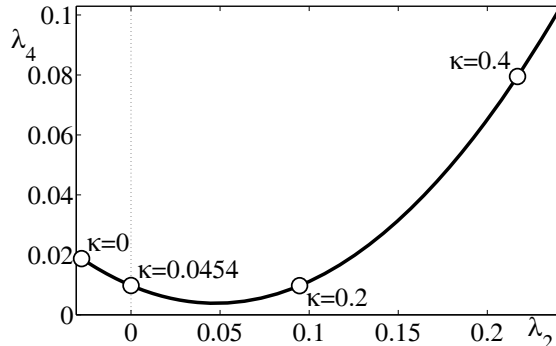
(76) shows that the transition case itself is imperfection insensitive. As expected, λ_i vanishes for odd values of i and $\mathbf{v}_j$ vanishes for $j \in \{3,5,7,\ldots\}$. This would still be the case, if the values of γ, κ, μ, or χ were changed. λ_2 and λ_4 are plotted for $p=1$ and for varying values of κ in Fig. 5. Again, the

dependence of λ_2 and λ_4 on κ is linear and quadratic, respectively. Along the primary path, $\tilde{\mathbf{K}}_T$ is a diagonal matrix, which for a two-degrees-of-freedom system verifies (26).
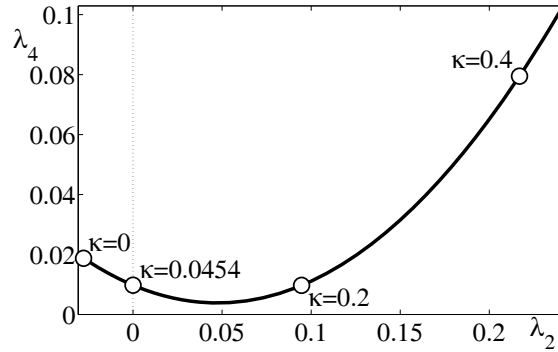
Fig. 5: Coefficients of asymptotic series expansion of λ for varying κ

The symmetric equilibrium paths for specific values of κ are shown in Fig. 6. The second bifurcation point C_1 is located on an unstable section of the primary path. As regards the qualitative behavior of the system if γ, κ, μ, and χ are increased, the same statements as given at the end of Subsection 6.1 hold.
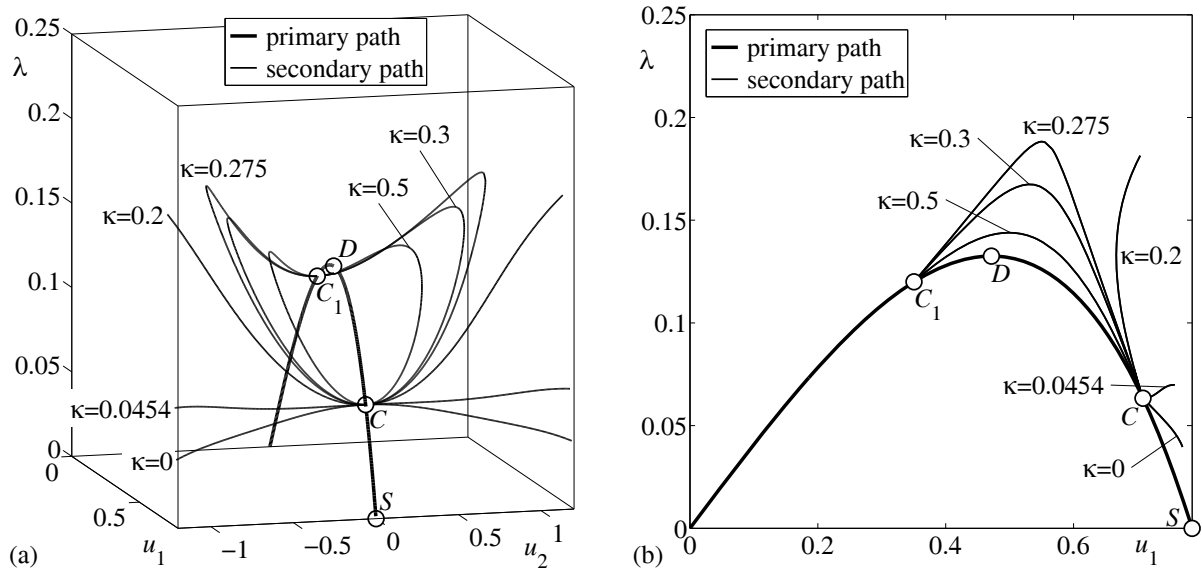
Fig. 6: (a) Load-displacement paths of the system given in Fig. 2(b), (b) projection onto the plane $u_2 = 0$

6.3.   Antisymmetric bifurcation

Fig. 7(a) shows a planar, static, two-degrees-of-freedom system, which bifurcates antisymmetrically. It is based on a parallelogram four-bar linkage. The coupler link ② remains always horizontal and carries a constant, vertical load kL, which may be conceived of as gravitational force. The grounded link ① is designed as an L-shaped bracket supported by a linear elastic spring k, which always remains vertical. Both legs of the bracket ① have the length L. A cantilevered bar ③ (length L) is assembled at the upper left joint and propped up by a linear elastic torsional spring c. Beam ③ carries the vertical load $\lambda\bar{P}$ at its free end. Two angular degrees of freedom u_1 and u_2 measure the angular position of bar ③ and bracket ①, respectively. Both angles are counted positive in clockwise

direction. The springs are strain-free for $u_1 = 0$ and $u_2 = 0$. This situation is delineated in gray, whereas the deflected position is shown in black. No parameters are varied.
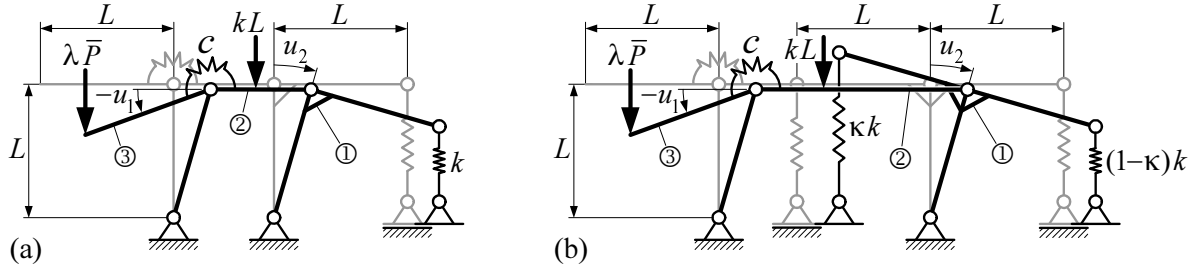
Fig. 7: Static systems with two degrees of freedom, which bifurcate
(a) antisymmetrically, (b) with zero-stiffness postbuckling behavior

The potential energy reads as

$$V(u_1, u_2, \lambda) = U(u_1, u_2) + W(u_1, u_2, \lambda), \tag{77}$$

with the strain energy

$$U(u_1, u_2) = \frac{1}{2} c u_1^2 + \frac{1}{2} k L^2 \left(1 - \cos(u_2) + \sin(u_2)\right)^2 \tag{78}$$

and the potential energy of the external loads

$$W(u_1, u_2, \lambda) = -\lambda \overline{P} L \left(1 - \cos(u_2) - \sin(u_1)\right) - k L \left(1 - \cos(u2)\right). \tag{79}$$

The tangent stiffness matrix along the primary path, where $u_2 = 0$, follows as

$$\tilde{\mathbf{K}}_T = \begin{bmatrix} c - \lambda \overline{P} L \sin(u_1) & 0 \\ 0 & -\lambda \overline{P} L \cos(u_1) \end{bmatrix}. \tag{80}$$

Therefore, the critical load is $\lambda_c = 0$ and V satisfies the conditions for antisymmetric bifurcation (52) and (53). Moreover, the antisymmetric bifurcation behavior is verified by the analytical expressions of the load-displacement paths

$$\lambda = -\frac{c u_1}{\overline{P} L \cos(u_1)}, \quad u_2 = 0 \tag{81}$$

for the primary path and

$$\lambda = -\frac{c u_1}{\overline{P} L \cos(u_1)}, \quad \lambda = -\frac{k L \left(2 \cos^2(u_2) - \cos(u_2) - 1\right)}{\overline{P} \sin(u_2)} \tag{82}$$

for the secondary path. $\tilde{\mathbf{K}}_T$ is a diagonal matrix, which for a two-degrees-of-freedom system conforms to the definition (52). The parameter values are chosen as $c = 1 \text{Nm}$, $k = 1 \text{N/m}$, $L = 1 \text{m}$, and $\overline{P} = 1 \text{N}$. Then, the values of the triangular array of coefficients (13) are

$$\begin{matrix} a_{1,0} \\ a_{2,1} & a_{2,0} \\ a_{3,2} & a_{3,1} & a_{3,0} \\ a_{4,3} & a_{4,2} & a_{4,1} & a_{4,0} \\ a_{5,4} & a_{5,3} & a_{5,2} & a_{5,1} & a_{5,0} \end{matrix} \quad = \quad \begin{matrix} 0 \\ -1 & 3p/2 \\ 0 & 0 & 0 \\ 0 & 0 & p^2/6 & -p^3/4 \\ 0 & 0 & 0 & 0 & 0. \end{matrix} \tag{83}$$

Moreover,

$$\lambda_1 = 3p/2, \quad \lambda_2 = 0, \quad \lambda_3 = -3p^3/8, \quad \lambda_4 = 0, \quad \lambda_5 = p^5/80, \quad \lambda_6 = 0, \quad \lambda_7 = -11p^7/13440,$$

$$\mathbf{v}_1 = \begin{pmatrix} 0 \\ p \end{pmatrix}, \quad \mathbf{v}_2 = \mathbf{0}, \quad \mathbf{v}_3 = \mathbf{0}, \quad \mathbf{v}_4 = \mathbf{0}, \quad \mathbf{v}_5 = \mathbf{0}, \quad \mathbf{v}_6 = \mathbf{0}, \quad \mathbf{v}_7 = \mathbf{0}.$$

$$(84)$$
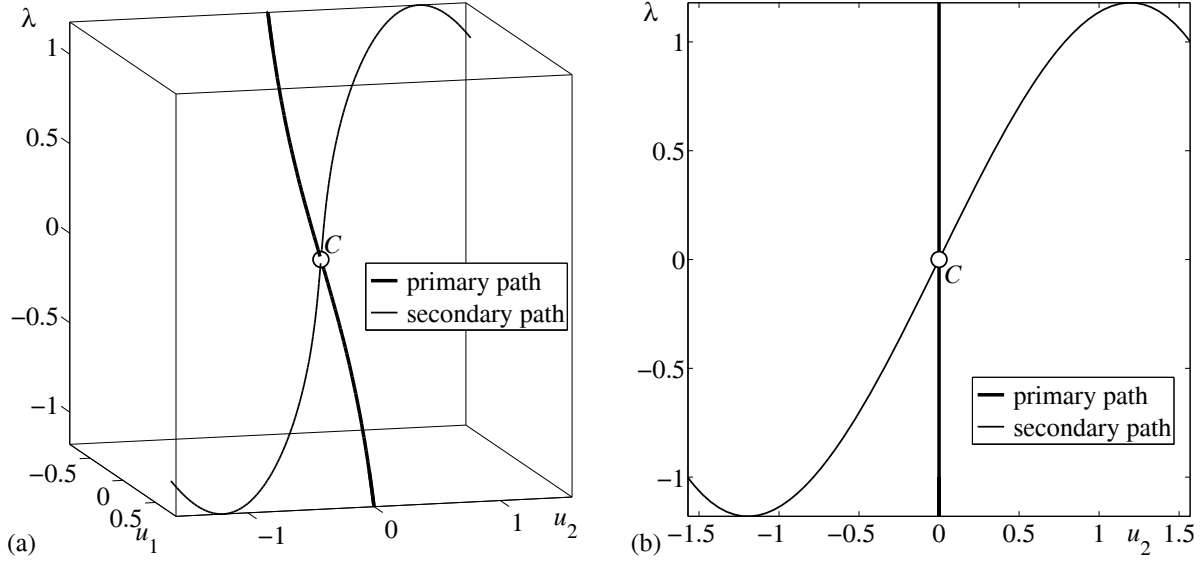
Fig.8: (a) Load-displacement paths of the system given in Fig. 7(a), (b) projection onto the plane $u_1 = 0$

It is emphasized that for antisymmetric bifurcation, $\mathbf{v}_3, \mathbf{v}_5, \mathbf{v}_7, \dots$ generally do not have to be equal to $\mathbf{0}$. The two non-trivial equations described by the second and fourth row of (83) are linear equations in λ_1. Moreover, they are identical. The equilibrium paths and their projection to the plane $u_1 = 0$ are shown in Fig. 8. The snap-through points on the secondary path are a consequence of the rotational (2π) periodicity of u_2.

From this example it can be concluded that antisymmetric bifurcation prevents conversion from imperfection sensitivity into imperfection insensitivity. Such a conversion would require abandoning antisymmetric bifurcation, which usually corresponds to qualitative modifications of the original structure. Such modifications may be undesirable or not feasible from an engineering perspective. It is unlikely that simple variations of parameters can render an antisymmetric bifurcation system imperfection insensitive.

6.4. Zero-stiffness postbuckling behavior

Fig. 7(b) shows a system which is similar to the antisymmetric bifurcation system of the previous Subsection. It is obtained by augmenting the original system with a mirror image of the L-shaped bracket, which is responsible for the antisymmetric bifurcation. This gives a T-shaped grounded link ①, supported by two vertical springs. Apart from their spring stiffness κk and $(1-\kappa)k$, respectively, no parameters of the previous example were changed. It can be shown that for any value of the parameter $\kappa \in [0,1]$, the critical load is $\lambda_C = 0$ and the primary path is defined by (81), i.e., equal to the case of antisymmetric bifurcation. For $\kappa = 0$, the original system is obtained, and for $\kappa = 1/2$, which will be used in the sequel, zero-stiffness postbuckling behavior is achieved.

In this case, the strain energy reads as

$$U(u_1,u_2) = \frac{1}{2}cu_1^2 + \frac{1}{2}\frac{k}{2}L^2\left(\left(1-\cos(u_2)+\sin(u_2)\right)^2 + \left(1-\cos(u_2)-\sin(u_2)\right)^2\right) \qquad (85)$$

and the potential energy of the external loads is defined by (79). As expected, (85) is the symmetric part $\left(U(u_1,u_2)+U(u_1,-u_2)\right)/2$ of the strain energy (78) of the associated antisymmetric bifurcation system. The primary equilibrium path is the same as in the previous example, given in (81). The secondary path follows as

$$u_1 = 0, \quad u_2 \in \mathbb{R}, \quad \lambda = 0. \qquad (86)$$

Hence, the conditions (65) and (66) for zero-stiffness postbuckling behavior and equivalently (67) are satisfied. The values of the triangular array of coefficients (13) are

$$
\begin{array}{llllll}
a_{1,0} & & & & & \\
a_{2,1} & a_{2,0} & & & & \\
a_{3,2} & a_{3,1} & a_{3,0} & & = & \\
a_{4,3} & a_{4,2} & a_{4,1} & a_{4,0} & & \\
a_{5,4} & a_{5,3} & a_{5,2} & a_{5,1} & a_{5,0} &
\end{array}
\qquad
\begin{array}{lllll}
0 & & & & \\
-1 & 0 & & & \\
0 & 0 & 0 & & \\
0 & 0 & p^2/6 & 0 & \\
0 & 0 & 0 & 0 & 0.
\end{array}
\qquad (87)
$$

Moreover,

$$\lambda_i = 0 \quad \forall i \in \mathbb{N}\backslash\{0\}, \qquad \mathbf{v}_1 = \begin{pmatrix} 0 \\ p \end{pmatrix}, \qquad \mathbf{v}_i = \mathbf{0} \quad \forall i \in \mathbb{N}\backslash\{0,1\}. \qquad (88)$$

The vanishing values in (87) and (88) reflect the fact that this system satisfies the criteria for symmetric bifurcation. The equilibrium paths and their projection onto the plane $u_2 = 0$ are shown in Fig. 9. In this projection, the secondary path degenerates to a point.
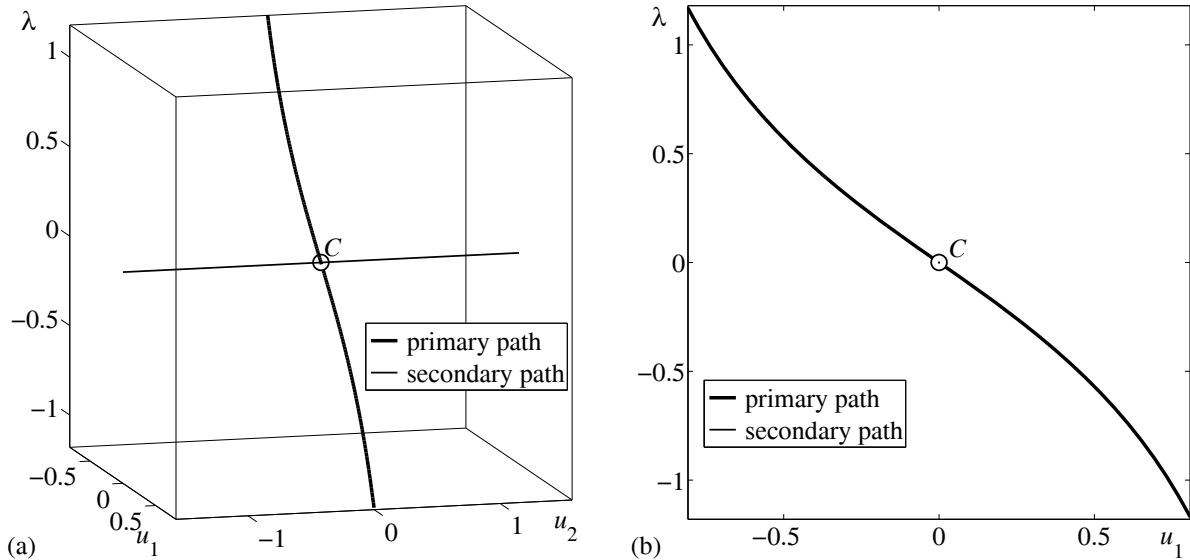
Fig. 9: (a) Load-displacement paths of the system given in Fig. 7(b), (b) projection onto the plane $u_2 = 0$

The example shows that zero-stiffness postbuckling does not necessarily indicate the transition from imperfection sensitivity to insensitivity, as is frequently the case. The reason for this is that for the special case of $\kappa = 1/2$, as delineated in this example, postbuckling happens with zero-stiffness, but for any other value $\kappa \in [0,1]$, the system behaves antisymmetric, i.e., imperfection sensitive.

7. Conclusions

The three categories *symmetric bifurcation*, *antisymmetric bifurcation*, and *zero-stiffness postbuckling behavior* were identified as distinct properties of a bifurcation system. Their role regarding the conversion from imperfection sensitivity into insensitivity was investigated. Qualitative conditions that ensure, facilitate, hamper, or prevent such a conversion were given. Symmetric and antisymmetric bifurcation is a global property of a system, whereas zero-stiffness postbuckling behavior can only be attributed to single equilibrium paths. Nevertheless, it may be regarded as a combination of symmetric and antisymmetric equilibrium paths.

In the framework of *Koiter*'s initial postbuckling analysis, the conditions (45), (62), and (67) were proposed as being sufficient for symmetric bifurcation, antisymmetric bifurcation, and zero-stiffness postbuckling behavior, respectively. In principle, these conditions involve examining infinitely many coefficients. Therefore, checking for the three categories of bifurcation behavior by means of (23), (52), and (53) as well as (65), and (66), respectively, is preferable. Often, it is obvious that the bifurcation behavior is symmetric, antisymmetric, or showing a zero-stiffness postbuckling path, i.e., *a priori* engineering knowledge renders testing for such categories superfluous.

Supplementing a general bifurcation system by its mirror image yields a symmetric bifurcation system. This was shown in the examples in Subsections 6.1 and 6.2. Augmenting an antisymmetric bifurcation system by its mirror image, zero-stiffness postbuckling behavior is obtained, which was demonstrated by the examples described in Subsections 6.3 and 6.4. However, this is obviously not the only way of designing systems that experience symmetric bifurcation or zero-stiffness postbuckling. For instance, in [10], some examples of symmetric bifurcation and zero-stiffness postbuckling paths are elaborated.

Symmetric bifurcation requires all underlined terms in (13) to vanish. However, this is not a sufficient condition for symmetry. There are also classes of bifurcation problems, where additional terms in (13) become zero, e.g. zero-stiffness bifurcation as noticed in (87).

An imperfection-insensitive structure must satisfy (16). Hence, imperfection insensitivity requires $\lambda_1 = 0$, which holds automatically for systems that bifurcate to a symmetric or a zero-stiffness postbuckling path. Generally, however, neither symmetry nor zero-stiffness postbuckling is necessary for the conversion from imperfection sensitivity into imperfection insensitivity. This facilitates the analysis of bifurcation problems by the FEM, since the discretization by means of finite elements may destroy symmetry properties.

If, in case of non-symmetric systems, $\lambda_1 \neq 0$, the vanishing of λ_1 must be enforced in the course of the conversion process. For the example discussed in Subsection 6.1 (non-symmetric bifurcation), this was done without difficulty by variation of parameters, but in other cases, undesirable structural modifications of the original design may be inevitable. This holds particularly for antisymmetric bifurcation systems, which do not change their antisymmetric bifurcation behavior if only parameter values are modified. In contrast, a qualitative modification of the original structure will be necessary so that equilibrium paths deviate from their originally antisymmetric (imperfection sensitive) shape.

Condition (16) implies that $\lambda_2 = 0$ is neither *necessary* nor *sufficient* for conversion from imperfection sensitivity into imperfection insensitivity. It is not necessary because a general non-symmetric bifurcation system with $\lambda_1 \neq 0$ and $\lambda_2 > 0$ could be made imperfection insensitive by enforcing $\lambda_1 = 0$, whereas λ_2 always remains positive. Moreover, $\lambda_2 = 0$ is not sufficient for such a conversion, which can be concluded from the example given in Subsection 6.4.

The ultimate load of a structure does not necessarily benefit from increasing the stiffness. In Subsections 6.1 and 6.2, the spring stiffness κk of a system was varied and it was found that this contributes to the conversion from imperfection sensitivity into imperfection insensitivity. However, raising the stiffness above a certain value will have adverse effects on the postbuckling behavior, at least for the analyzed cases. In fact, it leads to qualitative changes of the secondary path.

Example 6.3 demonstrated that antisymmetric bifurcation always entails imperfection sensitivity, which also follows from (16) and (49). The examples of non-symmetric and symmetric bifurcation given in Subsections 6.1 and 6.2 showed the possibility of converting an imperfection-sensitive into an imperfection-insensitive structure without modifying the prebuckling domain, particularly without changes of the buckling load.

Application of the considerations made herein to multiple-degrees-of-freedom systems, in particular to systems analyzed by the FEM, leaves scope for future scientific work. Moreover, the meaning of different characteristic patterns of vanishing coefficients in the triangular array (13) needs further clarification. It is expected that this will allow identification of additional qualitative design properties that are pivotal for the conversion from imperfection sensitivity into imperfection insensitivity.

Acknowledgements

References

[1] Bochenek B. *Problems of structural optimization for post-buckling behaviour*, Struct. Multidisciplinary Optim. 25(5-6), 423-435, 2003.

[2] Budiansky B. *Post-buckling behavior of cylinders under torsion*, in: Theory of thin shells - Proceedings of the second IUTAM symposium, Copenhagen, Denmark, 5-9 September,1967, Springer, Berlin, 212-233.

[3] Dym C.L. *Stability theory and its applications to structural mechanics*. Noordhoff International Publishing, Leyden, The Netherlands, 1974.

[4] Godoy L. *Sensitivity of post-critical states to changes in design parameters*, Int. J. Solids Struct. 33(15), 2177-2192, 1996.

[5] Huseyin K. *Multiple Parameter Stability Theory and its Applications*. Clarendon Press, Osford. 1986.

[6] Koiter W. *On the stability of elastic equilibrium*, Translation of '*Over de Stabiliteit van het Elastisch Evenwicht*' (1945), in: NASA TT F-10833, Polytechnic Institute Delft, (H.J. Paris Publisher, Amsterdam, 1967)

[7] Mang H.A., Schranz C., Mackenzie-Helnwein P. *Conversion from imperfection-sensitive into imperfection-insensitive elastic structures I: Theory*, Comput. Methods Appl. Mech. Engrg., 195, 1422-1457, 2006.

[8] Mróz R., Haftka R. *Design sensitivity analysis of non-linear structures in regular and critical states*, Int. J. Solids Struct. 31(15), 2071-2098, 1994.

[9] Reitinger R. S*tabilität und Optimierung imperfektionsempfindlicher Tragwerke [in German; Stability and optimization of imperfection-sensitive structures]*. Ph.D. dissertation, Universität Stuttgart, Institute of Structural Mechanics, 1994.

[10] Schranz C., Krenn B., Mang H.A. *Conversion from imperfection-sensitive into imperfection-insensitive elastic structures II: Numerical investigation*, Comput. Methods Appl. Mech. Engrg., 195, 1458-1479, 2006.

[11] Steinboeck A., Jia X., Hoefinger G., Mang H.A. *Symmetry and imperfection insensitivity - two independent properties of a structure?* Proc. of the 8th HSTAM (Hellenic Society for Theoretical and Applied Mechanics) International Congress on Mechanics, Patras, Greece, 12-14 July 2007.

[12] Tarnai T. *Zero stiffness elastic structures*, Int. J. of Mechanical Sciences, 45(3), 425-431, 2003.

[13] Thompson M.T., Hunt G.W. *Elastic Instability Phenomena*. John Wiley & Sons, New York, 1984

Chapter IV

Hilltop Buckling as the Alpha and Omega in Sensitivity Analysis of the Initial Postbuckling Behavior of Elastic Structures

Herbert A. Mang, Xin Jia, Gerhard Hoefinger

Institute for Mechanics of Materials and Structures, Vienna University of Technology, Karlsplatz 13/202, 1040 Vienna, Austria.

Abstract

The coincidence of a bifurcation point with a snap-through point is called hilltop buckling. In this paper, it either serves as the starting point – the A – or as the end – the Ω – in sensitivity analysis of the initial postbuckling behavior of elastic structures. It is shown that hilltop buckling is imperfection sensitive. In sensitivity analyses with hilltop buckling as the starting point (end), the bifurcation point and the snap-through point are diverging from (converging to) each other. Two classes of sensitivity analyses are identified by means of the consistently linearized eigenproblem. They determine the more (or less) effective mode of conversion of an originally imperfection-sensitive into an imperfection-insensitive structure. The results from the numerical investigation corroborate the theoretical findings. The present study is viewed as a step in the direction of better understanding the reasons for different modes of the initial postbuckling behavior of elastic structures and its interplay with the prebuckling behavior.

Keywords

consistently linearized eigenproblem, hilltop buckling, imperfection (in)sensitivity, Koiter's initial postbuckling analysis, sensitivity analysis, symmetric bifurcation, zero-stiffness postbuckling.

1. Introduction

The coincidence of a bifurcation point with a snap-through point is called hilltop buckling [1]. It can be realized by appropriately tuning a set of design parameters of a structure [2].

Assuming that hilltop buckling is imperfection sensitive, it may serve as the starting point – the Alpha – for sensitivity analysis of the buckling load and the initial postbuckling behavior by means of variation of a design parameter. The motivation for such an analysis may be improvement of this behavior through conversion of an originally imperfection-sensitive into an imperfection- insensitive structure [3], [4]. In the course of this analysis, the stability limit, represented by the bifurcation point, is increasing less strongly than the load corresponding to the snap-through point. Hence, the two points are diverging from each other.

Conversely, in sensitivity analysis the stability limit may be increasing more strongly than the snap-through load. In this case, the two load points are converging to each other. Their coincidence represents the end – the Omega – of sensitivity analysis of the buckling load and the initial postbuckling behavior because snap-through would otherwise replace bifurcation buckling as the relevant mode of loss of stability.

The purpose of this paper is to examine these two forms of sensitivity analyses of the buckling load and the initial postbuckling behavior. Examination tools include Koiter's initial postbuckling analysis [5] and the Finite Element Method (FEM).

It will be shown that hilltop buckling is imperfection sensitive. As a special form of transition from imperfection sensitivity to imperfection insensitivity, zero- stiffness postbuckling [6] will be mentioned.

The investigation is restricted to static, conservative, perfect systems with a finite number N of degrees of freedom as conforms to the FEM. The material behavior is assumed to be either rigid or linear elastic. Only symmetric bifurcation behavior with respect to a scalar variable η will be considered [6]. Multiple bifurcation will be excluded, especially multiple hilltop buckling is not discussed in this analysis, i.e. there is only a single secondary path. For a discussion on multiple hilltop branching phenomena and their influence on imperfection sensitivity refer to [1], [11]. The numerical results of examples presented there corroborate the following theoretical findings. Sensitivity analysis will be restricted to variation of one design parameter at a time.

2. Derivation of polynomials

2.1. Koiter's initial postbuckling analysis

Fig. 1 shows a projection of load-displacement paths of a system bifurcating at point C. The solid line represents the *primary* path, whereas the dashed line is a *secondary* path. The latter is parameterized by $\eta \in \mathbb{R}$, defined as zero at C. Herein, the subscript $\bullet_C$ means evaluation of a

quantity at C. The reference load $\bar{\mathbf{P}}$ is scaled by a dimensionless load factor λ, and $\mathbf{u}$ denotes the vector of generalized displacement coordinates.

In [3] and [6] Koiter's initial postbuckling analysis [5] was used to expand the out-of-balance force

$$\mathbf{G}(\mathbf{u},\lambda) := \mathbf{F^I}(\mathbf{u}) - \lambda\bar{\mathbf{P}} \in \mathbb{R}^N, \tag{1}$$

where $\mathbf{F^I}(\mathbf{u})$ denotes the internal forces, into an asymptotic series at C. For a static, conservative system, $\mathbf{G}$ can be derived from the potential energy function V as

$$\mathbf{G} = \frac{\partial V}{\partial \mathbf{u}}. \tag{2}$$
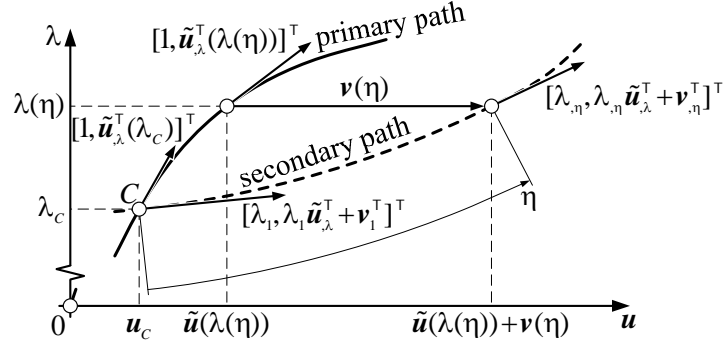
Fig. 1: On Koiter's initial postbuckling analysis [6]

$\mathbf{G}$ vanishes along equilibrium paths in the $\mathbf{u}-\lambda$ space. $\lambda(\eta)$ is the load level at the point of the secondary path associated with η, as outlined in Fig. 1. The point on the primary path characterized by the same load is described by the displacement vector $\tilde{\mathbf{u}}(\lambda(\eta))$. Quanti- ties evaluated along the primary path are labeled by an upper tilde. The displacement at the corresponding point of the secondary path can be expressed as $\mathbf{u}(\eta) = \tilde{\mathbf{u}}(\lambda(\eta)) + \mathbf{v}(\eta)$ where $\mathbf{v}$ is the displacement offset which vanishes trivially at C.

Hence,

$$\mathbf{G}(\eta) := \mathbf{G}\left(\tilde{\mathbf{u}}(\lambda(\eta)) + \mathbf{v}(\eta), \lambda(\eta)\right) = \mathbf{0} \tag{3}$$

must hold along the secondary path. Insertion of the asymptotic series expansions

$$\lambda(\eta) = \lambda_C + \lambda_1\eta + \lambda_2\eta^2 + \lambda_3\eta^3 + O(\eta^4) \tag{4}$$

$$\mathbf{v}(\eta) = \mathbf{v}_1\eta + \mathbf{v}_2\eta^2 + \mathbf{v}_3\eta^3 + O(\eta^4) \tag{5}$$

into (3) and expanding the resulting expressions into a series in terms of η yields

$$\mathbf{G} = \mathbf{G}_{0C} + \mathbf{G}_{1C}\eta + \mathbf{G}_{2C}\eta^2 + \mathbf{G}_{3C}\eta^3 + O(\eta^4) \tag{6}$$

with

$$\mathbf{G}_{nC} = \frac{\mathbf{G}_{,\eta^nC}}{n!} \ \forall \ n \in \mathbb{N}, \tag{7}$$

where $\mathbb{N}$ denotes the set of natural numbers including zero. Details of computation of $\mathbf{G}_{nC}$ are given in [6].

Since (3) must hold for any point along the secondary path, i.e. for arbitrary values of η, each coefficient $\mathbf{G}_{nC}$ of the series must vanish. This condition paves the way for successive calculation of the pairs of unknowns $(\mathbf{v}_1,\, \lambda_1)$, $(\mathbf{v}_2,\, \lambda_2)$, etc. described in [3].

2.2. Coefficients of the asymptotic series expansion of $\lambda(\eta) - \lambda_C$

For the present investigation only the first four coefficients of the series expansion of $\lambda(\eta)$ need to be known. They are given as follows [3]:

$$\lambda_1 = d_0, \tag{8}$$

$$\lambda_2 = a_1 \lambda_1^2 + b_1 \lambda_1 + d_1, \tag{9}$$

$$\lambda_3 = a_1^* \lambda_1^3 + b_1^* \lambda_1^2 + c_1^* \lambda_1 + b_1 \lambda_2 + d_2, \tag{10}$$

$$\lambda_4 = \hat{a}_1 \lambda_1^4 + \hat{b}_1 \lambda_1^3 + \hat{c}_1 \lambda_1^2 + \hat{d}_1 \lambda_1 + a_1 \lambda_2^2 + b_2 \lambda_2 + b_1 \lambda_3 + d_3, \tag{11}$$

where

$$c_1^* = 2a_1 \lambda_2 + b_2, \tag{12}$$

$$\hat{c}_1 = 3a_1^* \lambda_2 + \frac{1}{2} b_2^*, \tag{13}$$

$$\hat{d}_1 = 2b_1^* \lambda_2 + 2a_1 \lambda_3 + b_3, \tag{14}$$

whereas none of the other coefficients in the expressions for λ_3 and λ_4 depends on λ_2, and λ_2 and λ_3, respectively.

To get an idea of the structure of the coefficients in (8)-(11), the expressions for d_0 (b_0 in [3]), a_1, b_1, d_1, and a_1^* are listed in the following [3]:

$$d_0 = -\frac{1}{2} \frac{\mathbf{v}_1^T \cdot \mathbf{K}_{T,\mathbf{u}} : \mathbf{v}_1 \otimes \mathbf{v}_1}{\mathbf{v}_1^T \cdot \tilde{\mathbf{K}}_{T,\lambda} \cdot \mathbf{v}_1}, \tag{15}$$

$$a_1 = -\frac{1}{2} \frac{\mathbf{v}_1^T \cdot \tilde{\mathbf{K}}_{T,\lambda\lambda} \cdot \mathbf{v}_1}{\mathbf{v}_1^T \cdot \tilde{\mathbf{K}}_{T,\lambda} \cdot \mathbf{v}_1}, \tag{16}$$

$$b_1 = -\frac{\mathbf{v}_1^T \cdot \tilde{\mathbf{K}}_{T,\lambda} \cdot \mathbf{v}_2 + \dfrac{1}{2} \mathbf{v}_1^T \cdot \mathbf{K}_{T,\mathbf{u}\lambda} : \mathbf{v}_1 \otimes \mathbf{v}_1}{\mathbf{v}_1^T \cdot \tilde{\mathbf{K}}_{T,\lambda} \cdot \mathbf{v}_1}, \tag{17}$$

$$d_1 = -\frac{\mathbf{v}_1^T \cdot \mathbf{K}_{T,\mathbf{u}} : \mathbf{v}_1 \otimes \mathbf{v}_2 + \dfrac{1}{6} \mathbf{v}_1^T \cdot \mathbf{K}_{T,\mathbf{u}\mathbf{u}} \vdots \mathbf{v}_1 \otimes \mathbf{v}_1 \otimes \mathbf{v}_1}{\mathbf{v}_1^T \cdot \tilde{\mathbf{K}}_{T,\lambda} \cdot \mathbf{v}_1}, \tag{18}$$

$$a_1^* = -\frac{1}{6} \frac{\mathbf{v}_1^T \cdot \tilde{\mathbf{K}}_{T,\lambda\lambda\lambda} \cdot \mathbf{v}_1}{\mathbf{v}_1^T \cdot \tilde{\mathbf{K}}_{T,\lambda} \cdot \mathbf{v}_1}. \tag{19}$$

$\mathbf{K}_T(\mathbf{u}) = \mathbf{G}_{,\mathbf{u}}$ is the tangent stiffness matrix which generally refers to out-of-balance states, whereas

$$\tilde{\mathbf{K}}_T(\lambda) := \mathbf{K}_T(\tilde{\mathbf{u}}(\lambda)) \tag{20}$$

is the one that refers to the special case of equilibrium states on the primary path. $(\bullet)_{,\lambda}$ indicates the special differentiation with respect to λ along a direction parallel to the primary path [3]. Most of the coefficients in (8)-(11) are given in [3]. The remaining coefficients can be deduced from Appendix B in [3].

3. Specialization of the expressions for $\lambda_1, ..., \lambda_4$ for symmetric bifurcation

3.1. Conditions for symmetric bifurcation

Bifurcation is qualified as *symmetric* with respect to the parameter η if it obeys the definitions [6]:

$$\lambda(\eta) = \lambda(-\eta) \wedge \tag{21}$$

$$\mathbf{v}(\eta) = T(\mathbf{v}(-\eta)) \wedge \tag{22}$$

$$\tilde{\mathbf{u}}(\lambda(\eta)) = T(\tilde{\mathbf{u}}(\lambda(\eta))), \tag{23}$$

where the linear mapping $T : \mathbb{R}^N \to \mathbb{R}^N$ is an element of a symmetry group. Insertion of (4) into (21) yields

$$\lambda_1 = \lambda_3 = ... = 0. \tag{24}$$

3.2. Specialization of (8)-(11) for symmetric bifurcation

Substitution of (24) into (8)-(11) gives

$$0 = d_0, \tag{25}$$

$$\lambda_2 = d_1, \tag{26}$$

$$0 = b_1 \lambda_2 + d_2, \tag{27}$$

$$\lambda_4 = a_1 \lambda_2^2 + b_2 \lambda_2 + d_3. \tag{28}$$

According to [6], symmetric bifurcation requires

$$d_0 = d_2 = ... = 0. \tag{29}$$

Hence, following from (27),

$$b_1 = 0. \tag{30}$$

This corresponds with the result of a proof in [6] according to which b_1, b_1^*, $\hat{b}_1$, ..., $\hat{d}_1$, ... must vanish for symmetric bifurcation. Hence, following from (14), also

$$b_3 = 0. \tag{31}$$

4. Conditions for imperfection insensitivity

A necessary condition for imperfection insensitivity is given as [7]

$$\lambda_1 = 0 \tag{32}$$

which is automatically satisfied for symmetric bifurcation. Sufficient conditions for imperfection sensitivity are [7]

$$\lambda_1 = 0, \ \lambda_2 > 0. \tag{33}$$

Hence, symmetric bifurcation is not necessary for imper- fection insensitivity [8]. If $\lambda_1 = 0 \wedge \lambda_2 = 0$,

$$\lambda_3 = 0 \tag{34}$$

is a necessary condition for imperfection insensitivity which is automatically satisfied for symmetric bifurcation. Sufficient conditions for imperfection insensitivity in this case are

$$\lambda_3 = 0, \ \lambda_4 > 0. \tag{35}$$

Thus, for imperfection insensitivity the first non-vanishing coefficient in the asymptotic series expansion (4) must have an even subscript which is automatically the case for symmetric bifurcation, and must be positive.

5. Hilltop buckling

In the following it will be proved that hilltop buckling is imperfection sensitive. Introducing the parameter ξ, which refers to the primary path, into (16), gives

$$a_1 = -\frac{1}{2\lambda_{,\xi}}\left(\frac{\mathbf{v}_1^T \cdot \tilde{\mathbf{K}}_{T,\xi\xi} \cdot \mathbf{v}_1}{\mathbf{v}_1^T \cdot \tilde{\mathbf{K}}_{T,\xi} \cdot \mathbf{v}_1} - \frac{\lambda_{,\xi\xi}}{\lambda_{,\xi}}\right)\Bigg|_{\xi=\xi_C}, \tag{36}$$

with $\xi = \xi_C$ indicating the stability limit $\lambda = \lambda_C$.

At the snap-through point, $\lambda(\xi)$ has a local maximum:

$$\lambda_{,\xi} = 0,\ \lambda_{,\xi\xi} < 0. \tag{37}$$

Because of

$$\mathbf{v}_1^T \cdot \tilde{\mathbf{K}}_{T,\xi} \cdot \mathbf{v}_1 \neq 0,\ \left|\mathbf{v}_1^T \cdot \tilde{\mathbf{K}}_{T,\xi\xi} \cdot \mathbf{v}_1\right| \neq \infty, \tag{38}$$

the first term in parentheses of (36) is negligible. Thus

$$a_1 = -\infty. \tag{39}$$

Because of $\lambda_{,\xi\xi}\big/\lambda_{,\xi}^2$ with (37), a_1 has a pole of 2nd order.

Alternatively, the path parameter η, referring to the secondary path, is inserted into (16), which gives

$$a_1 = -\frac{1}{2\lambda_{,\eta}}\left(\frac{\mathbf{v}_1^T \cdot \tilde{\mathbf{K}}_{T,\eta\eta} \cdot \mathbf{v}_1}{\mathbf{v}_1^T \cdot \tilde{\mathbf{K}}_{T,\eta} \cdot \mathbf{v}_1} - \frac{\lambda_{,\eta\eta}}{\lambda_{,\eta}}\right)\Bigg|_{\eta=0}, \tag{40}$$

with $\eta = 0$ indicating the stability limit $\lambda = \lambda_C$.

Equating the right-hand side (40) to the one of (36) gives

$$\lambda_{,\eta\eta}\big|_{\eta=0} = \left(\frac{\lambda_{,\eta}\big|_{\eta=0}}{\lambda_{,\xi}\big|_{\xi=\xi_C}}\right)^2 \lambda_{,\xi\xi} - \left(\frac{\lambda_{,\eta}\big|_{\eta=0}}{\lambda_{,\xi}\big|_{\xi=\xi_C}}\right)^2 \frac{\mathbf{v}_1^T \cdot \tilde{\mathbf{K}}_{T,\xi\xi} \cdot \mathbf{v}_1}{\mathbf{v}_1^T \cdot \dfrac{\tilde{\mathbf{K}}_{T,\xi}}{\lambda_{,\xi}} \cdot \mathbf{v}_1}\Bigg|_{\xi=\xi_C}$$

$$+ \frac{\mathbf{v}_1^T \cdot \tilde{\mathbf{K}}_{T,\eta\eta} \cdot \mathbf{v}_1}{\mathbf{v}_1^T \cdot \dfrac{\tilde{\mathbf{K}}_{T,\eta}}{\lambda_{,\eta}} \cdot \mathbf{v}_1}\Bigg|_{\eta=0},\ \lambda_{,\xi} > 0, \tag{41}$$

where, for the time being, hilltop buckling is excluded. Inserting

$$\lambda_{,\eta}\big|_{\eta=0} = \lambda_1 \text{ and } \lambda_{,\eta\eta}\big|_{\eta=0} = 2\lambda_2, \tag{42}$$

which follows from (4), and

$$\mathbf{v}_1^T \cdot \frac{\tilde{\mathbf{K}}_{T,\eta}}{\lambda_{,\eta}} \cdot \mathbf{v}_1\Bigg|_{\eta=0} = \mathbf{v}_1^T \cdot \frac{\tilde{\mathbf{K}}_{T,\xi}}{\lambda_{,\xi}} \cdot \mathbf{v}_1\Bigg|_{\xi=\xi_C} = \mathbf{v}_1^T \cdot \tilde{\mathbf{K}}_{T,\lambda} \cdot \mathbf{v}_1\big|_{\lambda=\lambda_C} \tag{43}$$

into (41) yields

$$\lambda_2 = \frac{1}{2}\left(\frac{\lambda_1}{\lambda_{,\xi}\big|_{\xi=\xi_C}}\right)^2\left(\lambda_{,\xi\xi}\big|_{\xi=\xi_C} - \frac{\mathbf{v}_1^T \cdot \tilde{\mathbf{K}}_{T,\xi\xi}\big|_{\xi=\xi_C} \cdot \mathbf{v}_1}{\mathbf{v}_1^T \cdot \tilde{\mathbf{K}}_{T,\lambda}\big|_{\lambda=\lambda_C} \cdot \mathbf{v}_1}\right) +$$

$$+ \frac{1}{2}\frac{\mathbf{v}_1^T \cdot \tilde{\mathbf{K}}_{T,\eta\eta}\big|_{\eta=0} \cdot \mathbf{v}_1}{\mathbf{v}_1^T \cdot \tilde{\mathbf{K}}_{T,\lambda}\big|_{\lambda=\lambda_C} \cdot \mathbf{v}_1},$$

(44)

where [3]

$$-\infty < \mathbf{v}_1^T \cdot \tilde{\mathbf{K}}_{T,\xi}\big|_{\xi=\xi_C} \cdot \mathbf{v}_1 < 0.$$

(45)

In order not to *a priori* dismiss the antithesis, i.e. the possibility of imperfection insensitivity for hilltop buckling, the special case of

$$\lambda_{,\eta}\big|_{\eta=0} = \lambda_1 = 0$$

(46)

will be considered, resulting in

$$\lambda_2 = \frac{1}{2}\frac{\mathbf{v}_1^T \cdot \tilde{\mathbf{K}}_{T,\eta\eta}\big|_{\eta=0} \cdot \mathbf{v}_1}{\mathbf{v}_1^T \cdot \tilde{\mathbf{K}}_{T,\lambda}\big|_{\lambda=\lambda_C} \cdot \mathbf{v}_1},$$

(47)

where

$$0 \le \left|\mathbf{v}_1^T \cdot \tilde{\mathbf{K}}_{T,\eta\eta} \cdot \mathbf{v}_1\right| < \infty.$$

(48)

Following from (45), (47) and (48), $\lambda_2 = 0$ requires

$$\mathbf{v}_1^T \cdot \tilde{\mathbf{K}}_{T,\eta\eta}\big|_{\eta=0} \cdot \mathbf{v}_1 = 0.$$

(49)

Extending now the validity of (47) to hilltop buckling, i.e. replacing (41.2) by

$$\lambda_{,\xi} \ge 0,$$

(50)

requires extending the range in (45) from $(-\infty, 0)$ to $[-\infty, 0)$ and in (48) from $[0, \infty)$ to $[0, \infty]$. Hence, for hilltop buckling $\lambda_2 = 0$ represents an indeterminate expression with

$$\mathbf{v}_1^T \cdot \tilde{\mathbf{K}}_{T,\lambda}\big|_{\lambda=\lambda_C} \cdot \mathbf{v}_1 = -\infty \quad \wedge \quad \left|\mathbf{v}_1^T \cdot \tilde{\mathbf{K}}_{T,\eta\eta}\big|_{\eta=0} \cdot \mathbf{v}_1\right| = \infty$$

(51)

To show that hilltop buckling is necessarily imperfection sensitive, a design parameter κ is increased. Initially,

$$\kappa = \kappa_0 \ge 0, \quad \lambda_2(\kappa_0) < 0, \quad \lambda_{2,\kappa}(\kappa_0) > 0.$$

(52)

The purpose of this sensitivity study is conversion of an originally imperfection sensitive into an imperfection insensitive structure. As follows from (45) and its extension to (51.1), and from (47) and (51.2),

$$0 < \mathbf{v}_1^T \cdot \tilde{\mathbf{K}}_{T,\eta\eta}\big|_{\eta=0} \cdot \mathbf{v}_1\bigg|_{\kappa=\kappa_0} \le \infty$$

(53)

If hilltop buckling occurs for $\kappa = \kappa_0$,

$$\mathbf{v}_1^T \cdot \tilde{\mathbf{K}}_{T,\eta\eta}\big|_{\eta=0} \cdot \mathbf{v}_1\bigg|_{\kappa=\kappa_0} = \infty$$

(54)

Fig. 2(a) refers to this situation. It shows that hilltop buckling is imperfection sensitive.

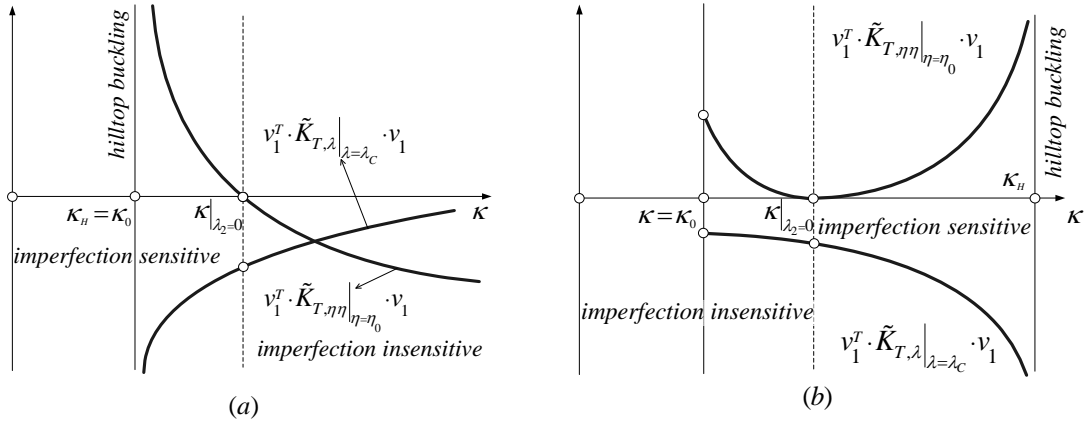If hilltop buckling occurs for $\kappa = \kappa_H > \kappa_0$,

Fig. 2: Hilltop buckling as (a) the A *and (b) the* Ω *of sensitivity analysis*

$$0 < \mathbf{v}_1^T \cdot \tilde{\mathbf{K}}_{T,\eta\eta}\Big|_{\eta=0} \cdot \mathbf{v}_1\Big|_{\kappa=\kappa_0} < \infty \tag{55}$$

$$\mathbf{v}_1^T \cdot \tilde{\mathbf{K}}_{T,\eta\eta}\Big|_{\eta=0} \cdot \mathbf{v}_1\Big|_{\kappa=\kappa_0} = \infty \tag{56}$$

(56) follows from the fact that for both cases

$$\left(\mathbf{v}_1^T \cdot \tilde{\mathbf{K}}_{T,\lambda}\Big|_{\lambda=\lambda_C} \cdot \mathbf{v}_1\right)_{,\kappa\kappa} < 0, \quad \mathbf{v}_1^T \cdot \tilde{\mathbf{K}}_{T,\eta\eta}\Big|_{\eta=0} \cdot \mathbf{v}_1\Big|_{\kappa=\kappa_0} > 0. \tag{57}$$

Fig. 2(b) refers to $\kappa = \kappa_H > \kappa_0$ It shows that also for this case hilltop buckling is imperfection sensitive. Information about λ_4 is obtained from specialization of (28) for $a_1 = -\infty^2$ and $\lambda_2 < 0$ and consideration of the following scheme:

$$\begin{array}{rclclcl} \lambda_4 &=& a_1\lambda_2^2 &+& d_3 &+& b_2\lambda_2 \\ && -\infty^2 &+& \infty^2 && \\ && &+& \infty^1 &-& \infty^1 \\ && && &-& \infty^0. \end{array} \tag{58}$$

In this scheme, "∞^2", "∞^1", and "∞^0" denote a pole of 2nd, 1st, and 0th order (with respect to a variable design parameter κ), noting that the latter is a positive, finite number. The scheme is based on the hypothesis that (58) cannot disintegrate at hilltop buckling. Numerical results have validated the scheme according to which

$$b_2 = \infty^1, \quad d_3 = \infty^2, \quad -\infty < \lambda_4 < 0. \tag{59}$$

Eq. (59) corroborates the conjecture that for the symmetric bifurcation at the hilltop all coefficients with an even subscript in the asymptotic series expansion (4) must be negative, finite numbers.

6. Classification of sensitivity analyses of the initial postbuckling behavior

6.1. Consistently linearized eigenvalue problem

With the help of the consistently linearized eigenproblem, sensitivity analyses of the initial postbuckling behavior can be categorized in two classes. For a specific value of κ, this eigenproblem is defined as [8], [9]

$$\left[\tilde{\mathbf{K}}_T + (\lambda^* - \lambda)\tilde{\mathbf{K}}_{T,\lambda}\right] \cdot \mathbf{v}^* = \mathbf{0}. \tag{60}$$

In (60), $(\lambda^* - \lambda) \in \mathbb{R}$ is the eigenvalue corresponding to the eigenvector $\mathbf{v}^* \in \mathbb{R}^N$. Because of (20), λ^* and $\mathbf{v}^*$ are functions of λ. If $\lambda^* = \lambda$, $\tilde{\mathbf{K}}_T$ is singular. Thus, a candidate for the stability limit is found [8]. The first eigenpair of (60) is $\left(\lambda_1^*,\ \mathbf{v}_1^*\right)$. At the stability limit,

$$\lambda_1^* = \lambda = \lambda_C, \quad \mathbf{v}_1^* = \mathbf{v}_1. \tag{61}$$

(Recall that λ_C and $\mathbf{v}_1$ appear on the right-hand side of (4) and (5), respectively.)

Furthermore, at the stability limit [3],

$$\mathbf{v}_{1,\lambda}^* = a_1 \mathbf{v}_1 \quad \wedge$$

$$\mathbf{v}_{1,\lambda\lambda}^* = 3\left(a_1^2 + a_1^*\right)\mathbf{v}_1 + \sum_{j=2}^{N} \frac{\mathbf{v}_j^{*T} \cdot \tilde{\mathbf{K}}_{T,\lambda\lambda} \cdot \mathbf{v}_1}{(\lambda_1^* - \lambda_j^*)(\mathbf{v}_j^{*T} \cdot \tilde{\mathbf{K}}_{T,\lambda} \cdot \mathbf{v}_j^*)} \, \mathbf{v}_j^*. \tag{62}$$

Equating (47) to (16) gives

$$\lambda_2 = -\frac{a_1}{\mathbf{v}_1^T \cdot \tilde{\mathbf{K}}_{T,\lambda\lambda} \cdot \mathbf{v}_1} \mathbf{v}_1^T \cdot \tilde{\mathbf{K}}_{T,\eta\eta} \cdot \mathbf{v}_1 \tag{63}$$

where [3]

$$a_1 = -\frac{1}{2} \lambda_{1,\lambda\lambda}^* \Big|_{\lambda=\lambda_C}. \tag{64}$$

Because $\mathbf{v}_1^T \cdot \tilde{\mathbf{K}}_{T,\lambda} \cdot \mathbf{v}_1$ does not vanish [3], the same applies to $a_1 / \mathbf{v}_1^T \cdot \tilde{\mathbf{K}}_{T,\lambda\lambda} \cdot \mathbf{v}_1$, as follows from (16). Consequently, $a_1 = 0$ requires $\mathbf{v}_1^T \cdot \tilde{\mathbf{K}}_{T,\lambda\lambda} \cdot \mathbf{v}_1 = 0$. It follows that

$$\frac{a_1}{\left(\mathbf{v}_1^T \cdot \tilde{\mathbf{K}}_{T,\lambda\lambda} \cdot \mathbf{v}_1\right)\Big|_{\lambda=\lambda_C}} = -\frac{1}{2} \frac{\lambda_{1,\lambda\lambda}^*}{\mathbf{v}_1^{*T} \cdot \tilde{\mathbf{K}}_{T,\lambda\lambda} \cdot \mathbf{v}_1^*}\Bigg|_{\lambda=\lambda_C} = \frac{0}{0} =$$

$$= -\frac{1}{2} \frac{\lambda_{1,\lambda\lambda\lambda}^*}{\left(2\mathbf{v}_1^{*T} \cdot \tilde{\mathbf{K}}_{T,\lambda\lambda} \cdot \mathbf{v}_{1,\lambda}^* + \mathbf{v}_1^{*T} \cdot \tilde{\mathbf{K}}_{T,\lambda\lambda\lambda} \cdot \mathbf{v}_1^*\right)}\Bigg|_{\lambda=\lambda_C} = \tag{65}$$

$$= \frac{3a_1^*}{\mathbf{v}_1^T \cdot \tilde{\mathbf{K}}_{T,\lambda\lambda\lambda} \cdot \mathbf{v}_1} \neq 0$$

where use of (19), (61.1) and (62.1) with $a_1 = 0$ was made and, following from (65),

$$a_1^* = -\frac{1}{6} \lambda_{1,\lambda\lambda\lambda}^* \Big|_{\lambda=\lambda_C}. \tag{66}$$

For class II, in contrast to class I, $a_1 = 0$ implies

$$a_1^* = 0 \tag{67}$$

which requires

$$\mathbf{v}_1^T \cdot \tilde{\mathbf{K}}_{T,\lambda\lambda\lambda} \cdot \mathbf{v}_1 = 0, \tag{68}$$

as follows from (65). Thus

$$\frac{a_1^*}{\mathbf{v}_1^T \cdot \tilde{\mathbf{K}}_{T,\lambda\lambda\lambda} \cdot \mathbf{v}_1} = \frac{\lambda_{1,\lambda\lambda\lambda}^*}{\left(2\mathbf{v}_1^{*T} \cdot \tilde{\mathbf{K}}_{T,\lambda\lambda} \cdot \mathbf{v}_{1,\lambda} + \mathbf{v}_1^{*T} \cdot \tilde{\mathbf{K}}_{T,\lambda\lambda\lambda} \cdot \mathbf{v}_1^*\right)\Big|_{\lambda=\lambda_C}} =$$

$$= \frac{0}{0} = -\frac{1}{6} \frac{\lambda_{1,\lambda\lambda\lambda\lambda}^*}{\left(2\mathbf{v}_{1,\lambda}^{*T} \cdot \tilde{\mathbf{K}}_{T,\lambda\lambda} \cdot \mathbf{v}_{1,\lambda}^* + 4\mathbf{v}_1^{*T} \cdot \tilde{\mathbf{K}}_{T,\lambda\lambda\lambda} \cdot \mathbf{v}_{1,\lambda}^*\right.}\cdots$$

$$\cdots\frac{}{\left.+2\mathbf{v}_1^{*T} \cdot \tilde{\mathbf{K}}_{T,\lambda\lambda} \cdot \mathbf{v}_{1,\lambda\lambda}^* + \mathbf{v}_1^{*T} \cdot \tilde{\mathbf{K}}_{T,\lambda\lambda\lambda\lambda} \cdot \mathbf{v}_1^*\right)\Big|_{\lambda=\lambda_C}} =$$

$$= -\frac{1}{6} \frac{\lambda_{1,\lambda\lambda\lambda\lambda}^*}{\left(2\mathbf{v}_1^{*T} \cdot \tilde{\mathbf{K}}_{T,\lambda\lambda} \cdot \mathbf{v}_{1,\lambda\lambda}^* + \mathbf{v}_1^{*T} \cdot \tilde{\mathbf{K}}_{T,\lambda\lambda\lambda\lambda} \cdot \mathbf{v}_1^*\right)\Big|_{\lambda=\lambda_C}} \neq 0. \tag{69}$$

For the special case of

$$\tilde{\mathbf{K}}_{T,\lambda\lambda} \cdot \mathbf{v}_1 = 0, \tag{70}$$

$$\frac{a_1^*}{\mathbf{v}_1^T \cdot \tilde{\mathbf{K}}_{T,\lambda\lambda\lambda} \cdot \mathbf{v}_1} = -\frac{1}{6} \frac{\lambda_{1,\lambda\lambda\lambda\lambda}^*}{\mathbf{v}_1^{*T} \cdot \tilde{\mathbf{K}}_{T,\lambda\lambda\lambda\lambda} \cdot \mathbf{v}_1^*}\Bigg|_{\lambda=\lambda_C} \neq 0. \tag{71}$$

The joint vanishing of a_1 and a_1^* represents a limiting case insofar as it correlates with a limiting value of $\lambda_2(a_1 = 0)$. (See Sections 6.2. and 6.3.)

6.2. Class I

This class is characterized by

$$\mathbf{v}_j^{*T} \cdot \tilde{\mathbf{K}}_{T,\lambda\lambda} \cdot \mathbf{v}_1 = 0 \quad \forall \ j \in \{2,3,\ldots,N\}, \tag{72}$$

resulting in

$$\mathbf{v}_{1,\lambda\lambda}^* = 3(a_1^2 + a_1^*)\mathbf{v}_1. \tag{73}$$

This remarkable orthogonality relation represents the special case that the curve described by the vector function $\mathbf{v}_1^*(\lambda)$ degenerates into a straight line.

For

$$\lambda_2 = 0, \tag{74}$$
$$a_1 < 0, \quad b_2 > 0, \quad \lambda_4 = d_3. \tag{75}$$

The signs of a_1 and b_2 are the same as for hilltop buckling. The sign of $\lambda_4 = d_3$ which follows from (28) is indeterminate. For

$$a_1 = 0, \tag{76}$$
$$\lambda_2 > 0. \tag{77}$$

For class I, (76) requires [2]

$$\tilde{\mathbf{K}}_{T,\lambda\lambda} \cdot \mathbf{v}_1 = \mathbf{0}. \tag{78}$$

Fig. 3(a) (3(b)) shows qualitative plots of a_1 and b_2 (λ_2, d_3, and λ_4) as functions of κ which denotes the stiffness of an elastic spring attached to the structure, details of which will be given in Chapter 7 (Numerical investigation).

Fig. 3 refers to a situation where hilltop buckling represents the starting point of sensitivity analysis, characterized by

$$\kappa = 0. \tag{79}$$

Fig. 3: Sensitivity analysis (class I, hilltop buckling as the starting point):
(a) $a_1(\kappa)$, $b_2(\kappa)$; (b) $\lambda_2(\kappa)$, $d_3(\kappa)$, $\lambda_4(\kappa)$

In Fig. 3(b),

$$d_3(\lambda_2 = 0) = \lambda_4(\lambda_2 = 0) > 0 , \tag{80}$$

indicating that at $\lambda_2 = 0$ the structure is already imperfection insensitive. For $d_3(\lambda_2 = 0) < 0$, the structure would still be imperfection sensitive at $\lambda_2 = 0$. For $d_3(\lambda_2 = 0) = 0$, the sign of $\lambda_6(\lambda_2 = 0, \lambda_4 = 0)$ would determine the initial postbuckling state of the structure. The linear dependence of λ_2 and λ_4 on κ represents a special situation.

6.3. Class II

In this class, (72) does not hold. Furthermore, contrary to class I,

$$\lambda_2 = 0 \tag{81}$$

jointly occurs with

$$a_1 = 0 \quad (\text{with } \tilde{\mathbf{K}}_{T,\lambda\lambda} \cdot \mathbf{v}_1 \neq \mathbf{0} \vee = \mathbf{0}) \tag{82}$$

and

$$a_1^* = 0 \quad (\text{with } \tilde{\mathbf{K}}_{T,\lambda\lambda\lambda} \cdot \mathbf{v}_1 \neq \mathbf{0}). \tag{83}$$

Substitution of (82) into (62.1) and of (82) and (83) into (62.2) gives

$$\mathbf{v}_{1,\lambda}^* = \mathbf{0} \quad \wedge \quad \mathbf{v}_{1,\lambda\lambda}^* = \sum_{j=2}^{N} \frac{\mathbf{v}_j^{*T} \cdot \tilde{\mathbf{K}}_{T,\lambda\lambda} \cdot \mathbf{v}_1}{(\lambda_1^* - \lambda_j^*)(\mathbf{v}_j^{*T} \cdot \tilde{\mathbf{K}}_{T,\lambda} \cdot \mathbf{v}_j^*)} \; \mathbf{v}_j^* \begin{cases} = \mathbf{0} \text{ if } \tilde{\mathbf{K}}_{T,\lambda\lambda} \cdot \mathbf{v}_1 = \mathbf{0} \\ \neq \mathbf{0} \text{ else} \end{cases} \tag{84}$$

indicating a singular point $\mathbf{v}_1^*(\lambda_C) = \mathbf{v}_1$ in the form of a cusp on the curve described by the vector function $\mathbf{v}_1^*(\lambda)$.

Fig. 4(a) (4(b)) shows qualitative plots of a_1 and b_2 (λ_2, d_3, and λ_4) as functions of κ which denotes the stiffness of an elastic spring attached to the structure, details of which will be given in Chapter 7 (Numerical investigation). Fig. 4 refers to a situation where hilltop buckling represents the starting point of sensitivity analysis, characterized by
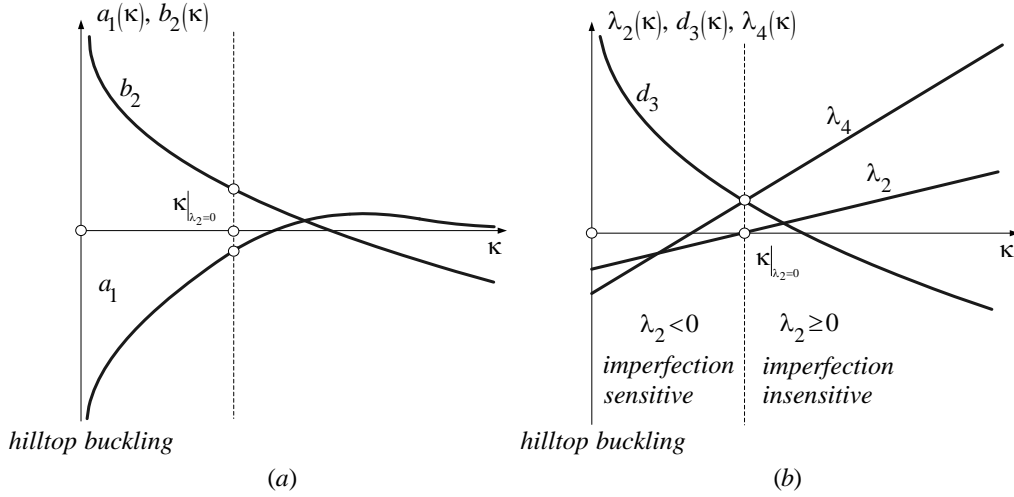
$$\kappa = 0 . \tag{85}$$

Fig. 4: Sensitivity analysis (class II, hilltop buckling as the starting point):
(a) $a_1(\kappa), b_2(\kappa)$; (b) $\lambda_2(\kappa), d_3(\kappa), \lambda_4(\kappa)$

Substitution of (81) into (28) and into its first derivative with respect to κ gives,

$$(d_3 - \lambda_4) = 0, \tag{86}$$

$$b_2 \, \lambda_{2,\kappa} + (d_3 - \lambda_4)_{,\kappa} = 0. \tag{87}$$

Because of (82) and, contrary to Fig. 3(a), of $\lim_{\kappa \to \infty} a_1 \neq 0$ (see Fig. 4(a)),

$$b_2 = 0 \quad \wedge \quad (d_3 - \lambda_4)_{,\kappa} = 0 \tag{88}$$

(see Figs. 4 and 5). According to Fig. 4(b),

$$d_3(\lambda_2 = 0) = \lambda_4(\lambda_2 = 0) < 0, \tag{89}$$

indicating that for $\lambda_2 = 0$ the structure is still imperfection sensitive.

Following from (88.2)

$$d_{3,\kappa}(\lambda_2 = 0) = \lambda_{4,\kappa}(\lambda_2 = 0) \tag{90}$$

(see Figs. 4(b) and 5(b)). Fig. 4 is based on $\mathbf{v}_{1,\lambda\lambda}^* \neq \mathbf{0}$.

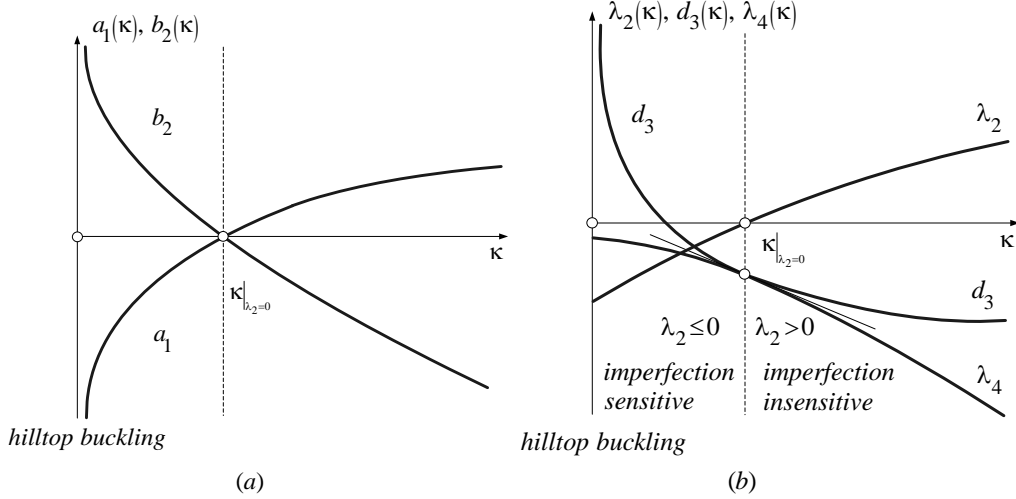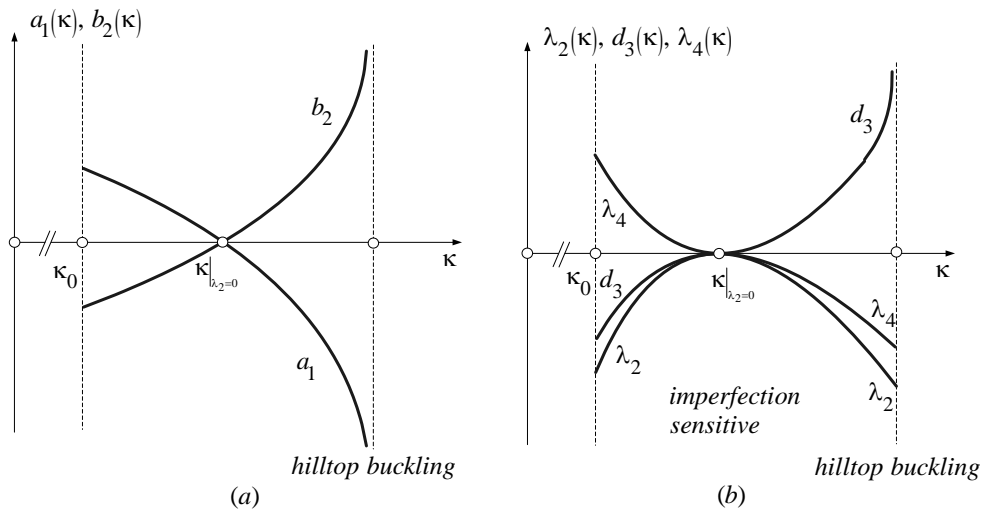Fig. 5: Sensitivity analysis (class II, hilltop buckling as the end):
(a) $a_1(\kappa), b_2(\kappa)$; (b) $\lambda_2(\kappa), d_3(\kappa), \lambda_4(\kappa)$

Fig. 5(a) (5(b)) shows qualitative plots of a_1 and b_2 (λ_2, d_3, and λ_4) as functions of κ standing for the thickness of the structure, details of which will be given in Chapter 7 (Numerical investigation).

The initial value of κ is denoted as κ_0. The curves illustrate a situation where hilltop buckling represents the end of sensitivity analysis because snap-through would become relevant to loss of stability if κ was further increased.

If $\mathbf{v}_{1,\lambda\lambda}^* = \mathbf{0}$, then also (see Fig. 5(b))

$$\lambda_{2,\kappa}(\lambda_2 = 0) = 0. \tag{91}$$

Furthermore, (86) and (88.2) disintegrate into (see Fig. 5(b))

$$d_3(\lambda_2 = 0) = \lambda_4(\lambda_2 = 0) = 0 \quad \wedge \quad d_{3,\kappa}(\lambda_2 = 0) = \lambda_{4,\kappa}(\lambda_2 = 0) = 0. \tag{92}$$

Substitution of (81), (82), (88.1), and (91) into the second derivative of (28) with respect to κ yields (see Fig. 5(b))

$$d_{3,\kappa\kappa}(\lambda_2 = 0) = \lambda_{4,\kappa\kappa}(\lambda_2 = 0) = 0. \tag{93}$$

At $\lambda_2 = 0$, there is no conversion from imperfection sensitivity into imperfection insensitivity. $\lambda_2 = 0$ marks the starting point of deterioration of the initial postbuckling behavior accompanied by continued improvement of the prebuckling behavior.

7. Numerical examples

The numerical investigation consists of one example each for the two classes of sensitivity analyses of the initial postbuckling behavior. In the example for class I (II), hilltop buckling is chosen as the starting point (end) of such sensitivity analysis. The example for class I (II) is solved analytically (numerically by the FEM).

7.1. Example for class I
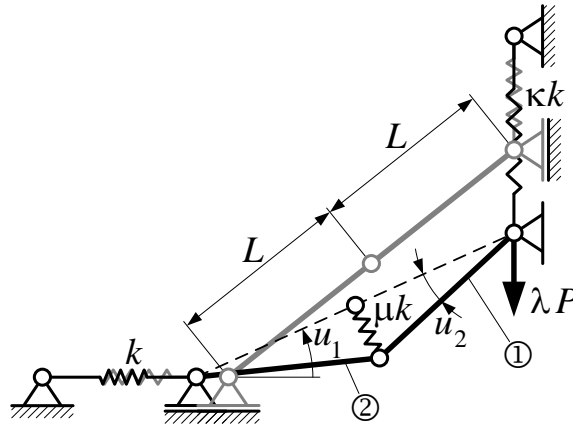
Fig. 6: Pin-jointed two-bar system [2]

Fig. 6 shows a planar, static, conservative system with two degrees of freedom. The description of this system closely follows [2] where additional details can be found. Both rigid bars, ① and ② have the same length L and in the non-buckled state they are in-line. The bars are linked at one end and supported by turning-and-sliding joints at their other ends. A horizontal linear elastic spring of stiffness k and a vertical linear elastic spring of stiffness κk are attached to turning-and-sliding joints. A spring of stiffness μk "pulls" the two bars back into their in-line position. The system is loaded by a vertical load λP at the vertical turning-and-sliding joint. The two displacement coordinates are the

angles u_1 and u_2, summarized in the vector $\mathbf{u} = [u_1, u_2]^{\mathrm{T}}$. In order to write the out-of-balance force $\mathbf{G}$ in the structure as defined in (1), other coordinates would have to be chosen. In fact, the angle u_1 would have to be replaced by the vertical position of the upper turning-and-sliding joint. This would only require a simple coordinate transformation. For convenience, however, the angle u_1 was chosen as a coordinate. The unloaded position, delineated in gray, is defined by $\mathbf{u} = [u_{10}, 0]^{\mathrm{T}}$. This system was first investigated in [4] and later on in [2].

The potential energy expression follows as

$$
\begin{aligned}
V(\mathbf{u}, \lambda) = {}& 2\kappa k L^2 \left(\sin(u_{10}) - \sin(u_1)\cos(u_2) \right)^2 \\
& + \frac{\mu k}{2} L^2 \sin^2(u_2) \\
& + 2 k L^2 \left(\cos(u_{10}) - \cos(u_1)\cos(u_2) \right)^2 \\
& - \lambda P 2 L \left(\sin(u_{10}) - \sin(u_1)\cos(u_2) \right).
\end{aligned}
\tag{94}
$$

The equilibrium equations $V_{,u_1} = 0$ and $V_{,u_2} = 0$ are satisfied for the primary path

$$
\begin{aligned}
& u_2 = 0, \\
& \lambda = \frac{2 L k}{P} \left((1-\kappa)\sin(u_1) - \cos(u_{10})\tan(u_1) + \kappa \sin(u_{10}) \right),
\end{aligned}
\tag{95}
$$

and for the secondary path

$$
\begin{aligned}
& u_2 = \pm \arccos\left(\frac{4}{4-\mu} \frac{\cos(u_{10})}{\cos(u_1)} \right), \\
& \lambda = \frac{2 L k}{P} \left(\frac{\mu - 4\kappa}{4-\mu} \cos(u_{10})\tan(u_1) + \kappa \sin(u_{10}) \right).
\end{aligned}
\tag{96}
$$

Since a perfect system is assumed, the sign of u_2 is indeterminate, i.e. it is not known into which direction the two bars will buckle. The tangent-stiffness matrix follows as

$$
\tilde{\mathbf{K}}_T = 4 k L^2 \operatorname{diag} \left\{
\begin{aligned}
& \kappa\left(1 + \sin(u_{10})\sin(u_1) - 2\sin^2(u_1)\right) \\
& + 1 + \cos(u_{10})\cos(u_1) - 2\cos^2(u_1) \quad , \\
& - \lambda \frac{P}{2 k L} \sin(u_1)
\end{aligned}
\right.
$$

$$
\left.
\begin{aligned}
& \kappa\left(\sin(u_{10})\sin(u_1) - \sin^2(u_1)\right) \\
& + \cos(u_{10})\cos(u_1) - \cos^2(u_1) \\
& - \lambda \frac{P}{2 k L} \sin(u_1)
\end{aligned}
\right\}.
\tag{97}
$$

Its derivative with respect to λ can be computed by

$$
\tilde{\mathbf{K}}_{T,\lambda} = V_{,\mathbf{uuu}} \cdot \tilde{\mathbf{u}}_{,\lambda} + \frac{\partial V_{,\mathbf{uu}}}{\partial \lambda},
\tag{98}
$$

where $\tilde{\mathbf{u}}_{,\lambda}$ is the derivative of the displacement vector along the primary path, which can be determined from the linear equation

$$\tilde{\mathbf{G}}_{,\lambda} = \tilde{\mathbf{K}}_T \cdot \tilde{\mathbf{u}}_{,\lambda} + \frac{\partial \tilde{\mathbf{G}}}{\partial \lambda} = \mathbf{0} .$$ (99)

The expression of $\tilde{\mathbf{K}}_{T,\lambda}$ looks similar to (97). For the sake of conciseness, it has been omitted. Hence, all terms necessary for solving the eigenproblem (60) are available.

$u_{10} \in (-\pi/2, \pi/2)$, $\mu \in \mathbb{R}^+$ and $\kappa \in \mathbb{R}^+$ are parameters that can be varied in order to achieve qualitative changes of the system. However, in this work, only κ was modified. The remaining two parameters were taken as $\mu = 3/5$ and $u_{10} = 0.67026$, in which case hilltop buckling occurs for $\kappa = 0$ representing the starting point of sensitivity analysis of the buckling load and the initial postbuckling behavior. The load-displacement path for hilltop buckling and its projection onto the plane $u_2 = 0$ are shown in Figs. 7(a) and 7(b), respectively. S labels the unloaded state. As the load is increased, the state will move up along the primary path until $C = D$ is reached. In case of a load-controlled system, snap-through will occur. However, a displacement-controlled system would bifurcate and the state would traverse one branch of the secondary path.

If $\eta = u_2$, the relevant coefficients of the series expansion (4) generally follow as

$$\lambda_1 = 0, \qquad \lambda_2 = \frac{kL}{P} \frac{(\kappa - \mu/4)}{\sqrt{1 - \frac{\cos^2(u_{10})}{(1 - \mu/4)^2}}}, \qquad \lambda_3 = 0, \qquad \lambda_4 = -\frac{\lambda_2}{12} \frac{1 - 4\frac{\cos^2(u_{10})}{(1 - \mu/4)^2}}{1 - \frac{\cos^2(u_{10})}{(1 - \mu/4)^2}} .$$ (100)

Thus, $\lambda_4 \propto \lambda_2$. For $\kappa = 0$ (hilltop buckling), this system is imperfection sensitive ($\lambda_2 < 0$), and λ_C exceeds the ultimate load of any imperfect system. Increasing the parameter κ, i.e. the stiffness of the vertical spring, improves the postbuckling behavior insofar as λ_2 eventually begins increasing monotonically. The system is imperfection insensitive for $\kappa > \mu/4$. Fig. 7(c) refers to the transition case $\kappa = \mu/4$. Remarkably, $\lambda = \lambda_C$ holds along the whole postbuckling path, which requires

$$\lambda_i = 0 \quad \forall \in \mathbb{N} \setminus \{0\} .$$ (101)

This situation is referred to as zero-stiffness postbuckling. In contrast to the present example, where zero-stiffness postbuckling is a special case of symmetric bifurcation, it may also be a special case of antisymmetric bifurcation [6]. However, this special case is of little practical interest because it does not represent a transition from imperfection sensitivity to imperfection insensitivity.

As κ is further increased, the critical displacement at the beginning of monotonically increasing prebuckling paths approaches 0. Eventually, at $\kappa = 1 - \cos(u_{10})$, the two turning points meet at $\mathbf{u} = \mathbf{0}$, where the primary path exhibits a saddle point D. This situation is shown in Fig. 7(d). A comparison of Figs. 7(b), 7(c), and 7(d) shows that the bifurcation point C is increasing less strongly with increasing κ than the snap through point D. Hence, the two points are diverging from each other.
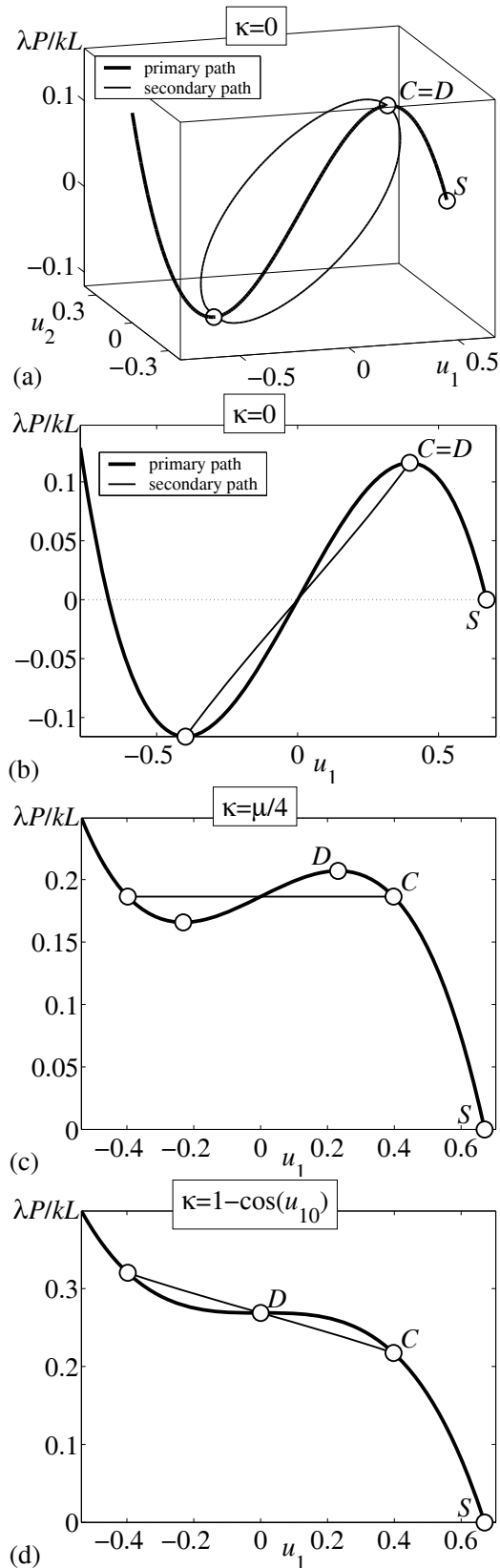
Fig. 7: Selected results from sensitivity analysis of the initial postbuckling behavior of the pin-jointed two-bar system shown in Fig. 5: (a) load-displacement path for hilltop buckling; (b), (c), (d) projections of load-displacement paths onto the plane $u_2 = 0$ for hilltop buckling, zero-stiffness postbuckling, and the beginning of monotonically increasing prebuckling paths
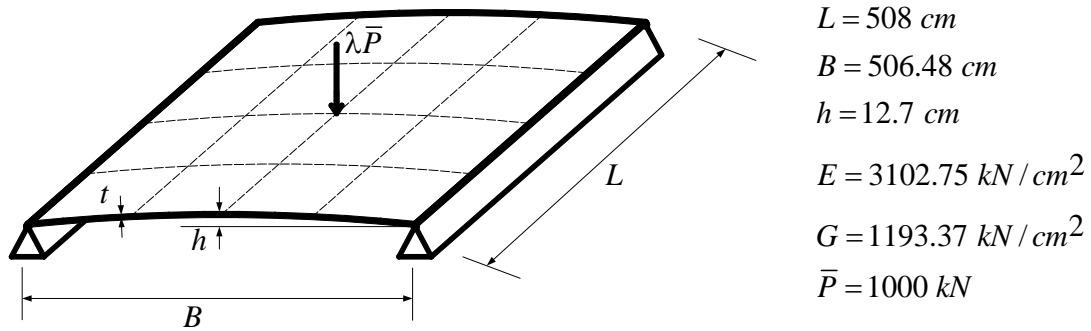
7.2.   Example for class II

$L = 508 \ cm$

$B = 506.48 \ cm$

$h = 12.7 \ cm$

$E = 3102.75 \ kN/cm^2$

$G = 1193.37 \ kN/cm^2$

$\overline{P} = 1000 \ kN$

Fig. 8: Shallow cylindrical shell subjected to a point load at the center [4]

Fig. 8 shows a shallow cylindrical shell subjected to a point load at the center. It contains the geometric data as well as values for the modulus of elasticity *E* and the shear modulus *G*. The reference load $\overline{P} = 1000 \ kN$ is scaled by a dimensionless load factor λ. The descrip- tion of sensitivity analysis of the initial postbuckling behavior of the shell is based on [4] where this structure was previously investigated and where additional details can be found.

In contrast to the first example, Koiter's initial postbuckling analysis was not used to compute post-buckling paths for this example. Instead of it, prebuckling and postbuckling analyses were performed by means of the FEM, using the finite element program MSC.Marc [10].

The parameter κ that is varied in the course of sensitivity analysis of the initial postbuckling behavior of the shell is the thickness. The initial value κ_0 was chosen as 5.35 *cm*. Load-displacement paths for $\kappa = 5.35 \ cm$, 6.35 *cm*, 7.35 *cm*, and 8.10 *cm* are shown in the left part of Fig. 9 where *u* denotes the displacement of the load point. The right part of Fig. 9 contains details of corresponding plots of the left part.

For each one of the four values of κ considered, the structure is imperfection sensitive. For the thinnest shell ($\kappa = 5.35 \ cm$), the slope of the postbuckling path at the stability limit is negative whereas the curvature is positive. The postbuckling path has a minimum followed by a maximum. For the second thinnest shell ($\kappa = 6.35 \ cm$), the slope of the postbuckling path at the stability limit is approximately zero, i.e. $\lambda_2 \approx 0$.

According to Fig. 5(b), for $\lambda_2 = 0$, also $\lambda_{2,\kappa} = 0$, $\lambda_4 = 0$, $\lambda_{4,\kappa} = 0$, and $\lambda_{4,\kappa\kappa} = 0$. Because of the negative curvature of the postbuckling path at the stability limit, the first non-vanishing coefficient of (4), which because of symmetric bifurcation must have an even subscript, is negative. For the second thickest shell ($\kappa = 7.35 \ cm$) and the thickest shell ($\kappa = 8.10 \ cm$), both the slope and the curvature of the postbuckling path are negative at the stability limit. For the thickest shell, hilltop buckling occurs. It represents the end of sensitivity analysis of the initial postbuckling behavior of the shell, because loss of stability would occur by snap-through if the thickness of the structure was further increased.
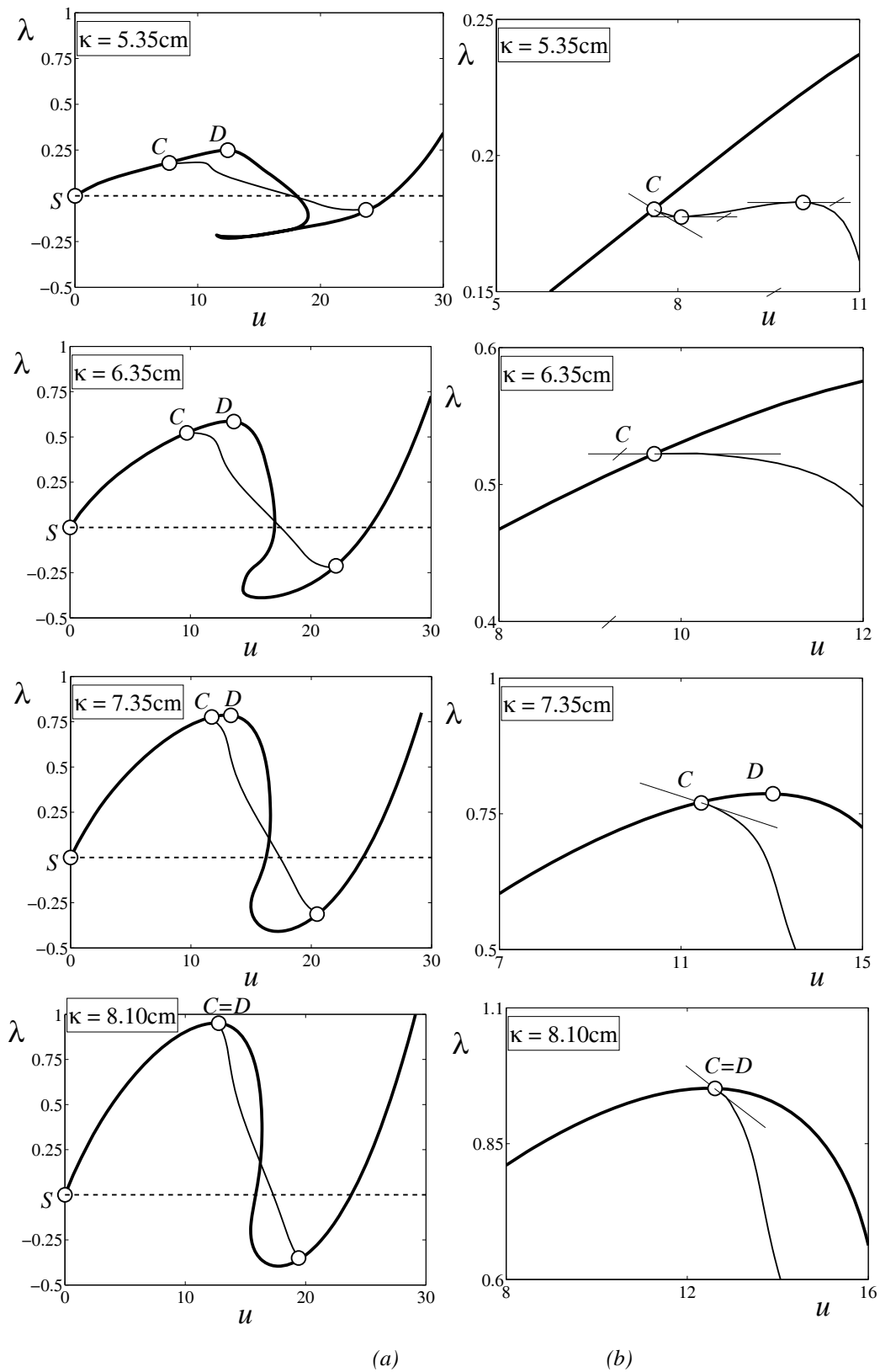
Fig.9: Selected results from sensitivity analysis of the initial postbuckling behavior of the shallow cylindrical shell shown in Figure 7: (a) Load-displacement paths for different values of the thickness of the shell, with the largest value referring to hilltop buckling; (b) details of load-displacement paths

A comparison of the plots in Fig. 9 shows that the bifurcation point C is increasing more strongly with increasing κ than the snap-through point D. Hence, the two points are converging to each other. This comparison also shows that $\lambda_2 = 0$ marks the starting point of deterioration of the initial postbuckling behavior accompanied by continued improvement of the pre- buckling behavior, characterized by

$$d\lambda_2 < 0 \ \wedge \ d\kappa > 0. \tag{102}$$

Fig. 9 elucidates that the increase of the thickness of the shell does not result in a transition from imperfection sensitivity to imperfection insensitivity.

8.   Conclusions

It was shown that hilltop buckling is imperfection sensitive.

It is conjectured that for symmetric bifurcation all non-vanishing coefficients in the asymptotic series expansion for the load level at an arbitrary point of the secondary path (see (4)) are negative, i.e. $\lambda_{2k} < 0 \ \forall k \in \mathbb{N} \setminus \{0\}$. This conjecture is based on a hypothesis representing the generalization of a scheme that was validated numerically for the special case of λ_4 (see (58)). Verification of this conjecture is planned.

Hilltop buckling as the starting point – the A – of sensitivity analysis of the initial postbuckling behavior of elastic structures is characterized by $\lambda_{2,\kappa} > 0$ with $d\lambda_2 > 0 \wedge d\kappa > 0$, where κ is a design parameter that is increased in the course of the analysis. It marks the starting point of an improvement of the initial postbuckling behavior of the structure, accompanied by an improvement of the prebuckling behavior. The bifurcation point and the snap-through point are diverging from each other.

Hilltop buckling as the end – the Ω – of such sensitivity analysis is characterized by $\lambda_{2,\kappa} < 0$, with $d\lambda_2 < 0 \wedge d\kappa > 0$. It is preceded by a deterioration of the initial postbuckling behavior of the structure, accompanied by an improvement of the prebuckling behavior. Hilltop buckling represents the end of sensitivity analysis because snap-through would become relevant to loss of stability if κ was further increased. The bifurcation point and the snap-through point are converging to each other.

Two classes of sensitivity analyses of the initial postbuckling behavior of elastic structures were identified. Class I is characterized by a remarkable orthogonality condition derived from the so-called consistently linearized eigenproblem (see (60)). It may be viewed as a special case of class II for which this condition does not hold. In mechanical terms, for the first class the decisive eigenvector of the eigenproblem, $\mathbf{v}_1^*(\lambda)$, describes a rectilinear motion, with λ representing the time. For class II, however, $\mathbf{v}_1^*(\lambda)$ describes a general motion. Hence, it is conjectured that class I is restricted to relatively simple problems.

The two classes of sensitivity analyses determine the mode of conversion of an originally imperfection- sensitive into an imperfection-insensitive structure. Such a conversion is the true motivation for this type of sensitivity analyses.

For class I, there is no restriction on the sign of $\lambda_4 (\lambda_2 = 0)$. Hence, for $\lambda_2 = 0$, the structure may either be already imperfection insensitive or still imperfection sensitive. As a special case, zero-stiffness postbuckling may occur (see Fig. 7(b)).

For class II, if $\mathbf{v}_{1,\lambda\lambda}^{*}(\lambda_C) \neq \mathbf{0}$, then $\lambda_{2,\kappa}(\lambda_2 = 0) > 0$, and $\lambda_4(\lambda_2 = 0) < 0$ (see Fig. 4(b)), but if $\mathbf{v}_{1,\lambda\lambda}^{*}(\lambda_C) = \mathbf{0}$, then $\lambda_{2,\kappa}(\lambda_2 = 0) = 0$, $\lambda_4(\lambda_2 = 0) = 0$, and $\lambda_{4,\kappa}(\lambda_2 = 0) = 0$, $\lambda_{4,\kappa\kappa}(\lambda_2 = 0) = 0$ (see Fig. 5(b)). For the second case there is no transition from imperfection sensitivity into imperfection insensitivity. Thus, the increase of the thickness of a structure, while improving its prebuckling behavior, does not result in such a transition. For class II, $\lambda_2 = 0$ correlates with a singular point in form of a cusp on the curve described by the vector function $\mathbf{v}_1^{*}(\lambda)$ at the point $\mathbf{v}_1^{*}(\lambda_C) = \mathbf{v}_1$ (see (84)). The type of the cusp depends on whether or not $\mathbf{v}_{1,\lambda\lambda}^{*}(\lambda_C)$ is zero.

The present investigation is viewed as a step in the direction of better understanding the reasons for the initial postbuckling behavior of a particular elastic structure and of its interplay with the prebuckling behavior. Such understanding will help to avoid the design of structures with unfavorable postbuckling characteristics. In this sense, the present study is aimed at changing the widespread opinion about postbuckling as a structural feature that can hardly be influenced.

Acknowledgements

References

[1] Fujii F, Noguchi H. *Multiple hill-top branching*. In Proc. 2nd Int. Conf. on Structural Stability and Dynamics, World Scientific, Singapore, 2002.

[2] Steinboeck A., Jia X. Hoefinger G., Mang H.A. *Remarkable postbuckling paths analyzed by means of the consistently linearized eigenproblem*. Int. J. Numer. Meth. Engng, 76, 156-182, 2008.

[3] Mang H.A., C. Schranz, P. Mackenzie-Helnwein. *Conversion from imperfection-sensitive into imperfection-insensitive elastic structures I: Theory*. Comput. Methods Appl. Mech. Engrg., 195, 1422-1457, 2006.

[4] Schranz C., Krenn B., Mang H.A. *Conversion from imperfection-sensitive into imperfection-insensitive elastic structures II: Numerical investigation*. Comput. Methods Appl. Mech. Engrg., 195 1458-1479, 2006.

[5] Koiter W. *On the stability of elastic equilibrium*, Translation of '*Over de Stabiliteit van het Elastisch Evenwicht*' (1945). In NASA TT F-10833, Polytechnic Institute Delft, H.J. Paris Publisher: Amsterdam, 1967.

[6] Steinboeck A, Jia X, Hoefinger G, Mang H.A. *Conditions for symmetric, antisymmetric, and zero-stiffness bifurcation in view of imperfection sensitivity and insensitivity*. Comput. Methods Appl. Mech. Engrg., 197, 3623-3636, 2008.

[7] Bochenek B. *Problems of structural optimization for post-buckling behaviour*. Struct. Multidisciplinary Optim., 25(5-6), 423-435, 2003.

[8] Helnwein P. *Zur initialen Abschätzbarkeit von Stabilitätsgrenzen auf nichtlinearen Last-Verschiebungspfaden elastischer Strukturen mittels der Methode der Finiten Elemente [in German; On ab initio assessability of stability limits on nonlinear load-displacement paths of elastic structures*

by means of the finite element method]. Ph.D. Thesis, Vienna University of Technology, Österreichischer Kunst- und Kulturverlag: Vienna, 1997.

[9] Mang H.A, Helnwein P. *Second-order a-priori estimates of bifurcation points on geometrically nonlinear prebuckling paths*. In Proc. Int. Conf. of Computational Engineering Science, Hawaii, USA. Springer: Berlin, 1995; II: 1511-1516.

[10] MSC.MARC volume A: *Theory and user information*, MSC.Marc manuals, 145-152, 2005.

[11] Ohsaki, M., Ikeda, K. *Imperfection sensitivity analysis of hill-top branching points with many symmetric bifurcation points*. International Journal of Solids and Structures, 43, 4704-4719, 2006.

Chapter V

Three Pending Questions in Structural Stability

Andreas Steinboeck[1], Gerhard Hoefinger[2], Xin Jia[2], and Herbert A. Mang[2]

[1] *Automation and Control Institute, Complex Dynamical Systems Group, Vienna University of Technology, Gusshausstrasse 27-29/376, 1040 Vienna, Austria*
[2] *Institute for Mechanics of Materials and Structures, Vienna University of Technology, Karlsplatz 13/202, 1040 Vienna, Austria*

Abstract

This analysis deals with three pending questions in structural stability:

- Are linear prebuckling paths and linear stability problems mutually conditional?

- Does the conversion from imperfection sensitivity into imperfection insensitivity by means of a modification of the original structural design require a symmetric postbuckling path?

- Is hilltop buckling, characterized by the coincidence of a bifurcation point and a snap-through point on a load-displacement path, necessarily imperfection sensitive?

The questions will be answered by means of both mathematical proofs and examples.

Keywords

linear prebuckling path, linear stability analysis, imperfection (in)sensitivity, symmetric postbuckling path, hilltop buckling.

1. Introduction

Despite the long history of structural stability as a field of great scientific relevance and practical importance, it still holds a number of questions which have not yet been rigorously answered. The reasons for some pieces of the structural stability landscape still being uncharted range from missing mathematical proofs to aspects that are commonly regarded as matters of course, which, at first glance, render thorough proofs dispensable. This is the motivation for delivering in this work some clear cut answers to the three questions listed in the abstract. Recently, they have been cursorily discussed in [11].

The questions are related to the analysis of load-displacement paths and, in particular, to *instability phenomena*, exhibiting either *imperfection sensitivity* or *insensitivity* [9]. After a brief theoretical introduction into the topic in Section 2, the Sections 3 through 5 answer the posed questions based on mathematical proofs and representative examples. The example problems are solved analytically or numerically or both. Their simple nature allows drawing focus on corroborating the theoretical findings of this work and permits quick repetition of the computations.

2. Theoretical foundations

For the analysis of static, conservative systems, the potential energy function $V(\mathbf{u}, \lambda): \mathbb{R}^N \times \mathbb{R} \to \mathbb{R}$ can serve as a basis. Here, $\mathbf{u} \in \mathbb{R}^N$ is the vector of generalized displacement coordinates, and $\lambda \in \mathbb{R}$ is a load multiplier which scales a constant reference load $\mathbf{P} \in \mathbb{R}^N$. It is assumed that the system is either discrete or has been discretized such that the number of degrees of freedom N is finite. The derivative

$$\mathbf{G}(\mathbf{u}, \lambda) := V_{,\mathbf{u}} = \mathbf{F}^I(\mathbf{u}) - \lambda \mathbf{P} \tag{1}$$

may be interpreted as an out-of-balance force. $\mathbf{F}^I(\mathbf{u}) \in \mathbb{R}^N$ is the vector of internal forces. The implicit equation

$$\mathbf{G}(\mathbf{u}, \lambda) = \mathbf{0} \tag{2}$$

defines the equilibrium paths of the system. If two equilibrium paths intersect, the system is said to *bifurcate* at the point of intersection. Hereinafter, bifurcation points are denoted as $(\mathbf{u}_C, \lambda_C)$, like point C in Fig. 1. The equilibrium path which contains the unloaded state is referred to as *primary* or *prebuckling* path $(\tilde{\mathbf{u}}(\lambda), \lambda)$. Any other equilibrium path is called a *secondary* or *postbuckling* path. In this work it is assumed that there is just *one* secondary path $(\mathbf{u}(\eta), \lambda(\eta))$, which is uniquely parameterized by $\eta \in \mathbb{R}$, such that $(\mathbf{u}(\eta), \lambda(\eta))|_{\eta=0} = (\mathbf{u}_C, \lambda_C)$.

The differential of (2)

$$\mathbf{K}_T \cdot d\mathbf{u} - d\lambda \mathbf{P} = \mathbf{0}, \tag{3}$$

with the symmetric tangent stiffness matrix $\mathbf{K}_T = \mathbf{F}^I_{,\mathbf{u}}(\mathbf{u})$ plays an important role for the solution of structural problems by the FEM.
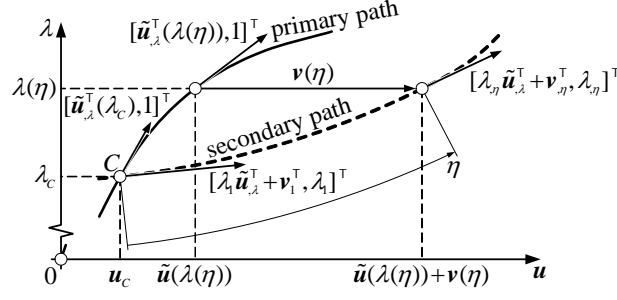
Fig. 1: On the series expansion of the secondary path at the bifurcation point C (adopted from [9])

The notation $\tilde{\mathbf{K}}_T = \mathbf{F}_{,\mathbf{u}}^I(\tilde{\mathbf{u}}(\lambda))$ is used for the specialization of $\mathbf{K}_T$ for the primary path. Along this path, apart from snap-through points, where $d\lambda = 0$, (3) can be written as

$$\tilde{\mathbf{K}}_T \cdot \tilde{\mathbf{u}}_{,\lambda} - \mathbf{P} = \mathbf{0}. \tag{4}$$

Differentiating a second time with respect to λ yields

$$\tilde{\mathbf{K}}_{T,\lambda} \cdot \tilde{\mathbf{u}}_{,\lambda} + \tilde{\mathbf{K}}_T \cdot \tilde{\mathbf{u}}_{,\lambda\lambda} = \mathbf{0}. \tag{5}$$

In the context of Koiter's initial postbuckling analysis [8], the displacement offset $\mathbf{v}(\eta) \in \mathbb{R}^N$ between the primary and the secondary path is introduced as outlined in Fig. 1. Therefore, with

$$\mathbf{u}(\eta) = \tilde{\mathbf{u}}(\lambda(\eta)) + \mathbf{v}(\eta), \tag{6}$$

the specialization of (2) for the secondary path reads as $\mathbf{G}(\eta) = \mathbf{G}(\tilde{\mathbf{u}}(\lambda(\eta)) + \mathbf{v}(\eta), \lambda(\eta)) = \mathbf{0}$. Insertion of the series expansions

$$\lambda(\eta) = \lambda_C + \lambda_1\eta + \lambda_2\eta^2 + \lambda_3\eta^3 + \mathcal{O}(\eta^4) \tag{7}$$

$$\mathbf{v}(\eta) = \qquad \mathbf{v}_1\eta + \mathbf{v}_2\eta^2 + \mathbf{v}_3\eta^3 + \mathcal{O}(\eta^4) \tag{8}$$

yields the new series expansion

$$\mathbf{G}(\eta) := \mathbf{G}_{0C} + \mathbf{G}_{1C}\eta + \mathbf{G}_{2C}\eta^2 + \mathbf{G}_{3C}\eta^3 + \mathcal{O}(\eta^4) = \mathbf{0} \tag{9}$$

with $\mathbf{G}_{nC} = \mathbf{G}_{,\eta^n}|_{\eta=0}/n! \; \forall n \in \mathbb{N}$. To simplify their computation, Mang *et al.* [9] used for tensorial quantities $\boldsymbol{f}(\mathbf{u}, \lambda)$ the differentiation rule

$$\boldsymbol{f}_{;\lambda}(\mathbf{u}, \lambda) := \boldsymbol{f}_{,\lambda}(\mathbf{u}, \lambda) + \left.\frac{\partial \boldsymbol{f}(\mathbf{u} + \alpha\,\tilde{\mathbf{u}}_{,\lambda}(\lambda), \lambda)}{\partial \alpha}\right|_{\alpha=0} \tag{10}$$

with $\alpha \in \mathbb{R}$. Then the first three coefficients in (9) read as

$$\mathbf{G}_{0C} = \mathbf{0},$$
$$\mathbf{G}_{1C} = \mathbf{G}_{,\mathbf{u}C} \cdot \mathbf{v}_1, \tag{11}$$
$$\mathbf{G}_{2C} = \mathbf{G}_{,\mathbf{u};\lambda C} \cdot \mathbf{v}_1\,\lambda_1 + \frac{1}{2}\mathbf{G}_{,\mathbf{uu}C} : \mathbf{v}_1 \otimes \mathbf{v}_1 + \mathbf{G}_{,\mathbf{u}C} \cdot \mathbf{v}_2.$$

Eq. (9) must be satisfied along the whole secondary path, independently of η. Therefore, $\mathbf{G}_{nC} = \mathbf{0}$ $\forall n \in \mathbb{N}$. From the latter conditions, the unknown pairs $(\mathbf{v}_1, \lambda_1), (\mathbf{v}_2, \lambda_2)$, etc. can be successively computed. The length of $\mathbf{v}_1 \neq \mathbf{0}$ (a null eigenvector of $\mathbf{K}_T(\mathbf{u}_C)$) can be chosen at will. Budiansky [5] suggested the orthogonality condition $\mathbf{v}_1 \cdot \mathbf{v}_i = 0 \quad \forall i > 1$, which renders the computation of the remaining unknowns $\lambda_1, \mathbf{v}_2, \lambda_2, \mathbf{v}_3$, etc. unique.

3. Are linear prebuckling paths and linear stability problems mutually conditional?

3.1. A linear prebuckling path

A prebuckling path is linear if it satisfies

$$\mathbf{A} \cdot \tilde{\mathbf{u}}(\lambda) + \mathbf{k}_1 + \lambda \mathbf{k}_2 = \mathbf{0} \qquad (12)$$

with some constant matrix $\mathbf{A} \in \mathbb{R}^{N \times N}$ and some constant vectors $\mathbf{k}_1, \mathbf{k}_2 \in \mathbb{R}^N$. Eq. (12) must hold for any value of λ, which requires $\mathbf{k}_1 \in \mathrm{im}(\mathbf{A}) \wedge \mathbf{k}_2 \in \mathrm{im}(\mathbf{A})$, where $\mathrm{im}(\mathbf{A})$ denotes the image of $\mathbf{A}$. The differential of (12) follows as

$$\mathbf{A} \cdot d\tilde{\mathbf{u}} + d\lambda \, \mathbf{k}_2 = \mathbf{0}. \qquad (13)$$

The formal similarity between (13) and the specialization of (3) for the primary path is somewhat misleading since $\mathbf{A}$ is constant. If $\mathbf{A}$ is singular, the system has at least one unconstrained degree of freedom. Ruling out such exceptional cases, (12) may be rewritten as

$$\tilde{\mathbf{u}}(\lambda) = -\mathbf{A}^{-1} \cdot (\mathbf{k}_1 + \lambda \mathbf{k}_2), \qquad (14)$$

or equivalently $\tilde{\mathbf{u}}(\lambda) = \tilde{\mathbf{u}}(0) + \lambda \mathbf{k}$ with

$$\tilde{\mathbf{u}}_{,\lambda} = \mathbf{k} = -\mathbf{A}^{-1} \cdot \mathbf{k}_2 = \mathrm{const.} \qquad (15)$$

This is both necessary and sufficient for a linear prebuckling path. The case $\mathbf{k} = \mathbf{0}$ is disregarded in the sequel, because it would imply a rigid system.

3.2. A linear stability problem

Linear stability problems are characterized by a tangent stiffness matrix of the form

$$\tilde{\mathbf{K}}_T = \mathbf{K}_0 + \lambda \mathbf{K}_1. \qquad (16)$$

It simplifies the computation of the buckling load λ_C because the condition for loss of stability, i.e. $\det(\tilde{\mathbf{K}}_T) = 0$, is just a polynomial equation in λ. Zienkiewicz and Taylor [15] obtain the result (16) for in-plane loaded plates, which indeed exhibit linear prebuckling paths. The reasonable assumption of stability in the unloaded state $\lambda = 0$ requires that the constant matrix $\mathbf{K}_0 = \mathbf{K}_0^T$ is positive definite. $\mathbf{K}_0$ is referred to as *small displacement stiffness*, whereas $\lambda \mathbf{K}_1 = \lambda \mathbf{K}_1^T$ is known as *geometric stiffness*.

The conditions for a structural stability problem to be considered as linear are that along the primary path (i) changes of the material tangent stiffness matrix are negligibly small, (ii) the displacements are sufficiently small, (iii) there is a linear relation between stresses and loads, and (iv) the loads do not depend on the displacements [1, 2, 3, 6, 14, 15].

With these conditions at hand, possible sources of nonlinearity can be identified as: (i) geometric nonlinearity, meaning that the strain-displacement relations are significantly nonlinear, (ii) nonlinear material behavior, and (iii) nonlinear boundary conditions [6, 15]. The following considerations are confined to the case (i), since it is almost trivial that the cases (ii) and (iii) generally entail both nonlinear prebuckling behavior and nonlinear stability problems.

The question whether linear prebuckling paths and linear stability problems are mutually conditional has been answered already in [13]. The present work is an extension of [13] insofar as the alternative proofs given in the sequel furnish the same results as [13].

3.3. A linear prebuckling path is not necessary for a linear stability problem

The following *proof by contraposition* demonstrates that a linear prebuckling path is not necessary for a linear stability problem.

For a linear stability problem with $\tilde{\mathbf{K}}_T$ from (16) it is assumed that $\mathbf{K}_1$ is regular, i.e. its null space is empty. Moreover, it is assumed that a linear stability problem implies a linear prebuckling path. Insertion of (15) and (16) into (5) leads to the contradiction $\mathbf{K}_1 \cdot \mathbf{k} = \mathbf{0}$. Consequently, the assumption that a linear stability problem implies a linear prebuckling path is wrong.

A question that may be raised at this point concerns the existence of conditions to achieve a linear prebuckling path if the stability problem is linear. Again, insertion of (15) and (16) into (5) furnishes the answer: A linear prebuckling path requires

$$\mathbf{K}_1 \cdot \tilde{\mathbf{u}}_{,\lambda} = \mathbf{0} \quad \forall \, \lambda \in \mathbb{R}. \tag{17}$$

3.4. A linear prebuckling path is not sufficient for a linear stability problem

The following *proof by contradiction* shows that a linear prebuckling path is not sufficient for a linear stability problem.

A linear prebuckling path is considered, i.e. $\tilde{\mathbf{u}}_{,\lambda}$ satisfies (15). Additionally, it is assumed that

$$\tilde{\mathbf{K}}_T = \mathbf{K}_0 + f(\lambda)\mathbf{K}_1, \tag{18}$$

with some differentiable function $f(\lambda) : \mathbb{R} \to \mathbb{R}$ obeying $f(0) = 0$. Thus, the assumption to be refuted is

$$\text{Eq. (15)} \Rightarrow f(\lambda) = \lambda. \tag{19}$$

Insertion of (15) and (18) into (5) yields

$$f_{,\lambda}(\lambda)\mathbf{K}_1 \cdot \mathbf{k} = \mathbf{0}, \tag{20}$$

which requires either $f_{,\lambda}(\lambda) = 0$ or $\mathbf{K}_1 = \mathbf{0}$ or $\mathbf{K}_1 \cdot \mathbf{k} = \mathbf{0}$. The cases $f_{,\lambda}(\lambda) = 0$ or $\mathbf{K}_1 = \mathbf{0}$ result in constancy of $\tilde{\mathbf{K}}_T$, meaning that loss of stability is impossible. Therefore, these trivial cases are ruled out. For the third possibility $\mathbf{K}_1 \cdot \mathbf{k} = \mathbf{0}$, proposition (19) is wrong. Hence, (15) is not sufficient for (16). It can be concluded from (20) that it is impossible to formulate sufficient conditions for a linear stability problem in terms of the prebuckling path $(\tilde{\mathbf{u}}(\lambda), \lambda)$. Thus, there is no analogue to (17). This conclusion is also plausible from a practical viewpoint. The postbuckling behavior must have an influence on the tangent stiffness matrix $\tilde{\mathbf{K}}_T$. Otherwise the same primary path would always entail the same matrix $\tilde{\mathbf{K}}_T$, which clearly contradicts the empirical evidence (cf. the example given in Section 4.5 and the results shown in Fig. 6). Therefore, the shape of the primary path alone cannot suffice to render a stability problem linear.

3.5. Linear prebuckling paths and (nontrivial) linear stability problems are mutually exclusive

The following *direct proof* shows that a nontrivial linear stability problem does not allow a linear prebuckling path. *Nontrivial* means that in (16) $\mathbf{K}_1 \neq \mathbf{0}$.

Substitution of (16) into (4) yields

$$\tilde{\mathbf{u}}_{,\lambda} = \tilde{\mathbf{K}}_T^{-1} \cdot \mathbf{P} = (\mathbf{K}_0 + \lambda \mathbf{K}_1)^{-1} \cdot \mathbf{P} = (\mathbf{I} + \lambda \mathbf{K}_0^{-1} \cdot \mathbf{K}_1)^{-1} \cdot \mathbf{K}_0^{-1} \cdot \mathbf{P}. \tag{21}$$

Let the eigenvectors of $\mathbf{K}_0^{-1} \cdot \mathbf{K}_1$ constitute the columns of $\mathbf{V}$. Hence, the *Jordan canonical form* is obtained as

$$\mathbf{J} = \mathbf{V}^{-1} \cdot \mathbf{K}_0^{-1} \cdot \mathbf{K}_1 \cdot \mathbf{V}. \tag{22}$$

Using this transformation in (21) gives

$$\tilde{\mathbf{u}}_{,\lambda} = \mathbf{V} \cdot (\mathbf{I} + \lambda \mathbf{J})^{-1} \cdot \mathbf{V}^{-1} \cdot \mathbf{K}_0^{-1} \cdot \mathbf{P} \tag{23}$$

and after premultiplication by $\mathbf{V}^{-1}$

$$\mathbf{V}^{-1} \cdot \tilde{\mathbf{u}}_{,\lambda} = (\mathbf{I} + \lambda \mathbf{J})^{-1} \cdot \mathbf{V}^{-1} \cdot \mathbf{K}_0^{-1} \cdot \mathbf{P}. \tag{24}$$

The last row of $(\mathbf{I} + \lambda \mathbf{J})^{-1}$ reads as

$$\begin{bmatrix} 0 & \cdots & 0 & \dfrac{1}{1 + \lambda J_{NN}} \end{bmatrix}. \tag{25}$$

Therefore, the left hand side of (24) is generally not constant w.r.t. λ, which would be necessary for a linear prebuckling path. This result is general because by permutation of columns in $\mathbf{V}$ any of the eigenvalues of $\mathbf{J}$ can take the position of J_{NN} in the last row.

3.6.   Example of a linear stability problem

The above theoretical considerations are illustrated by characteristic examples presented in [13]. First, a linear stability problem emerging from a two-degrees-of-freedom, planar system shown in Fig. 2(a) is analyzed.
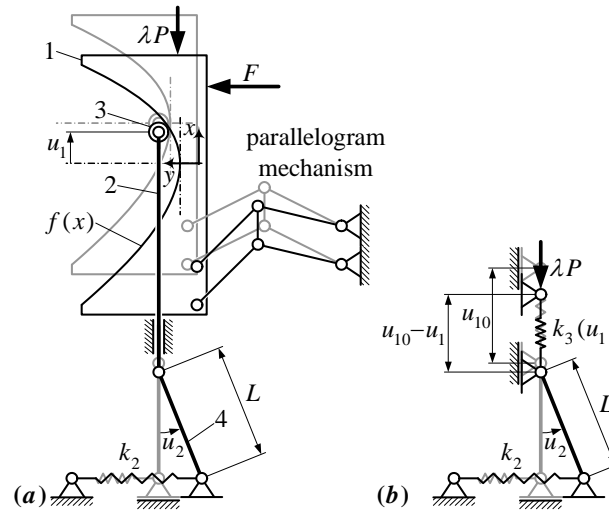
Fig. 2: Linear stability problem, (a) original system, (b) equivalent system with nonlinear spring k_3 [13]

The original, undisplaced position of the system is delineated in gray. The cam plate 1 can undergo any in-plane translation but its rotational degree of freedom is blocked by a parallelogram mechanism. Part 2 has only one translational degree of freedom in vertical direction. It is connected to part 1 by a negligibly small pivot 3 which slides along the cam contour

$$f(x) = \frac{k_0 P}{k_1 F} \left(\frac{P}{k_1} (e^{x k_1 / P} - 1) - x \right) \tag{26}$$

with constants $k_0, k_1 \in \mathbb{R}^+$ and a constant force $F \in \mathbb{R}^+$. The local coordinate system x-y is attached to part 1. $P \in \mathbb{R}^+$ is a constant reference load, amplified by the scalar parameter λ. The relative displacement u_1 and the angle u_2 serve as generalized coordinates. Apart from the linear spring k_2, which is unstrained for $u_2 = 0$, all components are rigid. Absence of friction is stipulated.

The mechanism with the parts 1, 2, and 3 may be thought of as a nonlinear spring. Its passivity (stability and monotonous spring characteristics) follows directly from the fact that $du_1 \, d\lambda \, P \geq 0$. Therefore, the two systems shown in Figs. 2(a) and 2(b), respectively, are equivalent if the spring characteristics $k_3(u_1)$ is identical to the nonlinear behavior of the mechanism.

The potential energy function of the system is

$$V = -\lambda P\big(u_1 + L(1 - \cos(u_2))\big) + F f(u_1) + \frac{k_2}{2}L^2 \sin^2(u_2). \tag{27}$$

The equilibrium equations $V_{,u_1} = 0$ and $V_{,u_2} = 0$ yield that the primary path is defined by the nonlinear relations

$$u_1 = \frac{P}{k_1}\ln\left(1 + \lambda\frac{k_1}{k_0}\right), \quad u_2 = 0. \tag{28}$$

The tangent stiffness matrix specialized for the primary path follows as

$$\tilde{\mathbf{K}}_T = \begin{bmatrix} k_0 + k_1\lambda & 0 \\ 0 & L(k_2 L - \lambda P) \end{bmatrix}. \tag{29}$$

Hence, the stability problem is linear with a regular matrix $\mathbf{K}_1$ according to (16). However, in Section 3.3, regularity of $\mathbf{K}_1$ was found to be in conflict with a linear prebuckling path.

3.7. Example of a linear prebuckling path
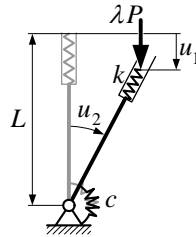
Fig. 3: System with a linear prebuckling path [13]

The second system to be analyzed is shown in Fig. 3. Apart from the linear elastic torsional spring c and the linear elastic spring k, all components are rigid. The displacement u_1 and the angle u_2 serve as generalized coordinates. In the unloaded initial state $\lambda = 0$ and $(u_1, u_2)^T = \mathbf{0}$ (delineated in gray) the springs are unstrained.

The potential energy function is readily found as

$$V = -\lambda P u_1 + \frac{1}{2}cu_2^2 + \frac{1}{2}k\left(L - \frac{L - u_1}{\cos(u_2)}\right)^2. \tag{30}$$

With the equilibrium equations $V_{,u_1} = 0$ and $V_{,u_2} = 0$, this results in a linear prebuckling path

$$u_1 = \frac{\lambda P}{k}, \quad u_2 = 0 \tag{31}$$

and in the tangent stiffness matrix

$$\tilde{\mathbf{K}}_T = \begin{bmatrix} k & 0 \\ 0 & c - P\lambda(L - P\lambda/k) \end{bmatrix}. \tag{32}$$

It follows from $\det(\tilde{\mathbf{K}}_T) = 0$ that there is no bifurcation point if $kL^2 \le 4c$. Evidently, the stability problem is nonlinear, which verifies the theoretical result of Section 3.4. An approximation of the stability problem as linear by neglecting the nonlinear term in (32) is only acceptable for large values of k or large values of L or both. This situation corresponds to the case of sufficiently small prebuckling displacements, as briefly discussed in Section 3.2.

4. Does the conversion from imperfection sensitivity into imperfection insensitivity require a symmetric postbuckling path?

Since Koiter [8] introduced a method for analyzing postbuckling paths of perfect structures in the vicinity of the bifurcation point, the question of imperfection sensitivity or insensitivity of these structures has experienced ongoing research interest. More recently, studies have focused on improving the buckling behavior [4, 9], which may mean to convert imperfection sensitive into imperfection insensitive structures. Therefore, it is necessary to clarify the role of characteristic properties of stability problems for the conversion process from imperfection sensitivity into imperfection insensitivity. The ultimate goal should be to provide the structural engineer with a set of rules for designing structures exhibiting imperfection insensitivity right from the outset.

As a contribution to this topic, the following considerations answer the question whether symmetric equilibrium paths are a necessary precondition for imperfection sensitivity. A mathematically more fundamental discussion and some insights concerning the role of antisymmetric load-displacement paths as well as zero-stiffness postbuckling paths can be found in [12].

4.1. Imperfection insensitivity

Bochenek [4] proposed to classify bifurcation at point C as imperfection insensitive if and only if $\lambda_{,\eta}(\eta)\,\mathrm{sign}(\eta) \ge 0$ in an open *local* domain around C with the equals sign holding only for $\eta = 0$. Bochenek referred to these properties as symmetric load-displacement behavior in the *vicinity* of C. By introduction of $m_{min} := \min\{m \mid m \in \mathbb{N}\backslash\{0\}, \lambda_m \ne 0\}$, Bochenek's condition can be expressed in terms of the coefficients λ_i from (7) as

$$m_{min} \text{ is even } \wedge \ \lambda_{m_{min}} > 0. \tag{33}$$

In any other case, the system is imperfection sensitive.

4.2. Symmetric equilibrium paths

Essentially, it is the potential energy function V that defines the load-displacement behavior of a structure. Therefore, it is reasonable to give a definition of symmetric load-displacement behavior in

terms of V. Let the linear mapping $\mathbf{T}:\mathbb{R}^N \to \mathbb{R}^N$ be an element of a group that describes mirror symmetry. In [12], the symmetry condition

$$V(\mathbf{u},\lambda) = V(\mathbf{T}(\mathbf{u}),\lambda) \quad \forall\,(\mathbf{u},\lambda) \in \mathbb{R}^N \times \mathbb{R} \tag{34}$$

was proposed. The uniqueness of the primary path requires $\tilde{\mathbf{u}}(\lambda) = \mathbf{T}(\tilde{\mathbf{u}}(\lambda))$. Specializing V for the secondary path, it may be expressed as a function of η. Hence, symmetry with respect to η requires $V(\eta) = V(-\eta)$ or with (6)

$$V(\tilde{\mathbf{u}}(\lambda(\eta)) + \mathbf{v}(\eta), \lambda(\eta)) = V(\tilde{\mathbf{u}}(\lambda(-\eta)) + \mathbf{v}(-\eta), \lambda(-\eta)) \quad \forall \eta \in \mathbb{R}. \tag{35}$$

A comparison of (34) and (35) shows that $\lambda(\eta) = \lambda(-\eta)$ and $\mathbf{v}(\eta) = \mathbf{T}(\mathbf{v}(-\eta))$. Therefore, necessary and sufficient conditions for the symmetry of the secondary path with respect to η are

$$\lambda(\eta) = \lambda(-\eta) \quad \wedge \tag{36}$$
$$\mathbf{v}(\eta) = \mathbf{T}(\mathbf{v}(-\eta)) \quad \wedge \tag{37}$$
$$\tilde{\mathbf{u}}(\lambda) = \mathbf{T}(\tilde{\mathbf{u}}(\lambda)). \tag{38}$$

In [12], these results were deduced by means of the series expansions (7) and (8). There, it was shown that for symmetric bifurcation problems a coordinate transformation allows to describe the symmetry with $\mathbf{T}(\mathbf{u}) = [\delta_{ij}(1 - 2\delta_{iN})]_{i=1...N, j=1...N} \cdot \mathbf{u}$ where δ_{ij} is the Kronecker symbol. Then, the symmetric structure of $\tilde{\mathbf{K}}_{T,\lambda^n}$ with $n \in \mathbb{N}$ can be used to demonstrate that symmetry is reflected by $\mathbf{v}_1 = [0,\ldots,0,p]^T$ with some $p \in \mathbb{R} \setminus \{0\}$, $\mathbf{v}_1 \cdot \mathbf{v}_i = 0 \quad \forall i > 1$, and $\mathbf{v}_i = \mathbf{0} \quad \forall i \in \{3,5,7,\ldots\}$, which corroborates (37).

Moreover, insertion of (7) into (36) yields $\lambda_1 = \lambda_3 = \lambda_5 = \ldots = 0$.

4.3. Symmetric postbuckling paths are not necessary for the conversion from imperfection sensitivity into imperfection insensitivity

Satisfaction of (33) is independent of (37) and (38). Consequently, symmetry is not necessary for imperfection insensitivity.

The condition (33) provides a means of classifying a system as imperfection sensitive or insensitive. To do so, it suffices to compute the coefficients λ_i up to an index $i = m$ such that $\lambda_m \neq 0$. In terms of the coefficients λ_i, the conversion from imperfection sensitivity into imperfection insensitivity is reflected by a sign reversal of $\lambda_{m_{min}}$ with even m_{min}. Evidently, this does not require symmetry. If, in contrast, m_{min} is odd, both a symmetric bifurcation path and imperfection insensitivity are unfeasible.

4.4. On the invariance of properties with respect to changes of the path parameter

The path parameter η should uniquely parameterize the postbuckling path and it should be zero at the bifurcation point C. Apart from these stipulations, the choice of η is *not* unique. The parameter η may be replaced by any bijective coordinate transformation $\eta \mapsto \bar{\eta}(\eta)$ which obeys $\bar{\eta}(0) = 0$. In contrast to symmetry, the property of imperfection sensitivity or insensitivity is invariant with respect to such transformations.

To show this, consider that a bijective transformation of the path parameter can be defined by $\eta(\bar{\eta}) = k_n \bar{\eta}^n + k_{n+1} \bar{\eta}^{n+1} + k_{n+2} \bar{\eta}^{n+2} + \ldots$ with $k_n \neq 0$. For bijectivity, n has to be odd. Application of this transformation to (7) yields

$$\lambda(\eta(\bar{\eta})) = \bar{\lambda}_{\bar{m}_{min}} \eta^{\bar{m}_{min}} + \bar{\lambda}_{\bar{m}_{min}+1} \eta^{\bar{m}_{min}+1} + \ldots \tag{39}$$

with $\bar{\lambda}_{\bar{m}_{min}} = \lambda_{m_{min}} k_n^{m_{min}}$ and $\bar{m}_{min} = n\, m_{min}$. Therefore, the property of imperfection sensitivity is invariant with respect to this type of coordinate changes. This is plausible from a physical perspective; imperfection sensitivity or insensitivity is an intrinsic property of a system. In contrast, symmetry can easily be lost through such transformations because the parameters $\bar{\lambda}_i$ in (39) may be coefficients of odd powers of $\bar{\eta}$, even if $\lambda(\eta)$ was a symmetric function.

4.5. Example

The following problem exemplifies the above theoretical findings. It closely follows the lines of an example presented in [12].

The transition from imperfection sensitivity to imperfection insensitivity requires modifications of the original structure. It is reasonable to formulate the problem such that the considered modifications can be controlled by a scalar parameter which will be denoted as κ. Hence, the analysis should furnish the range of values of κ where the structure is imperfection insensitive.
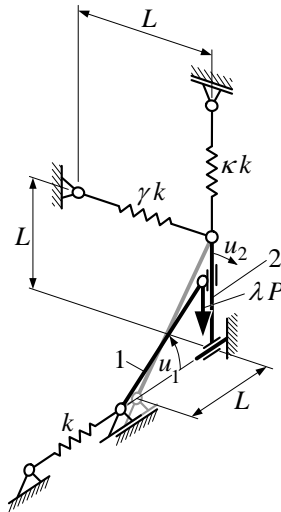

Fig. 4: System with non-symmetric secondary path

Fig. 4. shows a two-degrees-of-freedom system which exhibits a postbuckling path that is not symmetric. A rigid bar 1 is fitted with two turning-and-sliding joints. The second rigid bar 2 can only rotate with respect to a horizontal axis. The coordinate u_1 measures the angle between this axis and bar 1, whereas the coordinate u_2 defines the angular position of bar 2. The constant vertical reference load $P \in \mathbb{R}^+$ is applied to the system at the upper turning-and-sliding joint. It is amplified by the scalar parameter λ. The remaining components of the system are three linear elastic springs k, γk, and κk with parameters γ and $\kappa \in \mathbb{R}^+$. The unloaded state which is defined by $\lambda = 0$ and $(u_1, u_2) = (\pi/4, 0)$ is rendered in gray.

The potential function

$$
\begin{aligned}
V = -\lambda\,P\,L\left(1-\sqrt{2}\,\sin(u_1)\cos(u_2)\right) + \frac{1}{2}kL^2\Big(\left(1-\sqrt{2}\,\cos(u_1)\right)^2 \\
+ \kappa\left(1-\cos(u_2)\right)^2 + \gamma\left(1-\sqrt{3+2\left(\sin(u_2)-\cos(u_2)\right)}\right)^2\Big)
\end{aligned}
\tag{40}
$$

is not symmetric with respect to the coordinates u_1 and u_2. The equilibrium equations $V_{,u_1} = 0$ and $V_{,u_2} = 0$ yield the primary path

$$
\lambda(u_1) = \frac{kL}{P}\left(\sqrt{2}\,\sin(u_1) - \tan(u_1)\right)
\tag{41}
$$
$$
u_2 = 0.
$$

Because an analytical solution for the secondary path was not found, this path was computed using a numerical solver.

The coefficient λ_1 vanishes independently of κ and any other system parameter. Vanishing of λ_1 is a necessary condition for both symmetry and imperfection insensitivity. However, since $\lambda_3 \neq 0$, the postbuckling path is not symmetric. The parameter values are chosen as $L = 1\,\text{m}$, $k = 1\,\text{N/m}$, $\gamma = 0.07$, and $P = 1\,\text{N}$.

The design parameter κ is varied in order to achieve the desired conversion from imperfection sensitivity into imperfection insensitivity. For $\kappa \in [0, 0.08183]$, the buckling behavior is imperfection sensitive and imperfection insensitivity is achieved for $\kappa > 0.08183$. At the transition point $\kappa = 0.08183$, the first few coefficients of the series expansions (7) and (8) take the values

$$
\begin{aligned}
&\lambda_1 = 0, \quad \lambda_2 = 0, \quad \lambda_3 = 5.89\times10^{-2}, \\
&\lambda_4 = -6.87\times10^{-2}, \quad \lambda_5 = 5.50\times10^{-2}, \\
&\mathbf{v}_1 = \begin{pmatrix} 0 \\ 1 \end{pmatrix}, \quad \mathbf{v}_2 = \begin{pmatrix} 0.069 \\ 0 \end{pmatrix}, \quad \mathbf{v}_3 = \mathbf{0}, \\
&\mathbf{v}_4 = \begin{pmatrix} -0.015 \\ 0 \end{pmatrix}, \quad \mathbf{v}_5 = \mathbf{0}
\end{aligned}
\tag{42}
$$

if $\mathbf{v}_1$ is normalized to unit length. It can be shown that the dependence of the coefficients λ_2 and λ_4 on κ is linear and quadratic, respectively. Fig. 6 shows this dependency in a parametric plot of λ_2 and λ_4.
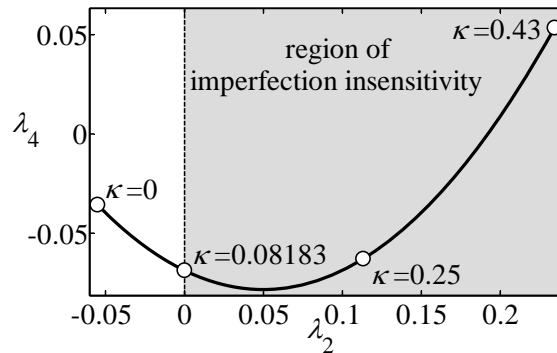

Fig. 5: Coefficients of asymptotic series expansion of λ for varying κ

It follows from (41) that the shape of the primary path depends only on the initial rise of bar 1, but not on the system parameters γ and κ. However, γ and κ do have an influence on the shape of the secondary path. Moreover, it can be shown that $\tilde{\mathbf{K}}_T$ is independent of κ, which implies that the bifurcation points are not influenced by variations of the design parameter κ. Indeed, the location of C is constant with respect to κ, as shown in Fig. 6. It contains load-displacement paths for representative values of κ. Evidently, the postbuckling paths are not symmetric and a conversion from imperfection sensitivity into insensitivity is achieved. A second bifurcation point C_1 and a snap-through point D are located on an unstable sector of the primary path. Moreover, Fig. 6 shows that increasing the stiffness by means of κ may lead to topological changes of the secondary path.

Apart from the constancy of the prebuckling behavior, it is worthwhile to note that for sufficiently large values of κ, the ultimate load of the postbuckling path exceeds the limit load at the point D of the primary path. An increase of the parameter γ would cause a larger buckling load λ_C, i.e. the point C approaches D. Consequently, stiffening the system by increasing γ is counterproductive insofar as the ultimate load of the system may drop.

This example shows that symmetry is not necessary for the conversion from imperfection sensitivity into insensitivity. However, $\lambda_1 = 0$ is a necessary condition for such a conversion. If, in contrast to the presented example, a system does not obey this condition, structural modifications of the original system may be necessary to enforce $\lambda_1 = 0$, before further measures are taken to shape the coefficient λ_2. Moreover, the considered example demonstrated that the conversion from imperfection sensitivity into insensitivity can be achieved without modifications of the primary path and the buckling load.
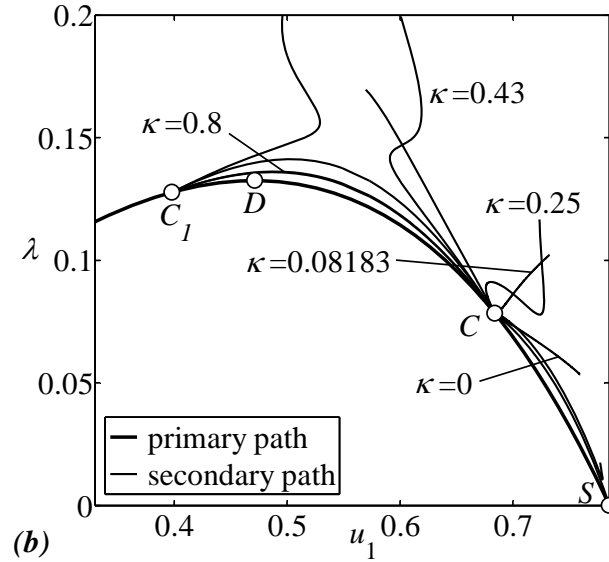

(a)

(b)
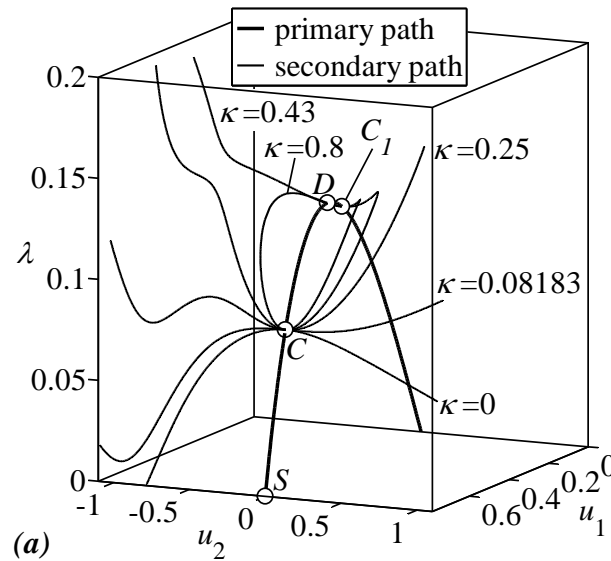
Fig. 6: (a) Load-displacement paths of the system shown in Fig. 4, (b) projection onto the plane $u_2 = 0$

5. Is hilltop buckling necessarily imperfection sensitive?

For the same motivation that sparked off the previous question, namely *ab initio* design for imperfection sensitivity, it seems reasonable to identify classes of stability problems where imperfection insensitivity is impossible. The following discussion will demonstrate why the prominent case of hilltop buckling falls into such an undesirable class.

5.1. Hilltop buckling

Hilltop buckling is characterized by the coincidence of a bifurcation point C and a snap through point D of a load-displacement path [7]. Multiple hilltop buckling is not discussed in this analysis, i.e. there is only a single secondary path. For a discussion on multiple hilltop branching phenomena and their influence on imperfection sensitivity refer to [10]. The results of examples presented there corroborate the following theoretical findings.

As described in 0, the equation $\mathbf{v}_1 \cdot \mathbf{G}_{3C} = 0$ with $\mathbf{G}_{3C}$ from (9) can be expressed as

$$a_1 \lambda_1^2 + b_1 \lambda_1 + c_1 = 0 \tag{43}$$

with

$$a_1 = -\frac{1}{2} \frac{\tilde{\mathbf{K}}_{T,\lambda\lambda}(\mathbf{u}_C) : \mathbf{v}_1 \otimes \mathbf{v}_1}{\tilde{\mathbf{K}}_{T,\lambda}(\mathbf{u}_C) : \mathbf{v}_1 \otimes \mathbf{v}_1} \tag{44}$$

and similar terms for b_1 and c_1 [9]. The parameter λ_2 is contained in c_1. So far, the primary path was parameterized by λ, but in the vicinity of snap-through points this does not allow a unique parameterization of the path. Therefore, a new path parameter ξ is introduced, which is single-valued along the primary path. At the stability limit $(\mathbf{u}_C, \lambda_C)$, it takes the value $\xi = \xi_C$, whereas $\xi < \xi_C$ holds along the prebuckling path.

Then, a_1 from (44) can be expressed in terms of ξ as

$$a_1 = -\frac{1}{2\lambda_{,\xi}} \left(\frac{\tilde{\mathbf{K}}_{T,\xi\xi} : \mathbf{v}_1 \otimes \mathbf{v}_1}{\tilde{\mathbf{K}}_{T,\xi} : \mathbf{v}_1 \otimes \mathbf{v}_1} - \frac{\lambda_{,\xi\xi}}{\lambda_{,\xi}} \right)\Bigg|_{\xi=\xi_C}. \tag{45}$$

At snap-through points, $\lambda(\xi)$ exhibits a local maximum, i.e. $\lambda_{,\xi} = 0$ and $\lambda_{,\xi\xi} < 0$, $\tilde{\mathbf{K}}_{T,\xi\xi} : \mathbf{v}_1 \otimes \mathbf{v}_1$ remains finite, and $\tilde{\mathbf{K}}_{T,\xi} : \mathbf{v}_1 \otimes \mathbf{v}_1$ does not vanish. Hence, snap-through points are characterized by $a_1 = -\infty$. In fact, a_1 exhibits a pole of second order at snap-through points (cf. [9]). Vice versa, if the stability limit does not coincide with the snap-through point, $\lambda_{,\xi} > 0$ and $a_1 > -\infty$. This case is considered in the subsequent section, unless stated otherwise.

5.2. Hilltop buckling is imperfection sensitive

The fundamental idea of the following proof is to study the mathematical expression for λ_2 if the bifurcation point C approaches the snap-through point D as a consequence of parametric changes of the original design. Finally, it can be shown that the transition case, where C and D converge, only allows $\lambda_2 < 0$.

The coefficient a_1 from (45) can also be computed in terms of η, i.e. the parameter of the secondary path:

$$a_1 = -\frac{1}{2\lambda_{,\eta}} \left(\frac{\tilde{\mathbf{K}}_{T,\eta\eta} : \mathbf{v}_1 \otimes \mathbf{v}_1}{\tilde{\mathbf{K}}_{T,\eta} : \mathbf{v}_1 \otimes \mathbf{v}_1} - \frac{\lambda_{,\eta\eta}}{\lambda_{,\eta}} \right)\Bigg|_{\eta=0}. \tag{46}$$

Equating the right-hand sides of (45) and (46) gives

$$\lambda_{,\eta\eta}\Big|_{\eta=0} = \frac{\tilde{\mathbf{K}}_{T,\eta\eta} : \mathbf{v}_1 \otimes \mathbf{v}_1}{\tilde{\mathbf{K}}_{T,\eta} / \lambda_{,\eta} : \mathbf{v}_1 \otimes \mathbf{v}_1}\Bigg|_{\eta=0} + \left(\frac{\lambda_{,\eta}\big|_{\eta=0}}{\lambda_{,\xi}\big|_{\xi=\xi_C}} \right)^2 \left(\lambda_{,\xi\xi} - \frac{\tilde{\mathbf{K}}_{T,\xi\xi} : \mathbf{v}_1 \otimes \mathbf{v}_1}{\tilde{\mathbf{K}}_{T,\xi} / \lambda_{,\xi} : \mathbf{v}_1 \otimes \mathbf{v}_1} \right)\Bigg|_{\xi=\xi_C}. \tag{47}$$

Insertion of

$$\lambda_{,\eta}\Big|_{\eta=0} = \lambda_1, \quad \lambda_{,\eta\eta}\Big|_{\eta=0} = 2\lambda_2, \tag{48}$$

which follow from (7), and the equivalence

$$\tilde{\mathbf{K}}_{T,\lambda}\Big|_{\lambda=\lambda_C} = \frac{\tilde{\mathbf{K}}_{T,\xi}}{\lambda_{,\xi}}\Bigg|_{\xi=\xi_C} = \frac{\tilde{\mathbf{K}}_{T,\eta}}{\lambda_{,\eta}}\Bigg|_{\eta=0} \tag{49}$$

into (47) yields

$$\lambda_2 = \frac{1}{2} \frac{\tilde{\mathbf{K}}_{T,\eta\eta}\big|_{\eta=0} : \mathbf{v}_1 \otimes \mathbf{v}_1}{\tilde{\mathbf{K}}_{T,\xi}\big|_{\xi=\xi_C} : \mathbf{v}_1 \otimes \mathbf{v}_1} \lambda_{,\xi}\Big|_{\xi=\xi_C} + \frac{1}{2} \left(\frac{\lambda_1}{\lambda_{,\xi}\big|_{\xi=\xi_C}} \right)^2 \left(\lambda_{,\xi\xi} - \frac{\tilde{\mathbf{K}}_{T,\xi\xi} : \mathbf{v}_1 \otimes \mathbf{v}_1}{\tilde{\mathbf{K}}_{T,\xi} / \lambda_{,\xi} : \mathbf{v}_1 \otimes \mathbf{v}_1} \right)\Bigg|_{\xi=\xi_C}. \tag{50}$$

If $\lambda_1 \neq 0$, the system is imperfection sensitive. Therefore, it only remains to analyze the case $\lambda_1 = 0$, which allows rewriting (50) as

$$\lambda_2 = \frac{1}{2} \frac{\tilde{\mathbf{K}}_{T,\eta\eta}\big|_{\eta=0} : \mathbf{v}_1 \otimes \mathbf{v}_1}{\tilde{\mathbf{K}}_{T,\xi}\big|_{\xi=\xi_C} : \mathbf{v}_1 \otimes \mathbf{v}_1} \lambda_{,\xi}\Big|_{\xi=\xi_C}. \tag{51}$$

Note that $\mathbf{v}_1$ is the null eigenvector of $\tilde{\mathbf{K}}_T\big|_{\lambda=\lambda_C}$. Thus,

$$\tilde{\mathbf{K}}_T : \mathbf{v}_1 \otimes \mathbf{v}_1 = \begin{cases} > 0 & \text{if } \xi < \xi_C \\ 0 & \text{if } \xi = \xi_C \\ < 0 & \text{else} \end{cases} \qquad (52)$$

holds along the prebuckling path and in the vicinity of the stability limit. Because of (52) and the fact that the eigenvalues of $\tilde{\mathbf{K}}_T$ cannot undergo discontinuous changes,

$$-\infty < \tilde{\mathbf{K}}_{T,\xi}\big|_{\xi=\xi_C} : \mathbf{v}_1 \otimes \mathbf{v}_1 < 0, \qquad (53)$$

or equivalently

$$-\infty < \tilde{\mathbf{K}}_{T,\lambda}\big|_{\lambda=\lambda_C} \lambda_{,\xi}\big|_{\xi=\xi_C} : \mathbf{v}_1 \otimes \mathbf{v}_1 < 0. \qquad (54)$$

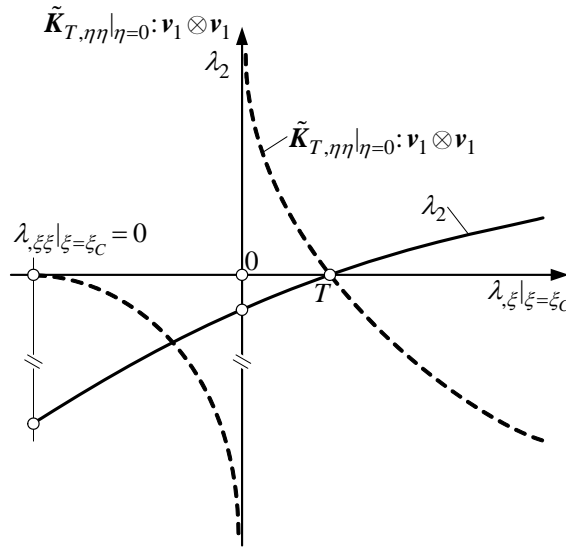Alternatively, (53) and (54) may be proved by means of the so-called *consistently linearized eigenproblem* [9].

Fig. 7: Values of $\tilde{\boldsymbol{K}}_{T,\eta\eta}\big|_{\eta=0} : \mathbf{v}_1 \otimes \mathbf{v}_1$ and λ_2 as the bifurcation point C moves along the primary path (qualitative plot)

A transition from imperfection sensitivity to imperfection insensitivity requires $\lambda_2 = 0$, which entails $\tilde{\mathbf{K}}_{T,\eta\eta}\big|_{\eta=0} : \mathbf{v}_1 \otimes \mathbf{v}_1 = 0$ in (51). The exceptional case of λ_2 being identically 0 is excluded in the sequel, because then the same arguments would apply to λ_4, which is relevant for imperfection sensitivity or insensitivity if $\lambda_1 = \lambda_2 = \lambda_3 = 0$. In fact, the following line of reasoning applies to $\lambda_{m_{min}}$, where m_{min} needs to be even. For simplicity, the expressions are given for the most frequent case $m_{min} = 2$.

In Fig. 7, which contains *qualitative* plots of $\tilde{\mathbf{K}}_{T,\eta\eta}\big|_{\eta=0} : \mathbf{v}_1 \otimes \mathbf{v}_1$ and λ_2, the transition from imperfection sensitivity to imperfection insensitivity occurs at point *T*. Both graphs start at the minimum value of $\lambda_{,\xi}\big|_{\xi=\xi_C}$, where $\lambda_{,\xi\xi}\big|_{\xi=\xi_C} = 0$ holds. At this point, the secondary path degenerates to a single point. However, this occurs beyond hilltop buckling $(\lambda_{,\xi}\big|_{\xi=\xi_C} = 0)$ and is, hence, only of minor interest.

The transition from imperfection sensitivity to imperfection insensitivity happens as $\tilde{\mathbf{K}}_{T,\eta\eta}|_{\eta=0}: \mathbf{v}_1 \otimes \mathbf{v}_1$ changes from 0 to a (finite) negative value. Therefore, $\tilde{\mathbf{K}}_{T,\eta\eta}|_{\eta=0}: \mathbf{v}_1 \otimes \mathbf{v}_1 = 0$ (point T in Fig. 7) may be considered as the *borderline case*.

If the same transition should take place for the hilltop buckling case characterized by $\lambda_{,\xi}|_{\xi=\xi_C} = 0$, $\tilde{\mathbf{K}}_{T,\eta\eta}|_{\eta=0}: \mathbf{v}_1 \otimes \mathbf{v}_1$ must change from a finite value to $\pm\infty$, which can be deduced from (51). Therefore, here, the *borderline case* is $\tilde{\mathbf{K}}_{T,\eta\eta}|_{\eta=0}: \mathbf{v}_1 \otimes \mathbf{v}_1 = \pm\infty$.

Since a smooth transition of the expression $\tilde{\mathbf{K}}_{T,\eta\eta}|_{\eta=0}: \mathbf{v}_1 \otimes \mathbf{v}_1$ from 0 to $\pm\infty$ within an infinitesimal increment of ξ or equivalently $\lambda_{,\xi}|_{\xi=\xi_C}$ is impossible, a bifurcation point C that refers to a transition case from imperfection sensitivity to imperfection insensitivity cannot converge to a snap-through point D. This finding is reflected in Fig. 7 since the transition point T cannot coincide with the hilltop buckling point 0. In fact, $\lambda_2 = 0$ and hilltop buckling are mutually disjoint events. Therefore, at hilltop buckling points only one sign of λ_2 is allowed. From a practical viewpoint and in agreement with numerical results, this sign is negative, i.e. $\lambda_2 < 0$. Any secondary path emerging from a hilltop buckling point is necessarily imperfection sensitive. Thus, hilltop branching may be interpreted as one of the most undesirable types of initial postbuckling behaviors.

5.3. Example

The undesirable properties of hilltop buckling are demonstrated by means of a planar, two-degrees-of-freedom system which is outlined in Fig. 8.
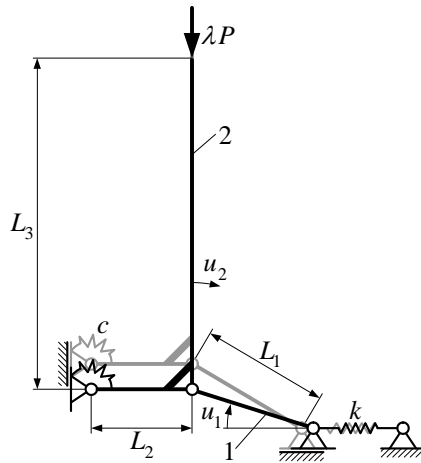

Fig. 8: System exhibiting hilltop buckling

The undisplaced position of the system is shown in gray. The angular position u_1 of bar 1 and the angular position u_2 of the knee 2 serve as generalized coordinates. A constant vertical reference load $P \in \mathbb{R}^+$, which is amplified by the load factor λ, is applied to the system at the top of part 2. A linear elastic torsional spring c counteracts rotations of the knee 2. The spring k is also linear elastic. In the

unloaded initial state $\lambda = 0$ and $(u_1, u_2) = (\pi/6, 0)$, the springs are unstrained. Snap-through can occur in the direction of u_1, whereas u_2 may be referred to as the bifurcation coordinate.

The potential energy function reads as

$$V = -\lambda P\left(L_3(1-\cos(u_2)) + L_1(1/2 - \sin(u_1))\right)$$
$$+ \frac{1}{2}c u_2^2 + \frac{1}{2}k\left(L_1\left(\sqrt{3}/2 - \cos(u_1)\right) + L_2(1-\cos(u_2))\right)^2. \tag{55}$$

The primary path

$$\lambda(u_1) = \frac{k L_1}{P}\tan(u_1)\left(\cos(u_1) - \sqrt{3}/2\right) \tag{56}$$
$$u_2 = 0$$

readily follows from the equilibrium equations $V_{,u_1} = 0$ and $V_{,u_2} = 0$. It is independent of c, L_2, and L_3. However, these parameters do have an influence on the secondary path, which was computed by means of a numerical solver. An analytical solution was not found. All load-displacement paths are symmetric with respect to the plane $u_2 = 0$.
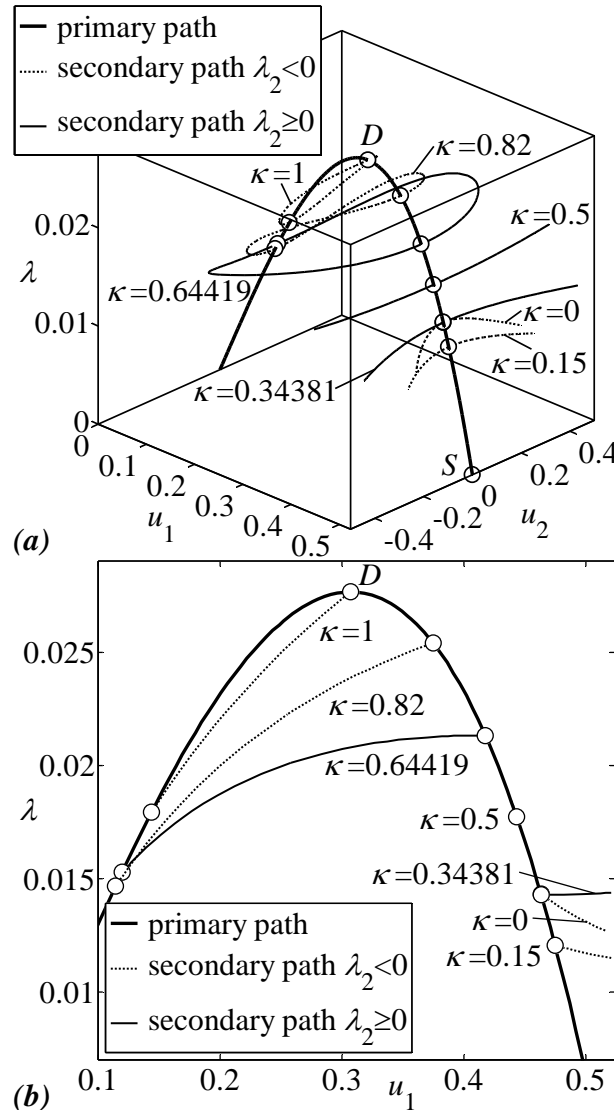

Fig. 9: (a) Load-displacement paths of the system shown in Fig. 8, (b) projection onto the plane $u_2 = 0$

Constant system parameters are chosen such that $k = P/L_1$ and $L_3 = 3L_1$. L_2 and c are defined as

$$L_2 = 0.8L_1(2\kappa - 1)$$
$$c = L_1 P(0.02 + \kappa^2 0.132678...)$$

(57)

where $\kappa \in [0,1]$ is a scalar design parameter. Fig. 8 is drawn for $L_2 > 0$. If $L_2 < 0$, the spring is c is on the opposite side of the vertical bar of part 2. Hilltop buckling occurs at $\kappa = 1$, whereas $\kappa < 1$ is associated with loss of stability caused by bifurcation. Fig. 9 shows the corresponding load-displacement paths. For $\kappa = 0.5$ ($L_2 = 0$), the projection of the secondary path onto the plane $u_2 = 0$ equals the primary path. As κ approaches the value 1, the bifurcation point C converges to the snap-through point D. Increasing κ further than 1 would be possible, yet, the practical relevance of bifurcation points located on an unstable section of the primary path is rather limited. Hence, the sensitivity analysis of the initial postbuckling behavior can be terminated at $\kappa = 1$.

For $\kappa = 0$, the system is imperfection sensitive. As κ is increased, it changes to imperfection insensitivity at $\kappa = 0.34381...$ and back to imperfection sensitivity at $\kappa = 0.64419...$ In line with Section 5.2, the hilltop buckling point ($\kappa = 1$) is imperfection sensitive. These findings follow from the sign of λ_2, which is shown in Fig. 10. The transition points $\lambda_2 = 0$ are marked with circles. For $\kappa \in [0,1]$, λ_2 is always finite.

Moreover, Fig. 10 contains the parameters a_1 and $\tilde{\mathbf{K}}_{T,\eta\eta}|_{\eta=0}: \mathbf{v}_1 \otimes \mathbf{v}_1$. In the limit $\kappa \to 1-$, $a_1 \to -\infty$ and $\tilde{\mathbf{K}}_{T,\eta\eta}|_{\eta=0}: \mathbf{v}_1 \otimes \mathbf{v}_1 \to +\infty$. Clearly, $\tilde{\mathbf{K}}_{T,\eta\eta}|_{\eta=0}: \mathbf{v}_1 \otimes \mathbf{v}_1$ cannot intersect the abscissa at $\kappa = 1$, which confirms the theory of Section 5.2. The hilltop buckling point is tied to an imperfection sensitive secondary path.

Note that modifications of κ generally have an influence on the buckling load λ_C (cf. Fig. 10) but not on the shape of the primary path. Therefore, modifications of κ may be appropriate means of improving the stability properties of the system. However, there are more intuitive and effective ways of doing so, like reducing L_2, reducing L_3, or increasing c.

6. Conclusions

In this work three pending questions of structural stability were answered. The main results of the presented analyses are:

- A linear prebuckling path is neither necessary nor sufficient for a linear stability problem.

- The conversion from imperfection sensitivity into imperfection insensitivity does not require a symmetric postbuckling path.

- Hilltop buckling is always imperfection sensitive.

These findings should help to prevent structural engineers from designing systems which are inherently imperfection sensitive and cannot be made imperfection insensitive without significant qualitative changes of the original design. Future research will be focused on the identification of

additional qualitative properties that are pivotal for the conversion from imperfection sensitivity into insensitivity.
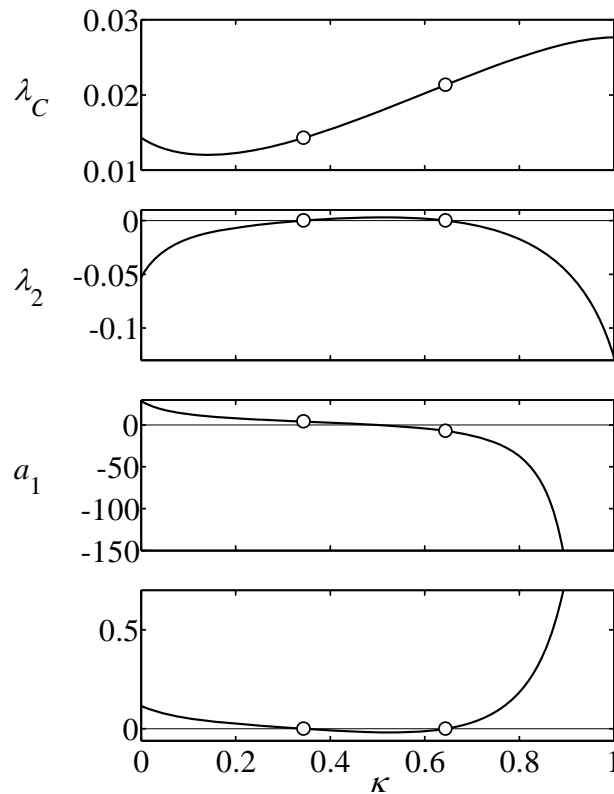

Fig. 10: Characteristic parameters for varying κ

Acknowledgements

References

[1] Bathe, K. J. *Finite element procedures in engineering analysis*, Prentice Hall, London, Sydney, Toronto, 1996.

[2] Bažant, Z. P. and Cedolin, L., *Stability of Structures, Elastic, Inelastic, Fracture, and Damage Theories*, Dover Publications, Mineola, New York, 1991.

[3] Belytschko, T. Liu, W. K., and Moran, B., *Nonlinear finite elements for continua and structures*, John Wiley & Sons, Chichester, New York, 2000.

[4] Bochenek, B. *Problems of structural optimization for post-buckling behavior*, Structural and Multidisciplinary Optimization, 25(5-6), 423-435, 2003.

[5] Budiansky, B. *Post-buckling behavior of cylinders under torsion*, Theory of thin shells - Proceedings of the second IUTAM symposium, Ed. F. I. Niordson, Springer, Berlin, 1969, 212-233.

[6] Felippa, C. A. *Nonlinear finite element methods*, Lecture notes, University of Colorado, Department of Aerospace Engineering Sciences, Retrieved August 29, 2007, http://www.colorado.edu/engineering/ CAS/courses.d/NFEM.d.

[7] Fujii, F., and Noguchi, H. *Multiple hill-top branching*, Proceedings of the 2nd International Conference on Structural Stability and Dynamics, Eds. C. M. Wang, G. R. Liu, and K. K. Ang, World Scientific, Singapore, 477-482, 2002.

[8] Koiter, W. *On the stability of elastic equilibrium*, Translation of '*Over de Stabiliteit van het Elastisch Evenwicht*' (1945), in: NASA TT F-10833, Polytechnic Institute Delft, H. J. Paris Publisher, Amsterdam, 1967.

[9] Mang, H. A., Schranz, C., and Mackenzie-Helnwein, P. *Conversion from imperfection-sensitive into imperfection-insensitive elastic structures I: Theory*, International Journal of Computer Methods in Applied Mechanics and Engineering, 195(13-16), 1422-1457, 2006.

[10] Ohsaki, M., and Ikeda, K. *Imperfection sensitivity analysis of hill-top branching with many symmetric bifurcation points*, International Journal of Solids and Structures, 43, 4704-4719, 2006.

[11] Steinboeck, A., Hoefinger, G., Jia, X., and Mang, H. A. *Answers to three not quite straightforward questions in structural stability*, Proceedings of the Sixth International Conference on Computation of Shell and Spatial Structures IASS-IACM 2008: Spanning Nano to Mega, Eds. J. F. Abel and J. R. Cooke, Cornell University, Ithaca, 2008.

[12] Steinboeck, A., Jia, X., Hoefinger, G., and Mang, H. A. *Conditions for symmetric, antisymmetric, and zero-stiffness bifurcation in view of imperfection sensitivity and insensitivity*, International Journal of Computer Methods in Applied Mechanics and Engineering, 197, 3623-3636, 2008.

[13] Steinboeck, A., and Mang, H. A. *Are linear prebuckling paths and linear stability problems mutually conditional?*, Computational Mechanics, 42(3), 441-445, 2008.

[14] Wriggers, P. *Nichtlineare Finite-Elemente-Methoden* [German, *Nonlinear finite element methods*], Springer Verlag, Berlin, Heidelberg, New York, 2001.

[15] Zienkiewicz, O. C., and Taylor, R. L. *The finite element method, volume 2, solid mechanics.* Butterworth-Heinemann, Oxford, England, 2000.

Chapter VI

Imperfection Sensitivity or Insensitivity of Zero-stiffness Postbuckling ... that is the Question

Xin Jia[1], Gerhard Hoefinger[1] and Herbert A. Mang[1]

[1] *Institute for Mechanics of Materials and Structures, Vienna University of Technology, Karlsplatz 13/202, 1040 Vienna, Austria*

Abstract

Zero-stiffness postbuckling of a structure is characterized by a secondary load-displacement path along which the load remains constant. In sensitivity analysis it is usually considered as a borderline case between imperfection sensitivity and imperfection insensitivity. However, it is unclear whether zero-stiffness postbuckling is imperfection sensitive or insensitive. In this paper, Koiter's initial postbuckling analysis is used as a tool for sensitivity analysis. Distinction between two kinds of imperfections is made on the basis of the behavior of the equilibrium path of the imperfect structure. New definitions of imperfection insensitivity of the postbuckling behavior are provided according to the classification of the imperfections. A structure with two degrees of freedom with a zero-stiffness postbuckling path is studied, considering four different imperfections. The results from this example show that zero-stiffness postbuckling is a transition case from imperfection sensitivity to imperfection insensitivity for imperfections of the first kind and that it is imperfection insensitive for imperfections of the second kind.

Keywords

zero-stiffness postbuckling, Koiter's initial postbuckling analysis, classification of imperfections, imperfection insensitivity, constant potential energy

1. Introduction

In the course of sensitivity analysis of the initial postbuckling behavior of a structure, a special case may occur that is referred to as *zero-stiffness postbuckling* [6]. It is characterized by a secondary path with a constant load. In this paper the question will be answered whether zero-stiffness postbuckling is imperfection sensitive or imperfection insensitive.

The investigation is restricted to static, conservative systems with a finite number N of degrees of freedom as conforms to the FEM. The material is assumed to be rigid. Multiple bifurcation will be excluded.

2. Theory

2.1. Koiter's initial postbuckling analysis [3]

The behavior of a static, conservative system can be deduced from the potential energy function $V(\mathbf{u}, \lambda) : \mathbf{R}^N \times \mathbf{R} \to \mathbf{R}$. The vector $\mathbf{u} \in \mathbf{R}^N$ contains the displacement coordinates. The parameter $\lambda \in \mathbf{R}$ is a load multiplier scaling a constant reference load $\mathbf{P} \in \mathbf{R}^N$. Therefore,

$$\mathbf{G}(\mathbf{u}, \lambda) := V,_{\mathbf{u}} = \mathbf{F}^I(\mathbf{u}) - \lambda \mathbf{P} \tag{1}$$

may be interpreted as an out-of-balance force which vanishes along any equilibrium path in the $u - \lambda -$ space. Here, $\mathbf{F}^I(\mathbf{u})$ is the vector of internal forces. The secondary path is parameterized by a scalar η, with $\eta = 0$ corresponding to the bifurcation point $(\mathbf{u}_C, \lambda_C)$. The displacement offset between the primary and the secondary path is defined by the vector $\mathbf{v}(\eta) \in \mathbf{R}^N$. Thus, $\overline{\mathbf{u}}(\eta) = \tilde{\mathbf{u}}(\lambda(\eta)) + \mathbf{v}(\eta)$ describes the displacement along the secondary path, where $\tilde{\mathbf{u}}(\lambda(\eta))$ denotes the displacement vector along the primary path. Insertion of the series expansions

$$\lambda(\eta) = \lambda_C + \lambda_1 \eta + \lambda_2 \eta^2 + \lambda_3 \eta^3 + O(\eta^4) \tag{2}$$

$$\mathbf{v}(\eta) = \quad \mathbf{v}_1 \eta + \mathbf{v}_2 \eta^2 + \mathbf{v}_3 \eta^3 + O(\eta^4) \tag{3}$$

into the specialization of $\mathbf{G}$ for the secondary path, i.e., $\mathbf{G}(\eta) = \mathbf{G}(\tilde{\mathbf{u}}(\lambda(\eta)) + \mathbf{v}(\eta), \lambda(\eta)) = \mathbf{0}$, yields the new series expansion

$$\mathbf{G}(\eta) = \mathbf{G}_{0C} + \mathbf{G}_{1C} \eta + \mathbf{G}_{2C} \eta^2 + O(\eta^3) = \mathbf{0} \tag{4}$$

with $\mathbf{G}_{nC} = \mathbf{G},_{\eta^n} \big|_{\eta=0} / n! \, \forall n \in \mathbf{N}$. Since (4) must hold for arbitrary values of η, $\mathbf{G}_{nC} = \mathbf{0} \, \forall n \in \mathbf{N}$. This condition paves the way for successive calculation of the unknowns $\mathbf{v}_1, \lambda_1, \mathbf{v}_2, \lambda_2$, etc.

2.2. Classification of imperfections

For perfect systems undergoing bifurcation buckling, the imperfections are classified in two categories depending on whether or not the imperfect system has a bifurcation point. Godoy [1], and Ikeda, *et al.* [2] introduce an imperfection vector $\mathbf{E}$ which is calculated from the potential energy function referring to the imperfect structure

$$V^* = V^*(\mathbf{u}, \lambda, \varepsilon) : \mathbf{R}^N \times \mathbf{R} \times \mathbf{R} \to \mathbf{R} \tag{5}$$

where $\varepsilon \in \mathbf{R}$ denotes the imperfection parameter, and * denotes variables or functions of the imperfect structure. The imperfection vector is defined as

$$\mathbf{E} = \frac{\partial^2 V^*}{\partial \mathbf{u} \partial \varepsilon}\bigg|_{\mathbf{u}=\tilde{\mathbf{u}}} . \tag{6}$$

$\mathbf{E}$ describes the difference of the out-of-balance force between the perfect and the imperfect structure depending on the imperfection parameter ε. The classification of imperfections gives:

$$\mathbf{E}^T \cdot \mathbf{v}_1 = 0 \text{ for imperfections of first kind, } \varepsilon_I, \tag{7}$$

$$\mathbf{E}^T \cdot \mathbf{v}_1 \neq 0 \text{ for imperfections of second kind, } \varepsilon_{II}. \tag{8}$$

2.3. Definitions of and criteria for imperfection insensitivity

Imperfections of first kind:

Definition I: $\varepsilon_I \in [-\varsigma, \varsigma]$, where ς is an arbitrary small positive value. If all imperfect structures in this interval are still stable at the bifurcation point C^*, then the *initial* postbuckling path of the corresponding perfect structure is *imperfection insensitive* with respect to ε_I.

Criterion I: If, in Eq. (2),

$$\lambda_{m_{\min}} > 0 \wedge m_{\min} \text{ is even, where } m_{\min} := \min\{m \mid m \in \mathbf{N}\backslash\{0\}, \lambda_m \neq 0\}, \tag{9}$$

then the *initial* postbuckling path is *imperfection insensitive* with respect to ε_I.

Imperfections of second kind:

Definition II: $\varepsilon_{II} \in [-\varsigma, 0) \cup (0, \varsigma]$, where ς is an arbitrary small positive value. If no imperfect structure in this interval has a load-displacement path with a snapthrough point $(\mathbf{u}_{D*}, \lambda_{D*})$ with $\lambda_{D*} < \lambda_C$, then the *initial* postbuckling path of the corresponding perfect structure is *imperfection insensitive* to ε_{II}.

Criterion II: See Definition II.

3. Condition for zero-stiffness postbuckling

For zero-stiffness postbuckling, the external load remains constant. Hence, all load coefficients in Eq. (2) vanish, i.e.,

$$\lambda = \lambda_C, \tag{10}$$

$$\lambda_i = 0 \ \forall \ i \in \mathbf{N}\backslash\{0\}. \tag{11}$$

Considering load coefficients $\lambda_i = \lambda_i(\mathbf{\kappa})$, where $\mathbf{\kappa} = \{\kappa_1, \kappa_2, ...\}$ is a set of design parameters,

$$\lambda_i(\mathbf{\kappa}) = C_0(\mathbf{\kappa}_0) \cdot C_i(\mathbf{\kappa}_i) \ \vee \ \mathbf{\kappa}_i \subseteq \mathbf{\kappa} \ \vee \ \mathbf{\kappa}_0 \subseteq \mathbf{\kappa} \tag{12}$$

with

$$C_0(\mathbf{\kappa}_0) = 0 \tag{13}$$

is a necessary and sufficient condition for zero-stiffness postbuckling.

4. Properties of zero-stiffness postbuckling

4.1. Internal force along a zero-stiffness equilibrium path

Substituting (10) into (1) and setting the result equal to zero yields

$$\mathbf{F}^I(\overline{\mathbf{u}}) = \lambda_C \cdot \mathbf{P} . \tag{14}$$

Eq. (14) shows that the internal force along the zero-stiffness path is a constant.

4.2. Potential energy along a zero-stiffness equilibrium path

Since the external load does not change along the zero-stiffness equilibrium path, the difference between the work done by the external load on the displacement at an arbitrary point on the secondary path and the one on the displacement at the bifurcation point is obtained as

$$W = (\lambda_C \cdot \mathbf{P}) \cdot \overline{\mathbf{u}} - (\lambda_C \cdot \mathbf{P}) \cdot \mathbf{u}_C , \tag{15}$$

The change of the strain energy is given as

$$\Delta U = U(\overline{\mathbf{u}}) - U(\mathbf{u}_C) . \tag{16}$$

By the law of conservation of energy,

$$W = \Delta U . \tag{17}$$

Insertion of (15) and (16) into (17) yields

$$V(\overline{\mathbf{u}}) = U(\overline{\mathbf{u}}) - (\lambda_C \cdot \mathbf{P}) \cdot \overline{\mathbf{u}} = U(\mathbf{u}_C) - (\lambda_C \cdot \mathbf{P}) \cdot \mathbf{u}_C = V(\mathbf{u}_C) . \tag{18}$$

Eq. (18) indicates that the potential energy along the zero-stiffness equilibrium path is a constant.

5. Examples

A planar, static, conservative system with two degrees of freedom (Fig. 1) is studied to illustrate the special situation of zero-stiffness postbuckling. It was originally studied in Schranz *et al.* [4] and later in Steinboeck *et al.* [5].
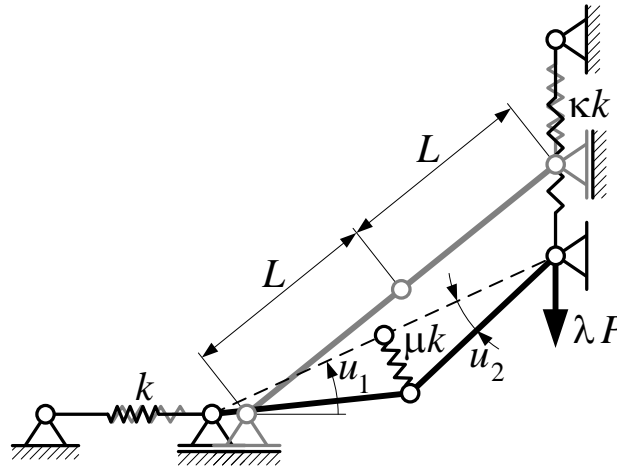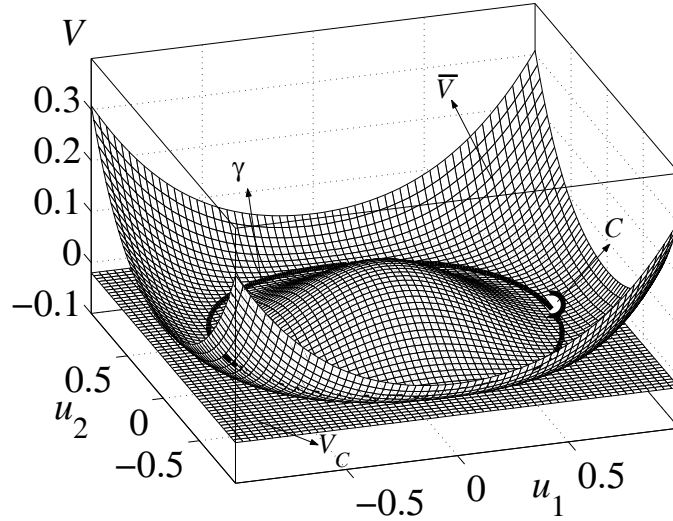

Fig. 1: Two-bar system

Fig. 2: Surface $\bar{V}(\mathbf{u})$ containing the curve $\gamma(\eta)$ which represents the zero-stiffness postbuckling mode

Fig. 2 shows the surface $\bar{V}(\mathbf{u}) = \left(\mathbf{u}, V(\bar{\mathbf{u}}, \lambda(\bar{\mathbf{u}}))\right) \ \forall \ \mathbf{u} \in \mathbf{R}^2$. Its intersection with the horizontal plane $V_C = \left(\mathbf{u}, V(\mathbf{u}_C)\right) \ \forall \ \mathbf{u} \in \mathbf{R}^2$ is the closed curve $\gamma(\eta) = \left(\bar{\mathbf{u}}(\eta), V(\bar{\mathbf{u}}(\eta), \lambda(\bar{\mathbf{u}}(\eta)))\right) \ \forall \ \eta \in \mathbf{R}$ which represents the potential energy along the zero-stiffness path containing the bifurcation point $C = \left(\mathbf{u}_C, V(\mathbf{u}_C)\right)$. In an infinitesimal neighborhood of $\gamma(\eta)$, $\bar{V}(\mathbf{u})$ coincides (apart from terms that are of higher order small) with the potential-energy surface $V(\mathbf{u}, \lambda)$. In the infinitesimal neighborhood of an arbitrary point on $\gamma(\eta)$, $V_{,\mathbf{uu}} \geq 0$, where the equals sign holds for $\gamma(\eta)$. Consequently, the zero-stiffness postbuckling path is stable. Therefore, zero-stiffness postbuckling can be classified as imperfection insensitive.
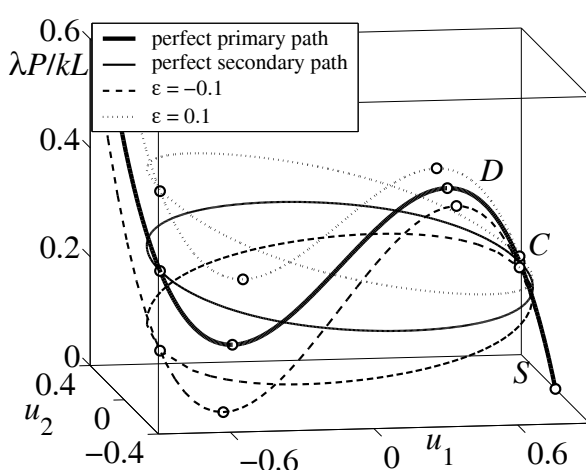
(a) Imperfection of stiffness of top spring

(b) Imperfection of stiffness of lateral spring

(c) Shift of load   (d) Change of initial angle between two rods
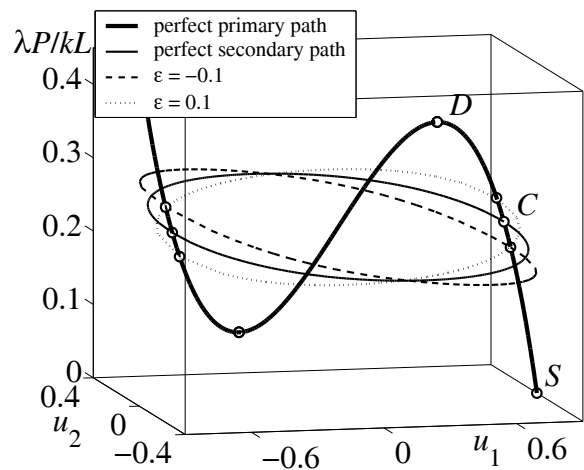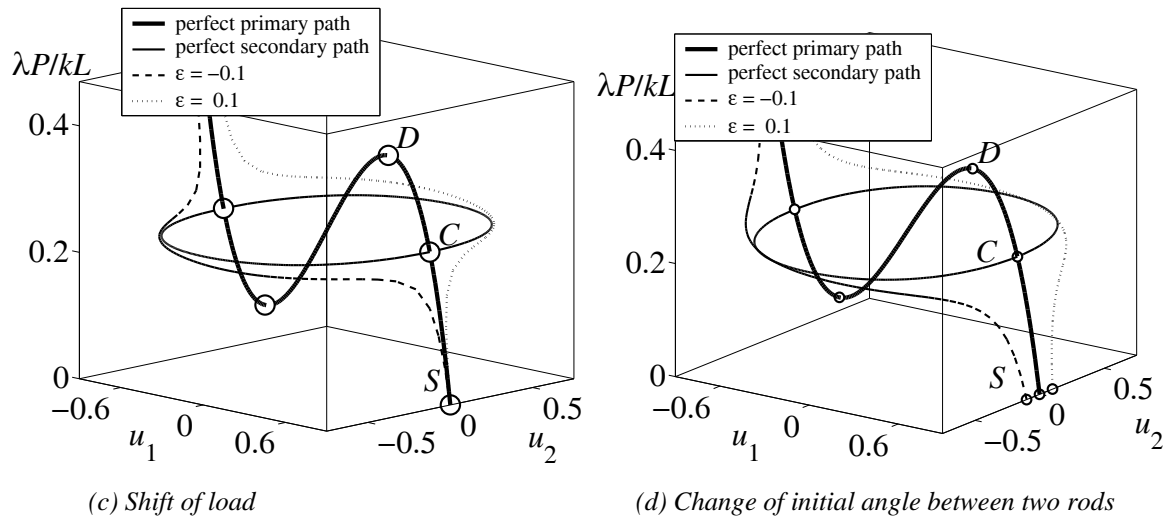
Fig. 3: Equilibrium paths of perfect and imperfect structures

Four different imperfections are considered herein, including an imperfection of the stiffness of the top spring, an imperfection of the stiffness of the lateral spring, a shift of the load and a change of the initial angle between two rods. The first two imperfections belong to the first kind, and the last two to the second kind of imperfections. Fig. 3 displays the equilibrium paths of the perfect and the imperfect structure for different imperfections.

6.   Conclusions

From the theoretical investigation and the results of the examples, it follows that zero-stiffness postbuckling

- represents a case of transition from imperfection sensitivity to insensitivity for imperfections of first kind;

- is characterized by a stable postbuckling equilibrium path with constant potential energy and, hence, is imperfection insensitive to imperfections of second kind.

References

[1] Godoy, L.A. *Theory of elastic stability: analysis and sensitivity*. Taylor & Francis, 2000.

[2] Ikeda, K. Ohsaki, M. *Generalized sensitivity and probabilistic analysis of buckling loads of structures*. Int. J. Non-linear Mech., 42, 733-743, 2007.

[3] Koiter W. *On the stability of elastic equilibrium*, Translation of '*Over de Stabiliteit van het Elastisch Evenwicht*'. In NASA TT F-10833, Polytechnic Institute Delft, H.J. Paris Publisher: Amsterdam, 1967.

[4] Schranz C., Krenn B., Mang H.A. *Conversion from imperfection-sensitive into imperfection-insensitive elastic structures II: Numerical investigation*. Comput. Methods Appl. Mech. Engrg., 195, 1458-1479, 2006.

[5] Steinboeck A, Jia X, Hoefinger G, Mang H.A. *Conditions for symmetric, antisymmetric, and zero-stiffness bifurcation in view of imperfection sensitivity and insensitivity*. Comput. Methods Appl. Mech. Engrg., 197, 3623-3636, 2008.

[6] Tarnai, T. *Zero stiffness elastic structures*, Int. J. Mech. Sci., 45(3), 425-431, 2003.

Chapter VII

Necessary and Sufficient Conditions for Zero-Stiffness Postbuckling

Xin Jia[1], Gerhard Hoefinger[1], and Herbert A. Mang[1]

[1] *Institute for Mechanics of Materials and Structures, Vienna University of Technology, Karlsplatz 13/202, 1040 Vienna, Austria*

Abstract

In the course of sensitivity analysis of the initial postbuckling behavior of elastic structures, a special case may occur which is referred to as zero-stiffness postbuckling. The purpose of this paper is to present sufficient and necessary conditions for this special case which is associated with a favorable form of transition from imperfection sensitivity to imperfection insensitivity in the course of sensitivity analysis of the initial postbuckling path. Koiter's initial postbuckling analysis is chosen as the vehicle for quantification of the initial postbuckling behavior.

1. Introduction

Tarnai [1] has pioneered research on zero-stiffness postbuckling. Schranz *et al.* [2] presented a numerical example which was further elaborated by Steinboeck *et al.* [3]. Jia *et al.* [4] have shown that zero-stiffness postbuckling is imperfection insensitive by investigation of the potential energy along the postbuckling path. The task of this work is to present sufficient and necessary conditions for zero-stiffness postbuckling with the help of Koiter's initial postbuckling analysis [5].

2. Necessary conditions for zero-stiffness postbuckling

The difference between the dimensionless load parameter λ at an arbitrary point on the secondary equilibrium path, characterized by the path parameter η, and the value of λ at the stability limit for which $\eta = 0$, is given as

$$\Delta\lambda(\kappa,\eta) = \lambda_1(\kappa)\eta + \lambda_2(\kappa)\eta^2 + \lambda_3(\kappa)\eta^3 + \lambda_4(\kappa)\eta^4 + O(\eta^5). \tag{1}$$

$\lambda_1, \lambda_2,...$ are coefficients depending on a design parameter κ. Steinboeck *et al.* [3] have shown that

$$\lambda_1(\kappa) = 0 \quad \forall \kappa \tag{2}$$

is a necessary condition for imperfection insensitivity and, consequently, for zero-stiffness postbuckling [4]. Additional necessary conditions for zero-stiffness postbuckling are

$$\lambda_2(\kappa = \bar{\kappa}) = 0 \;\Rightarrow\; d_2(\kappa = \bar{\kappa}) = 0 \;\Rightarrow\; \lambda_3(\kappa = \bar{\kappa}) = 0, \tag{3}$$

where $\bar{\kappa}$ is a specific value of κ. These conditions ensure that the first non-vanishing coefficient $\lambda_i(\kappa)$ in (1) is one with an even subscript. This situation is typical for the case of a restricted asymmetry [8] which is a consequence of (2).

Mang *et al.* [2] originally derived the relation

$$\lambda_4(\kappa) = a_1(\kappa)\lambda_2(\kappa)^2 + \bar{b}_2(\kappa)\lambda_2(\kappa) + \bar{d}_3(\kappa) \tag{4}$$

with $\bar{b}_2(\kappa) = b_1^2(\kappa) + b_2(\kappa)$, and $\bar{d}_3(\kappa) = b_1(\kappa)d_2(\kappa) + d_3(\kappa)$. The expressioins for a_1, b_1, b_2, and d_3 are given in [8]. Specialization of (4) for (3) gives

$$\lambda_4(\kappa = \bar{\kappa}) = \bar{d}_3(\kappa = \bar{\kappa}) \tag{5}$$

which is an additional necessary condition for zero-stiffness postbuckling. In general, however, $\lambda_4(\kappa = \bar{\kappa}) \neq 0$.

3. Sufficient condition for zero-stiffness postbuckling

With the help of the so-called consistently linearized eigenproblem [6], it is possible to distinguish between two different classes of problems as regards sensitivity analysis of the initial postbuckling path. For the first class,

$$\mathbf{v}_j^{*T} \cdot \tilde{\mathbf{K}}_{T,\lambda\lambda} \cdot \mathbf{v}_1^* = 0, \quad j = 2,3,...,n, \tag{6}$$

where $\tilde{\mathbf{K}}_{T,\lambda\lambda}$ is the second derivative of the tangent stiffness matrix, in the frame of the Finite Element Method, with respect to λ, and $\mathbf{v}_1^*$ and $\mathbf{v}_j^*$ stand for the first and the j-th eigenvector, respectively, of

the mentioned eigenproblem. This class is characterized by a prebuckling behavior that is restricted to axial deformations. For the second class,

$$\mathbf{v}_j^{*T} \cdot \tilde{\mathbf{K}}_{T,\lambda\lambda} \cdot \mathbf{v}_1^* \neq 0, \quad j = 2,3,...,n. \tag{7}$$

For this class,

$$\lambda_4\big|_{\lambda_2=0} < 0 \tag{8}$$

which is a sufficient condition for non-zero-stiffness postbuckling. Consequently, zero-stiffness postbuckling is impossible for this class of nonlinear stability problems which represents the general class of such problems.

4. Sufficient and necessary condition for zero-stiffness postbuckling

Non-zero-stiffness transitions from imperfection sensitivity to imperfection insensitivity are restricted to $\lambda_4\left(\kappa = \overline{\kappa}\right) \neq 0$ [7]. Hence, it is concluded that

$$\lambda_1\left(\kappa\right) = 0 \quad \forall \kappa, \qquad \lambda_2\left(\kappa = \overline{\kappa}\right) = \lambda_4\left(\kappa = \overline{\kappa}\right) = 0 \tag{9}$$

are sufficient and necessary conditions for zero-stiffness postbuckling, characterized by

$$\lambda_i\left(\kappa = \overline{\kappa}\right) = 0 \quad \forall i \in \mathbb{N}. \tag{10}$$

5. Numerical example

Details of an example involving zero-stiffness postbuckling in the course of sensitivity analysis of the initial postbuckling path can be found in [6]. For this example,

$$\frac{\lambda_4\left(\kappa\right)}{\lambda_2\left(\kappa\right)} = const. \tag{11}$$

For $\kappa = \overline{\kappa} = \mu/4$, where κ is a variable spring stiffness whereas μ is a costant spring stiffness,

$$\lambda_2\left(\kappa = \overline{\kappa}\right) = 0 \xrightarrow{\ (11)\ } \lambda_4\left(\kappa = \overline{\kappa}\right) = 0. \tag{12}$$

Hence, the sufficient and necessary conditions for zero-stiffness postbuckling, as given in (9), are satisfied.

6. Conclusions

Zero-stiffness postbuckling will occur if and only if $\lambda_1\left(\kappa\right) = 0 \ \forall \kappa, \ \lambda_2\left(\kappa = \overline{\kappa}\right) = \lambda_4\left(\kappa = \overline{\kappa}\right) = 0$.

$\lambda_4\left(\kappa = \overline{\kappa}\right) = 0$ requires $\mathbf{v}_j^{*T} \cdot \tilde{\mathbf{K}}_{T,\lambda\lambda} \cdot \mathbf{v}_1^* = 0, \quad j = 2,3,...,n.$

References

[1] Tarnai T., *Zero stiffness elastic structures*, Int. J. Mech. Sci., **45**(3), 425-431, 2003.

[2] Schranz C., Krenn B., and Mang H. A. *Conversion from imperfection-sensitive into imperfecction-insensitive elastic structures II: Numerical investigation*, Comput. Mech. Eng., **195**(13-16), 1422-1457 2006.

[3] Steinboeck A., Jia X., Hoefinger G., and Mang H. A. *Conditions for symmetric, antisymmetric, and zero-stiffness bifurcation in view of imperfection sensitivity and insensitivity*, Comput. Appl. Meth. Eng., **197**(45-48), 3626-3636, 2008.

[4] Jia X., Hoefinger G., and Mang H. A. *Imperfection sensitivity or insensitivity of zero-stiffness postbuckling...that is the question*, in: Proceedings of the International Symposium on Computational Structureal Engineering, Shanghai, China, (Springer, 2009), 103-110.

[5] Koiter W. *On the stability of elastic equilibrium*. (Translation of '*over de stabiliteit van het elastisch evenwicht'(1945)*), Techn. Rep., Polytechnic Institute Delft, H. J. Paris Publisher Amsterdam, NASA TT F-10, 833, 1967.

[6] Steinboeck A., Jia X., Hoefinger G., and Mang H. A. *Remarkable postbuckling paths analyzed by means of the consistently linearized eigenproblem*, Int. J. Numer. Meth. Engng., **76**(2), 156-182, 2008.

[7] Mang H. A., Hoefinger G., and Jia X. *On the interdependency of primary and initial secondary equilibrium paths in sensitivity analysis of elastic structures*, submitted for publication, 2010.

[8] Mang H. A., Hoefinger G., and Jia X. *On the predictability of zero-stiffness postbuckling*, Z. Angew. Math. Mech., **90**(10-11), 837-846, 2010.

Chapter VIII

Conversion of Imperfection-sensitive Elastic Structures into Imperfection-insensitive Ones by Adding Tensile Members

Xin Jia[1], Herbert Mang[1]

[1] *Institute for Mechanics of Materials and Structures, Vienna University of Technology, Karlsplatz 13/202, 1040 Vienna, Austria*

Abstract

The benefit of an increase of the stability limit of a structure in consequence of a modification of the original design may largely be lost through deterioration of the postbuckling behavior. Therefore, it may be useful to concentrate on design changes that result in a significant improvement of the postbuckling behavior without decrease of the stability limit. It is shown that the possibility of converting imperfection-sensitive structures into imperfection-insensitive ones by adding tensile members is not restricted to academic examples such as the von Mises truss. An arch bridge serves as the demonstration object. The reason for disregarding the option of adding compressive members to the original structure is to exclude the possibility of buckling of these members.

Keywords

bifurcation buckling, consistently linearized eigenproblem, imperfection (in)sensitivity, Koiter's initial postbuckling analysis, *von Mises* truss, arch bridge

1. Introduction

In contrast to imperfection-insensitive structures, imperfection-sensitive ones cannot carry the buckling loads of corresponding perfect structures. Design changes leading to an increase of the stability limit will be counterproductive if such an increase is accompanied by a significant deterioration of the prebuckling behavior, i.e. if the imperfection sensitivity of the original structure is markedly increased.

An example for such a design change is the increase of the thickness of a shallow cylindrical shell [1]. It results in the convergence of the bifurcation point, which represents the stability limit, to the snap-through point [2]. The load levels related to these two points increase with increasing thickness of the shell. At the same time, the postbuckling behavior gets worse which is reflected by the increase of the difference between the stability limit of the perfect structure and the snap-through point of the imperfect one.

The aim of this paper is to utilize the beneficial effect of attaching a vertical elastic spring to the vertex of a *von Mises* truss for a real-life structure. Approximate postbuckling analysis of such a truss, subjected to a vertical load at the vertex, is an example that can be solved analytically [3]. Whereas the *von Mises* truss without the spring is imperfection sensitive, it becomes imperfection insensitive provided the stiffness of the spring is large enough so that the increase of the load in the spring overcompensates the decrease in the load carried by the truss.

The paper is organized as follows: In section 2, the difference between bifurcation buckling from a general state of prebuckling deformations, as occurs in the majority of real-life structures, and from a membrane stress state will be mentioned in the context of the Finite Element Method (FEM). Section 3 contains an extension of Koiter's initial postbuckling analysis [4] to sensitivity investigations of the initial postbuckling behavior [5]. The first example presented in Section 4 is the aforementioned *von Mises* truss. It is an example for buckling from a nonlinear primary path, characterized by a membrane stress state. The second example is an arch bridge where loss of stability occurs from a general stress state.

2. Consistently linearized eigenproblem

The consistently linearized eigenproblem [10] is a vehicle for demonstrating the differences between bifurcation buckling from a general stress state and from a membrane stress state. The mathematical formulation of the consistently linearized eigenproblem for the first eigenpair $\left(\lambda_1^*(\lambda) - \lambda, \mathbf{v}_1^*(\lambda)\right)$ where λ denotes a dimensionless load factor by which the reference load vector $\bar{\mathbf{P}}$, in the frame of the FEM, is multiplied, reads as [6]

$$\left[\tilde{\mathbf{K}}_T + \left(\lambda_1^* - \lambda\right)\tilde{\mathbf{K}}_{T,\lambda}\right] \cdot \mathbf{v}_1^* = \mathbf{0} \tag{1}$$

where $\tilde{\mathbf{K}}_T$ is the tangent stiffness matrix and $\tilde{\mathbf{K}}_{T,\lambda}$ is its first derivative with respect to λ. At the stability limit,

$$\lambda_1^* = \lambda, \quad \mathbf{v}_1^* = \mathbf{v}_1, \quad \tilde{\mathbf{K}}_T \cdot \mathbf{v}_1 = \mathbf{0}, \tag{2}$$

with (2) representing the condition for loss of stability of equilibrium in the form of bifurcation buckling, characterized by

$$\mathrm{d}\lambda \geq 0. \tag{3}$$

The equal sign holds for the borderline case of hilltop buckling [2] for which also $d\mathbf{q}$, representing an infinitesimal increment of the vector of nodal displacements at the snap-through point, is an eigenvector.

Derivation of (1) with respect to λ yields

$$\left[\lambda_{1,\lambda}^* \tilde{\mathbf{K}}_{T,\lambda} + \left(\lambda_1^* - \lambda \right) \tilde{\mathbf{K}}_{T,\lambda\lambda} \right] \cdot \mathbf{v}_1^* + \left[\tilde{\mathbf{K}}_T + \left(\lambda_1^* - \lambda \right) \tilde{\mathbf{K}}_{T,\lambda} \right] \cdot \mathbf{v}_{1,\lambda}^* = \mathbf{0} \tag{4}$$

where [6]

$$\mathbf{v}_{1,\lambda}^* = \sum_{j=1}^{N} c_{1j} \mathbf{v}_j^*, \tag{5}$$

with

$$c_{11} = -\frac{1}{2} \frac{\mathbf{v}_1^{*\mathrm{T}} \cdot \tilde{\mathbf{K}}_{T,\lambda\lambda} \cdot \mathbf{v}_1^*}{\mathbf{v}_1^{*\mathrm{T}} \cdot \tilde{\mathbf{K}}_{T,\lambda} \cdot \mathbf{v}_1^*}, \quad c_{1j} = -\frac{\lambda_1^* - \lambda}{\lambda_1^* - \lambda_j^*} \frac{\mathbf{v}_j^{*\mathrm{T}} \cdot \tilde{\mathbf{K}}_{T,\lambda\lambda} \cdot \mathbf{v}_1^*}{\mathbf{v}_j^{*\mathrm{T}} \cdot \tilde{\mathbf{K}}_{T,\lambda} \cdot \mathbf{v}_j^*}, \quad j = 2,3,\ldots,N \tag{6}$$

where $\mathbf{v}_j^*$ is the eigenvector corresponding to the eigenvalue $\lambda_j^* - \lambda$. The coefficients c_{11} and c_{1j} depend on the normalization of the eigenvectors.

Premultiplication of (4) by $\mathbf{v}_1^{*T}$ and consideration of (1) gives

$$\frac{\lambda_{1,\lambda}^*}{\lambda_1^* - \lambda} = -\frac{\mathbf{v}_1^{*\mathrm{T}} \cdot \tilde{\mathbf{K}}_{T,\lambda\lambda} \cdot \mathbf{v}_1^*}{\mathbf{v}_1^{*\mathrm{T}} \cdot \tilde{\mathbf{K}}_{T,\lambda} \cdot \mathbf{v}_1^*}. \tag{7}$$

At the stability limit, following from (1), (4), (5), (6), and (7),

$$\frac{\lambda_{1,\lambda}^*}{\lambda_1^* - \lambda} = \frac{0}{0} = \frac{\lambda_{1,\lambda\lambda}^*}{\lambda_{1,\lambda}^* - 1} = -\lambda_{1,\lambda\lambda}^*. \tag{8}$$

Substitution of (8) and and $\lambda_1^* = \lambda$ (see (2)) into (7) gives

$$\lambda_{1,\lambda\lambda}^* = \frac{\mathbf{v}_1^{\mathrm{T}} \cdot \tilde{\mathbf{K}}_{T,\lambda\lambda} \cdot \mathbf{v}_1}{\mathbf{v}_1^{\mathrm{T}} \cdot \tilde{\mathbf{K}}_{T,\lambda} \cdot \mathbf{v}_1}. \tag{9}$$

For the special case of bifurcation from a membrane stress state [7],

$$\tilde{\mathbf{K}}_T \cdot \mathbf{v}_{1,\lambda\lambda}^* = \mathbf{0}, \tag{10}$$

$$\tilde{\mathbf{K}}_{T,\lambda\lambda} \cdot \mathbf{v}_1 = \lambda_{1,\lambda\lambda}^* \tilde{\mathbf{K}}_{T,\lambda} \cdot \mathbf{v}_1 \tag{11}$$

with $\lambda_{1,\lambda\lambda}^*$ according to (9). The relations (10) and (11) may be viewed as constraint conditions holding for this special stress state.
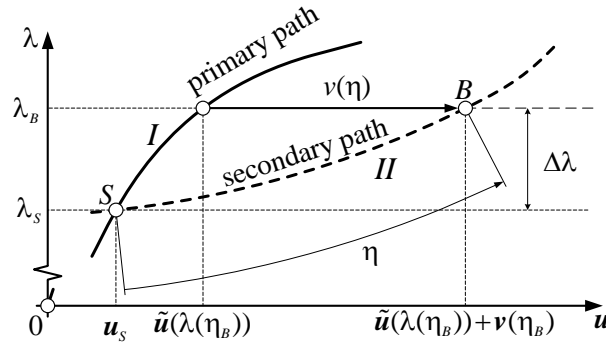
3. Koiter's initial postbuckling analysis

Fig. 1: Nonlinear primary path and secondary path for a specific value of the design parameter κ ($\tilde{\mathbf{u}}$ denotes the displacements of the primary path)

Fig. 1 shows a nonlinear primary path (I) and the secondary path (II) for a specific value of the design parameter κ that is increased from zero in the course of sensitivity analysis of the initial postbuckling path. For this value of κ, $\Delta\lambda$ (Fig. 1) is a function of the parameter η that describes the postbuckling path.

The series expansion of $\Delta\lambda(\kappa,\eta)$ is given as

$$\Delta\lambda(\kappa,\eta) = \lambda_1(\kappa)\eta + \lambda_2(\kappa)\eta^2 + \lambda_3(\kappa)\eta^3 + O(\eta^4). \tag{12}$$

$\lambda_1, \lambda_2, \dots$ are coefficients depending on κ. Steinboeck *et al.* [8] have shown that

$$\lambda_1(\kappa) = 0 \quad \forall \kappa \tag{13}$$

is a necessary condition for imperfection insensitivity. Making use of (13), the expression for the coefficient $\lambda_2(\kappa)$ is obtained as [5]

$$\lambda_2(\kappa) = d_1(\kappa) \tag{14}$$

with (omitting the argument κ)

$$d_1 = \frac{1}{\mathbf{v}_1^{\mathrm{T}} \cdot \tilde{\mathbf{K}}_{T,\lambda} \cdot \mathbf{v}_1} (\mathbf{v}_1^{\mathrm{T}} \cdot \tilde{\mathbf{K}}_{T,\mathbf{u}} : \mathbf{v}_1 \otimes \mathbf{v}_2 + \frac{1}{6} \mathbf{v}_1^{\mathrm{T}} \cdot \tilde{\mathbf{K}}_{T,\mathbf{uu}} \vdots \mathbf{v}_1 \otimes \mathbf{v}_1 \otimes \mathbf{v}_1) \tag{15}$$

where $\mathbf{v}_1$ is the eigenvector, and $\mathbf{v}_2 = \mathbf{v}_2(\kappa)$ denotes the first residual vector in the series expansion

$$\mathbf{v}(\kappa,\eta) = \mathbf{v}_1(\kappa)\eta + \mathbf{v}_2(\kappa)\eta^2 + \mathbf{v}_3(\kappa)\eta^3 + O(\eta^4) \tag{16}$$

for the displacement offset which vanishes at the stability limit S (Fig.1).

A sufficient condition for imperfection insensitivity for a specific value $\bar{\kappa}$ of the design parameter κ is

$$d_1(\kappa = \bar{\kappa}) > 0 \xrightarrow{\ (14)\ } \lambda_2(\kappa = \bar{\kappa}) > 0, \tag{17}$$

recalling that (14) is based on (13). This condition is not necessary because imperfection insensitivity is also given for

$$d_1(\kappa = \bar{\kappa}) = 0 \xrightarrow{\ (15)\ } \lambda_2(\kappa = \bar{\kappa}) = 0 \xrightarrow{\ [7]\ } \lambda_3(\kappa = \bar{\kappa}) = 0 \tag{18}$$

if

$$\lambda_4(\kappa = \bar{\kappa}) > 0. \tag{19}$$

If also

$$\lambda_4\left(\kappa=\bar{\kappa}\right)=0, \tag{20}$$

then, for the special case of bifurcation buckling from a membrane stress state,

$$\lambda_5\left(\kappa=\bar{\kappa}\right)=\lambda_6\left(\kappa=\bar{\kappa}\right)=\lambda_7\left(\kappa=\bar{\kappa}\right)=...=0 \xrightarrow{(12)} \Delta\lambda\left(\kappa=\bar{\kappa}\right)=0, \tag{21}$$

indicating zero-stiffness postbuckling which was shown to be imperfection insensitive [5]. Zero-stiffness postbuckling may be seen as a constraint condition for the postbuckling path that does not exist for the general case of bifurcation buckling.

A theoretical treatment of the sensitivity of structures with respect to imperfections is given e.g. in Bažant and Cedolin [11].

4. Numerical investigation

4.1. Von Mises truss

Fig. 2 shows the left half of a *von Mises* truss with a vertical elastic spring attached to the vertex of the structure at which a vertical load λP with $P=10^4 kN$ is applied. The length of the undeformed bar, L, is 100cm and the initial position of the load point, u_{10}, is 30.9 cm. The side length of the quadratic cross section, a, is chosen as 20 cm and the elastic modulus E, as $2.1\times10^7 kN/cm^2$. The spring constant is given as κk where $k=10^2\ kN/cm$ and $\kappa\in\mathbb{R}$ is a scaling parameter that represents the design parameter. In the prebuckling regime, the bar is straight. Hence, buckling occurs from a purely axial deformation state of the bar. For such a prebuckling deformation state the constraint conditions (10) and (11) must hold at the stability limit.
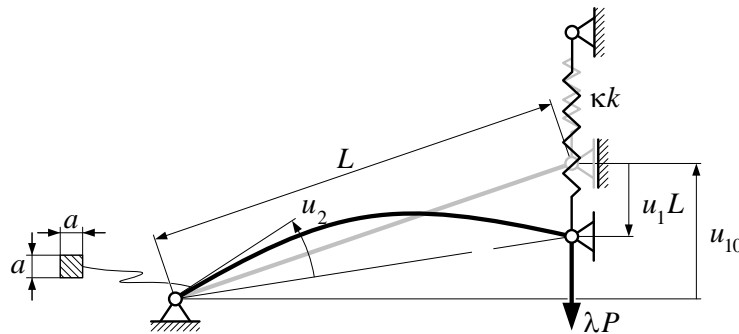

Fig. 2: Left half of a von Mises truss with a vertical elastic spring attached to the load point

Details of the analysis can be found in [6] where two solution strategies were pursued: (i) exact nonlinear theory and (ii) approximation of the deformed shape as a sine curve. In the latter case, it is stipulated that $\mathbf{u}=\left[u_1,u_2\right]^T$ suffices to define the configuration of the system, i.e. the model is reduced to a two-degrees-of-freedom scheme.

All parameters are tuned such that hilltop buckling occurs for $\kappa=0$ (Fig. (a)). The negative slope of the projection of the secondary path onto the plane $u_2=0$ at $S=D$ (denoting the coincidence of the bifurcation point S with the snap-through point D) indicates that a structure which experiences hilltop buckling is imperfection sensitive, as was proved theoretically in [2]. Increasing the stiffness of the spring by increasing κ, improves the postbuckling behavior, as expressed by a linear increase of

$\lambda_{2m}(\kappa)$, $\forall m \in \mathbb{N}$. Fig. (b) refers to a situation which is characterized by $\lambda_2 = 0$ and $\lambda_4 < 0$. Hence, zero-stiffness postbuckling does not occur here. The positive slope of the projection of the secondary path onto the plane $u_2 = 0$ in Fig. (c) shows that the initially imperfection-sensitive structure was converted into an imperfection-insensitive structure. The form of the projections of the secondary paths in Fig. onto the plane $u_2 = 0$ indicates symmetric bifurcation with respect to this plane, characterized by $\lambda_1 = \lambda_3 = \lambda_5 = ... = 0 \ \forall \kappa$. As was shown in [8], symmetric bifurcation is not necessary for imperfection insensitivity.
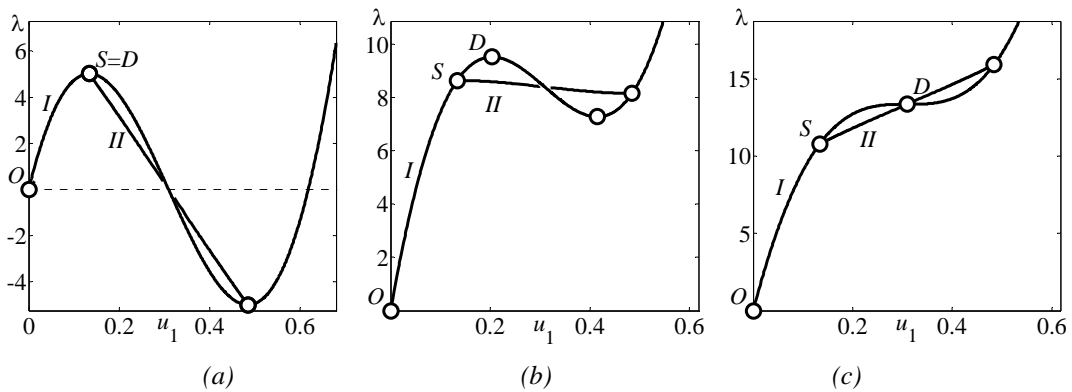

Fig. 3: Load-displacement paths of a von Mises truss for three different values of the spring stiffness: (a) $\kappa = 0$, *hilltop buckling, (b)* $\kappa = 27.2$ *(c)* $\kappa = 43.2$
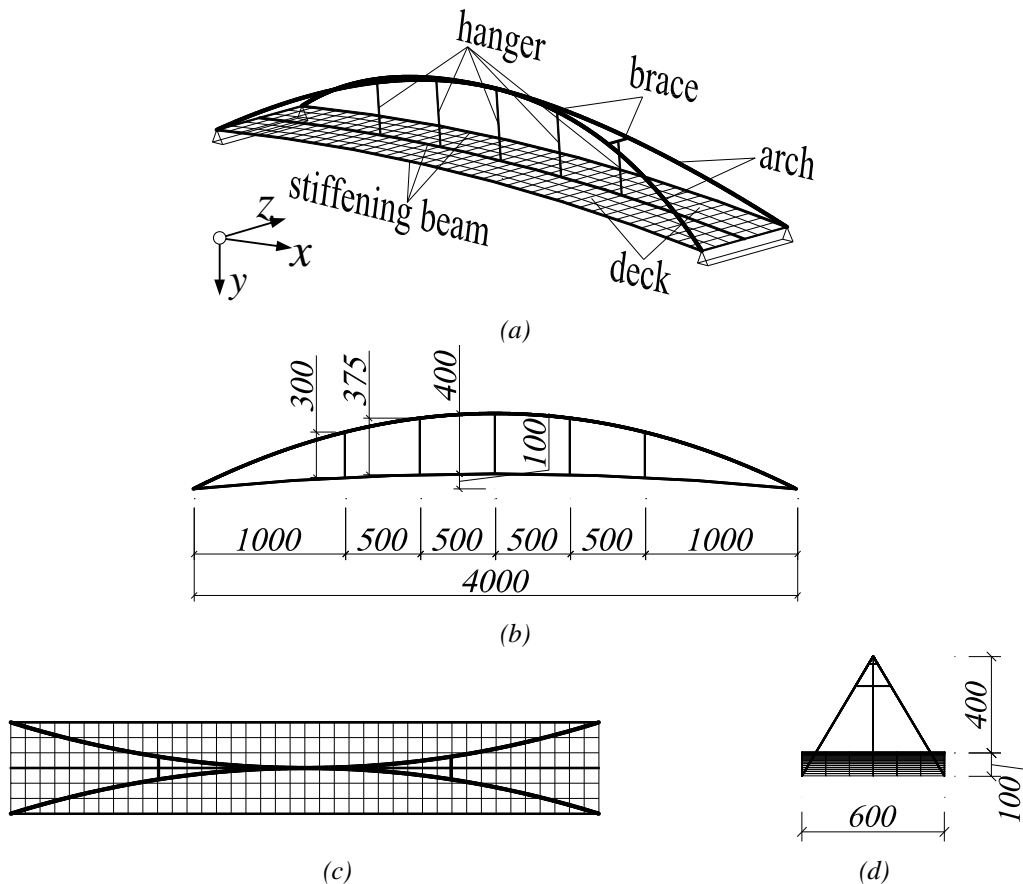
4.2. Arch bridge

Fig. 4: (a) Arch bridge, (b) view from the side, (c) floor plan, (d) front view; unit of numerical data: cm

Fig. 4(a) shows the investigated bridge. The two inclined, plane, parabolic arches with fixed supports meet at mid-span. They are connected by four transverse horizontal braces. The deck is a simply supported cylindrical shell with a rise of 100cm (Fig. 4(b)). It is suspended from the braces and the arches, respectively, by altogether five hangers and stiffened by three longitudinal beams, two of which along the longitudinal edges of the deck.

The elastic modulus, E_S, and Poisson's ratio, ν_S, of the steel used for the arch, the lateral braces, the stiffening beams, and the hangers, are given as $21000\ kN/cm^2$ and 0.3, respectively. The elastic modulus E_C and Poisson's ratio, ν_C, of the concrete used for the deck, are taken as $3500\ kN/cm^2$ and 0.1, respectively. For the given design, loss of stability of the bridge occurs by buckling of the deck. At the onset of buckling, the deck is mainly in compression. Hence, the influence of the reinforcement ratio and of cracking of concrete on the buckling load and the initial postbuckling behavior is negligible.

Fig. 5 shows the cross-sections of the members of the arch bridge. The diameter of the hangers is given as κd where $d = 1\ cm$ and $\kappa \in \mathbb{R}$ is a scaling factor that represents the design parameter. The thickness of the deck is chosen as 30 cm.

FE analysis of the arch bridge is carried out with MSC Marc 2005 [9]. The arches, braces, and stiffening beams are modelled with 2-node beam elements allowing consideration of twist [9]. The deck is discretized with 4-node shell elements [9]. Linear 2-node truss elements with constant cross-section [9] are used for modelling of the hangers. The uniform reference surface load applied to the deck is given as $p = 0.004\ kN/cm^2$ (including self weight and traffic load).
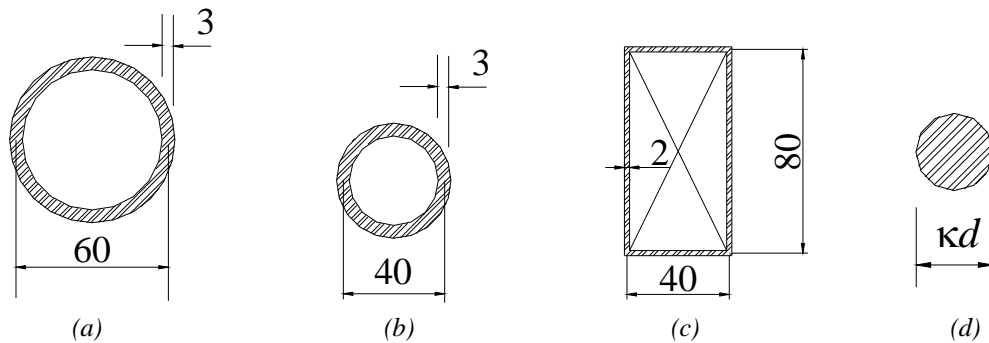

Fig. 5: Cross-section of (a) the arches, (b) the braces, (c) the stiffening beams, and (d) the hangers; unit of numerical data: cm
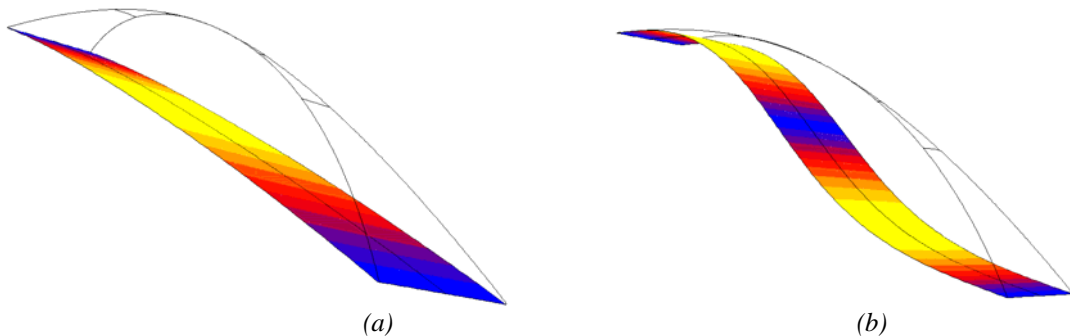

Fig. 6: (a) Deformed arch bridge without hangers just before buckling, (b) buckling mode

Fig. 6(a) shows the deformed arch bridge without hangers just before buckling. The value of the vertical displacement of the midpoint of the arch bridge, for the reference load, is 21.1 cm, which is 1/189 of the span. In contrast to the *von Mises* truss, the prebuckling stress state of the structure is not a membrane stress state because it contains e.g. bending deformations of the deck. Hence, the constraint condition for bifurcation buckling from a membrane stress state (Eq.(11)) is not satisfied. Fig. 6(b) shows the buckling mode.
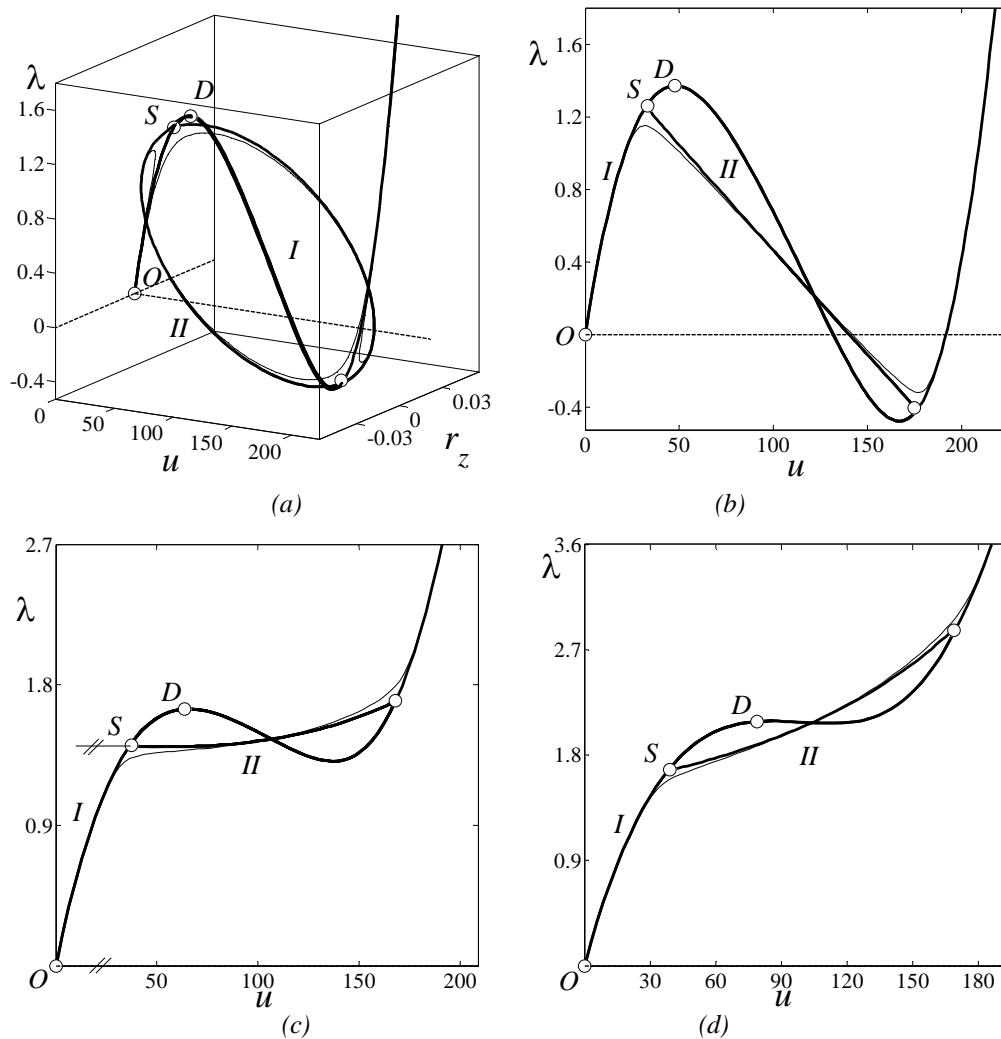

Fig. 7: Load-displacement paths of the midpoint of the deck of an arch bridge for three different values of the stiffness of the hangers; (a),(b) $\kappa = 0$, (c) $\kappa = 0.6182$, (d) $\kappa = 0.8000$ (Figs. 7(b) - (d) show the projection of the secondary path onto the plane $r_z = 0$)

Fig. 7(a) shows the load-displacement path of the midpoint of the deck of the arch bridge without hangers, i.e. for $\kappa = 0$, where u denotes the vertical displacement of this point and r_z stands for the rotation (in radian) of the tangent at this point in the direction of the $x - axis$, about the $z - axis$ (see Fig. 7(a)) The negative slope of the projection of the secondary path onto the plane $r_z = 0$ at the stability limit S (Fig. 7(b)) indicates that the structure without hangers is imperfection sensitive, i.e. $\lambda_1(\kappa = 0) = 0$, $\lambda_2(\kappa = 0) < 0$. The thin curve in Figs. 7(a) $-$ (d) refers to an imperfect structure. The imperfection was chosen as a perturbation of the geometric shape of the perfect structure, affine to the

eigenvector $\mathbf{v}_1$. The largest deviation of the geometric shape of the deck of the imperfect structure from the one of the perfect structure is 0.4%. As was found to be the case for the *von Mises* truss, loss of stability of the deck of the arch bridge occurs in the form of symmetric bifurcation with respect to the plane $r_z = 0$. Increasing the stiffness of the hangers by increasing κ to 0.6182, results in $\lambda_2 = 0$ and $\lambda_4 > 0$, indicating that the structure is already imperfection insensitive which is reflected by the positive curvature of the projection of the secondary path onto the plane $r_z = 0$ (Fig. 7(c)). For $\kappa = 0.8000$, the path of the imperfect structure and the projection of the secondary path onto the plane $r_z = 0$ are monotonic (Fig. 7(d)). Comparing Fig. 7(b) with Fig. 7(d), it is seen that the addition of tensile members in the form of hangers has resulted in the conversion of the originally imperfection-sensitive arch bridge into an imperfection-insensitive one. This conversion is accompanied by an increase of the stability limit. Moreover, for the reference load, the vertical displacement of the midpoint of the arch bridge is 12.9 cm, which is 1/310 of the span, as compared to 1/190 for the arch bridge without hangers.

5.   Conclusions

It was shown that conversion of imperfection-sensitive elastic structures into imperfection-insensitive ones by adding tensile members is not restricted to academic problems such as the *von Mises* truss where buckling occurs from a membrane stress state. A condition allowing to identify such a stress state by means of the consistently linearized eigenproblem was presented. An arch bridge for which this condition does not hold was used to demonstrate that the postbuckling behavior of the structure can be significantly improved by adding sufficiently stiff hangers which overcompensate the decrease in the load carried by the deck in the postbuckling regime.

Acknowledgements

References

[1] Schranz C, Krenn B, and Mang H.A. *Conversion from imperfection-sensitive into imperfection-insensitive elastic structures II: Numerical investigation*. International Journal of Computer Methods in Applied Mechanics and Engineering, 195, 1458-1479, 2006.

[2] Mang H.A, Jia X., and Hoefinger G. *Hilltop buckling as the* A *and* Ω *in sensitivity analysis of the initial postbuckling behavior of elastic structures*. Journal of Civil Engineering and Management, 15(1), 35-46, 2009.

[3] Brush D.O., and Almroth B.O. *Buckling of Bars, Plates, and Shells*. McGraw-Hill, New York, 1975.

[4] Koiter W. *On the stability of elastic equilibrium*, Translation of '*Over de Stabiliteit van het Elastisch Evenwicht*' (1945). In NASA TT F-10833, Polytechnic Institute Delft, H.J. Paris Publisher: Amsterdam, 1967.

[5] Mang H.A., Hoefinger G., and Jia X. *On the predictability of zero-stiffness postbuckling*. Z. Angew. Math. Mech., 90(10-11), 837-846, 2010.

[6] Steinboeck A., Jia X., Hoefinger G. and Mang H.A. *Remarkable postbuckling paths analyzed by means of the consistently linearized eigenproblem*. International Journal for Numerical Methods in Engineering, 76, 156-182, 2008.

[7] Mang H.A. and Hoefinger G. *Bifurcation buckling from a membrane stress state*. Submitted for publication, 2010.

[8] Steinboeck A., Hoefinger G. Jia X., and Mang H.A. *Three pending questions in structural stability*. Journal of the International Association for Shell and Spatial Structures, 50, 51-64, 2009.

[9] MSC.MARC. volume A: *Theory and user information*. MSC.Marc manuals, 2005.

[10] Helnwein P. *Zur initialen Abschätzbarkeit von Stabilitätsgrenzen auf nichtlinearen Last-Verschiebungspfaden elastischer Strukturen mittels der Methode der Finiten Elemente [in German; On ab initio assessability of stability limits on nonlinear load-displacement paths of elastic structures by means of the finite element method]*. PHD thesis, Vienna University of Technology, 1997.

[11] Bažant Z. P. and Cedolin L., *Stability of structures: elastic, inelastic, fracture, and damage theories, third edition*. 2010, World Scientific Publishing Company, Singapore.

CURRICULUM VITAE

M.Eng. Xin JIA

BIOGRAPHICAL INFORNATION

Date of birth:	19.04.1981
Place of Birth:	Jiangsu, China
Nationality:	Chinese
Marital status:	Married
Children:	1 Child
Postal Address:	Mittelgasse 17/7, 1060, Vienna, Austria
E-mail Address:	xin.jia@tuwien.ac.at

EDUCATION

09/1996 - 06/1999	High school, in No.1 High School of Xuzhou, Jiangsu, China
09/1999 - 06/2003	Undergraduate studies at the College of Civil Engineering of Tongji University, Shanghai, China; graduation to **B.Eng.**
09/2003 - 03/2006	Graduate studies at the Department of Geotechnical Engineering of Tongji University, Shanghai, China; graduation to **M.Eng.**
10/2006 - 12/2010	Doctoral studies at the Institute for Mechanics of Materials and Structures of Vienna University of Technology, Vienna, Austria.

RESEARCH INTERESTS

- Finite element method
- Structural stability
- Buckling and postbuckling analysis of structures
- Optimization of structures